

Omics-based characterization of chlorotoni-,
myxopyronin- and chelocardin-stress
in *Clostridioides difficile*

Inauguraldissertation

zur

Erlangung des akademischen Grades eines
Doktors der Naturwissenschaften (Dr. rer. nat.)

der

Mathematisch-Naturwissenschaftlichen Fakultät

der

Universität Greifswald

vorgelegt von

Madita Brauer

geboren am 17.09.1991

in Bremerhaven

Greifswald, den 12.07.2022

Dekan: Prof. Dr. Gerald Kerth

1. Gutachter: Prof. Dr. Katharina Riedel

2. Gutachter: Prof. Dr. Isabelle Martin-Verstraete

3. Gutachter: Prof. Dr. Franziska Faber

Tag der Promotion: 19.10.2022

*Dedicated to my grandmothers,
both of whom, each in their own way,
have always been a great example to me*

Table of contents

Abstract.....	9
Zusammenfassung.....	11
Original publications	13
Abbreviations	14
1. Introduction	15
1.1 Antibiotics and antibiotic resistances	15
1.1.1 The history of antibiotics.....	15
1.1.2 Antibiotic resistances.....	17
1.1.3 The requirement for new specialized antibiotics	18
1.2 <i>Clostridioides difficile</i> and its interplay with the microbiome and antibiotics....	19
1.2.1 <i>Clostridioides difficile</i> – a zoonotic pathogen with a versatile metabolism.....	19
1.2.2 <i>Clostridioides difficile</i> infections	22
1.2.3 Therapy of <i>C. difficile</i> infections.....	24
1.3 New candidates for the therapy of infections with <i>C. difficile</i>	26
1.3.1 Antibiotics under investigation for the therapy of <i>C. difficile</i> infections...26	
1.3.2 Promising drug targets in <i>C. difficile</i>	29
1.3.3 Screening of compounds with antimicrobial activity against <i>C. difficile</i> ..31	
2. Aim of the thesis.....	36
3. Results.....	37
3.1 Chlorotoniol A and its derivatives selectively inhibit growth of <i>C. difficile</i> and close relatives	38
3.1.1 Susceptibility of <i>C. difficile</i> and other intestinal species to chlorotoniols..39	
3.1.2 The protein inventory of bacteria with higher susceptibility to chlorotoniols	43
3.1.3 Systemic effects of chlorotoniol treatment on the metabolism of <i>C. difficile</i>	49
3.1.4 Systemic effects of ChA treatment on the complex microbial communities of the intestinal tract.....	62
3.2 Myxopyronin B as potential novel antibiotic for <i>C. difficile</i> therapy	74
3.2.1 Myxopyronin B is active against <i>C. difficile</i> including fidaxomicin- resistant strains but spares other intestinal anaerobes	75

3.2.2	The stress responses of <i>C. difficile</i> 630 to rifaximin, fidaxomicin, and myxopyronin B	76
3.2.3	Myxopyronin B interferes with toxin synthesis in <i>C. difficile</i>	79
3.3	The response of <i>C. difficile</i> to dissipation of the membrane potential by amidochelocardin	80
3.3.1	Susceptibility of <i>C. difficile</i> and selected anaerobic bacteria to chelocardins.....	81
3.3.2	The proteome response of <i>C. difficile</i> to amidochelocardin	82
3.3.3	Amidochelocardin accumulates in the membrane of <i>C. difficile</i> but does not cause cell deformation.....	84
3.3.4	<i>C. difficile</i> potentially accumulates aromatic compounds in response to amidochelocardin stress.....	86
4.	Discussion	88
4.1	Omics technologies in the context of antibiotic development.....	88
4.2	The complex intestinal community substantially contributes to host's health .	91
4.3	Transient metal toxicity and metal homeostasis as antibiotic target.....	94
4.4	Susceptibility to chlorotonils is correlated with tetrapyrrole biosynthesis and selenometabolism	96
4.5	Copper stress eventually limits selenium availability	98
4.6	The pros and cons of old and new drugs.....	100
4.7	The current role of membrane-active and broad-spectrum antibiotics	102
5.	Conclusion and outlook.....	105
6.	Materials and methods.....	107
6.1	Antibiotics.....	107
6.1.1	Natural products.....	107
6.1.2	Commercial antibiotics	107
6.2	<i>In vitro</i> experiments.....	108
6.2.1	Bacterial strains and handling	108
6.2.2	Physiological assays	112
6.2.3	Proteomics experiments.....	117
6.2.4	qPCR analysis	121
6.2.5	Inductively-coupled plasma-mass spectrometry analysis (ICP-MS)....	122
6.2.6	Metabolomics analysis	123

6.2.7	Subcellular localization analysis	125
6.2.8	Transmission electron microscopy.....	127
6.3	<i>In vivo</i> experiments: Metaproteomics analyses.....	129
6.3.1	Extraction of proteins.....	129
6.3.2	LC-MS/MS sample preparation and analysis.....	130
6.3.3	Database search and analysis.....	131
6.3	Comparative BLASTp analysis	132
6.4	Data visualization	133
6.5	Data availability	133
7.	References.....	134
8.	Appendix.....	161
8.1	Supplementary figures.....	161
8.2	CD Rom content.....	164
8.3	Eigenständigkeitserklärung.....	165
8.4	Conference contribution.....	166
8.5	Acknowledgments.....	167

Abstract

Clostridioides difficile is the leading cause of antibiotic-associated diarrhea referring to infections of the gastrointestinal tract in the course of (broad-spectrum)antibiotic therapy. While antibiotic therapy, preferentially with fidaxomicin or vancomycin, often stops the acute infection, recurrence events due to remaining spores and biofilm-associated cells are observed in up to 20% of cases. Therefore, new antibiotics, which spare the intestinal microbiota and eventually clear infections with *C. difficile* are urgently required. In this light, the presented work aimed at the evaluation and characterization of three natural product classes, namely chlorotonils, myxopyronins and chelocardins, with respect to their antimicrobial activity spectrum under anaerobic conditions and their potential for the therapy of *C. difficile* infections. Briefly, compounds of all three classes were screened for their activity against a panel of anaerobic bacteria. Subsequently, the systemic effects of selected derivatives of each compound class were analyzed in *C. difficile* using a proteomics approach. Finally, appropriate downstream experiments were performed to follow up on hypotheses drawn from the proteomics datasets. Thereby, all three compound classes demonstrated significant activity against *C. difficile*. However, chelocardins similarly inhibited the growth of other anaerobes excluding chelocardins as antibiotic candidates for *C. difficile* infection therapy. In contrast, chlorotonils demonstrated significantly higher *in vitro* activity against *C. difficile* and close relatives compared to a small panel of other anaerobes. In addition, it could be shown that chlorotonils affect intracellular metal homeostasis as demonstrated in a multi-omics approach. The data led to speculate that chlorotonils eventually affect cobalt and selenate availability in particular. Moreover, a metaproteomics approach verified that oral chlorotonil treatment only marginally affected the intestinal microbiota of piglets on taxonomic and functional level. Furthermore, the proteome stress response of *C. difficile* 630 to myxopyronin B, which similarly showed elevated activity against *C. difficile* compared to a few other anaerobes, indicated that the antibiotic inhibited early toxin synthesis comparatively to fidaxomicin. Finally, evidence is provided that *C. difficile* 630 responds to dissipation of its membrane potential by production and accumulation of aromatic metabolites.

Zusammenfassung

Clostridioides difficile ist der häufigste Erreger von Antibiotika-assoziierten Infektionen des Gastrointestinaltrakts als Folge einer (Breitspektrum)Antibiotika-Therapie. Infektionen mit *C. difficile* werden zumeist mit Fidaxomicin oder Vancomycin therapiert, was in den meisten Fällen zur Heilung der Infektion führt. Jedoch kommt es in bis zu zwanzig Prozent der Fälle zu wiederkehrenden Infektionen, die durch die von *C. difficile* produzierten Sporen oder Biofilm-assoziierte vegetative Zellen hervorgerufen werden. Aus diesem Grund werden dringend neue Antibiotika, die die Darmmikrobiota aussparen und idealerweise zur nachhaltigen Heilung der Infektion beitragen, benötigt. Die vorliegende Arbeit zielte daher darauf ab, drei neue Antibiotikaklassen mit Hinblick auf ihr Potential als Antibiotika für die Therapie von *C. difficile* Infektionen beziehungsweise das mit ihnen assoziierte Risiko eine *C. difficile* Infektion herbeizuführen zu evaluieren. Zunächst sollte dabei die Aktivität der Antibiotika-Klassen gegen anaerobe Bakterien nachgewiesen werden. Im Folgenden sollten die systemischen Effekte aller drei Substanzklassen mittels Proteomanalysen im Modellbakterium *C. difficile* untersucht werden, woraufhin abschließend Folgeexperimente generierte Hypothesen bestätigen sollten. Sowohl Chlorotonile und Myxopyronine als auch Chelocardine zeigten antimikrobielle Wirkung gegen *C. difficile*. Allerdings zeigten die Chelocardine zudem auch starke Aktivität gegen alle anderen getesteten Anaerobier, was die Chelocardine als Antibiotika für die Therapie von *C. difficile* Infektionen ausschließt. Im Gegensatz dazu zeigten insbesondere die Chlorotonile eine erhöhte Aktivität gegen *C. difficile* und nahe verwandete Spezies im Vergleich zu weniger nahe verwandten Spezies im Rahmen von *in vitro* Experimenten. Des Weiteren konnte eine Störung der intrazellulären Metallhomeostase in Folge von Chlorotonil-Stress in *C. difficile* im Rahmen einer multi-Omics Analyse beobachtet werden. Die vorliegenden Daten lassen zudem darauf schließen, dass Chlorotonile insbesondere den Cobalt- und Seleniumhaushalt stören. Außerdem konnte eine Metaproteomics Analyse zeigen, dass eine orale Chlorotonil-Gabe nur einen minimalen Effekt auf die taxonomische und funktionale Integrität der intestinale Mikrobiota von jungen Schweinen hat. Weitere Proteomstudien konnten darüber hinaus zeigen, dass Myxopyronin B, ähnlich wie Fidaxomicin, die frühe Toxinproduktion inhibiert und *C. difficile* 630 auf den Zusammenbruch seines Membranpotentials mit der Synthese und Akkumulation von aromatischen Metaboliten reagiert.

Original publications

Parts of the work presented here will be/have been published in:

- I. Brauer M., Herrmann J., Zühlke D., Müller R., Riedel K., Sievers S.
Myxopyronin B inhibits growth of a Fidaxomicin-resistant *Clostridioides difficile* isolate and interferes with toxin synthesis. *Gut Pathog* **14**, 4 (2022).
doi.org/10.1186/s13099-021-00475-9
- II. Brauer M., Hotop S.K., Wurster M., Herrmann J., Miethke M., Schlüter R., Zühlke D., Brönstrup M., Lalk M., Müller R., Sievers S., Bernhardt, J. Riedel, K.
Clostridioides difficile Modifies its Aromatic Compound Metabolism in Response to Amidochelocardin-Induced Membrane Stress. *mSphere*, e0030222. doi: 10.1128/msphere.00302-22
- III. Bublitz A., Brauer M.*, Wagner S.*, Hofer W., Müssen M., Deschner F., Lesker T.R., Neumann-Schaal M., Nübel U., Bartel J., Zühlke D., Bernecker S., Jansen R., Stadler M., Sievers S., Riedel K., Herrmann J., Müller R., Fuchs T.M., Strowig T.
Sparing of the microbiota by the natural product antibiotic chlorotoniil A prevents relapsing *Clostridioides difficile* infection (working title). *Cell Host Microbe*.
(in revision)
- IV. Wagner S., Brauer M., ..., Fuchs T.M.
Effects of antibiotics on the functionality of the swine gut microbiota determined by a MetaOmics approach (working title).
(in preparation)

Abbreviations

Abbreviations

AAA	Aromatic amino acids
ABC	ATP binding cassette
Ad	Add up to
a.u.	artificial units
BHI	Brain Heart Infusion
BHIS	Brain Heart Infusion – supplemented
BLASTp	Protein Basic local alignment search tool
CAMP	cationic antimicrobial peptides
Cbi	Cobinamide
CDCHD	Amidochelocardin
CDI	<i>Clostridioides difficile</i> infection
CDMM	Chemical defined minimal medium
ChA/B	Chlorotoniil A/B
CHD	Chelocardin
Ctrl	Control
DMSO	Dimethyl sulfoxide
Ecf	Energy-coupling factor
FC	Fold change
Fid	Fidaxomicin
FMT	Fecal microbiota transplantation
GC-MS	Gas chromatography – mass spectrometry
iBAQ	Intensity-based absolute quantification
ICP-MS	Inductive-coupled plasma – mass spectrometry
LC-MS/MS	Liquid chromatography – tandem mass spectrometry
LFQ	Label-free quantification
MIC	Minimal inhibitory concentrations
MyxB	Myxopyronin B
OD _{xx nm}	Optical density at xx nanometer
ON/OFF	Exclusively identified in treated/untreated cells
NMDS	Non-metric multidimensional scaling
NSAF	Normalized spectrum abundance factor
PCA	Principal component analysis
PTS	Phosphotransferase systems
Rif	Rifaximin
ROS	Reactive oxygen species
rpm	Rounds per minute
RT	Room temperature
(r)SAM	(radical) S-adenosylmethionine
SDS-PAGE	Sodium dodecyl sulfate polyacrylamide gel electrophoresis
Sec	Selenocysteine
TCA	Tricarboxylic acid cycle
TcdA/B	Toxin A/B
TEM	Transmission electron microscopy
w/v	Weight per volume

1. Introduction

Although tremendous progress has been achieved in recent decades, infectious diseases, including those caused by bacteria, viruses, fungi, protozoa and multicellular parasites, still rank among the most common causes of death (Spencer *et al.*, 2018; Bloom and Cadarette, 2019). In particular, infectious diseases are still highly prevalent in developing countries, whereas an overall higher standard of living and good healthcare have led to significant improvements in the industrialized part of the world (Hansen and Painsil, 2016; Wood *et al.*, 2017). Nevertheless, infectious diseases remain an important health care burden also in the industrialized part of the world (Liu *et al.*, 2016). Among others, emerging and antibiotic-resistant pathogens endanger human and animal health in all parts of the world due to the lack of effective therapeutic strategies to combat those pathogens (Morens *et al.*, 2004; Cassini *et al.*, 2019). Consequently, the search for and development of new strategies against long-standing as well as emerging pathogens is of utmost importance for maintaining and improving the state of health in the world. In this context, antibiotic research and development are pivotal aspects (Division, 2019).

1.1 Antibiotics and antibiotic resistances

1.1.1 The history of antibiotics

Since their commercialization in the mid 20th century, antibiotics are the most important treatment option against bacterial pathogens (Aminov, 2010). While originally defined as “small molecules that are produced by microorganisms and inhibit the growth of other microorganisms” (Waksman, 1947), the group of antibiotics today comprises a vast number of molecules of varying size, origin, and mode-of-action, which have in common that they either prevent the growth of bacterial pathogens (“bacteriostatic antibiotics”) or even lyse bacterial cells (“bactericidal antibiotics”) (Hutchings *et al.*, 2019).

Although antibiotics have been used for more than 2000 years, for instance, when the Chinese, Greeks and Egyptians already used moldy bread to cure wound infections it was not before the late 19th and the beginning of the 20th century that scientist became aware of antibiotics. After the discovery of microorganisms, such as the bacteria by Robert Hooke and Antoni van Leeuwenhoek between 1665 and 1676 (Gest, 2004), scientists systematically began to study the nature of infectious diseases and to search for effective treatment options. This led to the discovery of the first antibiotics, namely pyocyanase by Rudolf Emmerich and Oscar Löw in 1899 (Emmerich and Löw, 1899), salvarsan by Paul Ehrlich in 1909 (Ehrlich, 1910) and penicillin by Alexander Fleming in 1928 (Fleming, 1929) (Figure 1.1). In the following decades, further classes of antibiotics have been discovered, such as the cephalosporins, tetracyclines, macrolides and aminoglycosides (Gould, 2016)

Introduction

(Figure 1.1). Finally, the term “antibiotic” was introduced by Selman Waksman in 1941 (Waksman, 1941; Waksman, 1947).

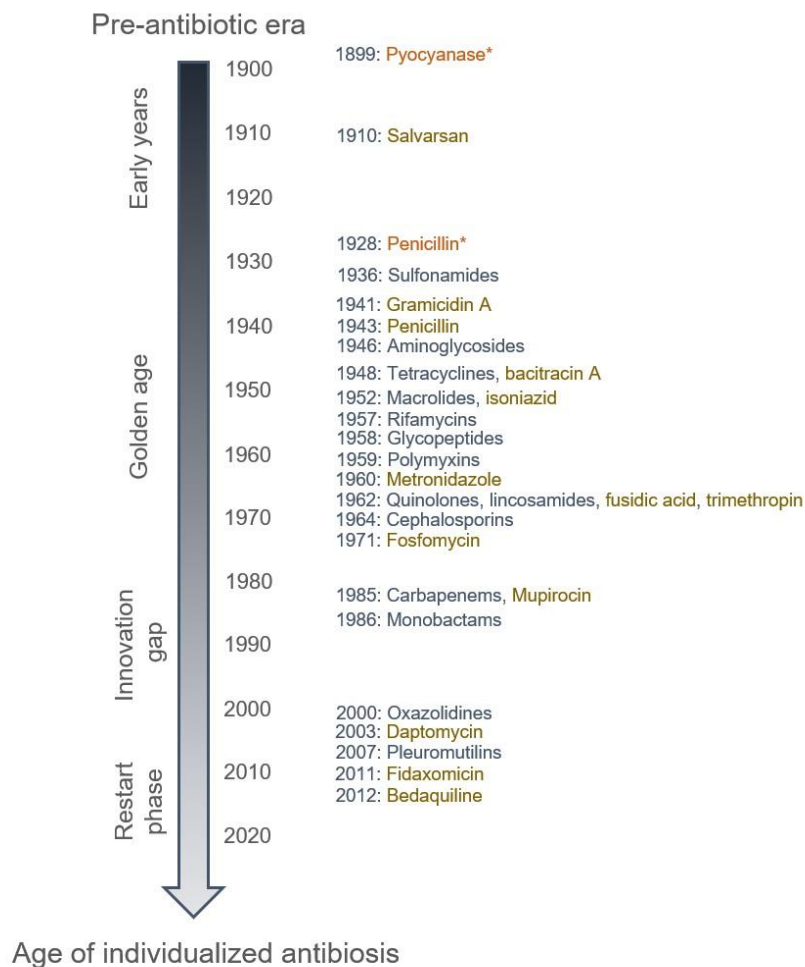


Figure 1.1: Timeline of antibiotic discovery. The most important antibiotic classes are displayed in the order of their introduction to the market. Substances presenting the only clinically relevant compound within their class are highlighted in yellow. * Penicillin has been discovered in 1928 but not commercially available before 1943. Modified from (Hutchings *et al.*, 2019).

In the first years, antibiotics were primarily isolated from Actinobacteria, such as various *Streptomyces* species (e.g., aminoglycosides, tetracyclines, macrolides), but also from other microorganisms, such as Myxobacteria (e.g., coralopyronins, myxopyronins) and several fungi (e.g., penicillins, cephalosporins, fusidic acid) (Barka *et al.*, 2016; Geers *et al.*, 2022). These “natural” antibiotics are mainly produced as secondary metabolites to support their producers in competition with other microorganisms in their environments, such as in soils and the sea (Lucas *et al.*, 2019). Naturally produced antibiotics are used by their producers for defense against other bacteria and eukaryotic predators and for colonization of new habitats but also, for instance, for communication or as siderophores (Lucas *et al.*, 2019; Pérez *et al.*, 2020).

As soon as the value of antibiotics for infectious disease management became evident, the repertoire of antibiotics was further expanded by scientists, who started to modify existing antibiotics to provide semi-synthetic antibiotics and to produce fully synthetic compounds (Christensen, 2021). For instance, methicillin and ampicillin were derived from penicillin and several generations of cephalosporins derived from cephalosporin-C were gradually introduced to the market (Christensen, 2021). The first fully synthetic antibiotic, Salvarsan (Ehrlich, 1910), was followed by the quinolones and sulfones (Colebrook, 1936; Leshner *et al.*, 1962).

1.1.2 Antibiotic resistances

Soon, a growing number of antibiotics became available and paved the way for the most outstanding improvements in medicine, such as surgeries and joint, organ and stem cell transplantations (Liu *et al.*, 2018; L. Evans *et al.*, 2021). However, as bacteria are well known for their adaptability and genetic flexibility, their frequent exposure to antibiotics selected for the first antibiotic-resistant clinical isolates soon after antibiotics were routinely used (Abraham and Chain, 1988; Aminov, 2010). Antibiotic resistance markers, referring to genetic elements that, for example, encode for enzymes able to modify or degrade antibiotics, for antibiotic efflux pumps or for modified target structures, are as old as antibiotics themselves. They are found in all kinds of environments where antibiotics are produced, even in deep sea sediments, and play an important role for the balance within ecosystems (Pal *et al.*, 2015; Blanco *et al.*, 2016; van Goethem *et al.*, 2018; Larsson and Flach, 2022). However, overuse of antibiotics in clinical settings accelerated the development and spread of antibiotic resistance markers, for instance via horizontal gene transfer, finally leading to the emergence of multidrug resistant bacteria (Aminov, 2010; Gould, 2016; Wintersdorff *et al.*, 2016).

It took some time until scientists identified the molecular mechanisms underlying antibiotic resistance development and its dissemination (D.I. Andersson *et al.*, 2020). Today, huge efforts are made to reduce antibiotic consumption world-wide and to reduce the introduction of antibiotics into the environment to slow down antibiotic resistance development and dissemination (McEwen and Collignon, 2018). Moreover, antibiotic stewardship strategies were developed to adapt antibiotic treatment schemes in order to optimize the use of antibiotics and preserve the efficacy of last-resort antibiotics used to treat multidrug and other difficult-to-treat pathogens, such as multi-drug resistant *Mycobacterium tuberculosis* and bacteria from the ESKAPE-group (*Enterococcus faecium*, *Staphylococcus aureus*, *Klebsiella pneumoniae*, *Acinetobacter baumannii*, *Pseudomonas aeruginosa*, and *Enterobacter* species) (Oliveira *et al.*, 2020; Nang *et al.*, 2021).

Introduction

Nevertheless, antibiotic consumption is increasing and the prevalence of antibiotic resistant pathogens is higher than ever before (Aslam *et al.*, 2018; Klein *et al.*, 2018). On the opposite side, the number of antibiotics in the development pipeline is low compared to the 1950s or to the number of anticancer and antihypertensive drugs, and is only slowly increasing after decades of stagnation (Plackett, 2020) (Figure 1.1). The restricted use of new antibiotics, which are withheld for relatively rare severe infections with high-concern pathogens, however, strongly limits the expected profit from new antibiotics. Consequently, the interest of many pharmaceutical companies to continue or resume their own work on antibiotics is rather low, and thus antibiotic research is mainly restricted to the academic sector and smaller companies (Silver, 2011; Da Farrell *et al.*, 2018). Therefore, only a few antibiotics have been added to the pool of antibiotics in the last two decades, such as daptomycin in 2003, pleuromutilins in 2007, fidaxomicin in 2011 and bedaquiline in 2012 (Hutchings *et al.*, 2019) (Figure 1.1).

1.1.3 The requirement for new specialized antibiotics

Alternative therapeutic options and preventive measures, such as monoclonal antibodies, phage therapy and probiotics, are in use and under investigation as well (Shen *et al.*, 2017; Wilcox *et al.*, 2017). However, antibiotics are still the preferred therapy against many important bacterial infections and a larger panel will be inevitable to keep up with bacterial infections in the future (Mulani *et al.*, 2019; Luong *et al.*, 2020). In addition to the general demand for new antibiotics, there is also growing interest in more specialized antibiotics (Yang *et al.*, 2021). In recent years, there has been an increasing gain in knowledge concerning individual infectious diseases and disease outcome has been linked to many other aspects of health, such as hormone status, diet and microbiota composition (Cho and Blaser, 2012; Myles, 2014). This more sophisticated understanding of infectious diseases has led to a demand for antibiotics with additional beneficial properties, such as immunomodulatory effects or antibiotics, which reduce the virulence of a pathogen during infection (Köhler *et al.*, 2010; Zimmermann *et al.*, 2018). Moreover, there is increasing awareness that many antibiotic treatment regimens are associated with adverse events, which eventually counterbalance the positive effect of antibiotic therapy (Gerber *et al.*, 2017; Tandan *et al.*, 2018). In particular, antibiotics that spare the gastrointestinal microbiota of a patient are urgently needed to reduce the risk of patients to develop antibiotic-associated diarrhea (Theriot *et al.*, 2014).

Especially, the microbiota associated with different body sites, such as the skin, oral cavity, vagina and intestinal tract, has recently gained considerable attention as profound first line of defense against various pathogens (Cho and Blaser, 2012; Theriot and Young, 2015;

Park and Lee, 2017; Anahtar *et al.*, 2018). Antibiotics that spare and/or restore the microbiota therefore substantially support the cure of an infection and/or prevent secondary infections, such as antibiotic-associated diarrhea and vaginosis (Theriot and Young, 2015; Anahtar *et al.*, 2018). For instance, the vaginal tract is protected against invading pathogens by probiotic lactic acid bacteria, which lower the pH to an acidic state, which is unfavorable for most pathogens (Tachedjian *et al.*, 2017). Antibiotic therapy of vaginal infections must consequently aim at the inhibition of the invading pathogen, but must simultaneously allow the re-colonization of the infection site with probiotic bacteria and concomitant restoration of the pH (Tachedjian *et al.*, 2017).

Likewise, the gastrointestinal microbiota protects against numerous pathogens through competition for nutrients, production of inhibitory metabolites and immunomodulatory effects. This effect, not only restricted to the intestinal microbiota, is also known as “colonization resistance”. Disruption of the colonization resistance provided by the intestinal microbiota, e.g., by antibiotic therapy, often leads to antibiotic-associated diarrhea (Buffie and Pamer, 2013). The most important causative agent of antibiotic-associated diarrhea is the spore-forming Gram-positive bacterium *Clostridioides difficile* (Theriot and Young, 2015).

In summary, antibiotics, which became available for broad-use in the middle of the 20th century, saved millions of lives and still form a cornerstone in modern medicine. However, the emergence of antibiotic resistances as well as of new pathogens severely threatens the achievements made to public health in the last century. Moreover, a more sophisticated understanding of many infectious diseases has led to a demand for more targeted drugs to accelerate and improve the therapy for a particular disease, while reducing the adverse events frequently observed with inappropriate antibiotic therapy. In consequence, new antibiotics, overcoming antibiotic resistances, revealing novel modes-of-action, and being optimized for specific requirements addressing important pathogens, such as multi-drug resistant pathogens or other hard-to-treat pathogens, such as *C. difficile*, are urgently required.

1.2 *Clostridioides difficile* and its interplay with the microbiome and antibiotics

1.2.1 *Clostridioides difficile* – a zoonotic pathogen with a versatile metabolism

C. difficile is an important anaerobic rod-shaped pathogen able to spread inside the intestinal tract under favorable conditions causing mild to severe forms of colitis (Figure 1.2) (Magill *et al.*, 2018; Suetens *et al.*, 2018). As an ubiquitous bacterium, *C. difficile* can be found in the intestine of many different mammals, especially in humans and livestock animals such as pigs and cattle, but also in many environmental sources such as manure

Introduction

and soil (Janezic *et al.*, 2014; Hernandez *et al.*, 2020; Lim *et al.*, 2020). Moreover, *C. difficile* is considered a zoonotic pathogen. For instance, *C. difficile* isolates derived from swine or cattle and associated farm workers of a respective farm are closely related indicating direct human-animal transmission (Debast *et al.*, 2009; Koene *et al.*, 2012; Knetsch *et al.*, 2014; Knight *et al.*, 2019; Tramuta *et al.*, 2021). The broad host spectrum of *C. difficile* can be explained by the environmental requirements of the pathogen. As an inhabitant of the intestinal tract, *C. difficile* not only prefers mammalian body temperature and anaerobic conditions but is, more importantly, dependent on the availability of a certain nutrient spectrum. The preferred nutrients of *C. difficile* comprise high amounts of small peptides, amino acids and some carbohydrates. In addition, the availability of so-called “germinants” required for germination of *C. difficile* spores is crucial for the pathogen (Theriot *et al.*, 2014; Jenior *et al.*, 2018).

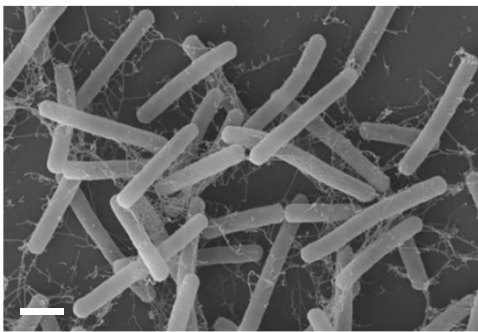


Figure 1.2: Scanning electron microscopy images of *C. difficile*. Provided and approved by Rabea Schlüter (Imaging Center, University of Greifswald) and Nicole Metzendorf (Institute of Microbiology, University of Greifswald). Scale bar = 1 μ m.

In more detail, *C. difficile* preferentially utilizes amino acids, such as proline, leucine, phenylalanine and glycine via Stickland fermentation (Neumann-Schaal *et al.*, 2015; Neumann-Schaal *et al.*, 2019). Although it was recently shown that *C. difficile* is able to grow in the absence of proline and branched chain amino acids (Gencic and Grahame, 2020), there is strong evidence that *C. difficile* is not able to compete with other microbes in the complex community of the intestinal tract in the absence of its preferred amino acids, particularly proline (Jenior *et al.*, 2017; Battaglioli *et al.*, 2018; Fletcher *et al.*, 2018; Lopez *et al.*, 2019; Fletcher *et al.*, 2021). In addition to amino acids, *C. difficile* is able to use carbohydrates via the glycolysis, the pentose-phosphate pathway and other carbohydrate degradation pathways as well as several other nutrients, such as ethanolamine derived from epithelial cells (Antunes *et al.*, 2012; Nawrocki *et al.*, 2018; Neumann-Schaal *et al.*, 2019). Carbohydrates are considered second-line nutrients for *C. difficile* and were neglected as a nutrient source for a long time. However, increasing evidence suggests a more central role of carbohydrates in the metabolism of *C. difficile* considering the expression of several phosphotransferase systems (PTS) and ATP binding cassette (ABC) transport systems during *in vivo* infection experiments (Theriot *et al.*, 2014; Jenior *et al.*, 2017, 2018). Intermediate fermentation products, such as pyruvate, are further degraded via the

pyruvate-formate lyase, pyruvate dehydrogenase or the butyrate fermentation pathway, which yields a range of short chain fatty acids (Neumann-Schaal *et al.*, 2019). Besides, the Wood-Ljungdahl pathway has recently gained attention as an important electron sink when reductive equivalents, such as the Stickland acceptor amino acids, become limited (Bouillaut *et al.*, 2019; Gencic and Grahame, 2020). The Wood-Ljungdahl pathway is used in a limited number of bacterial species to synthesize acetyl-CoA from CO₂ and H₂. Interestingly, the operon encoding the twelve proteins of the Wood-Ljungdahl pathway is present in all *C. difficile* genomes sequenced so far and is highly conserved (Köpke *et al.*, 2013).

Apart from the nutrient availability, bile acids play a central role for *C. difficile* inside the intestinal tract (Buffie *et al.*, 2015; Shen, 2020). While some of them, namely most secondary bile acids, such as lithocholate and deoxycholate, can prevent *C. difficile* sporulation (Buffie *et al.*, 2015; Thanissery *et al.*, 2017), others, such as cholate and taurocholate, are urgently required as signal molecules for the initiation of spore germination (Shen, 2020). Apart from that, bile acids are assumed to have large impact on other properties of *C. difficile*, including motility, toxin structure and biofilm formation (Dubois *et al.*, 2019; Sievers *et al.*, 2019; Tam *et al.*, 2020). However, the role of bile acids in the lifecycle of *C. difficile* is only partially understood and subject of ongoing research due to the complexity of this research field (Reed *et al.*, 2020). In addition to bile acids, *C. difficile* needs to cope with fluctuating oxygen conditions, the host immune system and secondary metabolites produced by other microbes. To cope with these stress factors within the intestinal tract, *C. difficile* has evolved an efficient stress response system with various signaling, regulatory and detoxification proteins, which allow the pathogen to deal with, e.g., molecular oxygen (Neumann-Schaal *et al.*, 2018; Kint *et al.*, 2020), bile acids (Sievers *et al.*, 2019), heme (Knippel *et al.*, 2020), and antimicrobial peptides (Woods *et al.*, 2018).

Overall, *C. difficile* is well equipped to survive in the variable environment of the mammalian gut and is furthermore provided with a large flexible genome allowing evolutionary adaptation to changing conditions (He *et al.*, 2010; Knight *et al.*, 2015; Kulecka *et al.*, 2021). Nevertheless, *C. difficile* is not able to establish inside the intestine of healthy humans as long as the complex and intact intestinal microbiota successfully protects its host by occupying the ecological niche required by *C. difficile*. Therefore, breakdown of the colonization resistance is a pre-requisite for an infection with *C. difficile* (Lopez *et al.*, 2020; Leslie *et al.*, 2021).

Introduction

1.2.2 *Clostridioides difficile* infections

The circumstances causing the intestinal imbalance, which paves *C. difficile*'s way to infection, are diverse and multifactorial, but increased age, antibiotic therapy, comorbidities, hospitalization, low alpha diversity of the microbiota and an overall weak immune response are assumed to be important risk factors (Peniche *et al.*, 2018; Czepiel *et al.*, 2021; van Werkhoven *et al.*, 2021). In concert, these factors change the microbiome structure and reduce its diversity, which are two key factors for colonization resistance against *C. difficile* (Kang *et al.*, 2019; Berkell *et al.*, 2021; Lesniak *et al.*, 2021). Despite the multifactorial nature of intestinal imbalance, antibiotics, especially broad-spectrum antibiotics such as carbapenems, cephalosporins and fluoroquinolones as well as other chemotherapeutic agents such as proton-pump inhibitors, often rank first in meta-analyses examining the factors most frequently correlated with *C. difficile* infections (Slimings and Riley, 2021; van Werkhoven *et al.*, 2021).

Infections with *C. difficile* are not only the most prevalent form of antibiotic-associated diarrhea but also rank amongst the most prevalent healthcare-associated infections in Europe (Cassini *et al.*, 2016; Motamedi *et al.*, 2021). Moreover, *C. difficile* infections often result in significant deterioration of the patient's health status and mortality rates are around ten percent (Czepiel *et al.*, 2021; Granata *et al.*, 2021). Therefore, infected patients often require substantial medical care and hospitalization, which additionally leads to a significant economic burden of the disease (Wiegand *et al.*, 2012; Rajasingham *et al.*, 2020). Despite great efforts to protect vulnerable patients, such as elderly and immunosuppressed patients, from *C. difficile* by appropriate hygiene management, the number of cases per year remains on a constant level (Finn *et al.*, 2021). Amongst others, rising numbers of *C. difficile* infections in the past decade are attributed to more virulent and transmittable strains and ribotypes, such as ribotype 027 (Kumar *et al.*, 2019; Almutairi *et al.*, 2021; Fu *et al.*, 2021). In addition, *C. difficile* infections are no longer exclusively healthcare-associated infections but community-acquired forms of *C. difficile* infections have become highly prevalent in recent years (Khanna *et al.*, 2012; Ofori *et al.*, 2018; Fu *et al.*, 2021).

An infection with *C. difficile* is initiated by the germination of *C. difficile* spores upon disruption of colonization resistance. This is the starting point for a bloom of the pathogen in the intestine (Figure 1.3), where it has been detected by different studies with an averaged abundance between 0.76% and 3%. In severe cases, the total load might be even higher (Khanna *et al.*, 2016; Seekatz *et al.*, 2016; Crobach *et al.*, 2020). In the following, the pathogen can cause a severe infection of the intestinal tract mediated mainly by the production of one or more enterotoxins (Figure 1.3) (Kordus *et al.*, 2021). These toxins damage the intestinal epithelium directly or indirectly by activating a proinflammatory

immune response (Ernst *et al.*, 2021; Landenberger *et al.*, 2021; McKee *et al.*, 2021). Epithelial damage, comprising necrosis of epithelial cells and destruction of the tight junctions, results in the typical symptoms of *C. difficile* infections, including diarrhea, colitis and, in severe cases, a so-called pseudomembranous colitis (Figure 1.3) (Kordus *et al.*, 2021).

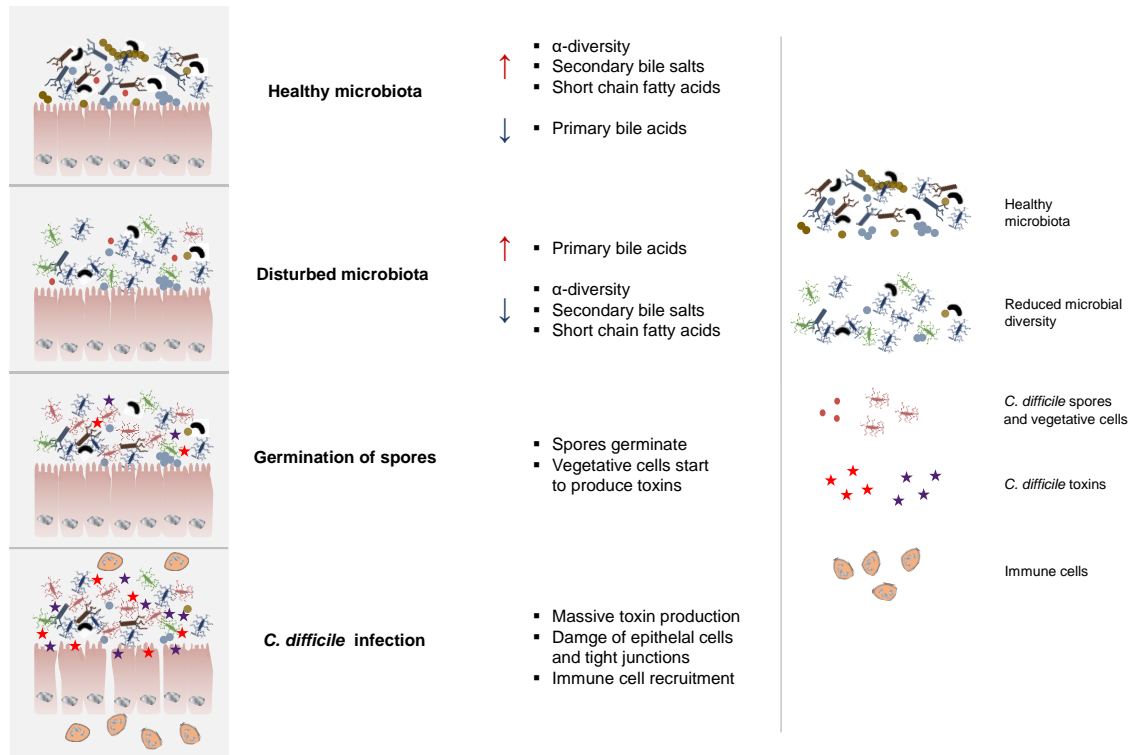


Figure 1.3: Schematic illustration of the steps towards an infection with *C. difficile*. Disruption of the healthy microbiota by, e.g., antibiotics, reduces the α -diversity of the microbial community and leads to an increase in primary bile acids, while secondary bile acids and short chain fatty acids are depleted. The changing conditions subsequently induce germination of *C. difficile* spores. The resulting vegetative cells eventually start to produce toxins. Toxins and the concomitantly induced immune response jointly cause damage of the intestinal epithelium. The figure was created in Microsoft PowerPoint according to recent literature cited above, e.g. Buffie *et al.*, 2015; Theriot and Young, 2015; Schäffer and Breitrück, 2018.

So far, three toxins have been described in *C. difficile*, of which most strains express at least one (Rupnik and Janezic, 2016). Two toxins, TcdA and TcdB, are encoded within one operon known as PaLoc (Eichel-Streiber *et al.*, 1992). Both toxins function as glucosyltransferases targeting members of the Rho and Ras protein families after translocation into host epithelial cells (Just *et al.*, 1995a; Just *et al.*, 1995b). Inactivation of Ras and Rho proteins results in membrane leakage and several functional disorders (Sun *et al.*, 2010). In contrast, the binary toxin Cdt is encoded separately from the PaLoc and acts as an ADP-ribosyltransferase (Perelle *et al.*, 1997; Gülke *et al.*, 2001). Damage mediated by the toxins causes an immune reaction, which together with the toxin damage further impairs the functionality of the intestinal epithelium and the microbiota (Kordus *et al.*, 2021). The regulation of *C. difficile* toxin synthesis is complex and involves various

Introduction

regulators and signaling systems. Moreover, expression of toxins is strictly linked to the availability of nutrients but also to several other environmental stimuli (Martin-Verstraete *et al.*, 2016). In addition to toxins directed against the host epithelial cells, *C. difficile* produces other, so far mainly overlooked, metabolites, which are directed against its competitors inside the intestine. The most prominent compound is para-cresol, which is produced from tryptophan by a very few bacterial species, including *C. difficile*, and which is toxic for most other bacteria (Passmore *et al.*, 2018). In concert, the toxin cocktail of *C. difficile* as well as the immune response, which is activated by the presence of *C. difficile*, ultimately damage the intestinal barrier leading to the characteristic symptoms, such as diarrhea. Finally, damage of colonic stem cells by *C. difficile*'s toxins results in delayed epithelial repair and long-lasting damages and dysfunctionality (Mileto *et al.*, 2020).

Mild forms of *C. difficile* infections might be self-limiting, but most often more severe forms require medical therapy. Such therapy is today mainly based on antibiotics accompanied by pre- and probiotic as well as immunomodulatory therapy.

1.2.3 Therapy of *C. difficile* infections

Although antibiotics, as the first line of defense against a *C. difficile* infection, are often able to stop the acute infection, recurrence of *C. difficile* infections is highly prevalent (Granata *et al.*, 2021). The collateral damage, which has been caused prior and during infection by the antibiotic therapy, the bacterial toxins, the host's immune response and metabolites produced by *C. difficile* directed against competing bacteria, often severely impair the recovery of the healthy microbiota and its colonization resistance. In turn, recurrence and re-infection rates are reported with up to 20 to 30% for a primary *C. difficile* infection (Granata *et al.*, 2021). Recurrence can thereby result both from reinfection events or due to the recovery of remaining biofilm-associated vegetative cells and spores (Castro-Córdova *et al.*, 2021; Normington *et al.*, 2021). Moreover, recurrence is linked to a persistently perturbed bile acid and short chain fatty profile and low alpha diversity of the microbiota (Buffie *et al.*, 2015; McDonald *et al.*, 2018; Lesniak *et al.*, 2021). While microbiota-sparing antibiotics are crucial to reduce the risk for antibiotic-associated diarrhea, clearance of a *C. difficile* infection inevitably requires a sustainable therapy with selective antibiotics allowing recovery of the healthy microbiota (Webb *et al.*, 2020; Binyamin *et al.*, 2021; Lesniak *et al.*, 2021). To prevent or overcome these issues, large efforts have been made to optimize preventive measures and to develop new therapeutic approaches. For instance, antibiotic treatment regimens have been intensively studied to identify high risk antibiotics, such as fluoroquinolones and cephalosporins, which are now avoided in high-risk patients (Dingle *et al.*, 2017; Slimings and Riley, 2021). In addition, new treatment options have been

evaluated leading to, for example, the introduction of the monoclonal antibody bezlotoxumab, which is successfully applied as co-drug to neutralize *C. difficile* toxins until the infection is cleared (Figure 1.4) (Wilcox *et al.*, 2017). Pre- and probiotic therapy with, e.g., *Lactobacillus acidophilus* and *Lactobacillus casei*, has gained upcoming interest to either prevent infections or to support antibiotic therapy (Figure 1.4) (Shen *et al.*, 2017). Building on the success of pre- and probiotics, fecal microbiota transplantations are an increasing field of research and have been successfully applied in severely ill patients (Figure 1.4) (Quraishi *et al.*, 2017; Hui *et al.*, 2019). However, bezlotoxumab and pre- and probiotic therapies are insufficiently as stand-alone therapy and fecal microbiota transplantations are subject of ongoing discussions due to several concerns, such as the risk of transmitting other intestinal pathogens (Yadav and Khanna, 2021). To overcome these issues, defined microbial communities are currently designed and delivery methods are optimized to specifically restore colonization resistance, while avoiding transmission of other pathogens (Kao *et al.*, 2021). However, such complex communities, which sufficiently resemble the complexity of the natural gastrointestinal microbiomes and enable reliable restoration of colonization resistance could not be established to date. Similarly, ongoing approaches to develop vaccines against *C. difficile*-specific antigens, such as the conserved cell wall glycopolymer PSII (Chu *et al.*, 2016), have not been successful until today (Heidebrecht *et al.*, 2021).

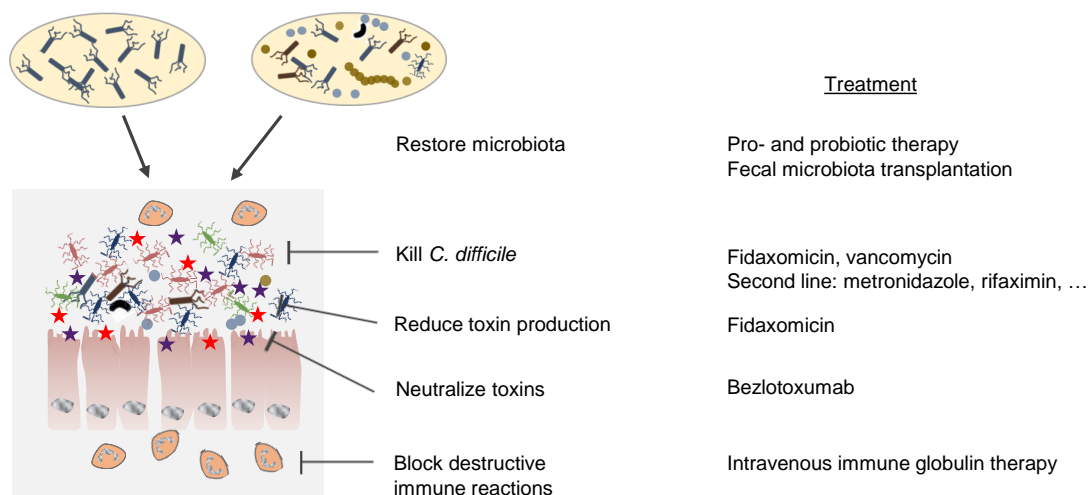


Figure 1.4: Treatment options for *C. difficile* infections and the currently available therapeutics. Treatment of infections with *C. difficile* is currently primarily based on antibiotic therapy. However, pre- and probiotic therapy and monoclonal antibodies, such as bezlotoxumab, are often used supportively. For severe cases, fecal microbiota transplantation is an additional option. The figure was created in Microsoft PowerPoint according to recent literature cited above, e.g. Chaar and Feuerstadt, 2021; Monaghan *et al.*, 2021.

Introduction

In consequence, treatment of *C. difficile* infections still largely depends on antibiotic therapy. Currently, fidaxomicin and vancomycin are recommended for therapy of *C. difficile* infections, whereas the former first-line antibiotic metronidazole as well as a number of other antibiotics might optionally be used as second-line antibiotics (Chaar and Feuerstadt, 2021). For instance, the rifamycin antibiotic rifaximin is used as a chaser antibiotic post-vancomycin therapy in severe cases to extend the antibiotic effect and due to the proven reduction in recurrence rates (Garey *et al.*, 2011; Ng *et al.*, 2019). The latest drug, fidaxomicin, is superior to most other available antibiotics due to the comparatively good clinical outcomes of patients, including comparatively high initial cure and low recurrence rates (Cornely *et al.*, 2012; Guery *et al.*, 2021; Gupta and Ananthkrishnan, 2021). The superiority of fidaxomicin is attributed to its high intestinal availability, its comparatively high selectivity for *C. difficile* and its ability to suppress toxin synthesis and spore formation as well as germination (Louie *et al.*, 2012). In concert, the growth advantage for competing commensal bacteria and the reduced toxin and spore levels significantly improve the patient outcomes (Louie *et al.*, 2012). Worryingly, a first fidaxomicin-resistant *C. difficile* strain was recently isolated from a patient and fidaxomicin-resistant strains were obtained during lab experiments (Leeds *et al.*, 2014; Schwanbeck *et al.*, 2019). These events remind that antibiotic resistances can quickly become an additional issue for the already difficult therapy of *C. difficile*, which thus far shows only neglectable levels of resistance against fidaxomicin and vancomycin (Liao *et al.*, 2012; Sholeh *et al.*, 2020).

In view of the high number of *C. difficile* infections, the substantial health decline, the economic burden associated with the infection, and the risk of antibiotic resistance development, there is an urgent demand for alternative antibiotics, which overcome current limitations and that can replace fidaxomicin in case of the continued spread of antibiotic resistances.

1.3 New candidates for the therapy of infections with *C. difficile*

1.3.1 Antibiotics under investigation for the therapy of *C. difficile* infections

New candidate antibiotics for the therapy of *C. difficile* infections should be as selective as possible, should have a new target or binding site, should be associated with low resistance rates and should be equipped with beneficial features, such as the ability to reduce toxin production and spore formation. Currently, a number of antimicrobial compounds are under investigation, comprising natural and synthetic compounds, including uncharacterized as well as approved antibiotics, which might be re-purposed for the therapy of *C. difficile* infections (Jarrad *et al.*, 2015; Petrosillo *et al.*, 2018; Monaghan *et al.*, 2021). Some of these compounds were only briefly mentioned as being active against *C. difficile*, whereas some

compounds have already passed the first clinical trials (Figure 1.5) (Butler *et al.*, 2022). The top group of next generation *C. difficile* antibiotics is currently formed by antibiotics such as ridinilazole, cadazolid, nitazoxanide, fusidic acid, thuricin CD, ramoplanin, surotomycin and teicoplanin. In addition, there are a range of other compounds currently under investigation such as rifaximin, rifampin, bacitracin, tigecycline, CRS3123, auranofin, NVB302, lacticin 3147, ebselen and aryldepsipeptide antimicrobials (Figure 1.5) (Petrosillo *et al.*, 2018; Monaghan *et al.*, 2021).

Promising candidate antibiotics, such as cadazolid, ridinilazole, surotomycin and ramoplanin, were all demonstrated to be highly active against and specific for *C. difficile* (Peláez *et al.*, 2005; Chilton *et al.*, 2014; Knight-Connoni *et al.*, 2016; Cho *et al.*, 2019). Especially, cadazolid, an oxazolidinone substituted with a fluoroquinolone moiety, is considered promising due to low gastrointestinal absorption, high tolerance and low rates of spontaneous resistance development (Baldoni *et al.*, 2014; Chilton *et al.*, 2014; Locher *et al.*, 2014a; Gehin *et al.*, 2015). Moreover, cadazolid was found to be non-inferior to vancomycin in clinical trials (Louie *et al.*, 2015; Muhammad *et al.*, 2020). Furthermore, toxin synthesis and spore formation were found to be inhibited by cadazolid (Locher *et al.*, 2014b). Similarly, ridinilazole was found to reduce toxin A and B levels resulting in an anti-inflammatory effect (Bassères *et al.*, 2016), while ramoplanin was found to adhere to *C. difficile* spores and immediately killed germinating cells (Kraus *et al.*, 2015). Ridinilazole and ramoplanin successfully cured *C. difficile* infections in rodent models (Freeman *et al.*, 2005; Sattar *et al.*, 2015) and randomized phase 1 and 2 trials could show that ridinilazole is well-tolerated in various doses and is non-inferior to vancomycin (Vickers *et al.*, 2015; Vickers *et al.*, 2017). Likewise, surotomycin was found to be non-inferior to vancomycin in clinical trials (Lee *et al.*, 2016; Daley *et al.*, 2017; Muhammad *et al.*, 2019). However, although surotomycin reached non-inferiority against vancomycin in a phase 3 trial, superiority could not be reached (Daley *et al.*, 2017) and both cadazolid and surotomycin failed to reach non-inferiority compared to vancomycin in two other phase 3 trials (Boix *et al.*, 2017; Gerding *et al.*, 2019). Today, only ridinilazole is in a phase 3 trial (Butler *et al.*, 2022).

In addition to these newly identified compounds, approved antibiotics, such as rifaximin, fusidic acid, bacitracin and teicoplanin, are considered to be re-purposed for the therapy of *C. difficile* infections (Figure 1.5) (Petrosillo *et al.*, 2018; AbdelKhalek *et al.*, 2020; Monaghan *et al.*, 2021). These antibiotics offer the advantage that they are already approved for clinical use and well characterized. Similarly, derivatives of established antibiotics, like desmethyl vancomycin, might be promising (Zhang *et al.*, 2012). In addition to antibiotics, a number of other therapeutics are in development, for instance, to suppress adhesion of *C. difficile* to

Introduction

host epithelial cells, e.g., by blocking surface-exposed proteins of *C. difficile* like the surface layer (S-layer) proteins and CotE, flagella proteins such as FliC or cell surface glycans of *C. difficile* (Bruxelle *et al.*, 2016; Bruxelle *et al.*, 2018; Maia *et al.*, 2020). Other compounds, such as the small molecule inhibitor ebselen and the inhibitor of endosomal acidification bafilomycin A1, are expected to prevent toxin B-mediated cytotoxicity (Stewart *et al.*, 2020; Monaghan *et al.*, 2021) or modulate the host immune system (Figure 1.5) (J. A. Andersson *et al.*, 2020). As for various other pathogens, small RNAs and phage therapy are likewise considered promising therapeutic strategies for *C. difficile* (Mondal *et al.*, 2020; Selle *et al.*, 2020).

<i>In vitro</i> activity and/or successful in animal models	Clinical trials	Clinical application	
Auranofin Thuricin CD Nisin Acyldepsipeptide-1 Phenylimidazole-derivatives	Cadazolid Ridinilazole Surotomycin Ramoplanin LFF571 Ibezapolstat CRS3123 SMT19969	Fidaxomicin Vancomycin (Metronidazole)	„New“ antibiotics
	Fusidic acid Bacitracin Teicoplanin Rifampin Nitazoxanide Tigecycline	Rifaximin	Repurposed antibiotics
Ebselen Bafilomycin Quinacrine Methyl cholate Phloretin Ambroxol	Amoxapine Doxapram Trifluoperazine Monensin Aminacrine Amodiaquinine Prazosin	Actoxumab OraCAB PolyCAB MK-3415, MK-6072, & MK-3415A	Adjuvant therapy
		Bezlotoxumab	

Figure 1.5: Antibiotics and adjuvants for the therapy of *C. difficile* infections currently in development or in clinical use. Compounds in development are grouped depending on whether they have been tested in clinical trials or whether data are limited to *in vitro* and animal studies. The figure was created in Microsoft PowerPoint based on current literature cited above, e.g., Petrosillo *et al.*, 2018; Chaar and Feuerstadt, 2021; Monaghan *et al.*, 2021; Butler *et al.*, 2022.

Finally, fecal microbiota transplantations, bile acid-based therapeutics and secondary metabolites of probiotic bacteria represent promising approaches based on natural defense strategies (Shen *et al.*, 2017; Hui *et al.*, 2019; Pal *et al.*, 2021).

However, regardless of the increasing list of compounds under investigation, none of the compounds has made it to market until now (Butler *et al.*, 2022). In addition, several of them will likely fail at some point due to missing non-inferiority, emerging resistances or other reasons (Ullah *et al.*, 2020). Especially therapeutics designed to reduce toxin production and their cytotoxic effects, as well as pre- and probiotic therapies are currently not expected to develop into stand-alone therapeutics (McFarland, 2015; Stewart *et al.*, 2020). In this light, it is inevitable to continue the search for new antibiotics in order to constantly replenish the pool of available antibiotics against *C. difficile*.

1.3.2 Promising drug targets in *C. difficile*

There are two opposite approaches to find new antimicrobial compounds. On the one hand, large screening experiments can be used to identify compounds with significant activity against a pathogen, such as *C. difficile*. These compounds could then be critically assessed with regard to the suitability of their target structure and their selectivity *in vivo*. On the other hand, promising new drug targets might be derived from accumulating knowledge on essential metabolic pathways and network structure of *C. difficile*.

Indeed, several studies used a computational approach to identify possible drug targets in *C. difficile*. For instance, metabolic network construction of *C. difficile* strain 630 revealed 79 essential genes and 39 essential gene pairs, some of which were even found to be unique in the genome of *C. difficile* (Larocque *et al.*, 2014). Based on these potential target genes, potential inhibitors for 29 of the essential genes, such as enzymes of the fatty biosynthesis pathway (*fabF*, *fabH*, *fabZ* and *fabG*), genes coding for the isoprene biosynthesis (*ispA*, *ispH* and *ispF*), genes involved in peptidoglycan biosynthesis (*glmU* and *murD*), as well as some metabolic genes, such as *crt1*, *ntpA*, *ntpB*, *gapA*, *gapB*, *glyA*, *hpt*, *foID*, *fhs*, *upsS*, *accC*, and *adk*, were identified (Larocque *et al.*, 2014). Another *in silico* analysis of the proteome of *C. difficile* 630 revealed 155 putative drug targets and nine pathways of above-average importance. The homoserine dehydrogenase, the aspartate-semialdehyde dehydrogenase and the aspartokinase were pointed out as most promising antibiotic targets due to their shared function in several essential pathways (Lohani *et al.*, 2017). Additionally, two analyses of essential genes in *C. difficile* strain R20291 further revealed an essential role of several pathways, including the branched chain amino acid fermentation, alanine, aspartate and glutamate metabolism, glycolysis/gluconeogenesis, pyrimidine and pyruvate metabolism and the peptidoglycan biosynthesis (Ezhilarasan *et al.*,

Introduction

2013; Kashaf *et al.*, 2017). The gene *murG* was pointed out by Ezhilarasan *et al.* as the most promising target (Ezhilarasan *et al.*, 2013). Likewise, an insertion mutant library analysis revealed 404 essential genes in *C. difficile* R20291, as none of the 70,000 insertion mutants were observed in these 404 genes. These genes were involved in DNA metabolism, transcription and translation as well as tRNA, fatty acid and folate or peptidoglycan biosynthesis (Dembek *et al.*, 2015).

These data consistently point to an essential role of fatty acid biosynthesis, amino acid metabolism and peptidoglycan biosynthesis in *C. difficile* as these pathways were repeatedly identified in these studies. However, although all these genes have in common that they are vulnerable points in the metabolism of *C. difficile*, the major challenge in the therapy of *C. difficile* infections is to find a drug, which is selective for *C. difficile*. To meet this demand, a drug must have a target, which is either unique to *C. difficile* or of substantially greater importance for *C. difficile* compared to other members of the intestinal microbiota. As a result, highly conserved enzymes and pathways might be rather unfavorable targets, while the catabolic or biosynthetic pathways, which are preferred by *C. difficile*, are favorable targets.

For instance, the proline reductase and the Wood-Ljungdahl pathway are assumed to be crucial for the competitive fitness of *C. difficile* as outlined above. However, they are rarely found in other bacteria (Jackson *et al.*, 2006; Gencic and Grahame, 2020). Additionally, the *de novo* biosynthesis pathway for the vitamin thiamine is considered an interesting antibiotic target due to the importance of the vitamin for *C. difficile* but a lack of a transport system for the uptake of this vitamin in the genome of *C. difficile* (Bousis *et al.*, 2019). In contrast, about 50% of all bacteria are able to synthesize the rare, essential nucleotide queuosine *de novo*, whereas *C. difficile* relies on the uptake of queuosine or its precursors from the environment via a specific transport system of the energy-coupling factor (Ecf)-transporter family (Yuan *et al.*, 2019). Furthermore, the tricarboxylic acid (TCA) cycle enzyme fumarate hydratase is an ubiquitous enzyme, which, however, occurs in nature as isoenzymes, of which *C. difficile* has a less common version (Woods *et al.*, 1988). Whereas most bacteria solely utilize an oxygen-stable version of the fumarate hydratase or encode for both enzyme types, some bacteria, such as *C. difficile*, only possess an ancient oxygen-sensitive version of the fumarate hydratase equipped with an iron-sulfur cluster (Lu and Imlay, 2021). The lack of sequence homology between both enzyme types makes the fumarate hydratase of *C. difficile* a selective antibiotic target.

Most interestingly, also the *fab* pathway, which encodes the bacterial type II fatty acid biosynthesis and which has been pointed out as highly essential by the metabolic network construction studies reviewed above, comprises a rare version of an important enzyme that

is considered as an Achilles' heel in *C. difficile*'s metabolism (Jones *et al.*, 2019; Marreddy *et al.*, 2019). Although the *fab* pathway is ubiquitous and relatively conserved in the bacterial world, the enoyl-acyl carrier protein of *C. difficile* is, as its fumarate hydratase, a less common form of four isoenzymes, FabI, FabK, FabL and FabV (Jones *et al.*, 2019; Marreddy *et al.*, 2019). While some bacteria, such as *E. faecalis* and some *Bacteroides*, *Enterobacterium* and *Lactobacillus* species, have two isoenzymes, many other bacteria have only one enzyme. However, most species, such as *E. faecium*, *Staphylococcus* and *Propionibacterium* species, utilize either FabI, FabL or FabV, which are structurally related and similarly inhibited by antibiotics, such as triclosan (Rana *et al.*, 2020). In contrast, a minority of bacterial genera, such as *C. difficile*, *Faecalibacterium*, *Streptococcus* and *Peptostreptococcus* species, utilize the less common isoenzyme FabK (Heath and Rock, 2000; Marrakchi *et al.*, 2003). Interestingly, *C. difficile* not only encodes a less common isoenzyme of the enoyl-acyl carrier protein, but additionally uses a less common transcriptional regulator, FabR, for the regulation of fatty acid biosynthesis. Whereas fatty acid biosynthesis in other bacteria is regulated by FabT, which allows exogenously supplied fatty acids to bypass inhibition of the *fab* pathway, FabR is prone to feedback inhibition by exogenous fatty acids resulting in additional repression of the *fab* operon in the presence of exogenously supplied fatty acids (Marreddy *et al.*, 2019).

In conclusion, all these findings offer the opportunity to discover compounds with powerful and selective activity against *C. difficile*, e.g., by targeting the fatty acid biosynthesis pathway of *C. difficile* or targeting ancient labile enzymes as the fumarate hydratase, while sparing most other members from the intestinal microbial community.

1.3.3 Screening of compounds with antimicrobial activity against *C. difficile*

Nevertheless, compounds directed to these identified target structures need to be identified. For this reason, screening approaches were developed to evaluate natural compounds, modified derivatives as well as synthetic compounds for their activity against *C. difficile*.

For example, Thanissery *et al.* (2018) established a screening pipeline to screen a palette of 2-aminoimidazole molecules, which were already active against other bacterial pathogens such as *S. aureus*, *Acinetobacter baumannii* and *Pseudomonas aeruginosa*. The authors not only tested the activity of the compounds against *C. difficile* but also included a number of other commensal bacteria in the screening panel. Moreover, toxin and sporulation assays were implemented downstream of the pipeline to screen for compounds with negative impact on toxin synthesis and sporulation in *C. difficile*. Ultimately, three of the eleven tested compounds were selected for further analysis (Thanissery *et al.*, 2018). Similarly, Pal *et al.* (2021) identified three promising compounds when screening the

Introduction

commercial AnalytiCon NATx library. The identified compounds not only showed good activity against a range of *C. difficile* strains but additionally did not affect growth of other members of the intestinal microbiota and did not show a cytotoxic effect on cell lines (Pal *et al.*, 2021).

Natural products, such as plant-derived antimicrobials, have been screened for their suitability as anti-*C. difficile* drugs, although their potential as stand-alone drugs is low (Roshan *et al.*, 2018; Schnizlein *et al.*, 2020; Tortajada-Girbés *et al.*, 2021). Furthermore, other groups have screened natural products, e.g., food ingredients, such as garlic, ginger and cinnamon, for their antibacterial activity in *C. difficile* (Roshan *et al.*, 2017).

Similarly, selected natural products provided by the Helmholtz Institute for Pharmaceutical Research (HIPS) in Saarbrücken were tested for their activity against *C. difficile* 630 Δ *erm*. To this end, three compounds were identified, which substantially delayed the growth of *C. difficile* 630 Δ *erm* (Bachelor's thesis (BT) Anna-Lena Wolmeringer, 2017). These compounds were subsequently chosen for further characterization and evaluation of their potential role in the lifecycle of *C. difficile*.

Chlorotonils

The first compound, chlorotonil A (ChA), is a secondary metabolite isolated from the myxobacterium *Sorangium cellulosum* So ce1525 (Figure 1.6) (Gerth *et al.*, 2008). Chlorotonil A has previously been shown antimicrobial activity against a number of relevant Gram-positive bacterial pathogens, such as *S. aureus* and *E. faecalis*, as well as anti-protozoal activity against *Plasmodium falciparum* (Held *et al.*, 2014; Jungmann *et al.*, 2015). Due to its most likely novel, although unknown, mode-of-action, chlorotonil A is considered a promising lead structure for antibiotic development. Consequently, a number of derivatives of chlorotonil A and its natural derivative ChB were synthesized, such as the epoxide derivative ChB1-Epo2 (Hofer *et al.*, 2022). The selectivity of chlorotonils for Gram-positive bacteria and the comparatively high bioavailability of chlorotonil A in the feces of rats and mice (Hofer *et al.*, 2022), led to the decision to test chlorotonil A and its derivatives for their antimicrobial activity against *C. difficile* 630 Δ erm. After the activity of chlorotonil A against *C. difficile* had been demonstrated *in vitro* (Anna-Lena Wolmeringer, 2017), the effect of chlorotonil A therapy on the complex intestinal microbiota of mice and piglets was studied *in vivo*. Thereby, chlorotonil A was found to be relatively selective for close relatives of *C. difficile*, supporting the hypothesis that chlorotonils might be promising antibiotic for the treatment of *C. difficile* infections (Bublitz *et al.*, in revision).

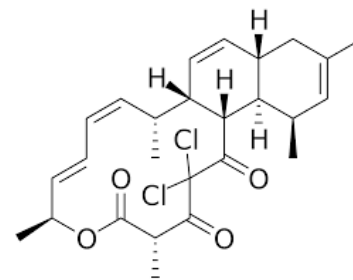


Figure 1.6: Chemical structure of chlorotonil A.
(Provided by the HIPS, Saarbrücken).

Introduction

Myxopyronins

Myxopyronins are alpha-pyrone antibiotics produced by *Myxococcus fulvus* fMx50 (Figure 1.7) (Irschik *et al.*, 1983). Alpha-pyrone antibiotics, such as myxopyronin A and B, coralopyronin and ripostatin, bind to the switch region of the bacterial RNA polymerase, thereby preventing the opening of the DNA:RNA clamp and, in turn, blocking the transcriptional process (Mukhopadhyay *et al.*, 2008; Srivastava *et al.*, 2011). Myxopyronin A/B as well as the other two compounds showed promising activity against clinically relevant bacterial species, such as *S. aureus*, *E. faecalis*, *S. pneumoniae*, and *Haemophilus influenzae* as well as *C. difficile* (Srivastava *et al.*, 2011). In addition, mutations conferring resistance to myxopyronins in *S. aureus* were shown to cause substantial fitness costs compared to mutations conferring rifampin resistance (Srivastava *et al.*, 2012). In consequence, development and dissemination of resistance to myxopyronins are expected to occur at lower rates than for rifamycins. Crystallography further provided insights into the exact binding site of myxopyronin and related compounds and showed that their binding is in close proximity, although not overlapping, to the binding site of fidaxomicin, which is likewise a RNA polymerase switch region inhibitor (Mukhopadhyay *et al.*, 2008; Srivastava *et al.*, 2011). Fidaxomicin blocks transcription at an earlier stage than rifamycins (Babakhani *et al.*, 2014). Interestingly, the early inhibition of the transcriptional process and the concomitant inability of the cell to respond to the antibiotic are discussed as the underlying reason for fidaxomicin's ability to reduce toxin production and spore formation in *C. difficile* (Louie *et al.*, 2012; Aldape *et al.*, 2017). Although differences between the mode-of-action of fidaxomicin and other switch region inhibitors have been demonstrated, the close proximity of their binding sites leads to the hypothesis that other RNA polymerase switch region inhibitors, such as myxopyronin A/B and coralopyronin, might be equally promising antibiotic candidates for the treatment of *C. difficile* infections. Additionally, the missing overlap between the binding sites potentially is expected to protect against cross-resistance between these antibiotics (Artsimovitch *et al.*, 2012). With the detailed characterization of the myxopyronin gene cluster in *M. fulvus* Mx f50 and the introduction of heterologous expression systems enabling high-yield production of myxopyronins (Sucipto *et al.*, 2017), myxopyronins have finally become available in sufficient quantity and quality, which further encourages the evaluation of myxopyronins against *C. difficile*.

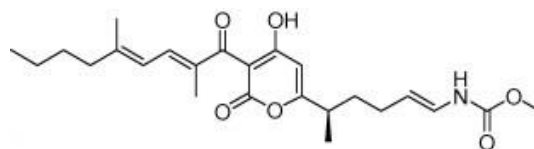


Figure 1.7: Chemical structure of myxopyronin B.
(Lira *et al.*, 2007)

Chelocardins

The atypical tetracycline chelocardin (CHD) has broad-spectrum antibiotic activity against a variety of important bacterial pathogens, including Gram-positive bacteria such as *S. aureus* and *E. faecalis*, but also several Gram-negative bacteria such as the ESKAPE pathogens.

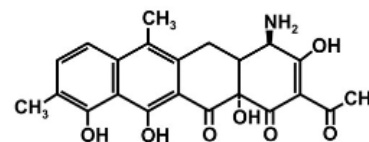


Figure 1.8: Chemical structure of amidochelocardin. (Provided by Jennifer Herrmann, HIPS, Saarbrücken).

Chelocardin, a natural product of the actinomycete *Amycolatopsis sulphurea*, is composed of four cyclic rings, which are typical for tetracyclines (Figure 1.8) (Mitscher *et al.*, 1970). However, in contrast to conventional tetracyclines, such as tetracycline, chlortetracycline and doxycycline, atypical tetracyclines, such as anhydrochlorotetracycline and chelocardin, do not primarily target protein biosynthesis by binding to the 30S subunit of the ribosome and are consequently not inhibited by classical tetracycline resistance determinants (Oliva and Chopra, 1992; Chopra, 1994; Stepanek *et al.*, 2016). In contrast, there is increasing evidence that chelocardin primarily acts on the bacterial membrane, whereas its derivative amidochelocardin, also known as 2-carboxamido-2-deacetyl-chelocardin (CDCHD), was even shown to exclusively kill bacteria via a membrane-directed mode-of-action (Oliva *et al.*, 1992; Stepanek *et al.*, 2016; Senges *et al.*, 2020). Moreover, most common antibiotic efflux systems do not protect bacteria against chelocardin (Hennesen *et al.*, 2020). Amidochelocardin is even superior compared to its lead compound due to its improved activity, e.g. by also inhibiting the growth of important ESKAPE pathogens and escaping efflux of the *Klebsiella* spp. ArcAB efflux system (Hennesen *et al.*, 2020). Despite first reports on the antibacterial activity of chelocardin from the 1960s and 70s (Mitscher *et al.*, 1970; Proctor *et al.*, 1978; Oliver and Sinclair, 2021) and a first successful clinical trial evaluating chelocardin as treatment option for urinary tract infections in 1977 (Molnar *et al.*, 1977), chelocardins had not been in focus for decades. In the view of growing urgency to find new antibiotics, the discovery of the biosynthetic gene cluster for chelocardin biosynthesis in the genome of *A. sulphurea* (Lukežič *et al.*, 2013) and the substantial improvements in biotechnological engineering led to the revival of chelocardins as future antibiotics. Heterologous expression and engineering of chelocardin finally provided new, optimized derivatives (Lešnik *et al.*, 2015; Lukežič *et al.*, 2019; Grandclaudon *et al.*, 2020; Lukežič *et al.*, 2020). Therefore, chelocardins, notably amidochelocardin, are highly promising broad-spectrum antibiotics anticipated to become important for the therapy of urinary tract infections.

2. Aim of the thesis

The central aim of this thesis was to characterize the antimicrobial activity of three natural product classes, namely the chlorotonils, myxopyronins and chelocardins, against anaerobic bacteria, in particular *C. difficile*. The work has been part of a joint research project performed in collaboration with the Friedrich-Loeffler Institute (Institute of Molecular Pathogenesis led by Prof. Thilo Fuchs, Jena, Germany), the Helmholtz Institute for Pharmaceutical Research (Department of Microbial Natural Products led by Prof. Rolf Müller, Saarbrücken, Germany) and the Helmholtz Institute for Infection Research (Department of Microbial Immune Regulation led by Prof. Till Strowig, Braunschweig, Germany).

In this thesis, the activity spectrum and the systemic effects of the natural product classes under anaerobic conditions were investigated in more detail. The first part of the study addressed the usefulness of chlorotonil A and myxopyronin B as lead structures for the development of new antibiotics for a selective therapy of *C. difficile* infections. The second part, in contrast, aimed at evaluating the potential risk for patients receiving the broad-spectrum antibiotics chelocardin or amidochelocardin to develop a *C. difficile* infection.

For this purpose, the susceptibility of several *C. difficile* isolates and other anaerobic bacterial species to the three compounds was determined. Next, the proteome signature of *C. difficile* 630 to all three compound classes was analyzed by liquid chromatography (LC)- tandem mass spectrometry (MS/MS). Finally, individual downstream experiments were performed to verify and to pursue hypotheses derived from the omics experiments to understand how *C. difficile* responds to a particular compound.

3. Results

To get an overview of the susceptibility of *C. difficile* to chlorotonils, chelocardins and myxopyronin B, all compounds were initially screened for their activity against a panel of five *C. difficile* strains in serial broth dilution assays. The panel of strains included isolates belonging to five different ribotypes, three of human and two of porcine origin, including the well-characterized strains 630 and R20291. In addition, all compounds were evaluated for their activity against a panel of other selected anaerobic bacteria to test for their potential selectivity for *C. difficile*. In the following, the stress response of *C. difficile* 630 to all three compounds and, when necessary, competitor antibiotics, was analyzed in detail on proteome level using a state-of-the-art LC-MS/MS approach. Eventually, individual assays and downstream experiments were performed with each respective compound to confirm the hypotheses derived from the proteomics stress signatures (Figure 3.0).

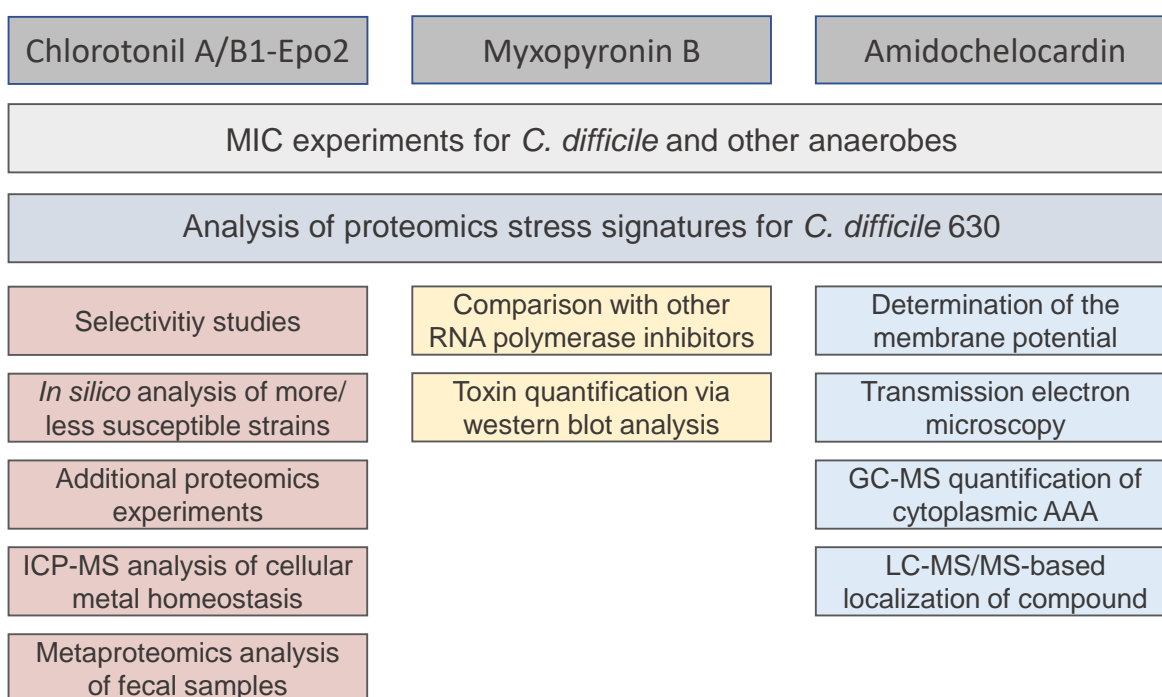


Figure 3.0: Overview of experiments performed to evaluate and characterize chlorotonils, myxopyronins and chelocardins with special focus on their activity and systemic effects against anaerobic bacteria, particularly *C. difficile*. MIC: minimal inhibitory concentrations, ICP-MS: inductively-coupled plasma-mass spectrometry, AAA: aromatic amino acids, GC-MS: Gas chromatography-mass spectrometry, LC-MS/MS: Liquid chromatography-tandem mass spectrometry.

Results

3.1 Chlorotoniol A and its derivatives selectively inhibit growth of *C. difficile* and close relatives

The first and largest part of this thesis aimed at the evaluation of chlorotoniols as possible new treatment option for *C. difficile* infections. A limited activity of chlorotoniols against Gram-negative bacteria and its previously demonstrated ability to inhibit the growth of *C. difficile* 630 Δ *erm* led to hypothesize that chlorotoniols might be promising for the therapy of *C. difficile* infections (Held *et al.*, 2014; Jungmann *et al.*, 2015; Anna-Lena Wolmeringer, BT, 2017). Therefore, the susceptibility of a range of *C. difficile* strains and selected other anaerobic bacteria to ChA and its derivatives was analyzed under *in vitro* conditions. Subsequently, the systemic effects of chlorotoniol-treatment on *C. difficile* and *Terrisporobacter glycolicus* under *in vitro* conditions were analyzed by LC-MS/MS. Moreover, a metaproteomics approach was applied to analyze the effect of chlorotoniols on the intestinal microbiota of piglets.

Parts of the results of this study have been included into two manuscripts and are reviewed in more detail in the following section.

Bublitz A., Brauer M.*, Wagner S.*, Hofer W., Müsken M., Deschner F., Lesker T.R., Neumann-Schaal M., Nübel U., Bartel J., Zühlke D., Bernecker S., Jansen R., Stadler M., Sievers S., Riedel K., Herrmann J., Müller R., Fuchs T.M., Strowig T. Spraying of the microbiota by the natural product antibiotic chlorotoniol A prevents relapsing *Clostridioides difficile* infection (working title). *Cell Host Microbe* (in revision)

Wagner S., Brauer M., ..., Fuchs T.M. Effects of antibiotics on the functionality of the swine gut microbiota determined by a MetaOmics approach (working title).
(in preparation)

* contributed equally

3.1.1 Susceptibility of *C. difficile* and other intestinal species to chlorotonils

As a starting point, the susceptibility of selected *C. difficile* isolates and intestinal commensals to ChA and its derivatives were studied to verify the activity of the compound class against anaerobic bacteria and to test for a possible selectivity of the compound for *C. difficile*.

3.1.1.1 Susceptibility of anaerobes to chlorotonils according to serial broth dilution assays

First, classical serial broth dilution assays were performed to analyze the minimal inhibitory concentrations of ChA and some of its derivatives against a panel of *C. difficile* strains. The five selected *C. difficile* strains were inhibited by either 3.2 µg/ml or 6.4 µg/ml ChA and ChB with the exception of strain 1780, which was not inhibited by ChB at the highest concentration tested (6.4 µg/ml) (Table 3.1.1). The other ChA derivatives inhibited all *C. difficile* strains at lower concentrations ranging between 0.1 µg/ml and 0.8 µg/ml, respectively (Table 3.1.1).

Table 3.1.1: Minimal inhibitory concentrations of chlorotonil A (ChA) and B (ChB) and selected derivatives of ChA against five different *C. difficile* strains in µg/ml according to serial broth dilution assays after 24 h of growth in BHIS. n ≥ 3.

	630	1780	R20291	rt126	rt78
ChA	6.4	6.4	3.2	3.2	6.4
ChA-Epo2	0.1	0.8	0.2	0.4	0.8
ChA-Epo2-Cl	0.2	0.4	0.2	0.2	0.2
ChA-Epo2-ONO2	0.4	0.8	0.4	0.4	0.4
ChB	6.4	> 6.4	3.2	6.4	6.4

Over the course of the project, a ChB derivative with improved solubility and stability, ChB1-Epo2, became available (Hofer *et al.*, 2022). Subsequently, serial broth dilution assays were repeated for selected *C. difficile* strains and this time vancomycin was included as a reference antibiotic. All *C. difficile* strains were inhibited by 6.4 µg/ml of ChA and 1.6 µg/ml or 0.8 µg/ml ChB1-Epo2 (Table 3.1.2). Vancomycin inhibited the growth of all strains at concentrations of either 2 µg/ml or 1 µg/ml (Table 3.1.2).

Results

Table 3.1.2: Minimal inhibitory concentrations of chlorotoniol A (ChA), its derivative ChB1-Epo2 and vancomycin against four different *C. difficile* strains in µg/ml according to serial broth dilution assays after 24 h of growth in BHIS. n ≥ 3.

	630	1780	R20291	VPI 10463
ChA	6.4	6.4	6.4	6.4
ChB1-Epo2	1.6	1.6	0.8	0.8
Vancomycin	2	2	1	1

Next, the susceptibility of commensal anaerobic bacteria to ChA and its derivative ChB1-Epo2 were determined to test for differential susceptibility between *C. difficile* and other members of the intestinal microbiota. The minimal inhibitory concentrations obtained for ChA ranged from below 0.0125 µg/ml for *Clostridium scindens* to above 6.4 µg/ml for *Bacteroides thetaiotaomicron*. ChB1-Epo2 inhibited the growth of tested strains at concentrations of 0.2 µg/ml to 6.4 µg/ml. Interestingly, the minimal inhibitory concentrations of ChB1-Epo2 were lower compared to ChA for some strains, namely *Terrisporobacter sp.*, *Bacteroides fragilis* and *B. thetaiotaomicron*, and higher for *Lactobacillus casei*, *Bifidobacterium longum*, *Clostridium scindens* and *Terrisporobacter glycolicus* (Table 3.1.3).

Table 3.1.3: Minimal inhibitory concentrations of chlorotoniol A (ChA) and its derivative ChB1-Epo2 against seven commensal intestinal anaerobes in µg/ml according to serial broth dilution assays after 24 h of growth in BHIS. n ≥ 3.

	<i>L. casei</i>	<i>B. longum</i>	<i>C. scindens</i>	<i>Terrisp sp.</i>	<i>T. glycolicus</i>	<i>B. fragilis</i>	<i>B. theta</i>
ChA	0.2	1.6	< 0.0125	0.1	0.2	6.4	> 6.4
ChB1-Epo2	0.8	6.4	0.05	0.2	1.6	1.6	6.4

Based on the higher susceptibility of *C. difficile* strains to ChB1-Epo2 in the serial broth dilution experiments and the improved solubility of ChB1-Epo2, the following experiments were mainly conducted with ChB1-Epo2 only.

3.1.1.2 Exponentially growing bacteria are more susceptible to chlorotonils

Interestingly, *C. difficile* 630 was significantly more sensitive to ChA and its derivative ChB1-Epo2 when the strain was stressed with serial dilutions of the compounds during exponential growth (Figure 3.1.1). While the strain tolerated up to 6.4 µg/ml in the serial broth dilution assays (Table 3.1.2), 6.25 ng/ml of ChA and ChB1-Epo2 were enough to temporarily reduce the optical density of exponentially growing cultures cultivated in chemical defined medium (Figure 3.1.1). Control experiments could show that this effect was independent from the different media that were used for serial broth dilution assays and growth experiments (Suppl. figure S1, suppl. table S1).

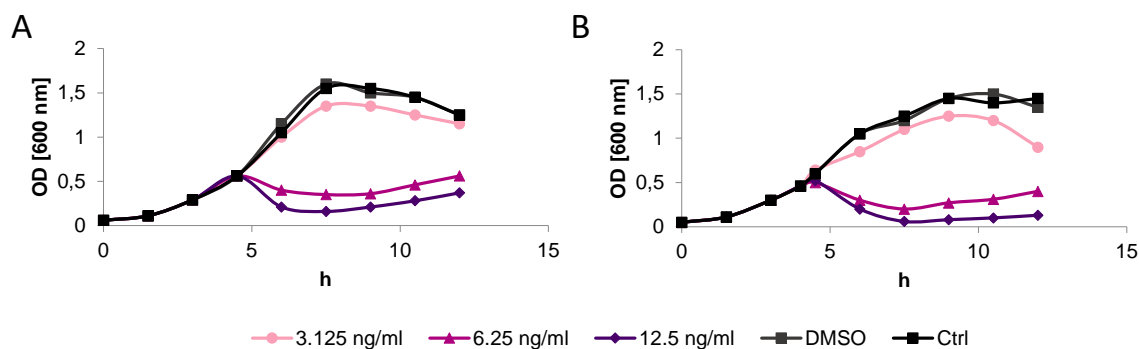


Figure 3.1.1: The growth of *C. difficile* is inhibited by low concentrations of chlorotonils. *C. difficile* 630 was grown to mid-exponential phase in CDMM and was treated with (A) chlorotonil A or (B) its derivative ChB1-Epo2. Exemplarily, selected growth curves for ChA and ChB1-Epo2 representing $n \geq 3$ biological replicates are shown.

To follow up on this interesting finding, the susceptibility of different *C. difficile* and commensal strains was re-analyzed in growth inhibition experiments. Instead of endpoint measurements performed in 96-well plates, exponentially growing bacteria were treated with four-fold serial dilutions of ChB1-Epo2. Subsequently, the growth rates of treated cells were compared to the growth rate of untreated cells. In contrast to the results from the serial broth dilution assays, the data revealed higher susceptibility of *C. difficile* and some close relatives to ChB1-Epo2 compared to other unrelated anaerobic bacteria (Figure 3.1.2). The non-clostridial species *B. longum*, *Enterococcus faecalis* and *L. casei* as well as a member of the Clostridia, namely *Intestinibacter bartlettii*, showed growth rates equal or higher than 25% compared to the control even with the highest concentration tested. In contrast, *C. difficile* and related clostridial species as well as *C. scindens* were highly sensitive and their growth rates were reduced to less than 25% compared to the controls for 25 ng/ml and higher concentrations of ChB1-Epo2 (Figure 3.1.2). *B. fragilis* and *B. thetaiotaomicron* were tested in Brain heart infusion (BHI) broth to allow comparability to the other species and supplemented BHI (BHIS) because both strains require heme and vitamin K1 for optimal growth. Although both strains grew significantly better in BHIS, they were inhibited by 1.6 $\mu\text{g/ml}$ and 400 ng/ml ChB1-Epo2 in both media. However, they were less inhibited by lower concentrations of ChB1-Epo2 compared to the clostridial species (Figure 3.1.2).

Results

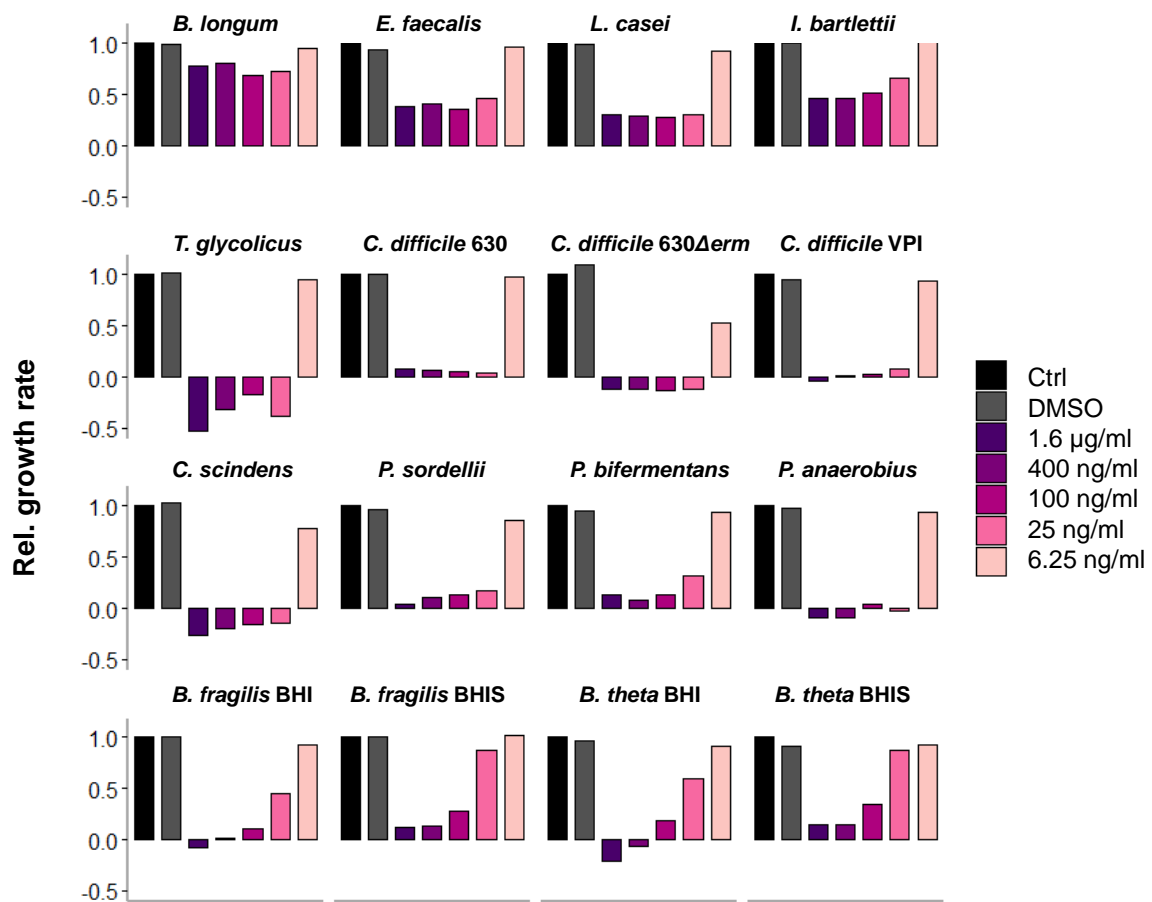


Figure 3.1.2: Relative growth rates of selected anaerobic bacteria after treatment with increasing concentrations of ChB1-Epo2. Growth rates of selected anaerobic bacteria treated with five different concentrations of ChB1-Epo2 or DMSO only in the mid-exponential phase were calculated and are depicted relative to the growth rates of the untreated cells. At least two biological replicates were performed. $n \geq 2$.

Three additional *C. difficile* strains were likewise substantially inhibited by low concentrations of ChB1-Epo2, although the porcine isolates rt78 and rt126 were slightly less susceptible compared to the other *C. difficile* strains (Figure 3.1.3).

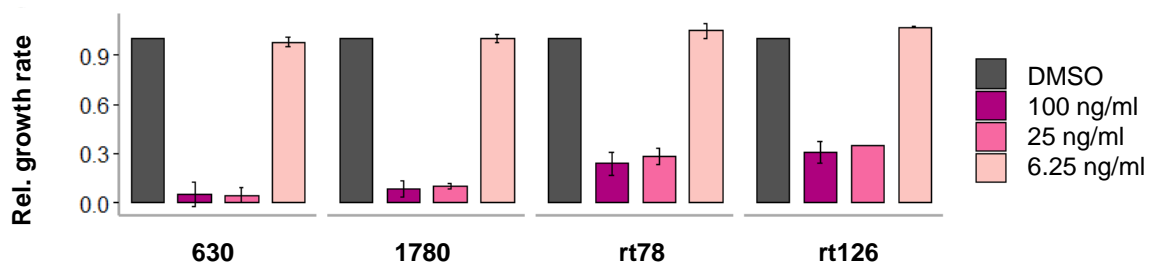


Figure 3.1.3: Relative growth rates of four *C. difficile* strains after treatment with increasing concentrations of ChB1-Epo2. Growth rates of selected *C. difficile* strains treated with 3 different concentrations of ChB1-Epo2 in the mid-exponential phase were calculated and are depicted relative to the growth rates of DMSO-treated cells. At least two biological replicates were performed. $n \geq 2$.

3.1.2 The protein inventory of bacteria with higher susceptibility to chlorotonils

It can be assumed that the increased sensitivity to chlorotonils of some species is caused by the presence or absence of a cellular structure or metabolic feature. Although there is a trend in the growth inhibition assay data that obligate anaerobes are more susceptible than facultative anaerobes, not all anaerobes are equally susceptible. To identify such a trait causative for increased susceptibility, the theoretical protein inventory of more susceptible and less susceptible strains was compared.

3.1.2.1 *In silico* analysis identifies differences between differentially susceptible bacteria in the amino acid and cofactor metabolism

To increase the reliability of the analysis, additional strains tested elsewhere in a 96-well format-based screening for their susceptibility to ChA and ChB1-Epo2 (Arne Bublitz, HZI, Braunschweig, **Suppl. figure S2**) were included. Briefly, the theoretical protein repertoire of 17 selected bacterial strains was compared using BLASTp (Camacho *et al.*, 2009). The group of bacteria with higher susceptibility comprised *C. difficile*, some other *Peptostreptococcaceae* and three other commensals, namely *Extibacter muris*, *C. scindens* and *Flavonifractor plautii*. In contrast, the group with low susceptibility to chlorotonils comprised the Gram-negative species *B. fragilis*, *B. thetaiotaomicron*, and *Akkermansia muciniphila* and the Gram-positive species *B. longum*, *Limosilactobacillus reuteri*, and *E. faecalis* (see **Suppl. figure S2**). The alignments were then reviewed for proteins, which were present in at least six more susceptible species than less susceptible species, and *vice versa*. Proteins, which were characteristic for bacteria with higher susceptibility, comprised an above average proportion of proteins belonging, e.g., to the functional categories “Regulation and signaling”, “Sporulation and germination”, “Motility and chemotaxis”, “Cofactors and vitamins”, “Amino acid fermentation”, and “Carbohydrate metabolism” based on the functional classification of the *C. difficile* homologs (**Figure 3.1.4, suppl. table S2**).

Results

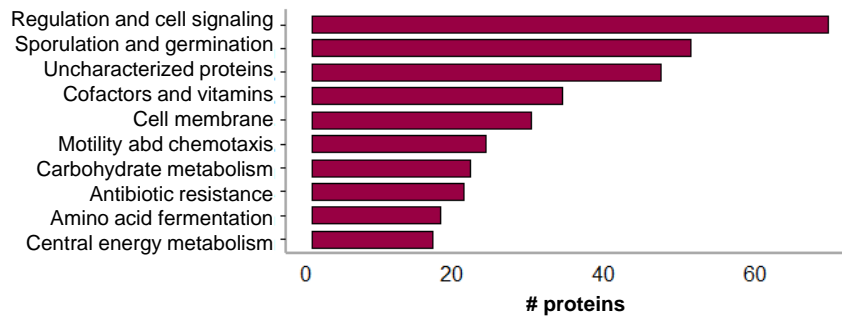


Figure 3.1.4: Homologous proteins enriched in the group of bacteria with higher susceptibility to chlorotoniils. A comparison of the theoretical protein repertoire of bacteria with higher or lower susceptibility to chlorotoniils using BLASTp revealed a number of proteins from different functional groups, which were present in at least six more strains with higher susceptibility than lower susceptibility. The ten functional categories comprising the highest number of homologous proteins in chlorotoniil-susceptible species are displayed.

A more detailed analysis of the proteins and their respective pathways revealed that Stickland fermentation pathways were enriched in the group of bacteria with higher susceptibility to chlorotoniils although homologous enzymes of most pathways were also found in the group of less susceptible bacteria (Suppl. table S2). Moreover, subunits of the selenium-dependent proline and glycine reductase were exclusively found in the group of bacteria with higher susceptibility (Figure 3.1.5). All species from the group with higher susceptibility are at least equipped with the glycine reductase with the exception of *F. plautii*. Similarly, proteins belonging to the cobalt-dependent cobalamin biosynthesis and proteins for cobalt acquisition were enriched in the group of bacteria with higher susceptibility, whereas only *B. fragilis* and *L. reuteri* had some more homologous enzymes (Figure 3.1.5, suppl. table S2).

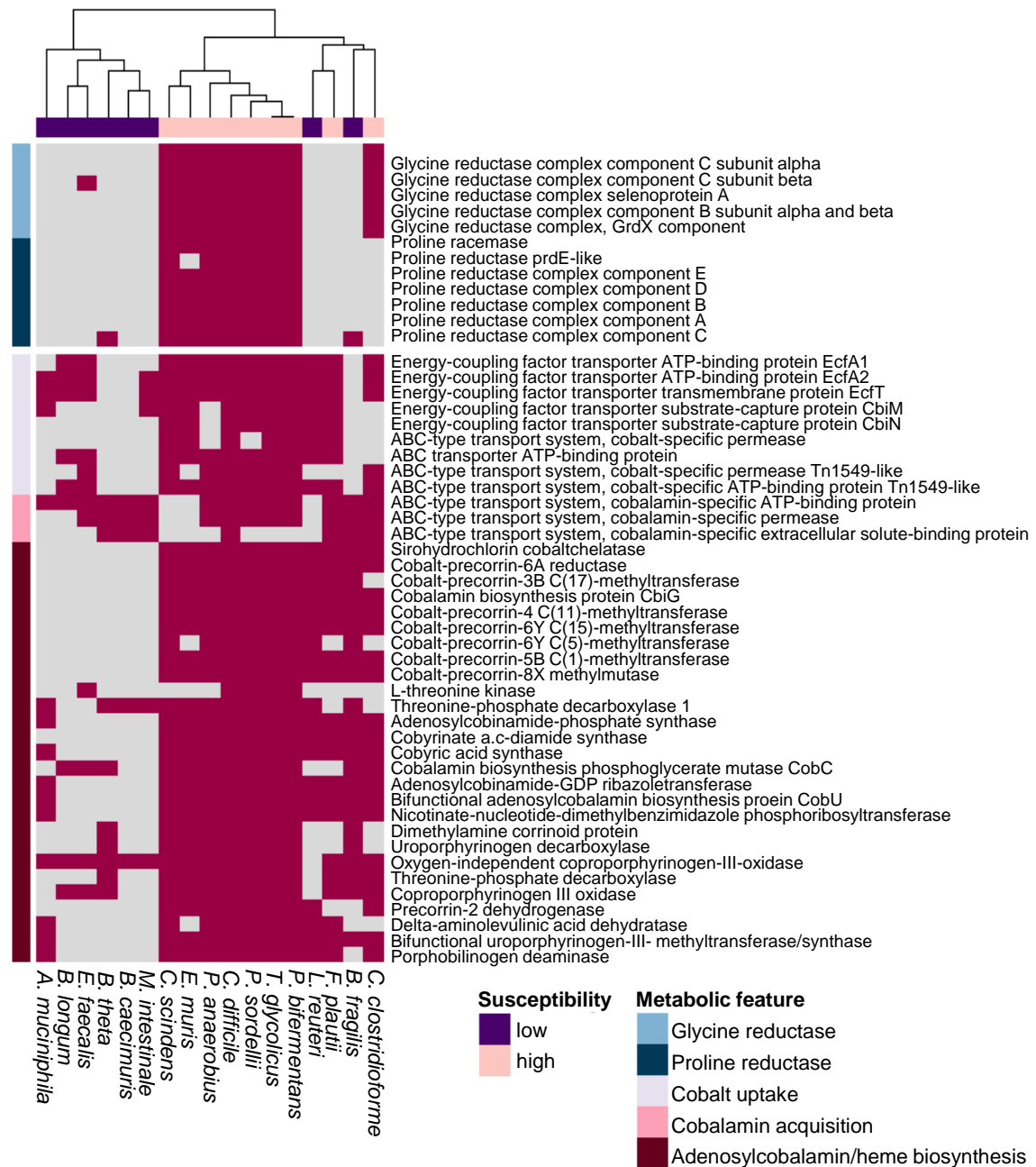


Figure 3.1.5: Presence of the selenoenzymes, proline and glycine reductase, and enzymes for cobalamin biosynthesis is correlated with higher susceptibility to chlorotonils. Based on a comparative whole proteome BLASTp analyses, the multi-enzyme complexes of the proline and glycine reductase were identified as characteristic for a panel of bacterial species with higher susceptibility to chlorotonils. Similarly, cobalamin biosynthesis proteins were enriched in the respective species with higher susceptibility to chlorotonils. Presence of a respective protein in the proteome of the analyzed species is indicated by magenta color. If no homologs could be identified, the putative absence is indicated by grey color. Column annotations show whether a strain revealed higher (rose) or lower (purple) susceptibility. Row annotations show the affiliation of the proteins to the selected metabolic feature.

Results

3.1.2.2 Bacteria with higher susceptibility to chlorotonils feature a specific seleno- and cobalamin metabolism

Based on the results of section **3.1.2.1**, the distribution of the proline and glycine reductase and of the cobalamin biosynthesis enzymes was examined in more detail. In addition, the distribution of enzymes involved in selenocompound metabolism required for the synthesis of the selenium-dependent proline/glycine reductase and of cobalamin-dependent enzymes were examined using publicly available datasets.

Selenium metabolism

The proline and glycine reductases are selenium-dependent multi-enzyme complexes. Their selenocysteine-containing subunits PrdB and GrdB are primarily found in Firmicutes species according to the InterPro database (data obtained from InterPro 09.05.2022) (**Figure 3.1.6 A**). More than 50% of the species for which PrdB and GrdB subunits can be found in the database are Clostridia species. In addition, a few homologs are assigned to the Actinobacteria or Proteobacteria (**Figure 3.1.6 A, suppl. table S3**). Since not all bacteria can synthesize the rare amino acid selenocysteine *de novo* (Zhang *et al.*, 2006; Peng *et al.*, 2016), the question was addressed whether the enzymes involved in selenium metabolism are likewise differentially abundant between species with higher or lower susceptibility to chlorotonils. To this end, a dataset published by Peng *et al.* (2016), who recently analyzed the distribution of selenocompound metabolism based on the analysis of 5,200 sequenced bacterial genomes, was used to analyze selenocompound metabolism in the selected species (Peng *et al.*, 2016). Thirteen of the seventeen bacterial strains analyzed in section **3.1.2.1** or closely related strains of the respective species were enclosed in the datasets of Peng *et al.* (2016). With the exception of *E. faecalis*, genes for the selenocompound producing enzymes were exclusively found in the genomes of bacteria with higher susceptibility to chlorotonils (**Figure 3.1.6 B**). All representatives of the bacteria with higher susceptibility are equipped with the genes encoding for the enzymes required for selenocysteine (Sec) synthesis (*selD*, *selA*, *selB*) and most of them also encode for the enzymes required for synthesis of the selenocofactor (Se cofactor) (*yqeB*, *yqeC*). Some species, including *C. difficile* and *T. glycolicus* are further equipped with *ybbB* encoding for the synthase of the rare tRNA base 5-methylaminomethyl-2-selenouridine (SeU) (**Figure 3.1.6 B**). In line with this, genes encoding for selenoenzymes, such as the formate dehydrogenase, the glycine reductase, and the heterodisulfide reductase, were exclusively found in the genomes of bacteria which also encoded for the respective selenocompound synthesis enzymes (**Figure 3.1.6 B**). No genes encoding for selenoenzymes could be identified in the genome of *E. faecalis*, although enzymes for selenocompound synthesis were predicted in its genome (**Figure 3.1.6 B**) (Zhang *et al.*, 2006; Peng *et al.*, 2016).

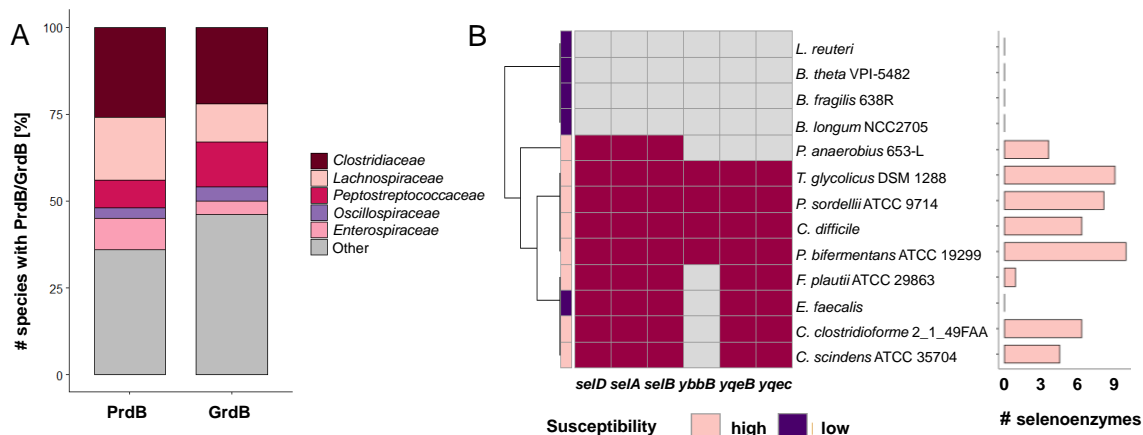


Figure 3.1.6: Differential distribution of selenocompound metabolism between bacteria with higher and lower susceptibility to chlorotonils. (A) Taxonomic distribution of the proline and glycine reductase subunits PrdB and GrdB according to sequences deposited to Uniprot. **(B)** Three different seleno-compounds are known thus far and are synthesized by SelD, SelA and SelB (Selenocysteine), YqeB and YqeC (selenocofactor) and YbbB (5-methylaminomethyl-2-selenouridine). Presence of the respective genes in the genome of the analyzed species is given by magenta color. If no homologs could be identified, the putative absence is indicated by grey color. Row annotations show whether a strain revealed higher (rose) or lower (purple) susceptibility to chlorotonils. The number of genes predicted to encode for selenoenzymes is given on the right.

Cobalamin metabolism

Similarly, Shelton *et al.* (2019) recently investigated bacterial cobalamin metabolism using genome sequences of 11,436 species. According to this analysis, genes of the *de novo* cobalamin biosynthesis were indeed mainly found in the genomes of commensals with higher susceptibility to chlorotonils (Figure 3.1.7 A). Moreover, the representatives *B. fragilis* and *A. muciniphila* are equipped with cobalamin biosynthesis enzymes but lack the first enzymes of the pathway. Therefore, they are only considered Cbi salvagers, which require cobinamide (Cbi) as precursor (Figure 3.1.7 A). In contrast, enzymes requiring vitamin B₁₂, a cofactor from the cobalamin group, were found in bacteria with higher as well as lower susceptibility. For example, genes encoding for the vitamin B₁₂-dependent methionine synthase, the vitamin B₁₂-dependent ribonucleotide reductase and the epoxyqueuosine reductase were found in several species. However, the species with higher susceptibility to chlorotonils revealed, on average, more predicted B₁₂-binding sites (Figure 3.1.7 B & C). The highest number of B₁₂-binding domains was detected in the genome of *T. glycolicus* DSM 1288 (Shelton *et al.*, 2019).

Results

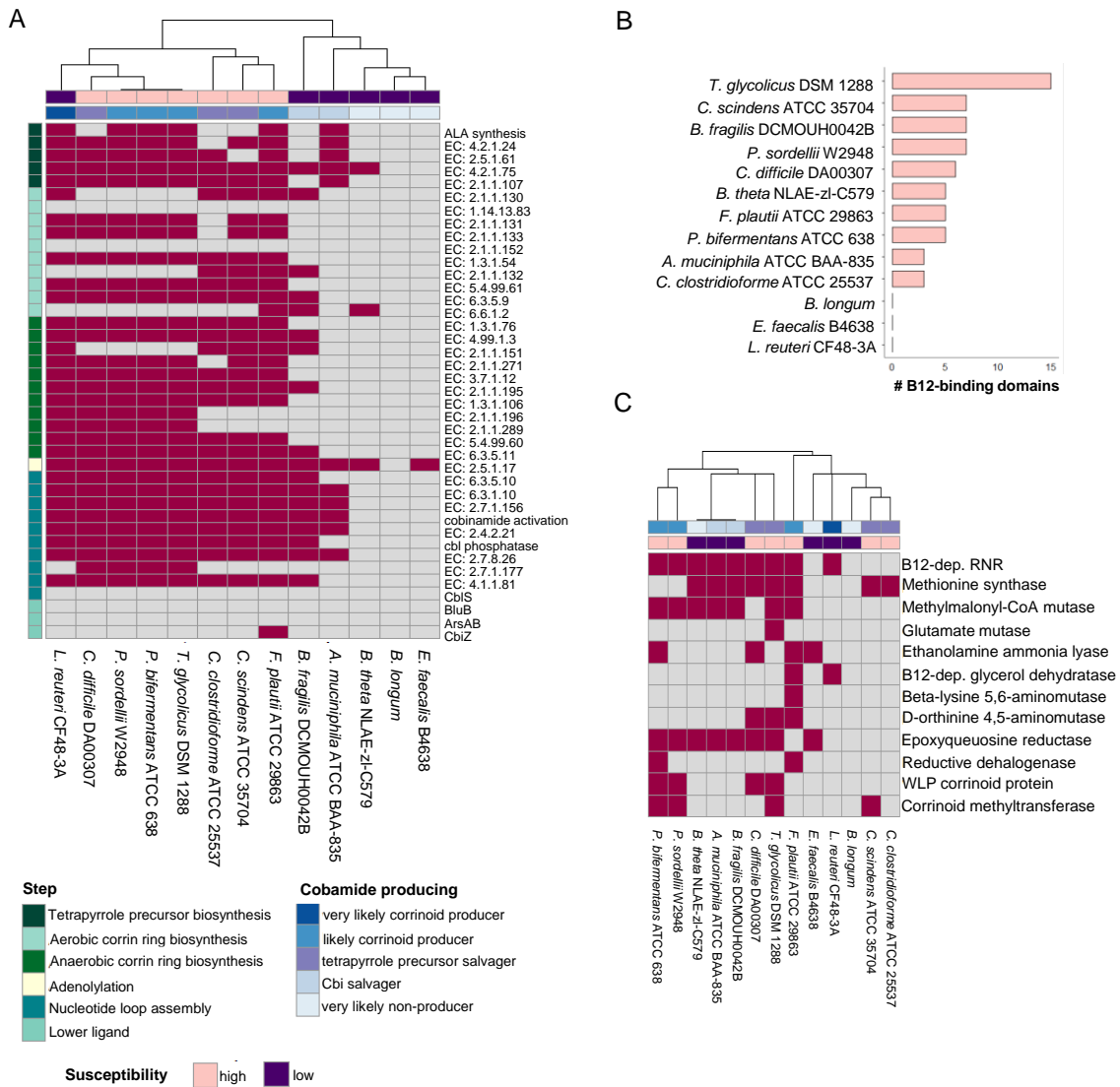


Figure 3.1.7: Differential distribution of cobalamin biosynthesis and vitamin B₁₂-dependent enzymes between bacteria with higher and lower susceptibility to chlorotoniis. (A) Overview of the cobalamin biosynthesis pathway and its enzymes. Presence of a respective protein in the proteome of the analyzed species is given by magenta color. If no homologs could be identified, the putative absence is indicated by grey color. Row annotations indicate the affiliation of the proteins to the step of the cobalamin biosynthesis pathway. Column annotations show whether a strain revealed higher or lower susceptibility and whether a strain is predicted to produce cobalamins. **(B)** The number of predicted vitamin B₁₂-binding sites varies between none and 10 sites. **(C)** B₁₂-dependent enzymes are found in the genomes of all selected species with the exception of *B. longum*. Column annotations show whether a strain revealed higher or lower susceptibility and whether a strain is predicted to produce cobalamins. Cbi: Cobinamide; RNR: ribonucleotide reductase.

3.1.3 Systemic effects of chlorotoniil treatment on the metabolism of *C. difficile*

Based on the results obtained in section 3.1.2, it was assumed that chlorotoniil treatment possibly affects *C. difficile* central metabolism, in particular Stickland fermentation and cofactor metabolism. With the aim to gain insights into the systemic effects of chlorotoniil stress, the stress responses of *C. difficile* 630 and *T. glycolicus* DSM 1288 to ChA and/or ChB1-Epo2 were analyzed on proteome level by LC-MS/MS. Therefore, strains were allowed to grow to mid-exponential phase and were treated with sublethal concentrations of the respective antibiotics. Subsequently, treated and untreated cells were harvested and lysed to extract the cytosolic protein fraction, which was subjected to a standard LC-MS/MS sample preparation and analysis workflow. Finally, LC-MS/MS raw data were searched against a strain-specific database and the data were used to evaluate how *C. difficile* and *T. glycolicus* respond to the different compound classes (Figure 3.1.8).

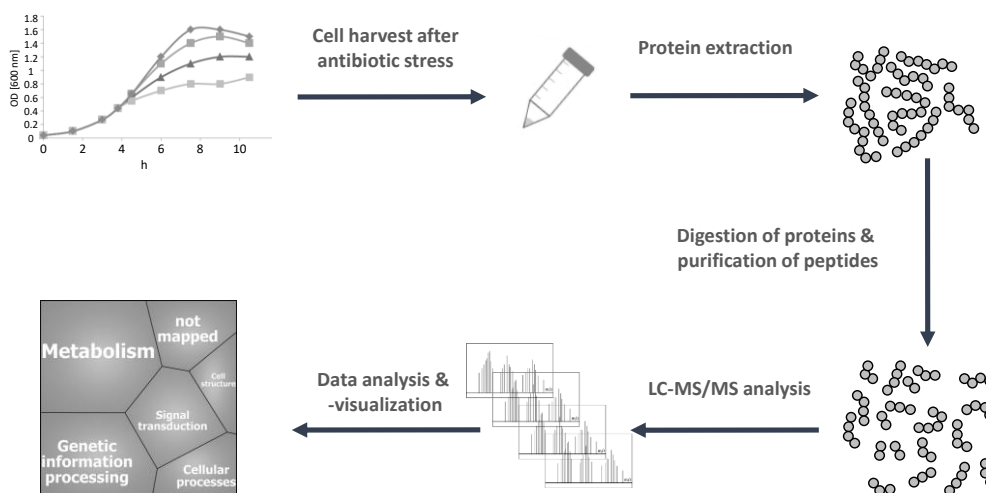


Figure 3.1.8: LC-MS/MS workflow. The stress response of *C. difficile* 630 to each of the selected new compounds and reference antibiotics was analyzed with the depicted workflow.

3.1.3.1 The proteome response of *C. difficile* to ChA and ChB1-Epo2 suggests osmo- and metal-stress and a disturbed energy metabolism

First, the proteome responses of *C. difficile* 630 to ChA and ChB1-Epo2 were analyzed. Exponentially growing cultures of *C. difficile* 630 were treated with 4.69 ng/ml of ChA or ChB1-Epo2, an equal volume of DMSO or were left untreated. 90 min following stress, cells were harvested and processed for analysis by LC-MS/MS as described above (Figure 3.1.8, Suppl. figure S3 A, B), leading to the identification of 1547 and 1499 proteins in the ChA and the ChB1-Epo2 experiment, respectively (Suppl. table S4, S5). The identified proteins covered the most important cellular functions, including macromolecule biosynthesis processes, energy, cofactor, and amino acid metabolism, and stress response/virulence

Results

networks and were mainly of cytoplasmic origin (Figure 3.1.9). Since it could be proven that the solvent DMSO has only a neglectable effect on *C. difficile*, the downstream data analysis focused on the comparison of chlorotoniil-stressed cells and solvent controls, only.

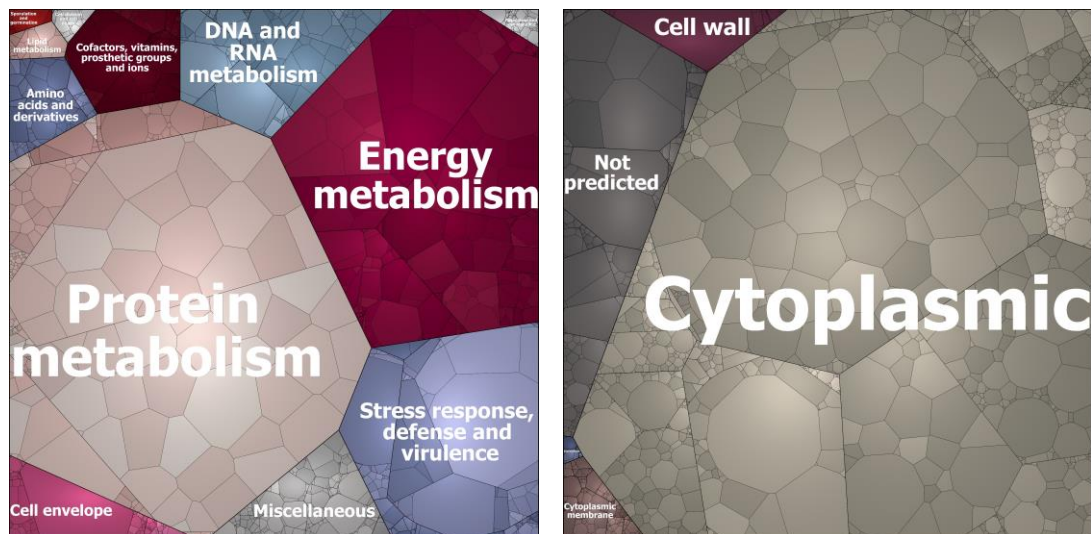


Figure 3.1.9: Relative abundance, functional assignment and localization of *C. difficile* proteins identified in the proteomics experiments. Proteomics experiments addressing the stress response of *C. difficile* 630 to sublethal concentrations of ChA or ChB1-Epo2 led to the identification of 1547 and 1499 proteins from various functional categories, mainly affiliated to the functional categories (1) protein metabolism, (2) energy metabolism, (3) stress response, defense and virulence, and (4) DNA and RNA metabolism (left panel). The proteins were mainly of cytoplasmic origin, minor fraction were cytoplasmic membrane or cell wall proteins according to PSORTb (right panel). Each cell of the Voronoi treemap represents a single protein and cell size correlates with overall abundance of the protein inside the bacterial cell.

Comparing the stress response of *C. difficile* 630 to ChA or ChB1-Epo2 to the proteome response of the solvent controls, fold changes could be calculated for 1,368 and 1,340 proteins, respectively (Suppl. table S4, S5). Statistical analysis indicated significant changes in protein abundance between treated and untreated controls for 9 and 7 proteins (\log_2 fold change (FC) ≥ 1 , adj. p value ≤ 0.05), respectively. In addition, 13 and 29 proteins were exclusively found in at least three replicates of the ChA- and ChB1-Epo2-stressed cells (ON), whereas 29 and 29 proteins were exclusively found in at least three replicates in the solvent controls (OFF).

In the ChA dataset, higher amounts of the enzymes for oxidative Stickland fermentation of aromatic amino acids (IorA, IorB, CD630_23820), the glycine betaine ABC-type transport proteins OpuCA and OpuCC, a TetR transcriptional regulator and three less characterized proteins were identified (CD630_08810, CD630_10060, CD630_17520) (Figure 3.1.10).

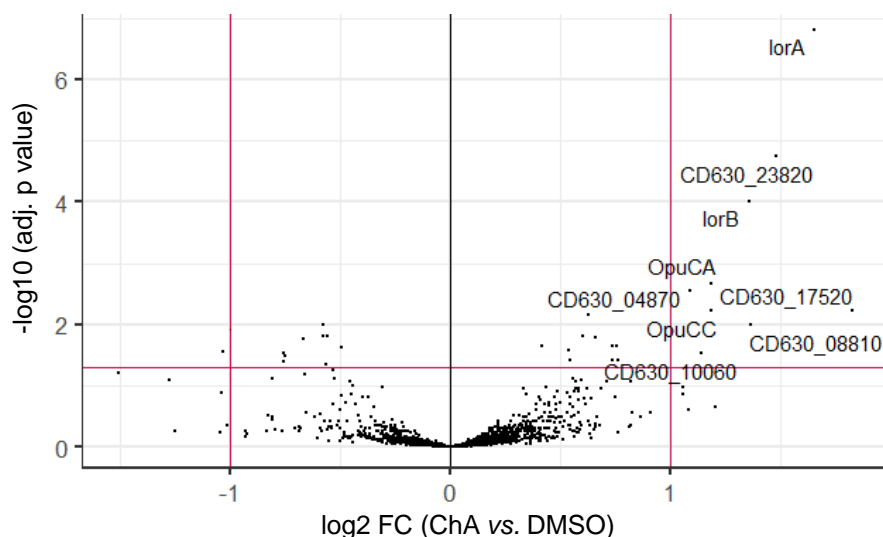


Figure 3.1.10: Volcano plot of the ChA-stress proteome signature. The proteome signature of *C. difficile* 630 in the presence of 4.69 ng/ml ChA vs. growth with an equal volume of DMSO indicated significant higher abundance of nine proteins (threshold: \log_2 fold change ≥ 1 ; p value ≤ 0.05). Proteins with significantly altered abundance following stress are labeled.

Following treatment with ChB1-Epo2, the small subunit ribosomal protein RpmE, a phosphonoacetate hydrolase, the thiamine biosynthesis protein ThiE and the argininosuccinate synthase ArgG, were identified in higher abundance in treated cells. Lower amounts in ChB1-Epo2-treated vs. DMSO-treated cells were observed for the cysteine synthase CysK, an ABC transport system protein and the proline ligase ProS2 (Figure 3.1.11).

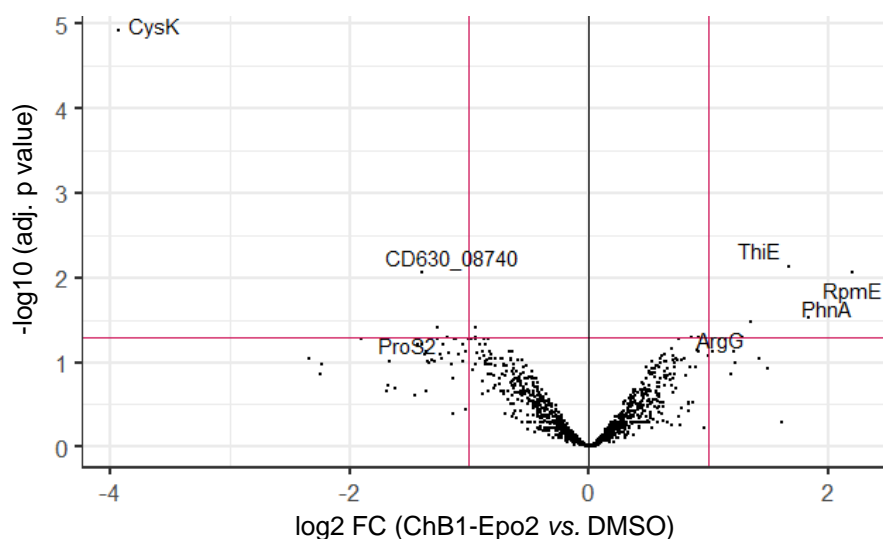


Figure 3.1.11: Volcano plot of the ChB1-Epo2-stress proteome signature. The proteome signature of *C. difficile* 630 in the presence of 4.69 ng/ml ChB1-Epo2 vs. growth with an equal volume of DMSO indicated significant higher or lower abundance of four and three proteins (threshold: \log_2 fold change ≥ 1 ; p value ≤ 0.05). Proteins with significantly altered abundance following stress are labeled.

Results

Interestingly, the ON/OFF proteins comprised several S-adenosylmethionine (SAM), metal- and [FeS]-cluster dependent enzymes according to their InterPro classification (Blum *et al.*, 2021). In addition, sequences of several ON/OFF proteins included a CXXC motive typically required for divalent metal and [FeS]-cluster binding.

In more detail, the 13 ON proteins following ChA treatment comprised an alpha-hydroxy acid FMN-dependent dehydrogenase with similarity to a glycolate dehydrogenase (CD630_23870), a putative glyoxalase/bleomycin resistance protein (CD630_36100), a metal-dependent hydrolase (CD630_31820) and a putative iron-dependent (2R)-sulfolactate sulfo-lyase subunit beta SuyB (Figure 3.1.12). In addition, e.g., the mannitol-specific PTS system protein MtlA was exclusively identified in the proteome signature of ChA-treated cells (Figure 3.1.12). By contrast, OFF proteins of ChA-treated cells included the cobalt-transport protein CbiM, three SAM- and [FeS]-cluster-dependent oxidoreductases, including the oxygen-independent coproporphyrinogen-III oxidase HemN, CD630_14140 and CD630_26330, a putative SAM-dependent methyltransferase, and some proteins with predicted metal binding sites (HydN1, CD630_35270, CD630_29270, CD630_36200, CD630_19960). Additionally, the keto-acid reductoisomerase IlvC and a putative serine/threonine protein kinase were only identified in the DMSO controls (Figure 3.1.12).

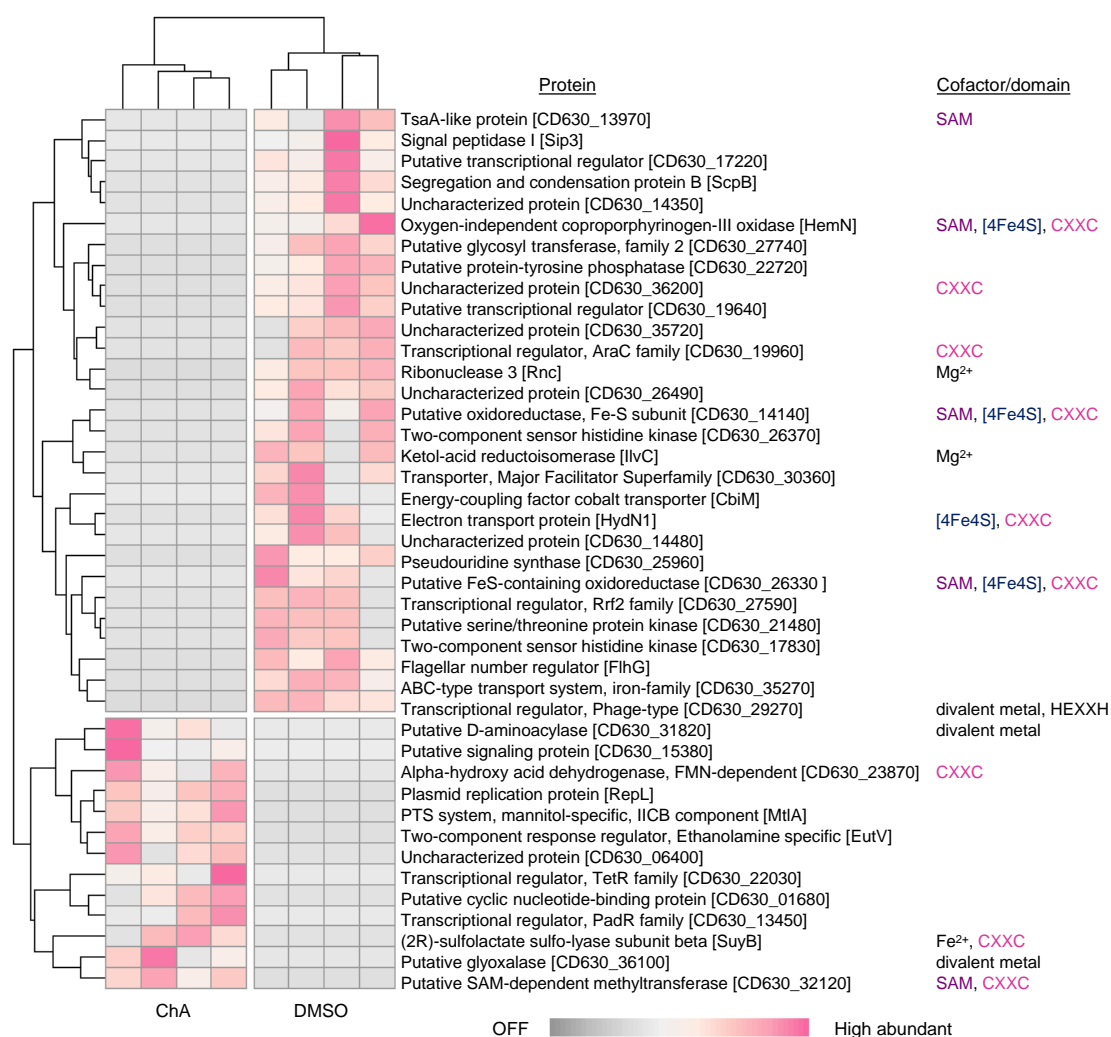


Figure 3.1.12: Heatmap of differentially abundant proteins in ChA- vs. DMSO-treated cells of *C. difficile*. The proteome stress signature of *C. difficile* 630 90 min after stress with 4.69 ng/ml ChA was compared to the proteome signature of cells treated with DMSO only. Proteins, which were exclusively present in ChA-treated cells or untreated cells, are displayed following z-transformation of the LFQ-based intensity data. Increased/decreased abundance following stress is displayed by the color gradient from red (high) to grey (OFF). Cofactors and domains with predicted metal-binding capacity are displayed on the right side. SAM: S-adenosyl methionine.

Similarly, approximately half of the ON proteins of the ChB1-Epo2 dataset contained conserved cysteine motives and several ON proteins are predicted to bind divalent metal ions. For instance, the ribosomal protein RpmE, the hydroxyphenylacetate decarboxylase HpdC, a [4Fe-4S]-cluster protein (CD630_31230), and the six-cysteine peptide CD630_27991 were among the ON proteins. In addition, the ON proteins included three PTS system proteins. In contrast, the OFF proteins included two D-alanyl-D-alanine carboxypeptidases (VanY3, DacF1), three SAM-dependent proteins (PfiE, CD630_12490, CD630_14140), the keto-acid reductoisomerase IlvC, the cobalt transport protein CbiQ and the ferrous iron transport protein FeoA3 (Figure 3.1.13).

Results

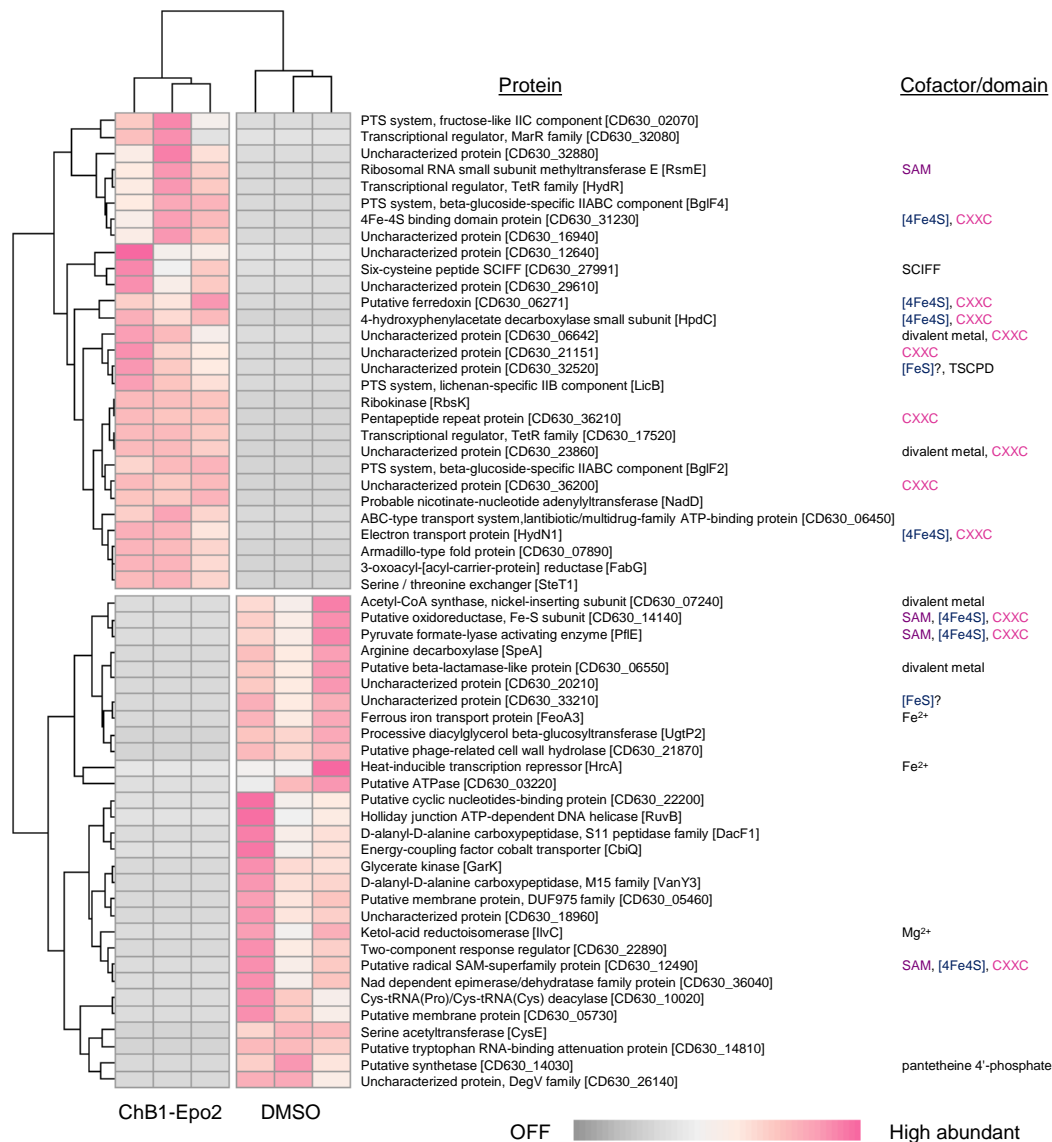


Figure 3.1.13: Heatmap of differentially abundant proteins in ChB1-Epo2- vs. DMSO-treated cells of *C. difficile*. The proteome stress signature of *C. difficile* 630 90 min after stress with 4.69 ng/ml ChB1-Epo2 was compared to the proteome signature of cells treated with DMSO only. Proteins, which were exclusively present in ChB1-Epo2-treated cells or untreated cells, are displayed following z-transformation of the LFQ-based intensity data. Increased/decreased abundance following stress is displayed by the color gradient from red (high) to grey (OFF). Cofactors and domains with predicted metal-binding capacity are displayed on the right side. SAM: S-adenosyl methionine. Adapted from Bublitz *et al.* (in revision).

Next, all identified proteins of the ChA- and ChB1-Epo2-stress proteome signatures were ranked according to their fold change and mean ranks of defined gene sets summarizing proteins from the same pathways or operons, or proteins with similar function were calculated (Suppl. table S4, S5). The gene set enrichment analysis indicated increased synthesis of proteins for the oxidative Stickland fermentation of aromatic amino acids and the proline reductase in response to treatment with both chlorotoniils (Figure 3.1.14 A). In contrast, cobalt transport proteins, butyrate fermentation enzymes, enzymes of the reductive part of the TCA cycle, pyruvate formate lyases, and cysteine and *de novo* purine biosynthesis enzymes were generally less abundant following stress with chlorotoniils

(Figure 3.1.14 A). Furthermore, proteins involved in glyoxalate metabolism, lysine biosynthesis and the oxidative part of the TCA cycle were overrepresented in the ChA dataset, whereas enzymes required for the synthesis of vitamins were overall of lower abundance (Figure 3.1.14 B). The ChB1-Epo2 dataset was further characterized by enrichment of ribosomal proteins and a few proteins required for metal resistance (Figure 3.1.14 C). In particular, the copper chaperone CopZ (FC: 1.55, rank: 6) and the copper-responsive regulator CsoR (FC: 1.23, rank: 11) caught attention by ranking among the top fifteen proteins in the ChB1-Epo2 dataset. Moreover, the enrichment of ribosomal proteins in the ChB1-Epo2 dataset was mainly driven by higher fold changes of proteins with predicted divalent metal binding sites or CXXC motives, such as RpmE, RpmF, RpmB, RpsR and RpsZ.

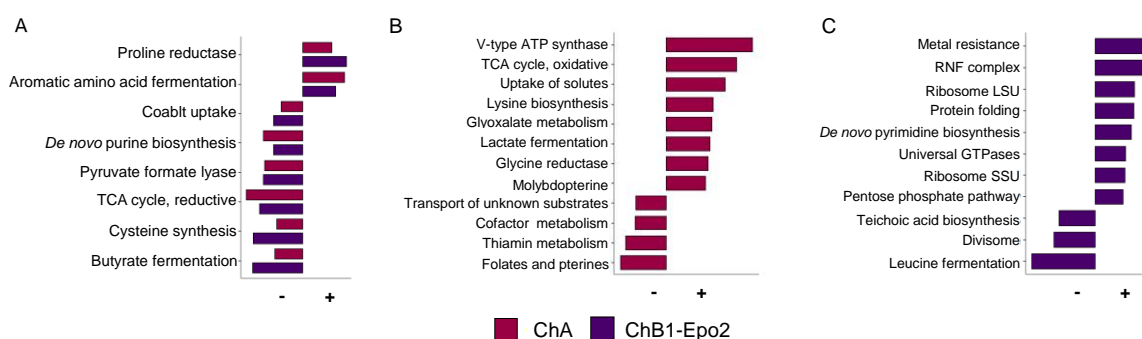


Figure 3.1.14: Top ten of gene sets affected the most by ChA- and/or ChB1-Epo2-treatment. Gene sets were defined as proteins from the same pathways or operons, or proteins with similar function and listed according to their mean rank sum based on \log_2 fold changes. **(A)** Gene sets equally affected by ChA and ChB1-Epo2 treatment. **(B)** Gene sets specifically affected by ChA treatment. **(C)** Gene sets specifically affected by ChB1-Epo2 treatment. TCA = tricarboxylic acid cycle; LSU = large ribosomal subunit; SSU = small ribosomal subunit.

3.1.3.2 The proteome of *C. difficile* upon long-term adaptation to ChB1-Epo2

The observed ability of *C. difficile* to grow in the presence of chlorotoniils in the absence of competing microbes and following adequate time for adaptation (Suppl. figure S4) led to the hypothesis that *C. difficile* is able to adapt its metabolism to overcome chlorotonil stress. To potentially identify changes in its proteome upon adaptation, *C. difficile* 630 was grown in the presence of ChB1-Epo2 or DMSO or without treatment to mid-exponential phase and cells were harvested when reaching OD_{600nm} 0.5 (Figure 3.1.15). ChB1-Epo2 was again chosen due to its better solubility compared to ChA.

Results

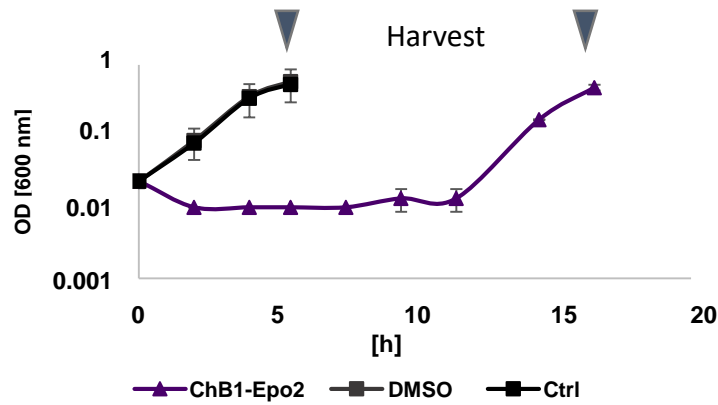


Figure 3.1.15: *C. difficile* slowly adapts to the chlorotoniol derivative ChB1-Epo2. *C. difficile* 630 was grown to mid-exponential phase in the absence and presence of 6.25 ng/ml ChB1-Epo2. At an OD_{600nm} of 0.5, cultures were harvested and analyzed by LC-MS/MS.

Proteomics analysis resulted in the identification of 1513 proteins with similar functional distribution and localization as shown above (Figure 3.1.9, suppl. table S6). A principal component analysis (PCA) of the generated dataset indicated that the proteome signatures of ChB1-Epo2-adapted cells did not substantially differ from the proteome signatures of untreated and DMSO-treated cultures (Figure 3.1.16). Only the third biological replicate of ChB1-Epo2-adapted cells clustered distinct from the controls in a PCA plot (Figure 3.1.16).

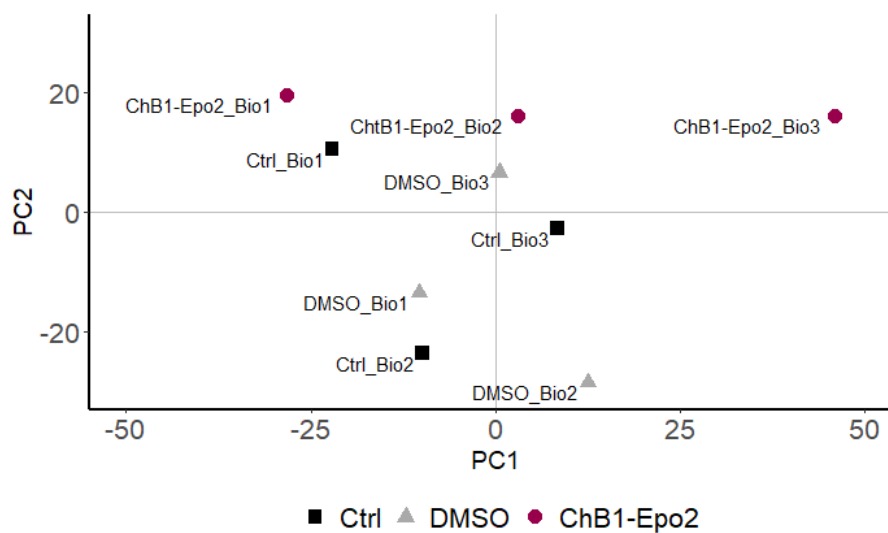


Figure 3.1.16: PCA plot of the ChB1-Epo2 adaptation dataset. The proteome signatures of *C. difficile* 630 cultures grown in the presence and absence of ChB1-Epo2 or an equal volume of DMSO were analyzed by PCA. The results indicate that the proteome signatures of cultures adapted to ChB1-Epo2 did not significantly differ from the proteome signatures of DMSO- and untreated cultures.

In accordance with the PCA, only one protein, namely the isoleucine 2-epimerase CD630_21580, was significantly higher abundant in the ChB1-Epo2-treated cells compared to the solvent controls (Figure 3.1.17). However, a few other proteins were exclusively identified in ChB1-Epo2- (ON) or DMSO-treated (OFF) cells as seen before for the stress signature. ON proteins comprised, e.g., the energy-coupling factor cobalt transport protein CbiM, a zinc-dependent M20-type amidohydrolase, a putative SAM-dependent methyltransferase/RNA-binding protein and a mannose-type PTS protein. In contrast, the OFF proteins included a [4Fe-4S]-cluster protein, a putative zinc-dependent deacetylase (CD630_19710) and the 3-oxoacyl-[acyl-carrier-protein]-reductase FabG (Figure 3.1.17).

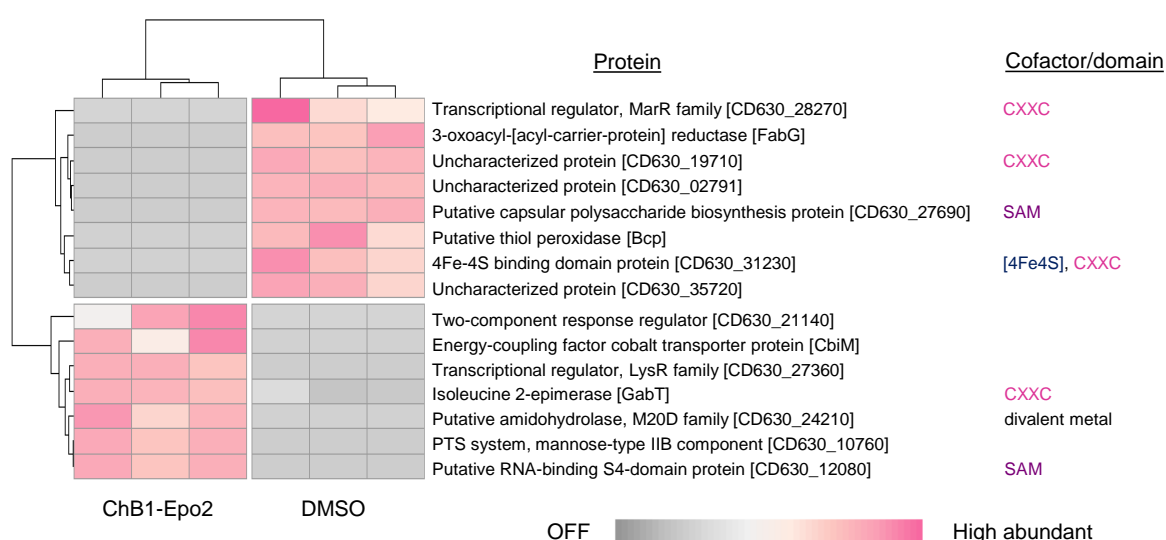


Figure 3.1.17: Heatmap of differentially abundant proteins of *C. difficile* grown in the presence or absence of ChB1-Epo2. The proteome stress signature of *C. difficile* grown to mid-exponential phase in the presence of 6.25 ng/ml ChB1-Epo2 was compared to the proteome signature of cells grown to mid-exponential phase in the presence of DMSO only. Proteins, which were significantly more or less abundant in ChB1-Epo2-treated cells or only present in treated or untreated cells, are displayed following z-transformation of the LFQ-based intensity data. Increased/decreased abundance following stress is displayed by the color gradient from red (high) to grey (OFF). Cofactors and domains with predicted metal-binding capacity are displayed on the right side. SAM: S-adenosyl methionine.

A more detailed analysis of the differences between the ChB1-Epo2-adapted cells of biological replicate three indicated that the observed different clustering was mainly mediated by substantially increased abundance of the glycine reductase subunit proteins. In addition, all ChB1-Epo2-adapted cultures revealed strikingly but non-significantly higher levels of the gluconeogenesis protein GapB and the glycogen biosynthesis proteins GlgB and GlgC (Suppl. table S6).

Results

3.1.3.3 The proteome stress response of *T. glycolicus* to ChB1-Epo2

The proteome signatures of *C. difficile* to both chlorotonils suggested disturbed metal homeostasis. To validate this finding, the proteome stress response signature of *T. glycolicus* DSM 1288, another highly susceptible representative of the intestinal microbiota, to ChB1-Epo2 was analyzed as well. Again ChB1-Epo2 was chosen due to its increased solubility compared to ChA. The experimental settings were chosen according to the experiments performed with *C. difficile* with the exception that *T. glycolicus* DSM 1288 was grown in BHI instead of CDMM (Figure 3.1.8, Suppl. figure S3 C). The analysis identified 1594 proteins mainly of cytoplasmic origin and assigned to the eggNOG functional categories “energy metabolism” and “information storage and processing”, followed by “cellular processes and signaling” (Figure 3.1.18, suppl. table S7).

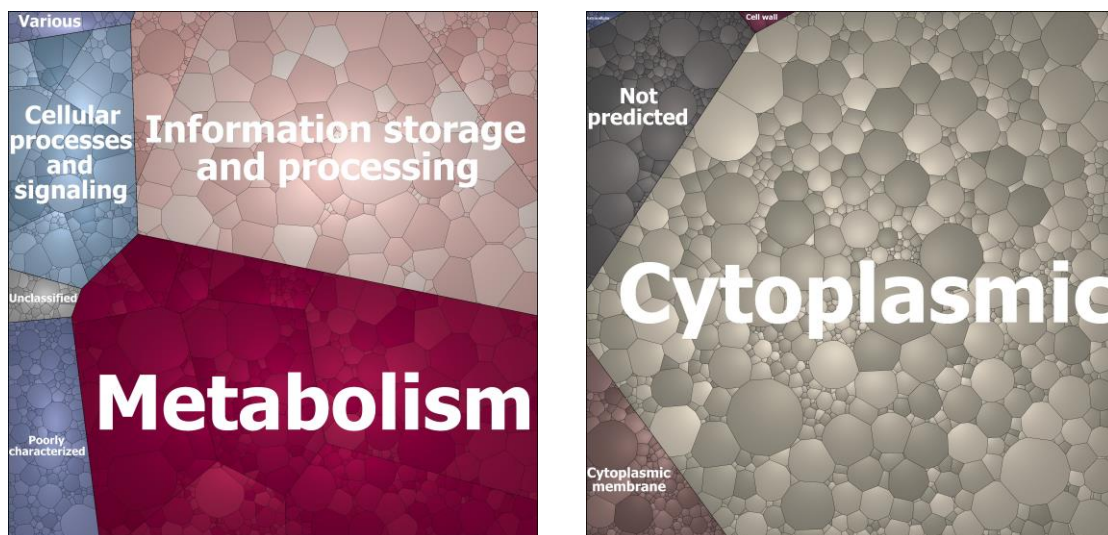


Figure 3.1.18: The proteome response of *T. glycolicus* to ChB1-Epo2. A proteomic experiment addressing the stress response of *T. glycolicus* DSM 1288 to a sublethal concentration of ChB1-Epo2 led to the identification of approximately 1594 proteins from various functional categories, mainly affiliated to the eggNOG classifications (1) metabolism, (2) information storage and processing, (3) cellular processes and signaling (left panel). Proteins were mainly of cytoplasmic origin or cytoplasmic membrane or cell wall proteins according to PSORTb (right panel). Each cell of the Voronoi treemap represents a single protein and cell size correlates with overall abundance of the protein inside the bacterial cell.

In line with the results obtained for the chlorotonil stress responses of *C. difficile*, only six proteins were found in significantly different amounts between DMSO- and ChB1-Epo2-treated cells. The proteins with the highest significant fold change were a glycine and a betaine reductase as observed for ChA-treated *C. difficile* cells. In addition, a metal-dependent dihydropyrimidase/amidohydrolase and a formate dehydrogenase subunit were enriched, while a protein of purine metabolism and a flagella biosynthesis protein were lower abundant upon stress (Figure 3.1.19). In addition, ON proteins exclusively identified in the ChB1-Epo2-treated cells comprised, e.g., the energy-coupling factor transport system ATP-binding protein CbiO, a formate/nitrite transporter and a [2Fe-2S]-dependent aldehyde

oxidoreductase. In contrast, some proteins from various other functional categories were not identified in ChB1-Epo2-treated cells but in the DMSO-treated cells, such as a radical SAM (rSAM) Elp3/MiaB/NifB protein (Figure 3.1.19). More detailed analysis of the respective proteins revealed that the significantly enriched formate dehydrogenase alpha subunit has 77.5% sequence homology to *C. difficile* 630 selenocysteine-dependent formate dehydrogenase H alpha subunit, suggesting that the *T. glycolicus* protein is most likely also a selenocysteine-containing protein.

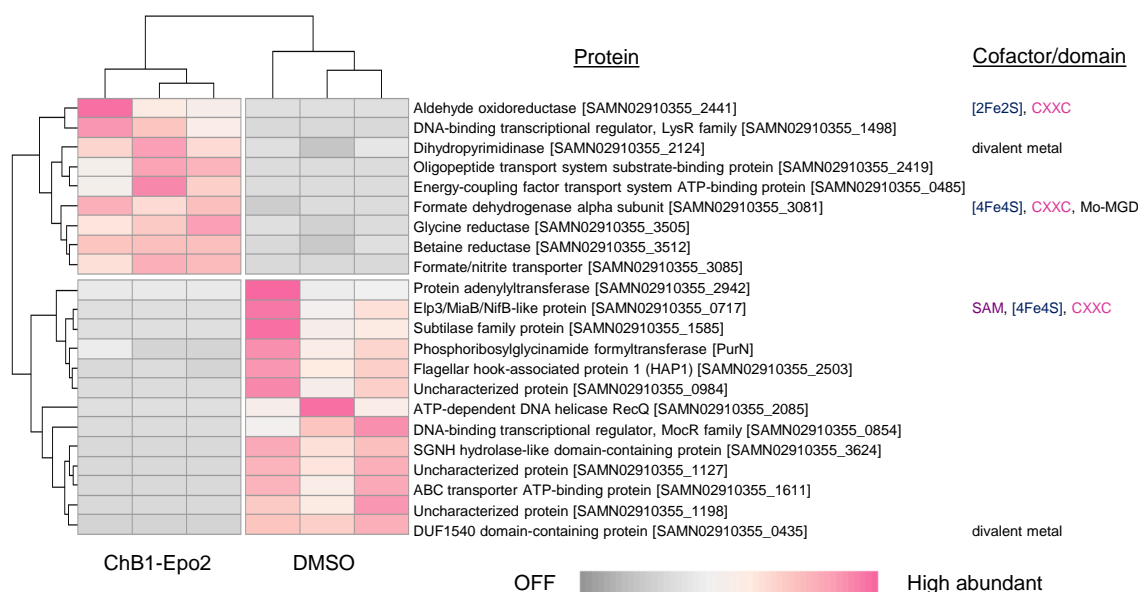


Figure 3.1.19: Heatmap of differentially abundant proteins in ChB1-Epo2- and DMSO-treated cells in *T. glycolicus*. The proteome stress signature of *T. glycolicus* following stress with 6.25 ng/ml ChB1-Epo2 for 90 min was compared to the proteome signature of cells treated with DMSO only. Proteins, which were significantly more or less abundant in ChB1-Epo2-treated cells or only present in treated or untreated cells, are displayed following z-transformation of the LFQ-based intensity data. Increased/decreased abundance following stress is displayed by the color gradient from red (high) to grey (low). Cofactors and domains with predicted metal-binding capacity are displayed on the right side. SAM: S-adenosyl methionine.

3.1.3.4 ChB1-Epo2 treatment disturbs the intracellular metal pool of *C. difficile* 630

The recurrent detection of metal-binding and -transport proteins among the differentially abundant proteins following ChA/ChB1-Epo2 treatment led to the decision to analyze the intracellular metal pool of *C. difficile* 630 following stress with ChB1-Epo2.

Briefly, the intracellular concentrations of mono- and divalent cations as well as their peak distribution under control and ChB1-Epo2 stress conditions were analyzed by inductively-coupled plasma-mass spectrometry (ICP-MS) for *C. difficile* 630 in the same experimental set up used for the stress proteome study. The data indeed revealed that the metal pool of *C. difficile* 630 was altered following stress (Suppl. table S8). Most prominent, the total amount of potassium and sodium were significantly different between treated and untreated

Results

cells (Figure 3.1.20 A). In addition, three transient metals, namely zinc, copper, and cadmium, were significantly more abundant in the cytoplasm upon stress (Figure 3.1.20 B, C & D). Besides, single peaks within the chromatograms of selenium and manganese were significantly changed compared to the controls (Figure 3.1.20 E & F).

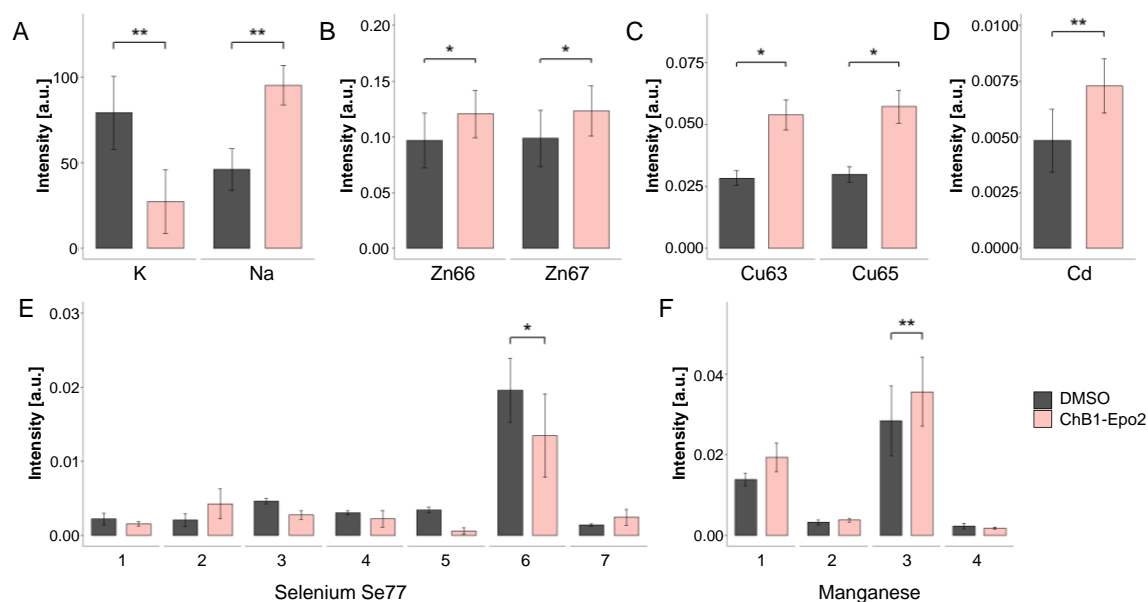


Figure 3.1.20: ICP-MS analysis of intracellular metal concentrations following ChB1-Epo2 treatment. The intracellular metal content of *C. difficile* 630 grown in the presence of 4.69 ng/ml ChB1-Epo2 for 90 minutes was comparatively analyzed by ICP-MS. Statistical analysis revealed significantly changed intracellular concentrations for (A) potassium (K) and sodium (Na), (B) both zinc (Zn) isotopes, (C) both copper (Cu) isotopes, and (D) cadmium (Cd). In addition, two single peaks were significantly altered in the (E) selenium (Se77) profile and the (F) manganese (Mn) profile, respectively. K = potassium, Na = sodium, Zn = zinc, Cu = copper, Cd = cadmium, * = p value ≤ 0.05 , ** = p value ≤ 0.01 , [a.u.] = artificial units.

3.1.3.5 ChA and ChB1-Epo2 bind divalent metals and selenium

Next, the question was addressed whether the disturbed metal pool is potentially directly induced by chlorotoniols and the result of non-covalent metal binding. Cell-free ICP-MS analysis of ChA and ChB1-Epo2 solved in DMSO revealed that both compounds bind divalent metals as well as selenate, but neither potassium nor sodium.

Metal-binding could reliably be confirmed for isotopes of magnesium (Mg25, Mg26), calcium (Ca46, Ca48), vanadium (V51), zinc (Zn66, Zn67), and selenium (Se82), which is most likely bound as selenate (Figure 3.2.1, suppl. table S9).

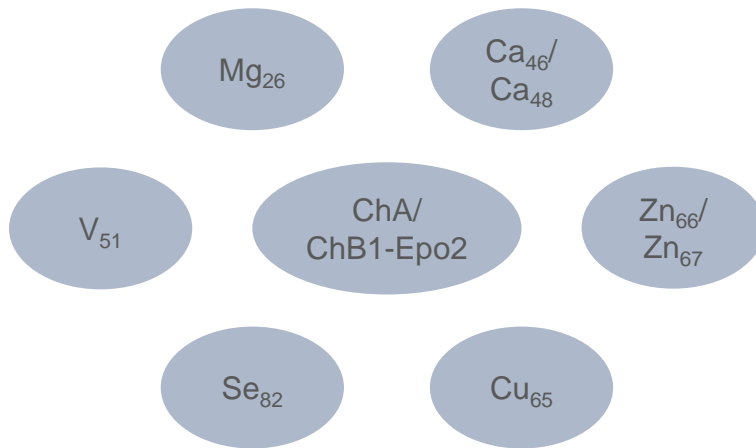


Figure 3.1.21: ChA/ChB1-Epo2 bind divalent metal cations and selenium.

Moreover, additional ICP-MS measurements performed with ChA and ChB1-Epo2 in concentrated trace salt buffer, copper sulfate or selenate solutions suggested increased binding of copper, selenate and other divalent metals if availability of these metals is artificially elevated. ICP-MS analysis of chlorotonils under physiologically relevant conditions is ongoing.

Results

3.1.4 Systemic effects of ChA treatment on the complex microbial communities of the intestinal tract

Based on the correlation between selenium/cobalamin metabolism and chlorotoniil susceptibility and the disturbed metal homeostasis observed *in vitro*, it was hypothesized that oral chlorotoniil treatment causes specific functional changes of the intestinal microbiota, particularly affecting the selenium and cobalamin metabolism or, more generally, metal stress-sensitive pathways. Furthermore, species that rely particularly on metal-dependent and metal-sensitive pathways might be the most affected by chlorotoniil treatment. As outlined in section 3.1.2, cobalamin and selenium metabolism are predominately found in the classes Clostridia and Proteobacteria. Backing up the hypothesis, previous analysis of fecal samples from ChA/ChB1-Epo2-treated piglets and mice by 16S rRNA gene sequencing revealed selective reduction of some Clostridia families, whereas Bacteroidetes families showed increased abundance upon ChA/ChB1-Epo2 treatment (Bublitz *et al.*, in revision). In order to test this hypothesis, functional changes of the microbiota in fecal samples of piglets were analyzed using a metaproteomics approach.

3.1.4.1 Piglet feeding trial

Briefly, two feeding trials with four and eight piglets bought at the age of four weeks were performed at the Friedrich-Loeffler Institute (Jena, Germany). To account for genetic diversity and maternally-inherited microbiota structure, six sibling pairs were selected, of which one was assigned the control (Ctrl) and one to the treatment group (ChA-treated = ChA) each (Table 3.1.4).

Table 3.1.4: Assignment of animals included in the piglet feeding trial to the experiments and treatment groups. The piglet feeding trial comprised two experiments with four and eight piglets. Two and four sibling piglets were bought and divided to the two treatment groups (control = Ctrl vs. ChA-treated = ChA).

Experiment	1				2							
Treatment group	Ctrl	ChA	Ctrl	ChA	Ctrl	ChA	Ctrl	ChA	Ctrl	ChA	Ctrl	ChA
Sibling pair	1	1	2	2	3	3	4	4	5	5	6	6
Animal	Ctrl_1	ChA_1	Ctrl_2	ChA_2	Ctrl_3	ChA_3	Ctrl_4	ChA_4	Ctrl_5	ChA_5	Ctrl_6	ChA_6

After two weeks of acclimatization, piglets either received two doses of 10 mg/kg body weight ChA with peanut butter as vehicle, or peanut butter only (= control treatment) on two consecutive days. Prior and 6 hours after the first dose and 1 day following the second dose fecal samples were collected and subjected to an analysis by LC-MS/MS (Figure 3.1.22). More detailed information of the piglet feeding trial can be found in Bublitz *et al.* (in revision).

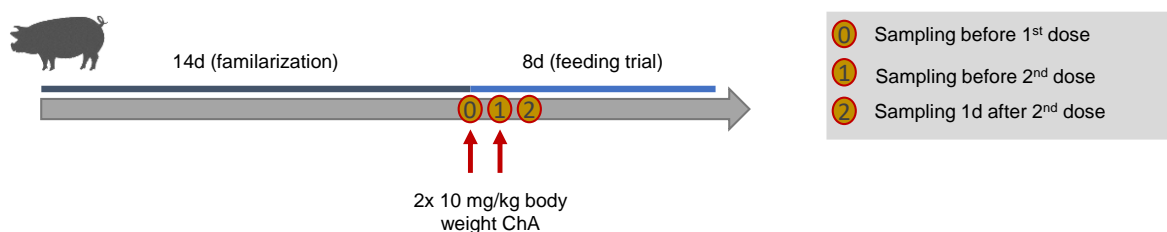


Figure 3.1.22: Overview of piglet feeding trial experimental design. To analyze the effect of ChA treatment on the intestinal microbiota of piglets, piglets were treated twice (d0, d1) with 10 mg/kg body weight ChA and feces samples were collected for the downstream analysis. Briefly, piglets were allowed to get accustomed with the new environment for 14 d. ChA in peanut butter (vehicle) or peanut butter only (control) were administered twice on two sequential days and fecal samples were collected directly before the treatment (d0), 6 h after the first (d1) and one day after the second dose (d2).

3.1.4.2 Metaproteomics sample preparation from fiber-rich piglet feces and customized database design

First, a protocol for the extraction of proteins from the fiber- and organic acid-rich fecal samples was established building on published protocols. As extensively reviewed in the literature, protein extraction from environmental samples is challenging due to the complexity of the samples and high content of interfering factors (Heyer *et al.*, 2017; Qian and Hettich, 2017; Isaac *et al.*, 2019). To that end, low-speed differential centrifugation and filtering steps (Juste *et al.*, 2014; Tanca *et al.*, 2015; Zhang *et al.*, 2016); phenol-, TriZOL-based and phenol-free extraction protocols (Heyer *et al.*, 2019; Gierse *et al.*, 2020) as well as 1D-gel-based and gel-free protein digestion protocols as used for the *in vitro* experiments (Heyer *et al.*, 2019; Gierse *et al.*, 2020) were compared. The best suited options, yielding the highest numbers of microbiota-derived proteins, were finally combined to a protocol. An overview of the entire workflow is given in Figure 3.1.23 and more detailed information can be found in the material and methods section.

Results

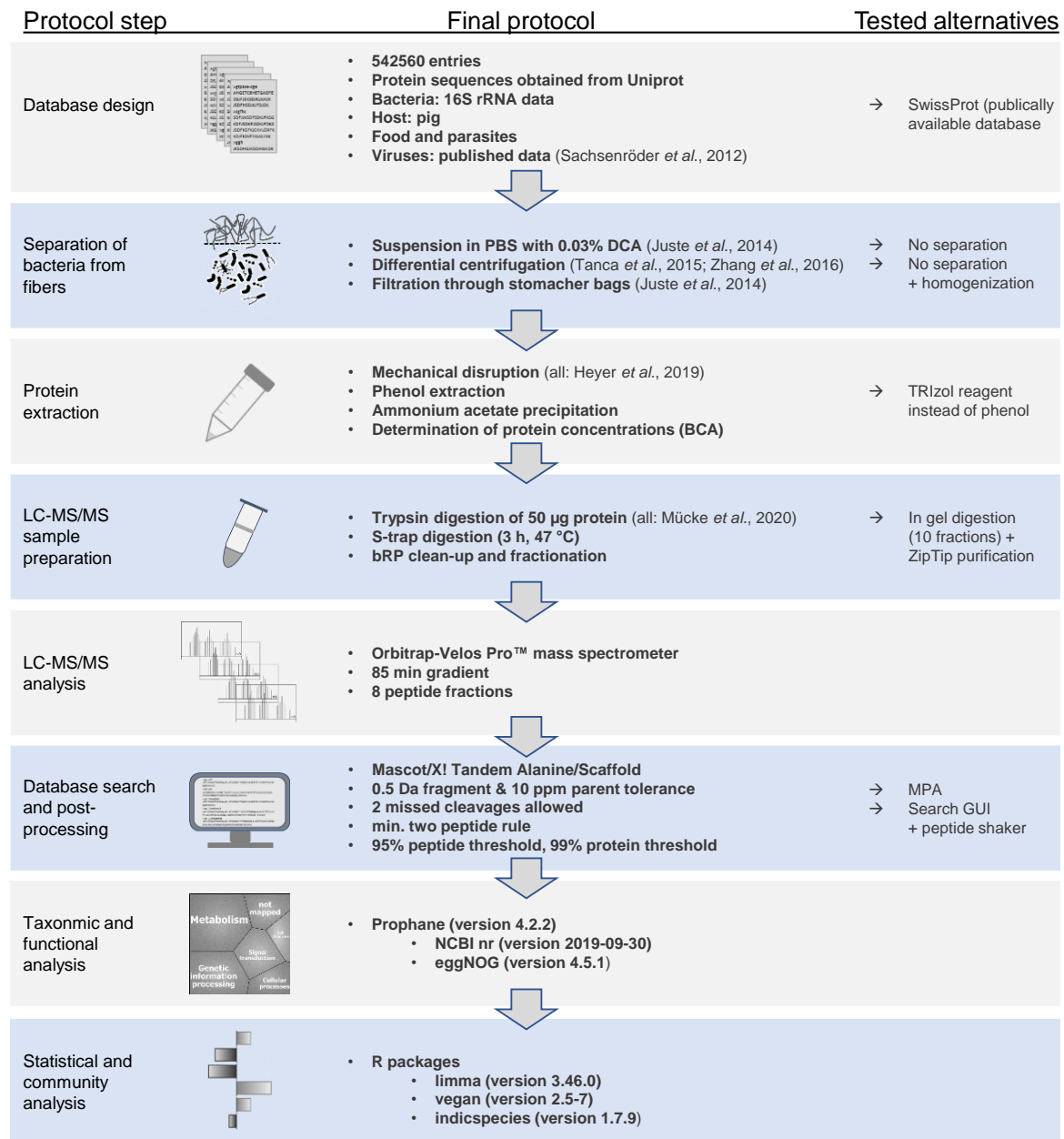


Figure 3.1.23: Metaproteomics workflow from protein extraction to statistical and community analysis. Feces samples were processed and analyzed by LC-MS/MS using a workflow optimized for fiber-rich sample material. Details for every step of the workflow are given in the “Protocol” column. For five steps, alternative protocols or tools were tested as outlined in the column “Tested alternatives”.

3.1.4.3 Inter-individual variability between piglets hampers microbiota analysis

Analysis of the 36 fecal samples with the final protocol resulted in the identification of 12,012 unique protein groups (Suppl. table S10). Hierarchical clustering analysis showed that clustering was mainly based on individual. In addition, sibling pairs (Ctrl1/ChA1, Ctrl2/ChA2, and Ctrl5/ChA5), and co-housing of animals affected sample clustering (Ctrl3, Ctrl4 and Ctrl6 vs. ChA3, ChA4 and ChA6, see Table 3.1.4) (Figure 3.1.24).

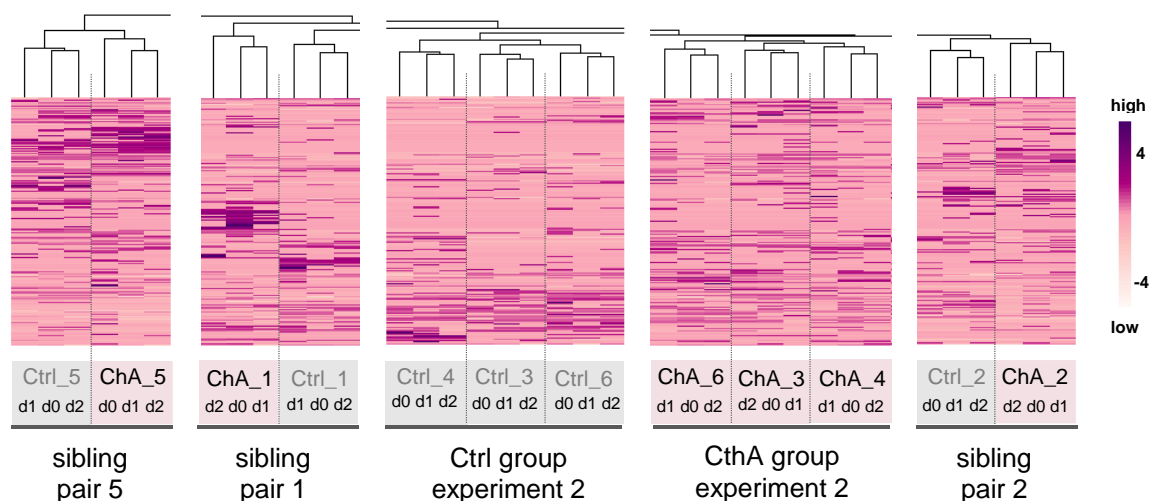


Figure 3.1.24: Hierarchical clustering of feces samples from untreated and ChA-treated animals. Relative intensities were scaled row-wise and subjected to hierarchical clustering. Clustering of all identified protein groups indicated high similarity in the metaproteome profiles of samples from the same animal. In addition, samples of related animals and co-housed animals clustered together. The color gradient indicates high (orange) and low (blue) abundance of a protein in a sample.

On average, 3,500 bacterial/archaeal protein groups were identified per sample (Figure 3.1.25 A). The number of identified protein groups varied between animals. However, at least in the control group numbers were comparable between days for single animals (Figure 3.1.25 A). In contrast, the numbers of the identified protein groups dropped in the ChA-treated animals with the exception of piglet 5 (Figure 3.1.25 A). Most protein groups were annotated as bacterial (80.4%), whereas the remaining protein groups were of host (13.1%), food (4.2%), archaeal (0.7%), parasitic (0.14%) or viral (0.02%) origin (Figure 3.1.25 B). The relative abundance of identified food protein, especially of straw proteins, was more variable in the ChA-treated group than in the control group (Figure 3.1.25 B & C).

Results

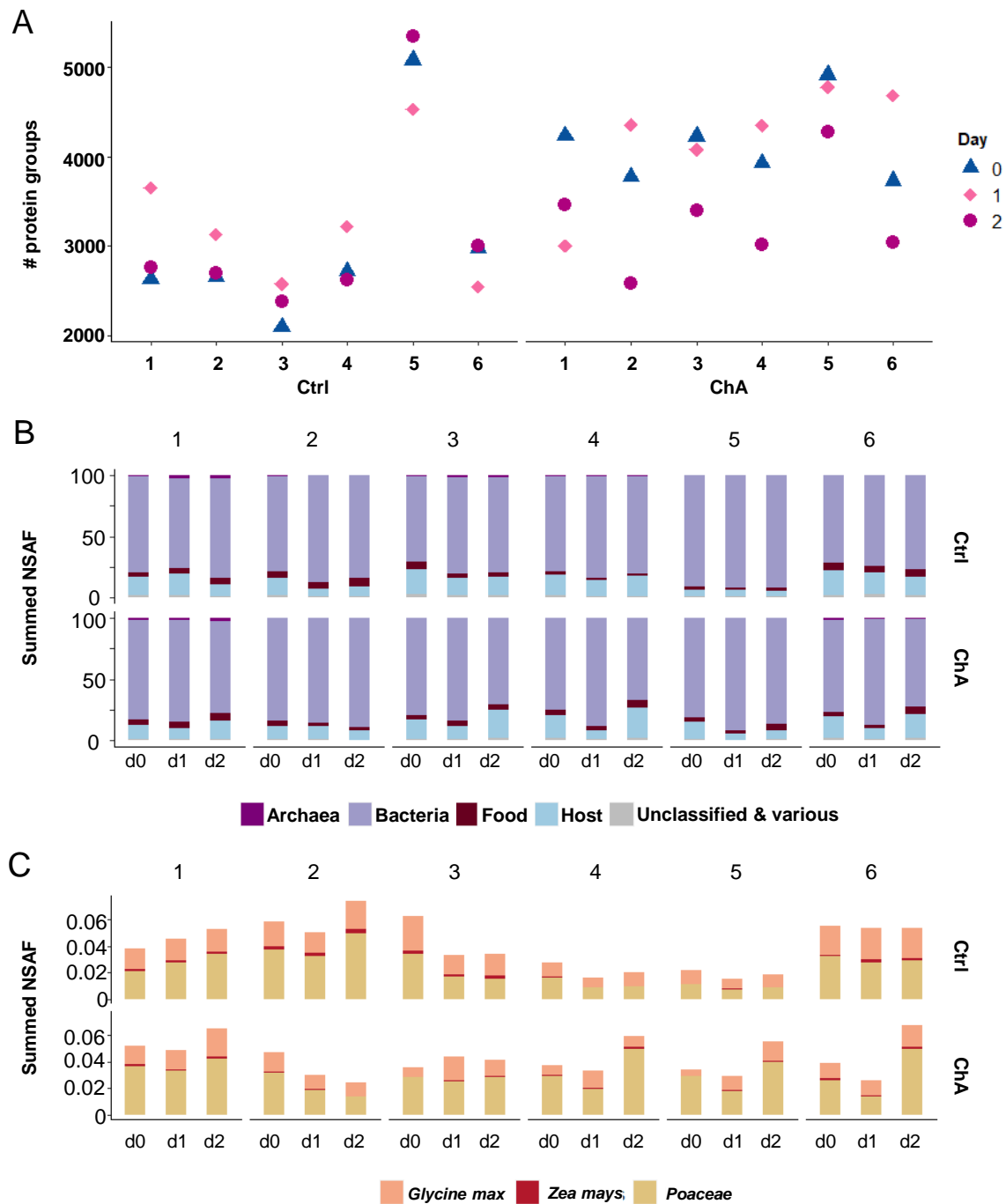


Figure 3.1.25: Taxonomic composition of fecal samples on protein level. (A) The number of identified bacterial protein groups varied between piglets (numbered 1 to 6) and were lower for ChA-treated piglets (ChA) compared to the control group (Ctrl) on day 2. **(B)** Most protein groups were of bacterial origin or were annotated as food or host proteins. **(C)** Variation in identified protein groups between days and animals might partly result from different food intake of piglets as suggested by variations of the summed NASF for soy (*Glycine max*), maize (*Zea mays*) and straw (*Poaceae*). Piglets with the same number are siblings. NSAF: Normalized spectral abundance factor. Animals with the same number present siblings.

3.1.4.4 Taxonomic stability of the piglet microbiota following ChA treatment

The drop in identified bacterial protein groups indicated an effect of ChA treatment on the microbiota of fecal samples from the ChA-treated piglets. First, the taxonomic composition of fecal samples was analyzed to evaluate whether ChA treatment reduced the bacterial load in general or diminished the abundance of specific taxa or functional groups. On average, the group of bacterial and archaeal proteins was dominated by protein groups affiliated to the phyla Firmicutes and Bacteroidetes (Figure 3.1.26 A). On lower levels most protein groups were affiliated to the classes Clostridia and Bacteroidia with a predominance of *Prevotellaceae* (Bacteroidia) on the family level followed by the *Ruminococcaceae*, the *Lachnospiraceae* and the *Clostridiaceae* (Clostridia) (Figure 3.1.26 A). Analysis of the Shannon diversity of microbial communities from all samples suggested that the diversity of the microbial community of some ChA-treated piglets, especially on day 2, was reduced compared to day 0, whereas the diversity of the microbial community of piglets from the control group did not change over days. In particular, for piglets 2, 5, and 6 the Shannon diversity and the numbers of identified genera dropped (Figure 3.1.26 B & C), which is line with the results from 16S rRNA gene sequencing-based data reported previously (Bublitz *et al.*, in revision).

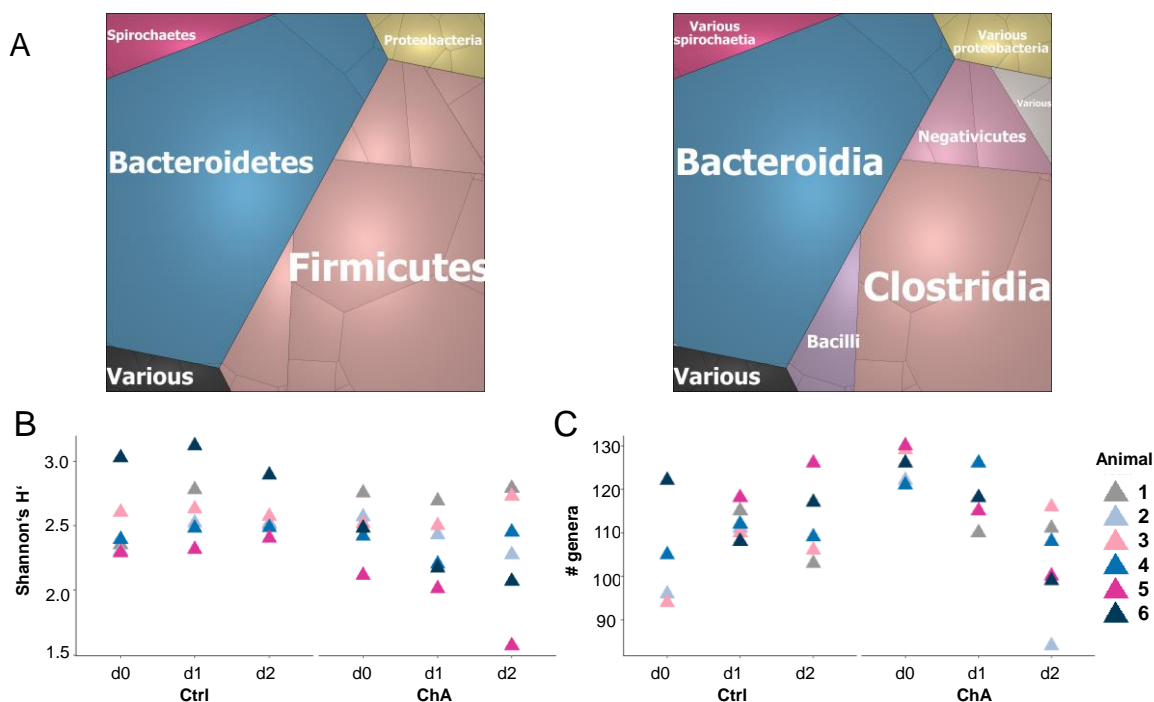


Figure 3.1.26: Taxonomic profile of the piglet intestinal microbiota and its diversity over during the feeding trial with ChA. (A) The bacterial community of feces samples was dominated by the phyla Firmicutes and Bacteroidetes, which were in turn dominated by the classes Clostridia and Bacteroidia. **(B)** Shannon diversity indices dropped for some ChA-treated animals and **(C)** concomitantly decrease the number of genera identified by the metaproteomics analysis decreased. Animals with the same number in the two treatment groups present siblings.

Results

Based on the observed reduction of the Shannon diversity of microbial communities from ChA-treated animals, it was hypothesized that community composition of samples from ChA-treated piglets following treatment could be different from the community composition of samples from day 0. Non-metric multidimensional scaling (NMDS) of all bacterial and archaeal protein groups on the taxonomic level, more specifically on family level, indicated a clustering of samples by individual. However, NMDS did not indicate an effect of ChA-treatment on the microbiota composition as indicated by clustering of samples from all three days for ChA-treated and untreated samples (Figure 3.1.27).

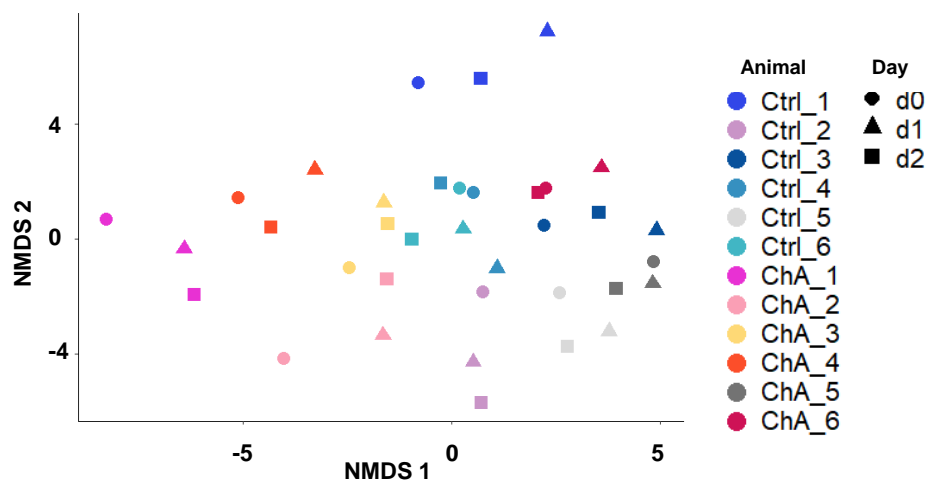


Figure 3.1.27: NMDS plot of fecal samples from ChA- and untreated piglets on family level. Non-metric multidimensional scaling (NMDS) of all bacterial and archaeal protein groups on family level indicated clustering of fecal samples from the same animal and of fecal samples from related and co-housed animals.

Accordingly, individual fecal community profiles were comparable between animals and days for the major bacterial phyla Clostridia, Bacteroidia and Proteobacteria (Figure 3.1.28). For the ChA-treated piglets 1, 2, 5 and 6 a trend towards slightly reduced relative abundance of Clostridia could be observed. However, statistical analysis using the R packages *limma* on class, order and family level to test for significant changes between the two treatment groups or between fecal samples from the earlier and the later sample points accordingly did not indicate significant changes within the community profiles on taxonomic level. A likely reason for this is that microbial community profiles of each piglet were so diverse that they obscured treatment-related differences.

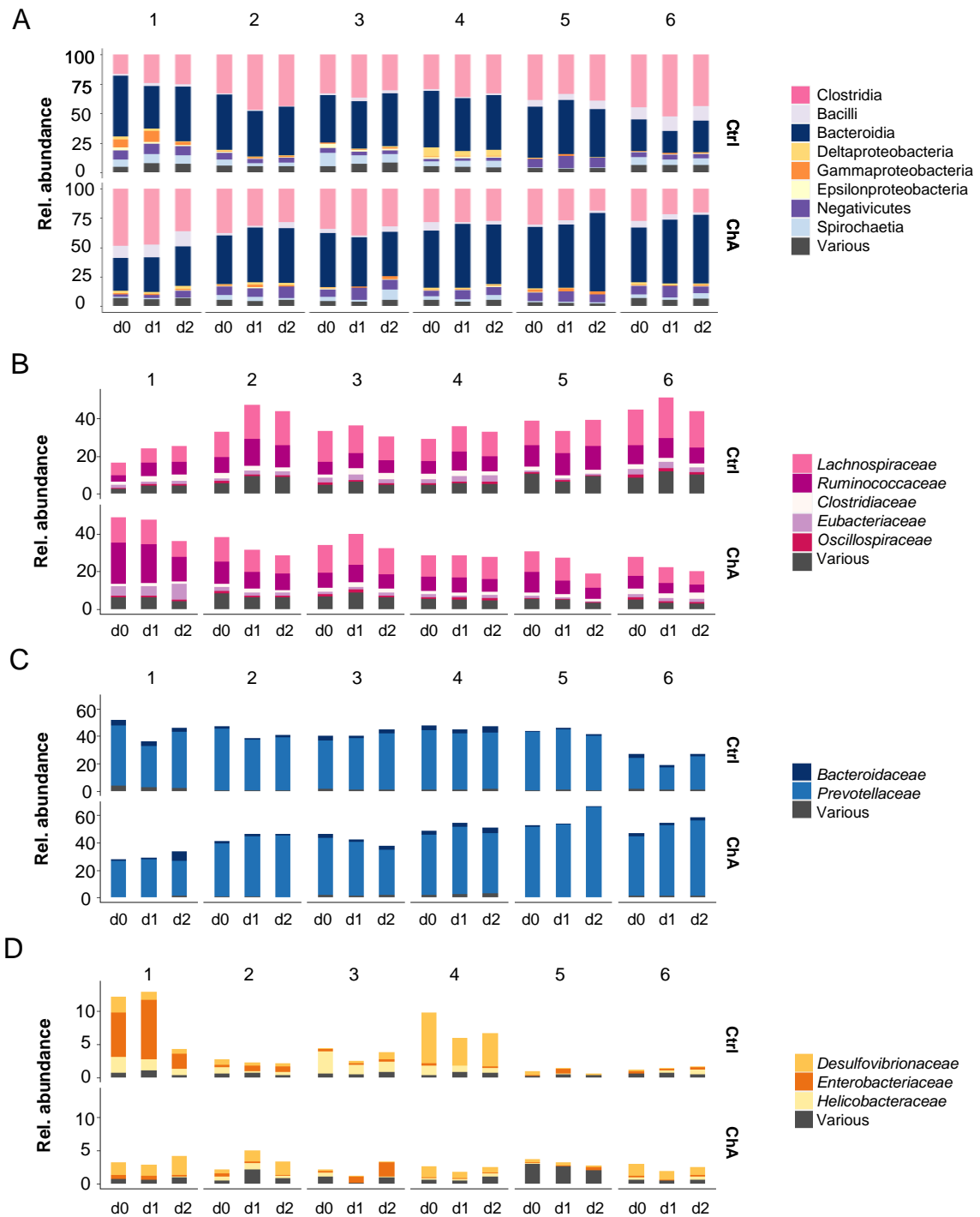


Figure 3.1.28: Detailed taxonomic profiles of untreated and ChA-treated piglets before and two days following treatment. (A) Taxonomic profiles of individual animals before (day 1) and on day 2 and 3 following treatment on class level were mostly stable in untreated as well as ChA-treated animals. **(B)** A slight reduction was observed for the class Clostridia and its most prevalent families in some ChA-treated animals. **(C)** By contrast, a slight increase of the class Bacteroidia and its most prevalent families was observed in the same animals. **(D)** The class of the proteobacteria, which often blooms following antibiotic therapy did not respond to the ChA-treatment. Animals with the same number present siblings.

Results

3.1.4.5 Functional stability of the piglet microbiota after ChA administration

Given the only minor changes on the taxonomic composition of piglet fecal samples, it was speculated that the functional composition of the samples is likewise not affected by ChA treatment. Most identified protein groups were assigned to the three main eggNOG categories “metabolism”, “information storage and processing” and “cellular processes and signaling” (Figure 3.1.29 A). This is as expected given their high abundance in the bacterial cell (Turnbaugh *et al.*, 2009; Verberkmoes *et al.*, 2009). In particular, a majority of the protein groups were either assigned to energy production and conversion, carbohydrate transport and metabolism or amino acid transport and metabolism. In addition, many proteins were involved in translation and post-translational modification (translation, ribosomal structure and biogenesis; posttranslational modification, protein turnover, chaperons). As expected, the functional profiles of the different fecal samples from untreated and ChA-treated piglets were stable for all animals and days on the first level (Figure 3.1.29 B).

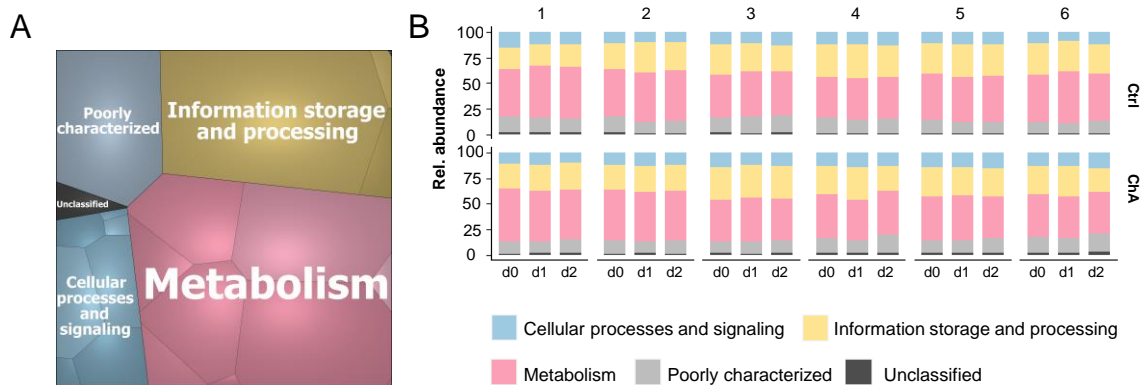


Figure 3.1.29: The microbiota profile on functional level. (A) 84.8% of all identified protein groups were assigned to the three main eggNOG categories Metabolism, Information storage and processing and Cellular processes and signaling and their averaged proportion is displayed in the left panel. An overview on the subfunctions of the respective categories is given on the right. **(B)** Comparative analysis of the functional microbiota of all piglet feces samples revealed that the functional assignment is highly conserved among piglets, stable over the days and independent of the ChA-treatment. Animals with the same number present siblings.

NMDS of bacterial and archaeal protein groups on the eggNOG sub-category level indicated a clustering of samples from the same piglet for the control group with the exception of samples from piglets of the first trial (Ctrl_1 & Ctrl_2). In contrast, samples of ChA-treated piglets formed less distinct clusters and either samples from day 1 or day 2 or both days were found less close to the sample point from day 0 (Figure 3.1.30).

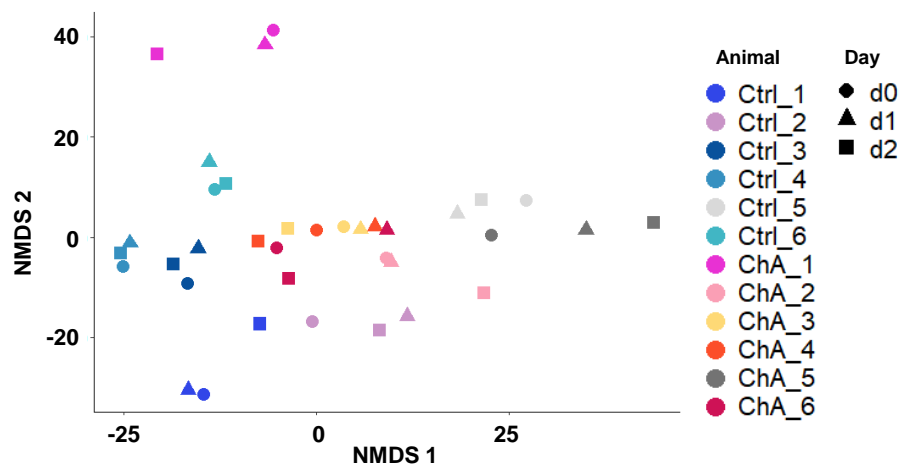


Figure 3.1.30: NMDS plot of fecal samples from ChA- and untreated piglets on functional level indicates individual profiles of samples derived from the same animal. NMDS of all bacterial and archaeal protein groups on eggnoG sub-category level indicated clustering of fecal samples from the same animal and more dense clusters of fecal samples from untreated piglets compared to ChA-treated piglets. Animal name code: “treatment_sibling pair”.

Since the NMDS plot suggested differences in the functional composition of the fecal samples from ChA-treated piglets between day 0 and the days following treatment, a statistical analysis using the R package *limma* was conducted to possibly identify changes between samples from ChA-treated and untreated animals as well as between days. Since no significant differences were identified as before on taxonomic level, it was speculated that the observed trends in the NMDS plot were individual for each piglet. Therefore, functional profiles were analyzed by comparing individual functional profiles of fecal samples from ChA-treated and untreated piglets. Given that disturbed metal homeostasis was observed in this thesis in *C. difficile* following ChA/ChB1-Epo2 stress, and the role of selenium metabolism for chlorotoni susceptibility proposed here, a particular attention was given to the sub-categories “cell envelope biogenesis”, “inorganic ion transport and metabolism” and “coenzyme transport and metabolism” (Figure 3.1.31 A, B & C). Moreover, the categories “amino acid transport and metabolism” and “carbohydrate metabolism” were analyzed in more detail (Figure 3.1.31 D, E). However, no marked differences were found between ChA-treated and untreated animals and between samples from different days for any of the functional categories. A likely reason for this could be that, e.g., the categories “cell wall/membrane/envelope biogenesis” and “inorganic ion transport and metabolism” were dominated by TonB-dependent transporters and OmpA-family proteins affiliated to Bacteroidetes families.

Results

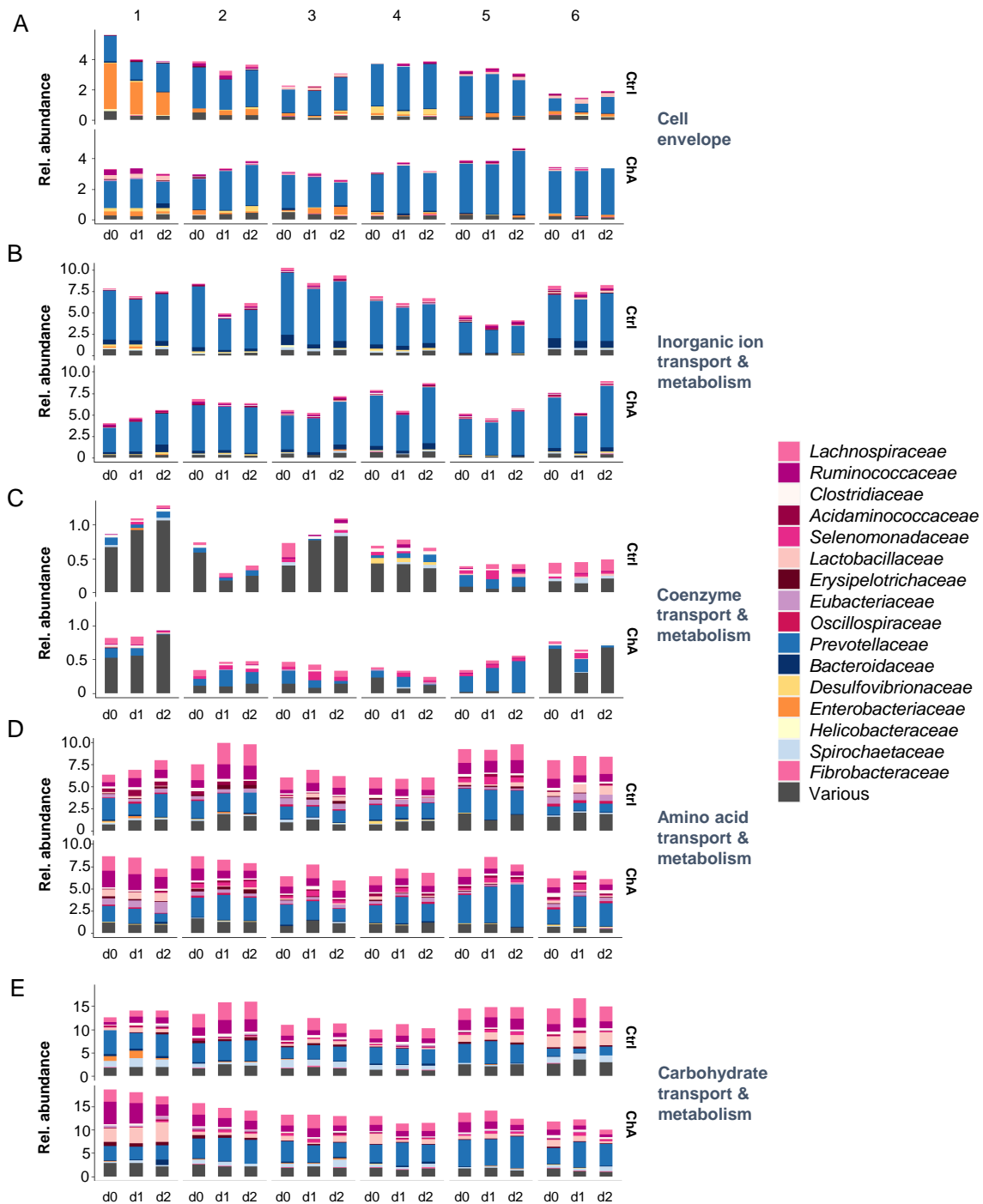


Figure 3.1.31: Detailed functional profiles of untreated and ChA-treated piglets before and two days following treatment for selected functional subcategories. The functional repertoire of feces samples from untreated and ChA-treated piglets before and two days following treatment was visually analyzed on eggNOG "sub" level. The total abundance of protein groups assigned to selected functions and the relative contribution of bacterial families to the respective functions are presented. **(A)** Cell wall/membrane/envelope biogenesis. **(B)** Inorganic ion transport and metabolism **(C)** Coenzyme transport and metabolism **(D)** Amino acid transport and metabolism **(E)** Carbohydrate transport and metabolism. Animals with the same number present siblings.

Finally, the metaproteomics dataset was searched for proteins affiliated with the selenocompound and cobalamin metabolism, and the proline and glycine reductase subunits to specifically test for changes in the abundance of these protein groups. However, only two protein groups annotated as selenate reductases, YgfK subunits were identified in one and five of 36 samples and a cobalamin synthesis protein was identified in seven of 36 samples. Similarly, only 15 different protein groups annotated as either D-proline reductase (9) or selenoprotein B, glycine betaine sarcosine D-proline reductase family protein (6) were identified in one to 30 of 36 samples. Since these protein groups were underrepresented in the dataset, they did not allow for reliable statistical analysis.

In conclusion, *C. difficile* and close relatives are particularly sensitive to chlorotonils, which is eventually linked to their dependency on selenium-dependent enzymes and cobalamin biosynthesis. Moreover, chlorotonil treatment affected the metabolism of *C. difficile* 630 and *T. glycolicus* DSM 1288, in particular the metal homeostasis possibly due to the ability of chlorotonils to bind divalent metals. In addition, diverse pathways were affected by chlorotonil treatment suggesting global disturbance of the cellular homeostasis following chlorotonil treatment. In contrast, the highly complex of the piglet microbiota was only marginally affected by ChA treatment.

Results

3.2 Myxopyronin B as potential novel antibiotic for *C. difficile* therapy

The panel of antibiotics recommended for the treatment of *C. difficile* infections includes two RNA polymerase inhibitors. First, fidaxomicin, which targets the RNA polymerase's "switch region", is considered the current gold standard for therapy of *C. difficile* infections (Louie *et al.*, 2012). In addition, rifaximin, which binds adjacent to the active center of the RNA polymerase, is recommended as post-vancomycin chaser for severe cases of *C. difficile* infections (Ng *et al.*, 2019). RNA polymerase inhibitors seem to be well suited for the therapy of *C. difficile* infections, which is amongst others attributed to their selectivity *in vivo* (Ponziani *et al.*, 2017). In this light, it can be speculated that other RNA polymerase inhibitors, especially other "switch region inhibitors", might be valuable alternatives for the treatment of *C. difficile* infections in the case that they do not show cross-resistance with fidaxomicin. Therefore, the "switch region" inhibitor myxopyronin B was evaluated as potential new lead structure for the design of new antibiotics for the therapy of *C. difficile* infections.

The results of this study have been published in Gut Pathogens in 2022 and are reviewed in more detail in the following section.

Brauer M., Herrmann J., Zühlke D., Müller R., Riedel K., and Sievers S. Myxopyronin B inhibits growth of a Fidaxomicin-resistant *Clostridioides difficile* isolate and interferes with toxin synthesis. *Gut Pathogens* **14**, 4 (2022).

<https://doi.org/10.1186/s13099-021-00475-9>

3.2.1 Myxopyronin B is active against *C. difficile* including fidaxomicin-resistant strains but spares other intestinal anaerobes

As a starting point, minimal inhibitory concentrations of myxopyronin A and B as well as rifaximin against a selection of *C. difficile* strains belonging to five different ribotypes were determined in serial broth dilution assays to confirm the activity of myxopyronins against *C. difficile*. As expected from previous reports, all strains were susceptible to myxopyronins with minimal inhibitory concentrations ranging between 0.125 µg/ml and 16 µg/ml (Table 3.2.1). However, four of the strains were slightly more susceptible to myxopyronin B and all strains were more susceptible to rifaximin (Table 3.2.1).

Table 3.2.1: Minimal inhibitory concentrations of myxopyronin A and B and rifaximin against five different *C. difficile* strains in µg/ml according to serial broth dilution assays after 24 h of growth in BHIS. n ≥ 3.

	630	1780	R20291	rt126	rt78
Myxopyronin A	8	0.5	16	1	1
Myxopyronin B	8	0.125	4	0.25	0.5
Rifaximin	0.002	0.004	0.004	0.002	0.002

To exclude cross-resistance between fidaxomicin and myxopyronins, which both bind to the switch region of the RNA polymerase (Mukhopadhyay *et al.*, 2008), serial broth dilution assays were repeated for strain 630 and an additional fidaxomicin-resistant isolate, Goe-91 (Schwanbeck *et al.*, 2019). This time fidaxomicin was included. As expected, the minimal inhibitory concentration of fidaxomicin against strain Goe-91 was substantially higher with 128 µg/ml compared to 0.0125 µg/ml against strain 630 (Table 3.2.2). Nevertheless, minimal inhibitory concentrations of myxopyronin B and rifaximin against both *C. difficile* strains were equal with 8 µg/ml and 0.002 µg/ml, respectively (Table 3.2.2).

Table 3.2.2: Minimal inhibitory concentrations of rifaximin, fidaxomicin and myxopyronin B for *C. difficile* strains 630 and Goe-91 in µg/ml according to serial broth dilution assays after 24 h of growth in BHIS. n ≥ 3.

	630	Goe-91
Rifaximin	0.002	0.002
Fidaxomicin	0.015625	128
Myxopyronin B	8	8

Results

Next, the susceptibility of other selected anaerobic bacteria from the gastrointestinal tract to myxopyronin B was tested. As a pre-requisite, antibiotics for the therapy of *C. difficile* infections should ideally spare the healthy intestinal microbiota as outlined in the previous sections (Jenior *et al.*, 2018). *C. scindens* was found to be as susceptible as *C. difficile* and *Terrisporobacter* sp. was inhibited by 16 µg/ml (Table 3.2.3). In contrast, *B. longum* as well as the Gram-negative representative *B. fragilis* were not inhibited by 16 µg/ml, which was the highest concentration that could be tested against all strains. *L. casei* and *B. thetaiotaomicron*, for which higher concentrations could be tested as well, showed a growth inhibition in the presence of 64 µg/ml or were even able to grow with this concentration (Table 3.2.3).

Table 3.2.3: Minimal inhibitory concentrations of myxopyronin B against six commensal intestinal anaerobes in µg/ml according to serial broth dilution assays after 24 h of growth in BHIS. $n \geq 3$. *Terrisp.* = *T. glycolicus*, *B. theta* = *B. thetaiotaomicron*. $n \geq 3$.

	<i>L. casei</i>	<i>B. longum</i>	<i>C. scindens</i>	<i>Terrisp.</i>	<i>B. fragilis</i>	<i>B. theta.</i>
Myxopyronin B	> 64	> 16	2	16	> 16	64

3.2.2 The stress responses of *C. difficile* 630 to rifaximin, fidaxomicin, and myxopyronin B
Based on the similar binding sites of myxopyronin B and fidaxomicin it was assumed that myxopyronin B might have similar beneficial features as fidaxomicin. For instance, fidaxomicin is known to reduce sporulation and toxin production in *C. difficile* and to kill its germinating spores via a hitherto still not fully understood mechanism (Louie *et al.*, 2012; Aldape *et al.*, 2017). With the aim to get a global overview on how myxopyronin B affects *C. difficile*'s metabolism, a comparative LC-MS/MS approach was applied to analyze the effect of myxopyronin B on *C. difficile* in direct comparison to fidaxomicin and rifaximin. *C. difficile* cells were exposed to sublethal concentrations of either rifaximin (1.75 ng/ml), fidaxomicin (6 ng/ml) or myxopyronin B (500 ng/ml), or were treated with the solvent, DMSO, only, in mid-exponential phase and were allowed to grow in the presence of the antibiotics for 90 minutes (Suppl. figure S3 D-F). Subsequently, their proteome was analyzed by LC-MS/MS as described in section 3.1.3.

Overall, 1612, 1667, 1613 and 1579 proteins were identified with a minimum of 2 unique peptides in at least two out of three biological replicates in the DMSO-, rifaximin-, fidaxomicin- and myxopyronin B-sample sets (Suppl. table S11). The vast majority of proteins (1474) were shared between all stress conditions. In addition, 12 proteins were exclusively identified in the DMSO sample set, 26 proteins were exclusively identified in the rifaximin-treated cells, 16 proteins were exclusively identified in the fidaxomicin-treated cells

and 8 proteins were exclusively identified in the myxopyronin B-treated cells. Several more proteins were shared between two or three cultivation conditions but were not identified in all sample conditions (Figure 3.2.1 A). A majority of proteins were assigned to the functional categories “protein metabolism”, “energy metabolism” and “DNA and RNA metabolism” (Figure 3.2.1 B, left panel). Moreover, about 70% of the identified proteins were of cytosolic origin according to PSORTb. In addition, 11% of proteins were membrane proteins, 2% were cell wall proteins, 1% were extracellular proteins and 14% proteins could not be assigned by PSORTb (Figure 3.2.1 B, right panel). Statistical analysis followed by hierarchical cluster analysis revealed significant changes between all stress conditions (Figure 3.2.1 C). Overall, similar pathways were affected by all three antibiotics or shared between at least two antibiotics, whereas some changes were specific for a respective antibiotic (Figure 3.2.1 C).

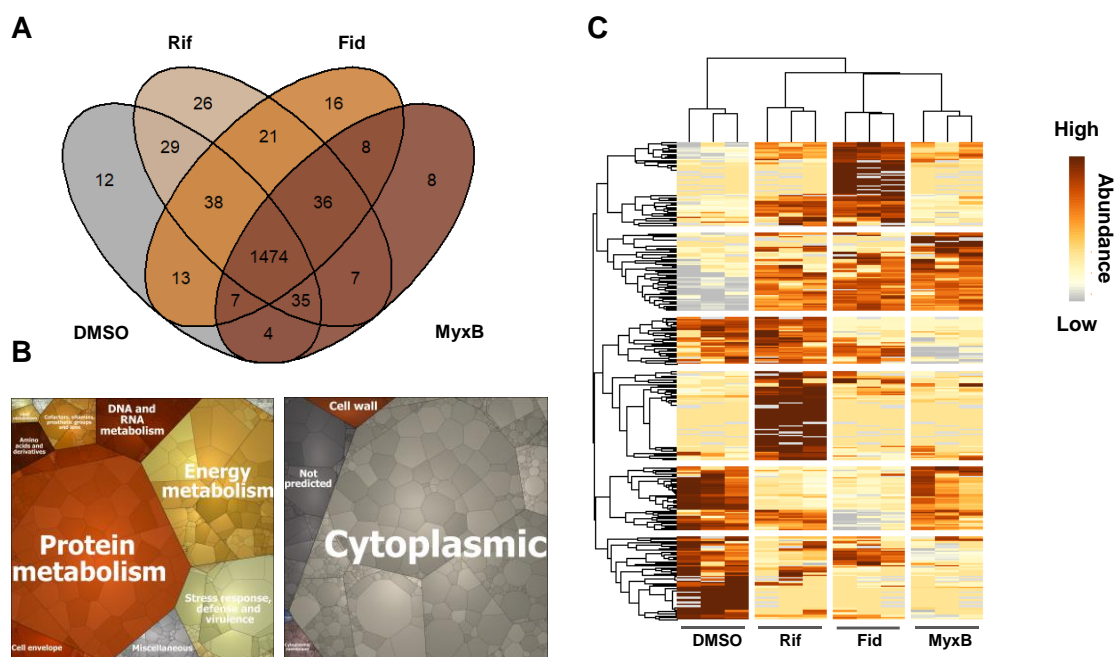


Figure 3.2.1: Comparative proteome analysis of rifaximin-, fidaxomicin- and myxopyronin B-treatment in *C. difficile*. (A) All proteins identified with at least two unique peptides in at least two out of three biological replicates in a respective condition are displayed within a Venn diagram. (B) Left panel: Identified proteins were visualized as Voronoi treemaps. Every cell represents an identified protein, which were clustered according to their functional assignments. Right panel: PSORTb analysis of all identified proteins revealed that a majority of proteins belonged to the cytosolic fraction with additional proteins belonging to the cytoplasmic membrane, cell wall and extracellular fractions. In addition, 14% of proteins could not be assigned. Cell size correlates with overall abundance of the protein inside the cell. (C) All proteins, which were found in significantly altered amounts after treatment with at least one antibiotic or which were either exclusively identified in at least one treatment condition or exclusively in the DMSO-treated cells are displayed as a heatmap. DMSO: DMSO-treated cells; Rif: rifaximin-treated cells; Fid: fidaxomicin-treated cells; MyxB: myxopyronin B-treated cells. Adapted from Brauer *et al.* (2022).

Results

Proteins with significantly altered abundance were found in several metabolic pathways suggesting substantial remodeling of the cellular metabolism. For instance, proteins from various functional categories such as, flagella synthesis and membrane transport were found more abundant after treatment with all three antibiotics, whereas proteins for the biosynthesis of cysteine as well as some phage proteins were lower abundant after treatment with each antibiotic (Figure 3.2.2). In contrast, differences between the three signatures were observed for proteins from other functional categories, especially the energy metabolism. For example, proteins required for branched chain amino acid fermentation were found in lower amounts in myxopyronin B-treated cells compared to all other conditions while proteins from the butyrate fermentation pathway were reduced in fidaxomicin- and rifaximin-treated cells. Most strikingly, chemotaxis proteins were among the proteins that were exclusively identified in rifaximin-treated cells (Figure 3.2.2). As none of these effects seem to be directly linked to the antibiotics' mode-of-action or accountable for other important clinical effects of the antibiotics, these findings are not further discussed.



Figure 3.2.2: Changes in the proteome signature of *C. difficile* upon treatment with rifaximin, fidaxomicin and myxopyronin B. Proteomics stress signatures *C. difficile* cells treated with sublethal concentrations of rifaximin, fidaxomicin, and myxopyronin B were visualized as Voronoi treemaps. Every cell represents an identified protein, which were clustered according to their functional assignments. Cell size correlates with overall abundance of the protein inside the cell and color code represents the log₂ fold change of treated vs. untreated cells. Light colors = low abundance; dark colors = high abundance.

3.2.3 Myxopyronin B interferes with toxin synthesis in *C. difficile*

In order to further evaluate whether myxopyronin B might be similarly efficient for the cure of *C. difficile* infections as fidaxomicin, the proteome signature data of myxopyronin B-treated *C. difficile* cells were screened towards a possible reduction of the pathogen's virulence. Indeed, this analysis revealed that the abundance of toxin A (TcdA) in myxopyronin B-treated cells was, similarly to fidaxomicin-treated cells, lower compared to the DMSO controls (\log_2 fold change -1.5 and -1.9). In contrast, toxin A levels were twice as high in the rifaximin-treated cells compared to the controls (\log_2 fold change 1.9) (Figure 3.2.3 A). To validate this effect and to get additional information on the production levels of toxin B, which was not identified by mass spectrometry, protein samples from the stress experiment were re-analyzed by Western blot analysis with antibodies directed against either toxin A or toxin B, respectively. As observed in the proteomics data set, toxin A levels were higher after rifaximin treatment while toxin A levels were lower after fidaxomicin and myxopyronin B treatment compared to the controls (Figure 3.2.3 B). This effect was even more pronounced for toxin B. Although toxin B levels in fidaxomicin- and myxopyronin B-treated cells were not much reduced compared to the controls as observed for toxin A, toxin B levels were significantly lower in fidaxomicin- and myxopyronin B-treated cells than in rifaximin-treated cells (Figure 3.2.3 B).

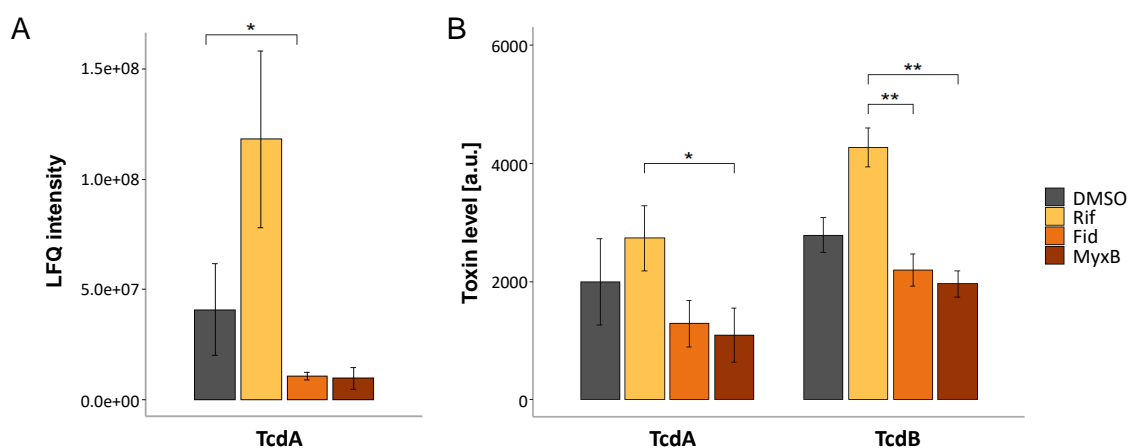


Figure 3.2.3: Both, fidaxomicin- and myxopyronin B suppressed early phase toxin synthesis. (A) LFQ protein intensities of toxin A (TcdA) in *C. difficile* after treatment with rifaximin, fidaxomicin, myxopyronin B or DMSO only. **(B)** Toxin A (TcdA) and B (TcdB) levels in *C. difficile* after treatment with rifaximin, fidaxomicin, myxopyronin B or DMSO only according to Western blot analysis. DMSO: DMSO-treated cells; Rif: rifaximin-treated cells; Fid: fidaxomicin-treated cells; MyxB: myxopyronin B-treated cells; p values: * ≤ 0.05 , ** ≤ 0.01 . [a.u.]: artificial units. Adapted from Brauer *et al.* (2022).

Results

3.3 The response of *C. difficile* to dissipation of the membrane potential by amidochelocardin

Chelocardin and its derivative amidochelocardin have broad-spectrum activity against several oxygen-tolerant Gram-positive and Gram-negative bacteria, such as *Enterococcus faecalis*, *Klebsiella* spp. and *S. aureus* (Lešnik *et al.*, 2015; Hennessen *et al.*, 2020). While chelocardin was previously shown to target both, the ribosome and the cell membrane (Oliva *et al.*, 1992; Stepanek *et al.*, 2016), the bactericidal effect of amidochelocardin seems to be restricted to the bacterial cell membrane (Senges *et al.*, 2020). Despite tremendous efforts to reduce the prescription of broad-spectrum antibiotics due to the high number of adverse events, including secondary infections with *C. difficile*, broad-spectrum antibiotic therapy is still required under certain circumstances (L. Evans *et al.*, 2021; Rhee *et al.*, 2021). Since not all broad-spectrum antibiotics equally prime patients to an infection with *C. difficile* (Gerding, 2004; Webb *et al.*, 2020), the question should be addressed to which extent chelocardin therapy might render patients susceptible to *C. difficile*. Therefore, the susceptibility of *C. difficile* and other anaerobes to chelocardins was assessed. In addition, amidochelocardin was used to study how *C. difficile* generally responds to surface-active antibiotics with respect to the promising role of the membrane as antibiotic target (Wu *et al.*, 2013).

The results of this study have been published in mSphere and are reviewed in more detail in the following section.

Brauer M., Hotop S.K., Wurster M., Herrmann J., Miethke M., Schlüter R., Zühlke D., Brönstrup M., Lalk M., Müller R., Sievers S., Bernhardt, J. Riedel, K.

Clostridioides difficile Modifies its Aromatic Compound Metabolism in Response to Amidochelocardin-Induced Membrane Stress. *mSphere*, e0030222. doi:

10.1128/msphere.00302-22

<https://journals.asm.org/doi/10.1128/msphere.00302-22>

3.3.1 Susceptibility of *C. difficile* and selected anaerobic bacteria to chelocardins

The susceptibility of several anaerobic bacteria to chelocardin and amidochelocardin was evaluated in serial broth dilution assays as done in the previous sections. The obtained results revealed that all tested *C. difficile* strains were similarly susceptible to both chelocardin and amidochelocardin with minimal inhibitory concentrations of 2 µg/ml or 4 µg/ml, respectively (Table 3.3.1). In comparison, minimal inhibitory concentrations of the typical tetracycline doxycycline ranged between 0.03125 µg/ml for the more susceptible strains and 8 µg/ml for strain 630 known to encode for the tetracycline resistance marker *tetM* (Table 3.3.1).

Table 3.3.1: Minimal inhibitory concentrations of chelocardin (CHD), amidochelocardin (CDCHD) and doxycycline against five different *C. difficile* strains in µg/ml according to serial broth dilution assays after 24 h of growth in BHIS. n ≥ 3.

	630	1780	R20291	rt126	rt78
CHD	2	2	2	2	4
CDCHD	2	4	4	2	2
Doxycycline	8	0.03125	0.03125	4	1

Likewise, all other anaerobic bacteria were similarly susceptible to amidochelocardin (Table 3.3.2). Minimal inhibitory concentrations were comparable to the minimal inhibitory concentrations between 2 µg/ml and 16 µg/ml observed previously for other aerobic pathogens such as *Enterococcus faecalis*, *Klebsiella* spp. and *S. aureus* (Lešnik *et al.*, 2015; Hennesen *et al.*, 2020).

Table 3.3.2: Minimal inhibitory concentrations of amidochelocardin (CDCHD) against seven commensal intestinal anaerobes in µg/ml according to serial broth dilution assays after 24 h of growth in BHIS. n ≥ 3. *Terrisp.* = *T. glycolicus*, *B. theta* = *B. thetaiotaomicron*. n ≥ 3.

	<i>L. casei</i>	<i>B. longum</i>	<i>C. scindens</i>	<i>Terrisp.</i>	<i>T. glycolicus</i>	<i>B. fragilis</i>	<i>B. theta.</i>
CDCHD	4	0.5	2	2	2	4	4

A more detailed analysis of the proteome stress signature revealed four major findings including 16 proteins, which were higher abundant following amidochelecardin treatment in a concentration-dependent manner (Figure 3.3.2). First, a significantly higher abundance of ClnR and ClnA from the antimicrobial peptide efflux system ClnAB could be observed. Second, all proteins from the operon encoding chorismate biosynthesis enzymes and the two enzymes required for biosynthesis of the aromatic amino acids phenylalanine and tyrosine were found in increasing amounts upon treatment. Third, two putative phenazine biosynthesis proteins, CD630_17610 and CD630_30350, and an additional protein encoded adjacent to the respective enzymes, CD630_17590 and CD630_30340, were found to be the most significantly enriched proteins. Last, a PadR-type regulator putatively involved in mediating a phenol stress response was found in higher amounts upon treatment (Figure 3.3.2).

In addition, a leucine-sodium symporter was one of the two significantly lower abundant proteins and 40% of all proteins that were exclusively identified in the control samples but not in the samples treated with the highest concentration (OFF) were either membrane or membrane transport-associated proteins (Suppl. table S12).

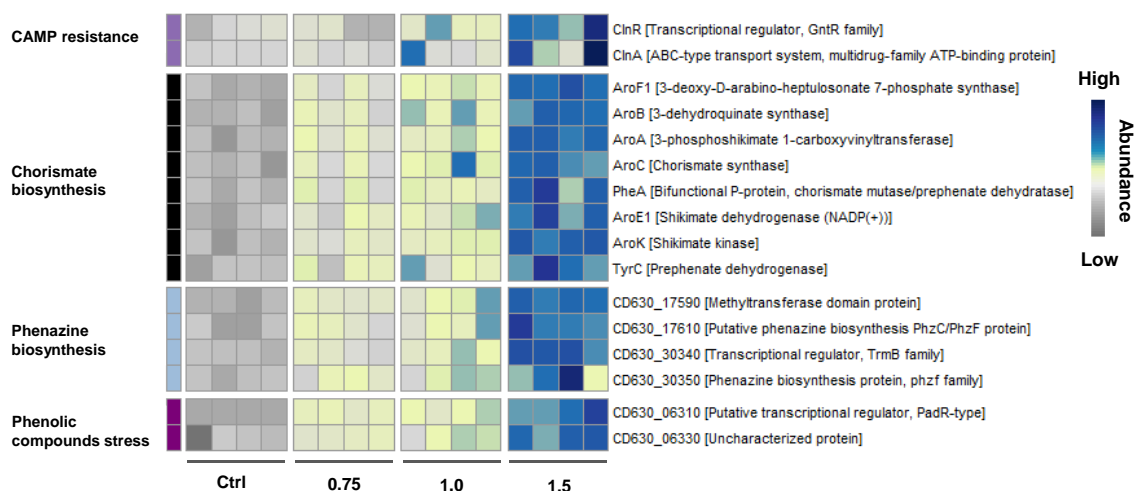


Figure 3.3.2: The proteome response of *C. difficile* to increasing concentrations of amidochelecardin is characterized by increased abundance of 16 proteins. 16 proteins, which were higher abundant upon amidochelecardin treatment in a concentration-dependent manner, belonged to four different functional categories. Z-transformed abundances are displayed as a heatmap. CAMP: cationic antimicrobial peptides. Adapted from Brauer *et al.* (re-submitted).

The evenly increased abundance of proteins of predicted operons suggested that the observed effects are regulated on transcriptional level. Consequently, the expression of selected genes from the five putative transcriptional units were analyzed by qPCR validating the effects observed on proteome level (Figure 3.3.3).

Results

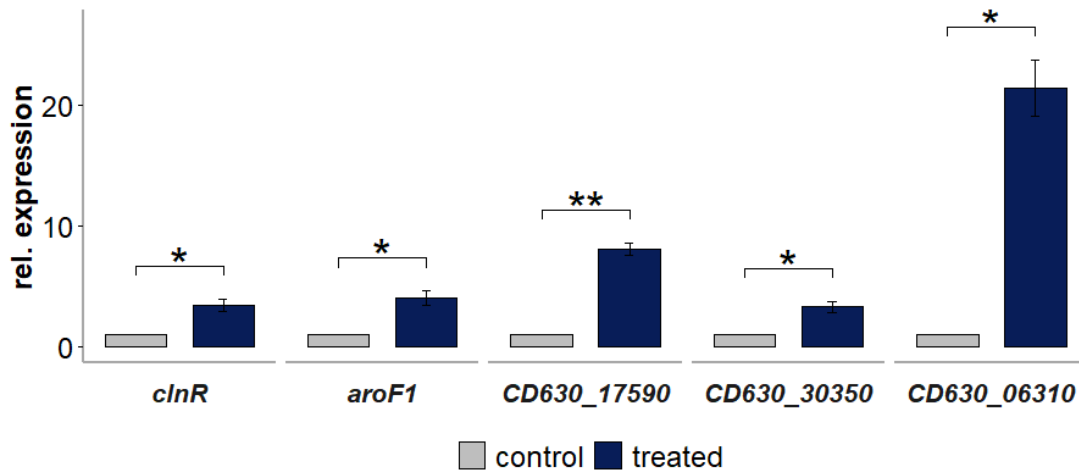


Figure 3.3.3: mRNA expression levels of represented genes from the putative operons encoding proteins of higher abundance following amidochelocardin stress. One gene of each putative operon was selected and its relative expression following treatment with 1.5 µg/ml amidochelocardin was analyzed by qPCR. Adapted from Brauer *et al.* (re-submitted).

3.3.3 Amidochelocardin accumulates in the membrane of *C. difficile* but does not cause cell deformation

To validate the membrane-directed activity of amidochelocardin indicated by the higher abundance of ClnRAB and lower abundance of many membrane-associated proteins, the membrane potential of *C. difficile* 630 cells in the presence of increasing amidochelocardin concentrations was analyzed in five-minute intervals using the cationic fluorescent dye DISC₅(3). Indeed, a time- and concentration-dependent dissipation of *C. difficile*'s proton motive force could be induced by amidochelocardin treatment (Figure 3.3.3 A). Previous studies further reported that the bactericidal effect of chelocardins does not involve pore formation although chelocardin was reported to accumulate in the bacterial cell membrane. To further proof this hypothesis, the intra- and extracellular ATP levels of amidochelocardin-treated *C. difficile* cells were quantified. Indeed, the intracellular levels of ATP were comparable between treated and untreated cells (Figure 3.3.4 B). The extracellular levels of ATP were found to slightly increase, which might, however, rather be the result of cell lysis instead of leakage given that intracellular levels remained constant (Figure 3.3.3 B).

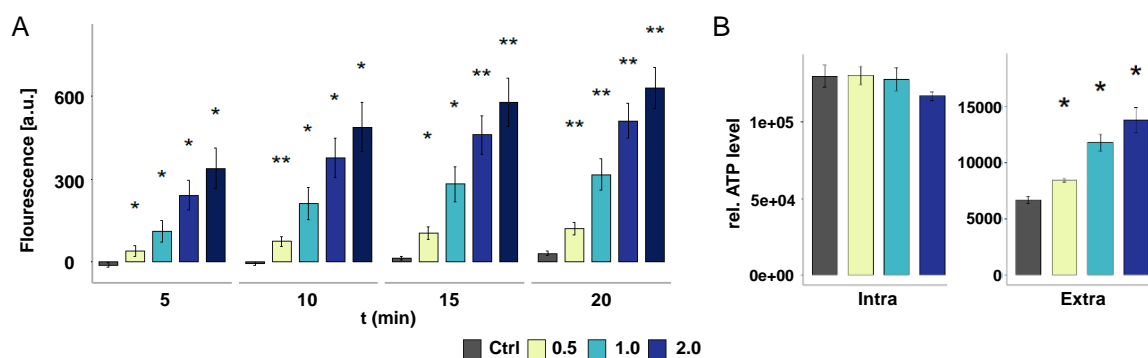


Figure 3.3.4: Amidochelocardin dissipates the proton motive force but only marginally permeabilizes the cell envelope. (A) Upon treatment with increasing concentrations of amidochelocardin a time- and concentration-dependent dissipation of the proton motive force could be observed in *C. difficile*. (B) Intra- and extracellular levels of ATP were quantified in *C. difficile* samples harvested 90 min after treatment with increasing concentrations of amidochelocardin. Adapted from Brauer *et al.* (re-submitted).

Furthermore, the effect of amidochelocardin treatment on *C. difficile* was analyzed by transmission electron microscopy (TEM) analysis to test for morphological changes, such as cell wall thickening, membrane blebbing or cell lysis. However, the cell morphology of *C. difficile* was not affected by amidochelocardin treatment as demonstrated by TEM micrographs (Figure 3.3.5).

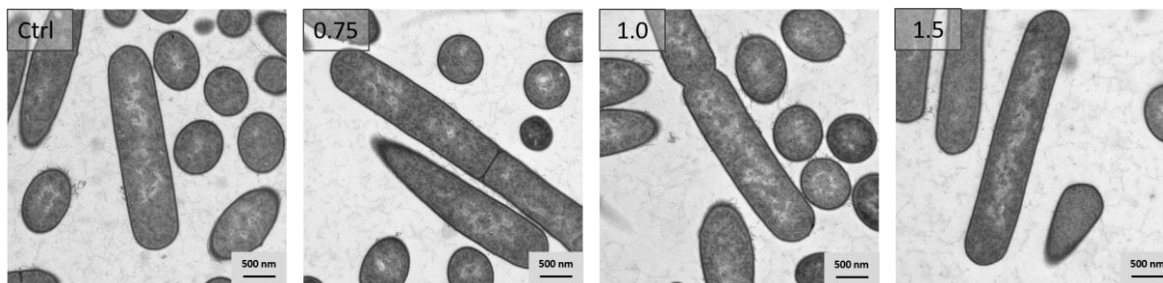


Figure 3.3.5: Transmission electron microscopy analysis of amidochelocardin-treated *C. difficile* cells. The cell morphology of *C. difficile* following treatment with three different concentrations of amidochelocardin (0.75 $\mu\text{g}/\text{ml}$, 1.0 $\mu\text{g}/\text{ml}$, and 1.5 $\mu\text{g}/\text{ml}$) for 90 min was analyzed by transmission electron microscopy. Adapted from Brauer *et al.* (re-submitted).

The membrane-directed activity of amidochelocardin led to the assumption that amidochelocardin might be retained in the cell envelope and might be directly responsible for the disturbed membrane integrity. Therefore, the relative concentrations of amidochelocardin in the cell envelope and the cytoplasm were quantified by targeted LC-MS/MS. The analysis revealed that the amount of amidochelocardin detected in the cytoplasm was higher compared to the amount detected in the envelope but the ratio of envelope-to-cytoplasm (40:60) was higher compared to ratios reported for tetracycline (20:80) and erythromycin (1:99) in *E. coli* (Figure 3.3.6) (Prochnow *et al.*, 2019).

Results

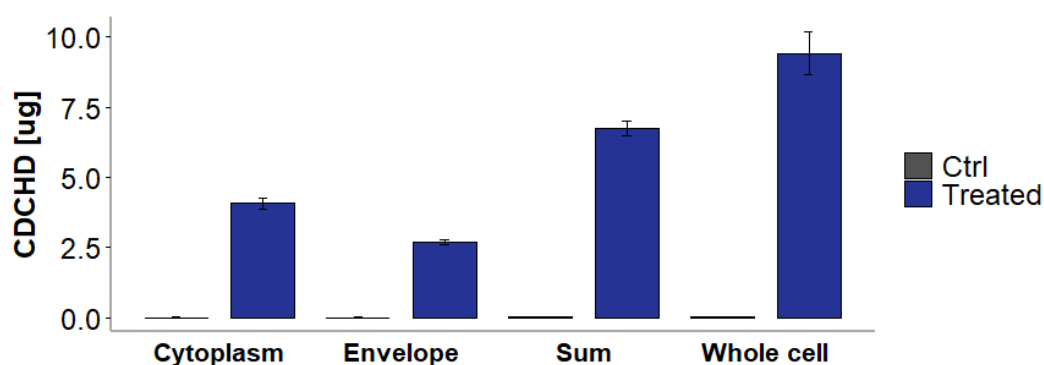


Figure 3.3.6: 40% of amidochelocardin is retained within the envelope of *C. difficile*. Amidochelocardin concentrations in *C. difficile* treated with 10 µg/ml amidochelocardin for 10 min were determined in the cytoplasm, envelope and in whole cell extracts. In addition, the sum of cytoplasmic and envelope amidochelocardin concentrations are given to account for loss during the experiment. Ctrl: control. Adapted from Brauer *et al.* (re-submitted).

3.3.4 *C. difficile* potentially accumulates aromatic compounds in response to amidochelocardin stress

Next, the dataset was further evaluated with regard to the question how *C. difficile* eventually protects itself against amidochelocardin. As mentioned above, the proteome response of *C. difficile* to amidochelocardin stress comprised higher abundance of the enzymes of the chorismate biosynthesis pathway, which provides chorismate for the biosynthesis of aromatic amino acids and many other aromatic compounds (Hubrich *et al.*, 2021) (Figure 3.3.7 A & B). Together with the increased levels of the putative phenazine biosynthesis proteins and the PadR-type regulator, these data strongly suggest a role of aromatic compounds in mediating amidochelocardin-stress in *C. difficile*. Since two additional enzymes encoded within the chorismate biosynthesis operon, namely the phenylalanine and tyrosine biosynthesis enzymes PheA and TyrC, were also higher abundant following stress, it was speculated that the increased synthesis of chorismate biosynthesis enzymes was required to respond to an increased demand for aromatic amino acids (Figure 3.3.7 B). Therefore, the relative cytoplasmic levels of the three aromatic amino acids phenylalanine, tyrosine and tryptophan were determined by a comparative GC-MS approach. The obtained data revealed that the relative intracellular levels of the two aromatic amino acids, tyrosine and phenylalanine, which are produced *de novo* by *C. difficile* 630, remained constant (Figure 3.3.7 C). In contrast, tryptophan, which cannot be synthesized by *C. difficile* 630, was found to be enriched in the cytoplasm upon amidochelocardin stress (Figure 3.3.7 C). Unfortunately, neither chorismate nor any of the other intermediates of its biosynthesis pathway could be identified by GC-MS.

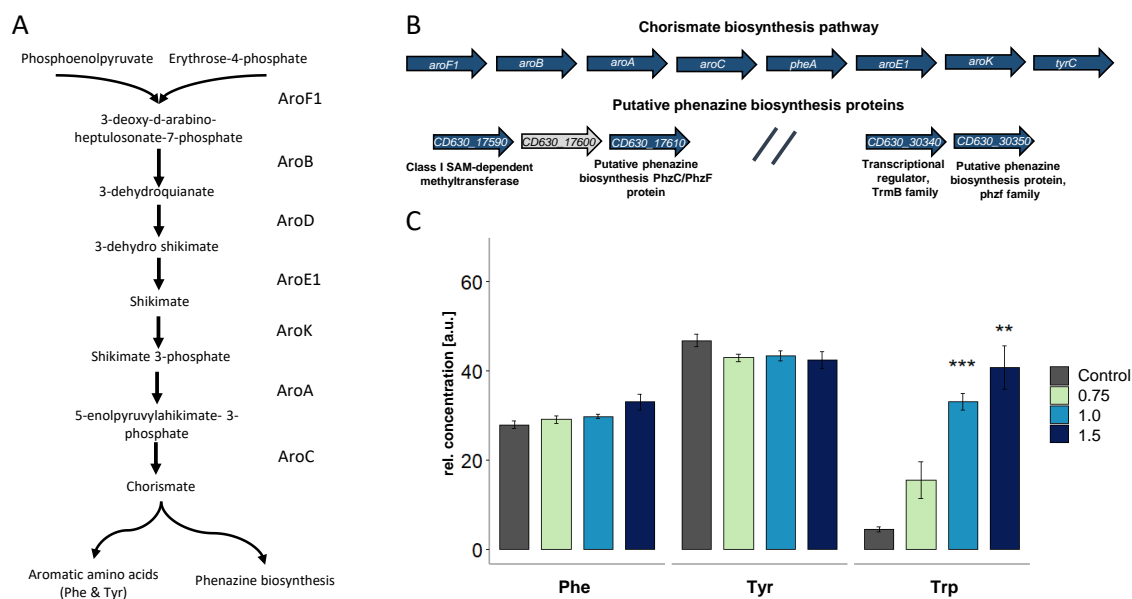


Figure 3.3.7: Aromatic compound metabolism in *C. difficile* upon amidochelecardin stress. (A) Chorismate, the precursor for aromatic amino acids and various other aromatic compounds, such as quinones and phenazines, is produced by *C. difficile de novo* from phosphoenolpyruvate and erythrose-4-phosphate. **(B)** The enzymes required for chorismate biosynthesis are encoded within one operon together with the enzymes required for phenylalanine, *pheA*, and tyrosine, *tyrC*, biosynthesis. Distinct two genes encoding putative phenazine biosynthesis enzymes are located within a class I SAM-dependent methyltransferase and an uncharacterized protein or TrmB transcriptional regulator. With the exception of the uncharacterized gene *CD630_17600*, all gene products of the respective operons were found in significantly increased amounts upon amidochelecardin stress (highlighted in blue). **(C)** Relative intracellular concentrations of phenylalanine (Phe), tyrosine (Tyr) and tryptophan (Trp) were determined in *C. difficile* 90 min after treatment with three different amidochelecardin concentrations. a.u.: artificial units. Adapted from Brauer *et al.* (re-submitted).

In addition, a BLAST search in the genome of *C. difficile* 630 for other prominent enzymes involved in the synthesis of phenazines in other bacteria was not successful. Likewise, a detailed analysis of the genes encoded adjacent to the respective phenazine biosynthesis proteins did not reveal additional indications on the role of these enzymes or putatively produced aromatic compounds. As mentioned above, both phenazine biosynthesis-like proteins were accompanied by an additional protein from the same operon. While *CD630_30350* seemed to be co-transcribed with a TrmB-type transcriptional regulator, *CD630_30340*, *CD630_17610* was accompanied by a class I SAM-dependent methyltransferase, *CD630_17590*. The other proteins encoded in proximity to the phenazine biosynthesis-like proteins were either not identified by the proteomics approach or did not show altered abundance.

4. Discussion

Although still considered a central cornerstone of modern medicine as the most important preventive and therapeutic measure against bacterial pathogens (Aminov, 2010), antibiotics have lost their sense of superiority being inactive against newly emerging and resistant bacterial pathogens (Gould, 2016; Oliveira *et al.*, 2020). In addition, the improved data and surveillance situation revealed that especially broad-spectrum antibiotic therapy is associated with occasionally high numbers of adverse events, which in some cases even counterbalance the benefit of the antibiotic therapy (Gerber *et al.*, 2017; Tandan *et al.*, 2018). The infection of the intestinal tract with *C. difficile* preceding antimicrobial therapy is probable the best example for both, an adverse event following broad-spectrum antimicrobial therapy and an infection that can hitherto only insufficiently be cured with the antibiotics on hand (Theriot and Young, 2015; Czepiel *et al.*, 2021; van Werkhoven *et al.*, 2021). In view of the occasionally high numbers of *C. difficile* infections, including a high percentage of recurrent events, more efficient therapeutic strategies to treat *C. difficile* infections are urgently required (Granata *et al.*, 2021). Screening of a panel of natural products provided by the Helmholtz Institute for Pharmaceutical Research (HIPS, Saarbrücken, Germany) revealed the antimicrobial activity of chlorotonils, myxopyronins and chelocardins against *C. difficile* and selected other anaerobes. While the activity of myxopyronins against *C. difficile* and other anaerobes had previously been demonstrated (Srivastava *et al.*, 2011), chlorotonils and chelocardins had not been tested under anaerobic conditions before. Bearing in mind that the direct target of both compound classes is hitherto unknown, the proven activity under anaerobic conditions contributes to the increased understanding of the modes-of-action of both compounds. For instance, antibiotics that target the respiratory chain components do not inhibit the growth of *C. difficile* and other anaerobes, which lack a respiratory chain (Schieferdecker *et al.*, 2014; Boersch *et al.*, 2018). Starting from this initial screening, the (omics)data presented in this thesis shed light on *C. difficile*'s stress response to all three compounds evaluating the compounds' value for the therapy of *C. difficile* infections and providing insight into the mechanisms underlying their antimicrobial activity. In particular, ChA and its derivatives prove to be interesting considering their high activity against *C. difficile* compared to some less related species during exponential growth phase, which is in line with high selectivity of the compound *in vivo* (Bublitz *et al.*, in revision).

4.1 Omics technologies in the context of antibiotic development

Omics technologies, including shot-gun proteomics approaches, have been proven to be of great value in antimicrobial research, e.g., for mode-of-action studies and to understand bacterial tolerance and resistance mechanisms (Khodadadi *et al.*, 2020; O'Rourke *et al.*,

2020; Tsakou *et al.*, 2020). For instance, stress response signature libraries have been established for selected antibiotics using model organisms, such as *B. subtilis* and *E. coli* (O'Rourke *et al.*, 2020; Senges *et al.*, 2020). These stress response libraries can subsequently be used to map the stress response signature of a model bacterium to a new antibiotic onto the previously obtained signatures allowing to draw conclusions concerning the mode-of-action or possible tolerance and resistance mechanisms (Stepanek *et al.*, 2016; Khodadadi *et al.*, 2020; Wüllner *et al.*, 2022). Stress response signatures can be obtained by using all kind of omics techniques like transcriptomics and proteomics (O'Rourke *et al.*, 2020; Senges *et al.*, 2020).

Shotgun transcriptomics experiments are often superior to proteomics and metabolomics experiments in terms of sequencing depth and identification bias (Kumar *et al.*, 2016). Sequencing of messenger RNA (mRNA) is easier than the analysis of metabolites and mRNA can, in contrast to certain proteins, completely be extracted from the cytosol despite a different cellular location of the gene products. Moreover, third-generation sequencing technologies, such as Oxford Nanopore Technology (ONT) and Pacific Biosciences (PacBio), support long sequencing reads allowing reliable detection and quantification of transcripts (Jenjaroenpun *et al.*, 2018). Nevertheless, proteomics and metabolomics datasets better reflect the cellular processes than transcriptomics datasets, which miss post-transcriptional regulation events and do not allow conclusions on enzyme activity (Kumar *et al.*, 2016). However, metabolomics approaches are rarely performed as untargeted approaches due to the high complexity of metabolites and their highly diverse nature with varying stability and different requirements depending on the metabolites to be detected (Choi and Verpoorte, 2014; Pinu *et al.*, 2019). In this light, proteomics technologies eventually come with a good balance by providing the possibility of an untargeted high-throughput analysis while providing a more reliable overview of the cellular inventory. Consequently, a bottom-up, label- and gel-free LC-MS/MS approach was applied here to generate antibiotic stress signatures of *C. difficile* to the selected antibiotics. Bottom-up proteomics approaches require the proteolytic digestion of proteins, e.g. with trypsin, followed by the analysis of peptides by LC-MS/MS. Although this approach is limited in terms of accuracy resulting from peptide ambiguity, it enables the identification of a large number of proteins and benefits, e.g., from better ionization rates of peptides over proteins (Donnelly *et al.*, 2019; Cupp-Sutton and Wu, 2020). Fractionation of peptides prior to the LC-MS/MS analysis or two-dimensional (2D)-LC set ups can further improve identifications rates of bottom-up approaches (Washburn *et al.*, 2001; Hinzke *et al.*, 2019). For instance, basic reversed-phase fractionation of digested peptides has been used in this study to increase identification rates (Yu *et al.*, 2017).

Discussion

A limitation of most shot-gun (meta)proteomics analyses is the detection limit, e.g. excluding peptides of lower abundant proteins in highly complex samples and variable detectability of peptides due to high hydrophobicity or low ionization rates (Dupree *et al.*, 2020; Kongpracha *et al.*, 2022). For example, membrane proteins are often underrepresented in untargeted whole cell proteomics experiments, due to their hydrophobic transmembrane domains, even if they are not removed from the sample during cell lysis and sample preparation (Kongpracha *et al.*, 2022). Consequently, membrane proteins are underrepresented in the here presented proteome signatures compared to transcriptome signatures reported elsewhere (O'Rourke *et al.*, 2020; Bublitz *et al.*, in revision). The effect of depletion of lower abundant proteins was even more pronounced in the metaproteome dataset, which mainly comprises protein groups from the most abundant functional categories.

In addition, all omics-based analyses are hampered by temporal dynamics and noise resulting from differential gene expression within subpopulations (Raj and van Oudenaarden, 2008; Mitosch *et al.*, 2017). Diversification within bacterial communities by responding differently to the same stress is discussed as an important feature of bacterial communities to secure survival (Mitosch *et al.*, 2017). Consequently, conventional omics techniques provide the sum of the responses of all cells to a certain stress. By contrast, single cell omics analyses allow a more differentiated insight into the response of a bacterial population but are not yet available for routine use on proteome level (Raj and van Oudenaarden, 2008; Ctortecka and Mechtler, 2021; Perkel, 2021). Furthermore, temporal dynamics and noise are, amongst others, causative for reported discrepancies between different omics datasets (Cai *et al.*, 2006; Newman *et al.*, 2006; Locke *et al.*, 2011). In the particular case of omics-based antibiotic research, off-target and post-antibiotic effects additionally hamper the analysis of the bacterial stress response (Dwyer *et al.*, 2014; Lobritz *et al.*, 2015; zur Abel Wiesch *et al.*, 2015). Although off-target and post-antibiotic effects might be specific for an antibiotic and significantly contribute to the antimicrobial effect, they are often difficult to differentiate from the original effect and arise, e.g., from reduced growth rates, changes in membrane permeability or from interaction of the antibiotic and its solvent (Belenky *et al.*, 2015; Lobritz *et al.*, 2015; Stokes *et al.*, 2019). This makes it difficult to compare omics stress response signatures derived from different experimental set ups and model organisms. For example, the stress response signature of *C. difficile* 630 to amidochelocardin differed from the signatures previously obtained for *B. subtilis* and chelocardin/amidochelocardin (Stepanek *et al.*, 2016; Senges *et al.*, 2020). For instance, marker proteins, such as LiaH, PspA and ribosomal proteins, previously found in elevated amounts in *B. subtilis* in response to chelocardins were not observed in *C. difficile* 630, whereas neither Stepanek *et al.* nor Senges *et al.* reported an effect on aromatic metabolite synthesis. However, Stepanek *et al.* and Senges *et al.* applied pulsed-chased metabolic-

labelling and used a 2D-gel-based MALDI-TOF approach for protein identification to analyze the protein synthesis rate in the first ten minutes following stress to study the compounds' mode-of-action (Stepanek *et al.*, 2016; Senges *et al.*, 2020). In contrast, the *C. difficile* 630 signature presented here addressed the question how the pathogen adapts its proteome in the presence of the compound within 90 minutes. Likewise, similarities between the fidaxomicin stress signature presented in section 3.2 and a fidaxomicin stress signature in *C. difficile* 630 Δ *erm* also generated in 2D-gel- and MALDI-TOF-based approach were restricted to some findings as discussed in more detail in Brauer *et al.* (2022).

Despite these limitations, omics have great value for antibiotic research by providing valuable insights into the systemic effects of new compounds and providing a starting point to draw hypotheses on the mechanisms underlying their antimicrobial activity. Thereby, omics substantially contribute to the identification and evaluation of highly specialized and selective antibiotics, which are urgently required as explained in detail in the introduction.

4.2 The complex intestinal community substantially contributes to host's health

Many bacteria, including *C. difficile*, reside inside a complex, competitive environment like the soil and the intestinal tract (Thompson *et al.*, 2017; Nayfach *et al.*, 2021). In the gastrointestinal tract, *C. difficile* most likely resides within biofilm-like structures attached to the mucus and inside the lumen (Soavelomandroso *et al.*, 2017; Normington *et al.*, 2021). A recent report by our lab, further supports the hypothesis that *C. difficile* forms aggregate-like biofilms consisting of flagellated cells, which allow various nutrients to access the inner part of these biofilms while waste products can diffuse (Brauer *et al.*, 2021). In line with this, an increasing number of studies report that *C. difficile* utilizes numerous metabolic pathways during colonization and infection although knowledge of *C. difficile*'s *in vivo* lifestyle is still mainly based on mono-associated animal and *in vitro* models (Theriot *et al.*, 2014; Jenoir *et al.*, 2017; Poquet *et al.*, 2018; Tremblay *et al.*, 2021). However, despite the metabolic flexibility, colonization and expansion inside the ecological niche are severely dependent on the ability of *C. difficile* and other enteropathogens to compete with other microorganisms for nutrient and trace elements (Bauer *et al.*, 2018). In particular, *C. difficile*'s competitive fitness is correlated with the availability of proline, other amino acids and a number of vitamins and trace elements, such as selenium (Battaglioli *et al.*, 2018; Jenior *et al.*, 2018; Lopez *et al.*, 2019; Lopez *et al.*, 2020). Consequently, a diverse bacterial community and the presence of other amino acid fermenting bacteria in the intestine protects against *C. difficile*, whereas reduction of bacterial diversity by unselective antibiotic therapy disrupts colonization resistance (Lopez *et al.*, 2020; Girinathan *et al.*, 2021). By using a metaproteomics approach, it could be validated that chlorotoniol treatment does not

Discussion

significantly affect the composition of the intestinal community of piglets although a drop in detected bacterial proteins and community diversity, and a trend towards reduction of the relative abundance of some Clostridia families, particularly, *Lachnospiraceae* and *Clostridiaceae*, could be observed. These findings are in line with results from 16S rRNA sequencing approaches reported by Bublitz *et al.* (in revision). More importantly, the metaproteomics approach could additionally validate that the functional profile of the intestinal community of ChA-treated piglets was mostly stable following treatment. Changes on the taxonomic level do not necessarily correlate with functional changes due to the redundancy of most functions performed by different members of the microbiota (Turnbaugh *et al.*, 2009; Lozupone *et al.*, 2012; Tian *et al.*, 2020). *Vice versa*, functional changes might occur despite taxonomic stability (Heintz-Buschart and Wilmes, 2018). In this light, metaproteomics is a well-suited tool to address the functional aspects of intestinal microbiota homeostasis (Li and Figeys, 2020).

As extensively reviewed in the literature, healthy individuals often have an individual and comparatively stable intestinal microbiota, which is shaped by diet, hormone status and several other factors (Eckburg *et al.*, 2005; Lozupone *et al.*, 2012; Yuan *et al.*, 2020). The individuality of the community profiles became clearly visible in the piglet feeding trial. In contrast to many other studies using in-breed mice or hamster models, the pig was chosen as a model organism due to the similarities between the human and porcine intestinal microbiota, physiology and diet (Rose *et al.*, 2022). However, gnotobiotic piglets and in-breed lines are rarely available and domestic pigs have been used in the piglet feeding trial. Consequently, feces community profiles from individual piglets clearly differed in their taxonomic composition. For instance, the microbiota of piglet number 1 of the control group differed from the other analyzed microbiota by high numbers of Proteobacteria. Community profiles of sibling animals and animals housed together during the feeding trial were more similar to each other as previously observed in human studies (Turnbaugh *et al.*, 2009). The individuality of the communities, however, hampered proper statistical analysis. Moreover, fluctuations between the days could be observed for ChA-treated as well as for untreated piglets further impeding comparative analysis. The minor fluctuations in the community profiles possibly arose from different food intake reflected by the varying numbers of fiber-derived proteins identified by LC-MS/MS or were caused by the young age of the piglets. In the early years, the community profile is subject to changes introduced, for instance, by changing diet following weaning (Lozupone *et al.*, 2012). Due to a limited amount of ChA and the application of the compound per kilogram body weight, piglets were bought at the age of four weeks directly following weaning and were only allowed to acclimatize to their new environment and diet for two weeks.

More pronounced changes of the intestinal community profile, however, can only be introduced by severe events, such as antibiotic therapy, which often severely disturbs the community structure, sometimes even in the long-term (Dethlefsen and Relman, 2011; Lozupone *et al.*, 2012; Reyman *et al.*, 2022). Depending on the activity spectrum of an antibiotic, more or less species are eventually eradicated from the community and might provide an ecological niche for other species, including enteropathogens, such as *Salmonella enterica*, *E. coli*, *E. faecalis* and *C. difficile* (Ng *et al.*, 2013; Ferreyra *et al.*, 2014; Faber *et al.*, 2016). In addition, a community shift might affect the functional repertoire of the gut and thereby additionally affect health of the host. The microbial community not only provides protection against enteropathogens but provides the host with nutrient and vitamins (Rodionov *et al.*, 2019; Hadadi *et al.*, 2021). For instance, the microbiota degrades various polysaccharides, such as xylan, not usable by the host and synthesizes essential vitamins, such as vitamin B₁₂, which are taken up by the host (Rodionov *et al.*, 2003; Flint *et al.*, 2012; Rodionov *et al.*, 2019). Likewise, the intestinal microbiota significantly contributes to host immunity (Zheng *et al.*, 2020; Zhao and Maynard, 2022). In this light, it was crucial to show that chlorotoniils only marginally affect the taxonomic and functional profile of the intestinal community at clinically relevant concentrations.

Nevertheless, it needs to be mentioned that the metaproteomics analysis had limitations. As mentioned above, the piglet microbiotas were highly different from each other impairing proper statistical analysis. Moreover, the depth of the analysis was limited to the most central functions performed by the microbiota, such as energy metabolism, translation and DNA and RNA metabolism as discussed in the previous section. Unfortunately, lower abundant taxa and functional features are overlooked by the analyses. For instance, the family *Peptostreptococcaceae* was rarely and only insufficiently detected. Similarly, many pathways involved in vitamin and cofactor metabolism, including selenium and cobalamin metabolism, are not detected and no conclusion on the abundance of proteins from these pathways could be drawn. This is also true for the multi-enzyme complexes of the glycine and proline reductase, which were found enriched in species with higher susceptibility to chlorotoniils. Despite their high abundance in species utilizing these enzymes, their overall abundance in the intestine is too low to draw reliable conclusions.

Moreover, fecal samples were used instead of intestinal samples. The community composition inside the gastrointestinal tract highly differs along the longitudinal as well as the transversal axis due to nutrient, oxygen and pH gradients (Eckburg *et al.*, 2005; Pereira and Berry, 2017). While the upper intestinal tract shows lower diversity, the lower intestinal tract reveals higher diversity and is dominated by Bacteroidetes and Firmicutes (Yuan *et al.*, 2020). The luminal microbiota is dominated by Firmicutes and Bacteroidetes, whereas

Discussion

the crypts reveal higher abundance of Alphaproteobacteria and lower abundance of Firmicutes (Chen *et al.*, 2012; Saffarian *et al.*, 2019). With this respect, fecal samples can only be used as a proxy for the study of the “intestinal community”. Nevertheless, it has multiple times been demonstrated that the community profile of fecal samples resembles the community profile found inside in the colon and can be used to study community changes in the large intestine (Looft *et al.*, 2014; Gierse *et al.*, 2020).

In conclusion, the metaproteomics support previous findings, which showed that chlorotoniils only marginally affect the intestinal community structure and function. However, more sensitive approaches have to be chosen to analyze lower abundant features of such complex samples as discussed in more detail in section 4.1 and machine-learning-based statistical analysis might detect hitherto overlooked effects.

4.3 Transient metal toxicity and metal homeostasis as antibiotic target

In contrast, analyses of the systemic effects of chlorotoniil treatment on *C. difficile* 630 and *T. glycolicus* DSM 1288 *in vitro* revealed that ChA and ChB1-Epo2 substantially affect the metal homeostasis of bacteria but apart induce a rather unspecific response.

Interestingly, a similar stress response as observed in *C. difficile* in the presence of ChA and ChB1-Epo2 has previously been observed in *S. aureus* following treatment with VU0026291, an antibiotic affecting metal homeostasis (Juttukonda *et al.*, 2020). Juttukonda *et al.* reported metal-mediated killing of *S. aureus* by VU0026291 via increasing the intracellular levels of copper and zinc with a concomitant slight decrease in manganese concentrations as well as production of reactive oxygen species (ROS). Increased extracellular copper concentrations further exacerbated the antibacterial activity of VU0026921, whereas cobalt had a protective effect. Furthermore, the authors observed a pleiotropic transcriptional response including an induction of genes encoding for proteins with putative metal-buffering function and ROS detoxifying enzymes (Juttukonda *et al.*, 2020). Similarly, the chlorotoniil omics stress responses presented here and elsewhere (Bublitz *et al.*, in revision) indicated an effect on multiple metabolic features, and indicated osmotic stress, redirection of the energy metabolism, and glyoxal stress. More importantly, it seems likely that the increased abundance of some of the proteins with predicted metal binding capacity elevated in response to ChB1-Epo2, such as some ribosomal proteins, is required by *C. difficile* 630 to buffer excess of copper, cadmium and zinc in the cytoplasm as observed for *S. aureus* (Juttukonda *et al.*, 2020). Several ribosomal proteins, such as RpmE and RpmF, detected in increased amounts following stress, were previously shown to bind zinc and were found in increased amounts following copper stress in *S. aureus* (Panina *et al.*, 2003; Tarrant *et al.*, 2019).

Metals, such as magnesium, calcium, zinc, and manganese, are important cofactors for several metalloproteins and are involved in DNA maintenance (Waldron and Robinson, 2009). Calcium is further required as germinant by *C. difficile* (Kochan *et al.*, 2017). In contrast, transient metals, like copper, zinc and cadmium, are severely toxic if present in excess (Waldron and Robinson, 2009; Chandrangsu *et al.*, 2017). Although the mechanisms of metal toxicity are still discussed, their destructive effect on the metabolism is based on mismetallation of metalloenzymes and cofactors, damage of vulnerable cysteine residues, the production of ROS via Fenton-like reactions and the depletion of other transient metals whenever one metal is present in excess (Begg *et al.*, 2015; Barwinska-Sendra and Waldron, 2017; Hassan *et al.*, 2017; Tan *et al.*, 2017). Most importantly, metal toxicity has very often been linked to damage of iron-sulfur cluster-dependent enzymes as well as damage of the enzymes for the biosynthesis of iron-sulfur clusters and tetrapyrroles, such as cobalamins (Xu and Imlay, 2012; Azzouzi *et al.*, 2013; Tan *et al.*, 2017; Wang *et al.*, 2019; Steunou *et al.*, 2020). In this light, it seems likely that high numbers of SAM- and [4Fe4S]-dependent enzymes affected by ChA/ChB1-Epo2 treatment reflect disruption of the iron-sulfur clusters and/or their depletion. Anaerobes, such as *C. difficile*, are particularly prone to metal toxicity due to their high amounts of enzymes containing labile [4Fe4S]-clusters, including SAM-dependent enzymes, as well as enzymes with sensitive cysteine catalytic residues (Azzouzi *et al.*, 2013; Bird *et al.*, 2013; Chandrangsu *et al.*, 2017; Tan *et al.*, 2017). Of note, the intracellular iron levels were not significantly affected as reported previously for cadmium, zinc and copper stress (Hassan *et al.*, 2017; Alquethamy *et al.*, 2021), excluding iron limitation as reason for the accumulation of [4Fe4S]- and metal-dependent enzymes.

Furthermore, several studies reported that exposure of various bacteria to silver, copper or cadmium disrupts energy metabolism and disturbs membrane biogenesis (Ong *et al.*, 2015; Tarrant *et al.*, 2019; Wang *et al.*, 2019; Neville *et al.*, 2020; Wang *et al.*, 2021). Disruption of the membrane barrier function following metal stress is assumed to be an indirect effect of the disturbed central metabolism, such as the depletion of acetyl-CoA required for membrane lipid biosynthesis (Neville *et al.*, 2020). Other prominent targets of transient metal toxicity include the glycolysis enzymes GapA, and phosphofructokinase Pfk due to their conserved cysteine residues in the catalytic center (Ong *et al.*, 2015; Tarrant *et al.*, 2019). Assuming that copper affected glycolysis in *C. difficile* could explain the strikingly but non-significantly increased abundance of the gluconeogenesis enzymes GapB, GlgC and GlgD, in *C. difficile* upon adaptation to ChB1-Epo2 on proteome level and following stress on transcriptome level reported by Bublitz *et al.* (in revision). Gluconeogenesis might present a way for *C. difficile* to sequester glucose and avoid accumulation of glycolytic intermediates upon inactivation of GapA by copper and zinc. Similarly, potassium efflux,

Discussion

which allows intracellular accumulation of protons and a concomitant reduction of the intracellular pH, is known as a bacterial response to detoxify negatively charged glycolytic intermediates (Chandrangsu *et al.*, 2014; Healy *et al.*, 2014). In this light, the observed reduction of intracellular potassium in response to ChB1-Epo2 might likewise indicate glycolytic stress. Alternatively, the decreased potassium and increased sodium levels in ChB1-Epo2-treated cells could be directly or indirectly caused by chlorotonil treatment or the disturbed transient metal pool. The increased abundance of the osmoproteins OpuCA and OpuCC in *C. difficile* following ChA treatment similarly indicate osmoprotection in response to ChA.

Due to their essential but toxic role, transient metals have recently gained attention for antimicrobial therapy (Weekley and He, 2017; Murdoch and Skaar, 2022). In addition to Juttukonda *et al.*, several other studies describe the pleiotropic effects of antimicrobial substances that modulate metal homeostasis (Chan *et al.*, 2017; Harbison-Price *et al.*, 2020; Juttukonda *et al.*, 2020; van Zuylen *et al.*, 2021). Interestingly, Juttukonda *et al.* further reported that it was not possible to generate VU0026291-resistant strains and concluded that the inability of *S. aureus* to adapt to VU0026291 is the result of the multiple cellular targets (Juttukonda *et al.*, 2020). Similarly, Chan *et al.* reported an inability of *E. coli* to adapt to the dithiopyrrolone, which also disturbs metal homeostasis (Chan *et al.*, 2017). Likewise, bacteria often fail to adequately adapt to excess of silver, copper or cadmium (Randall *et al.*, 2013; Wang *et al.*, 2021).

It was interesting to see that the metal-buffering effect was more pronounced in the ChB1-Epo2 stress signature in *C. difficile* 630. However, also the ChA stress signature indicated a disturbed cell homeostasis, including dysregulation of, e.g., [4Fe4S]-dependent proteins, and disturbed osmoregulation. Since *C. difficile* as well as other Clostridia are devoid of cuprous enzymes and cadmium is not used as metal cofactor (Argüello *et al.*, 2013), the increased levels of these metals in *C. difficile* upon ChB1-Epo2 treatment are unlikely a desirable event. Consequently, it can be concluded that the disturbed metal homeostasis contributed to the antimicrobial effect of the chlorotonils in *C. difficile*.

4.4 Susceptibility to chlorotonils is correlated with tetrapyrrole biosynthesis and selenometabolism

However, metal toxicity is severely problematic for all anaerobic bacteria. Therefore, it was speculated that species with higher susceptibility, such as *C. difficile*, must have a feature, such as a cellular structure, metabolic pathway, enzyme complex, or altered nutrient or cofactor requirements, that is causative for the increased sensitivity. Interestingly, it was possible to correlate the higher susceptibility to chlorotonils with the presence of the enzymatic repertoire for *de novo* selenocompound and cobalamin biosynthesis as well as

increased numbers of cobalamin-dependent and selenoenzymes when comparing the theoretical protein repertoire of selected species tested elsewhere (Arne Bublitz, HZI Braunschweig). With respect to the deleterious effect of transient metals on tetrapyrrole synthesis, which includes the synthesis of cobalamins, and the frequently observed depletion of essential metals when copper or zinc are present in excess, this correlation appears to be highly interesting. The hypothesis that the ability of *de novo* selenocompound and cobalamin biosynthesis eventually increases chlorotoniil-sensitivity is further supported by the observation that representatives of the *Bifidobacteria*, devoid of selenium- and cobalamin-dependent enzymes and devoid of glycolysis, are the least sensitive species in the *in vitro* strain panels addressing the differential sensitivity of anaerobes to chlorotoniils (Suppl. figure S2).

Although selenocysteine-containing enzymes are ubiquitously found in all domains of life, Clostridia and Deltaproteobacteria comprise an above average number of species equipped with enzymes involved in synthesis of selenocompounds (Peng *et al.*, 2016). Selenium is incorporated into selenoenzymes as selenocysteine and provides unique catalytic properties for certain enzymes involved, for example, in catabolic reactions under anaerobic conditions (R.M. Evans *et al.*, 2021). For the synthesis of selenocysteine a specific tRNA is charged with serine first. Subsequently, selenophosphate provided by the selenophosphate synthase SelD is used as selenium donor by the Sec synthase SelA to convert the serine to selenocysteine (Turanov *et al.*, 2011). In addition, some other enzymes are required for the synthesis of other selenocompounds, namely YqeB and YqeC for the synthesis of the selenocofactor (Se cofactor) and YbbB for the synthesis of the rare tRNA base 5-methylaminomethyl-2-selenouridine (SeU) (Zhang *et al.*, 2008; Sierant *et al.*, 2018). Additionally, an above average number of selenoenzymes, such as formate dehydrogenase, glycine reductase, and heterodisulfide reductase, can be found in the genome of the species equipped with enzymes required for selenocysteine synthesis (Peng *et al.*, 2016). Interestingly, families affected by chlorotoniil treatment, such as *Peptostreptococcaceae*, *Lachnospiraceae* and some *Ruminococcaceae* are often equipped with selenocompound synthesis and selenoenzymes, whereas the phyla Bacteroidetes and Verrucomicrobiota, and the family *Bifidobacteriaceae*, which were found in increased abundance following chlorotoniil treatment, often lack selenoenzymes (Zhang *et al.*, 2006; Peng *et al.*, 2016; Bublitz *et al.*, in revision).

Similarly, despite the vast distribution of cobalamin-dependent enzymes, only one third of bacterial species is able to synthesize cobalamins *de novo*, particularly Actinobacteria, Proteobacteria and Firmicutes (Shelton *et al.*, 2019). The term “cobalamin” summarizes a group of cobalt-containing cyclic tetrapyrrolidines with the lower ligand 5,6-

Discussion

dimethylbenzimidazole (DMB) attached in the α -position and an upper ligand in the β -position (Balabanova *et al.*, 2021). Depending on the upper ligand, 5'-deoxyadenosylcobalamin (AdoCbl), also known as vitamin B₁₂, methyl-cobalamin (MeCbl), hydroxocobalamin (OHCbl) or cyanocobalamin (CNCbl) is produced (Balabanova *et al.*, 2021). Cobalamins, especially vitamin B₁₂, are important cofactors for enzymes, such as the B₁₂-dependent ribonucleotide reductase, the B₁₂-dependent methionine synthase, the epoxyqueuosine reductase, and the methyl-malonyl-CoA mutase (Shelton *et al.*, 2019). *Peptostreptococcaceae*, including the genus *Terrisporobacter*, *Lachnospiracaceae*, and the genus *Clostridium sensu stricto* 1 are classified as (very) likely corrinoid producer and tetrapyrrole precursor salvagers (Shelton *et al.*, 2019) and were diminished in chlorotonil-treated animals (Bublitz *et al.*, in revision). In contrast, not affected taxa, such as more than 90% of all Bacteroidetes, most *Enterococcus* and *Lactobacillus* and all *Prevotellaceae*, *Verrucomicrobiaceae* and *Bifidobacterium* species, were either classified as non-producers or Cbi salvagers, which require Cbi as precursors due to the lack of the enzymes for tetrapyrrole precursor biosynthesis (Shelton *et al.*, 2019).

4.5 Copper stress eventually limits selenium availability

The assumption that cobalamin metabolism is disturbed by chlorotonil treatment is substantially supported by the finding that cobalt transport proteins were repeatedly identified among the ON/OFF proteins in the chlorotonil-stress and the ChB1-Epo2 adaptation proteome signature of *C. difficile* 630 as well as in the *T. glycolicus* stress signature indicating cobalt limitation. It can be speculated that the proposed cobalt limitation is caused by the ability of chlorotonils to bind transient metals, such as zinc and eventually cobalt under physiological conditions, as shown by ICP-MS measurements. However, the intracellular cobalt levels were not significantly affected following stress with ChB1-Epo2. The cobalt limitation indicated by the proteomics data can eventually be explained by the higher copper-affinity of the required cobalt-chaperons providing cobalt during cobalamin synthesis. According to the Irving-Williams series, enzyme complexes with copper are the most stable protein-metal complexes followed by zinc, nickel, cobalt, iron and manganese complexes (Irving and Williams, 1948; Foster *et al.*, 2014; Osman *et al.*, 2021). Excess of copper is therefore expected to limit cobalt availability even if intracellular levels are not affected.

Similarly, excess of zinc has been shown to limit selenium availability for *C. difficile* (Lopez *et al.*, 2019). It can be expected that copper has a similar effect, which is supported by the finding that the most pronounced intracellular selenium peak was reduced in ChB1-Epo2-treated cells compared to DMSO controls. This way, the disturbed metal pool and/or the demonstrated affinity of chlorotonils to the selenium isotope Se₈₂ eventually explain why

selenium metabolism is correlated with increased sensitivity to chlorotolils. Worth mentioning, one of *C. difficile*'s key enzymes, the proline reductase, is a selenoenzyme (Jackson *et al.*, 2006). The proline reductase is rarely found in the bacterial world and its presence is mainly limited to Clostridia (Jackson *et al.*, 2006; Christgen and Becker, 2019). Only 271 homologous proteins of the selenocysteine-containing subunit PrdB of *C. difficile*'s proline reductase belonging to 192 bacterial species, comprising mainly Clostridia (116) and Bacilli (37) species, have been submitted to the Uniprot database until today (Suppl. table S3) (data obtained from InterPro 09.05.2022 (Blum *et al.*, 2021)). Inside the competitive environment of the intestinal tract, which is rich of collagen-derived proline, the proline reductase is an advantageous enzyme (Huang *et al.*, 2018; Jenior *et al.*, 2018). In particular for *C. difficile*, the selenium-dependent enzyme is a key metabolic trait required by the pathogen to compete inside the intestine (Reed and Theriot, 2021). For instance, several studies showed preferentially utilization of proline by *C. difficile* *in vitro* and *in vivo* (Neumann-Schaal *et al.*, 2015; Jenior *et al.*, 2017; Battaglioli *et al.*, 2018; Fletcher *et al.*, 2018; Jenior *et al.*, 2018). Competition experiments further revealed that *C. difficile* is outcompeted by other amino acid fermenting bacteria, while growth is alleviated in the presence of saccharolytic bacteria (Lopez *et al.*, 2020; Girinathan *et al.*, 2021; Reed *et al.*, 2022). Similarly, proline reductase deletion mutants were shown to be outcompeted *in vitro* and to be attenuated in mice infection models (Lopez *et al.*, 2019; Lopez *et al.*, 2020). Likewise, auranofin- or zinc-induced selenium limitation significantly reduced *C. difficile*'s fitness by inhibiting selenium-dependent proline fermentation in *C. difficile* (Jackson-Rosario *et al.*, 2009; Lopez *et al.*, 2019).

In this light, it can be speculated that a disturbed selenium metabolism contributes to the antimicrobial effect of chlorotolils in *C. difficile* and close relatives and the observed selectivity of the compounds *in vivo* (Bublitz *et al.*, in revision). This hypothesis is further supported by the finding that one of the few proteins found in higher amounts in ChB1-Epo2-treated *T. glycolicus* cultures is the putatively selenium-dependent formate dehydrogenase H alpha subunit. The gene set enrichment analyses of both *C. difficile* stress signatures further revealed, although non-significantly, higher amounts of the proline and/or glycine reductase subunits. Interestingly, disruption of the selenium metabolism has further been shown to cause a switch towards mannitol fermentation in *C. difficile* R20291 to compensate for the lack of energy (McAllister *et al.*, 2021). In line with this, both the adaptation proteome signature presented above as well as the stress transcriptome signature reported by Bublitz *et al.* (in revision) indicate increased mannitol acquisition and utilization in *C. difficile* 630 in the presence of ChB1-Epo2.

Discussion

In concert, these data support the idea that *C. difficile*'s increased susceptibility to chlorotolils is partly caused by *C. difficile*'s dependency for selenium and its selenoenzymes. In this context, it was interesting to find that homologous proteins of *C. difficile*'s proline reductase, which are almost exclusively found in Clostridia, can be found in the genomes of *S. cellulosum* ce1525 (personal communication, HIPS Saarbrücken) and So0157-2 (Suppl. table S3), the producing strain of ChA and another representative of the genus. Assuming that the producing strain is dependent on selenium, it might be beneficial for the strain to sequester selenium from the environment using chlorotolils.

4.6 The pros and cons of old and new drugs

Most antibiotics that could be added to the pool of clinically relevant antibiotics in the last decade were derivatives of approved antibiotics modified to improve their activity, extend the activity spectrum, modulate their bioavailability and/or overcome antibiotic resistance mechanisms (Hutchings *et al.*, 2019; Butler *et al.*, 2022). This approach can comparatively fast and easily provide new compounds. However, these new antibiotics have limited added value, e.g., due to the risk of cross-resistance and the limited possibilities to use them simultaneously or alternately with other antibiotics in form of synergistic drug combinations (Karakonstantis *et al.*, 2020; Scudeller *et al.*, 2021). Therefore, antibiotics with new target sites are preferred.

In this light, it might be counterintuitive to consider an RNA polymerase switch region inhibitor, such as myxopyronin B, for *C. difficile* infection therapy. One of the first-line drugs for the treatment of *C. difficile* infections, fidaxomicin, also targets the RNA polymerase switch region (Artsimovitch *et al.*, 2012). However, structural binding site analyses suggested that the binding sites of fidaxomicin and other switch region inhibitors, such as myxopyronin B and corralopyronin, do not overlap (Artsimovitch *et al.*, 2012). Indeed, serial broth dilution assays demonstrated that at least a point mutation in *rpoB* conferring fidaxomicin resistance does not protect *C. difficile* Goe-91 against myxopyronin B. Although it cannot be excluded that other mutations confer cross-resistance, this is rather unlikely with respect to the different binding sites in the switch region.

The RNA polymerase seems to be well a suited antibiotic target in *C. difficile*. In addition to fidaxomicin, the classical RNA polymerase inhibitor rifaximin is additionally on the list of antibiotics recommended for *C. difficile* infections (Chaar and Feuerstadt, 2021). Rifaximin, which is also in use for the treatment of other gastrointestinal infections, such as traveller's disease and irritable bowel syndrome, shows high bioavailability in the gut lumen with only minimal absorption (Koo *et al.*, 2009; Chey *et al.*, 2020). In addition, several clinical trials

already proved the usefulness of rifaximin as an antibiotic for *C. difficile* infections (Basu *et al.*, 2010; Garey *et al.*, 2011; Major *et al.*, 2019; Ng *et al.*, 2019). Although the reasons for the selectivity are not completely understood, both, fidaxomicin and rifaximin, are comparatively selective for *C. difficile* (Finegold *et al.*, 2009; Louie *et al.*, 2012; Ponziani *et al.*, 2017). The initial data presented here give reason to hope that myxopyronin B is likewise more potent against *C. difficile* compared to other anaerobic commensals, such as Actinobacteria and Lactobacillales. Furthermore, myxopyronin B prevented early toxin synthesis in *C. difficile* 630 *in vitro* to a similar degree as fidaxomicin. In contrast, rifaximin elevated early toxin synthesis similar to other antibiotics analyzed previously (Aldape *et al.*, 2013; Aldape *et al.*, 2018). It is assumed that toxin synthesis is induced by the bacterial SOS response, which is triggered by antibiotic-mediated transcription arrest (Walter *et al.*, 2014; Willing *et al.*, 2015). Although the mechanisms underlying fidaxomicin's ability to reduce toxin synthesis in *C. difficile* are hitherto not fully understood, it is assumed that the early interruption of the transcriptional process by fidaxomicin, and presumably myxopyronin B, circumvents induction of toxin synthesis (Aldape *et al.*, 2017). Hitherto this effect was supposed to be exclusive for fidaxomicin what is now questioned by the data presented here. Possibly, prevention of toxin synthesis is a more general feature of RNA polymerase switch region inhibitors. Further studies with myxopyronin B and other switch region inhibitors will be necessary to proof this hypothesis. In addition, it would be interesting to test whether myxopyronin B is able to reduce sporulation as observed for fidaxomicin (Louie *et al.*, 2012).

Furthermore, resistance rates to RNA polymerase switch region inhibitors seem to be considerably low. Although fidaxomicin is used in the clinical context since 2011 almost no fidaxomicin-resistant isolates were observed until now (Sholeh *et al.*, 2020). In contrast, mutations conferring resistance to rifamycins are frequently observed (Sholeh *et al.*, 2020). Therefore, rifaximin is still only used as a "chaser antibiotic" in combination with other antibiotics because of varying levels of rifaximin resistance in *C. difficile* that dim the hopes associated with rifaximin therapy (Garey *et al.*, 2011; Major *et al.*, 2019; Ng *et al.*, 2019; Sholeh *et al.*, 2020). An important reason for the high resistance rates to rifaximin are the low fitness costs associated with mutations in *rpoB* conferring rifaximin resistance (Dang *et al.*, 2016). In contrast, mutations conferring resistance against myxopyronins were shown to have significantly higher fitness costs in *S. aureus* (Srivastava *et al.*, 2012). Therefore, the development and dissemination of resistances to myxopyronins are considered as substantially less likely.

Taken together, RNA polymerase inhibitors seem to be well suited for the therapy of *C. difficile* infections due to their selectivity for *C. difficile*. Furthermore, it can be speculated

Discussion

that RNA polymerase switch region inhibitors, such as fidaxomicin and myxopyronin B, might in general be potent anti-*C. difficile* antibiotics due to their proposed negative impact on toxin synthesis. Eventually, myxopyronin B might then become a promising lead structure for the targeted design of an antibiotic optimized for the therapy of *C. difficile* infections. Indeed, the biosynthetic gene cluster of myxopyronins is well characterized and efforts have been made to obtain more active, soluble and stable compounds (Sucipto *et al.*, 2017). *In vivo* studies will be necessary, e.g., to proof myxopyronin B's potential selectivity for *C. difficile* although it could already be shown that up to 100 mg/kg body weight myxopyronin B were well tolerated by mice when applied subcutaneous (Irschik *et al.*, 1983).

4.7 The current role of membrane-active and broad-spectrum antibiotics

Interestingly, already minor chemical modifications of an antibiotic, such as addition or replacement of single moieties, can change the activity, activity spectrum or bioavailability of a compound (Cyphert *et al.*, 2017; Mitcheltree *et al.*, 2021; Zhang *et al.*, 2021). For instance, minor differences in the biosynthetic gene clusters for oxytetracycline and chelocardin biosynthesis are responsible for a bifurcation point in the biosynthetic route and slightly different molecule structures having different modes-of-action (Lukežič *et al.*, 2020). While oxytetracycline is a typical protein biosynthesis inhibitor binding to the 30S subunit of the ribosome, chelocardin first and foremost targets the cell membrane potential. Only at higher concentrations chelocardin is assumed to additionally target protein biosynthesis (Stepanek *et al.*, 2016). The membrane-directed action of chelocardin is in line with observations made for other atypical tetracyclines before (Oliva and Chopra, 1992; Chopra, 1994). Moreover, membrane-associated lesions in *B. subtilis* cells treated with tetracycline and anhydrotetracycline, a tetracycline supposed to lack antibiotic activity, have been observed before by using transmission electron microscopy analysis. These results provide evidence that the lesions were not the result of the protein synthesis inhibition but a direct effect of the tetracycline derivative (Wenzel *et al.*, 2021). Based on this report, it can be speculated that all tetracyclines in general have two cellular targets but primarily target the membrane or the ribosome depending on their chemical structure. As validated as part of this thesis, the chelocardin derivative amidochelocardin primarily targets the cell membrane and is retained inside the membrane in comparatively high amounts compared to other antibiotics analyzed previously (Prochnow *et al.*, 2019).

Structurally, chelocardin and its derivative amidochelocardin only differ by an amide moiety replacing a methyl group in amidochelocardin. Nevertheless, amidochelocardin is not only assumed to solely affect the cell membrane, but is further able to efficiently escape multi-drug efflux and to overcome antibiotic resistance in several important nosocomial

pathogens (Hennesen *et al.*, 2020). Due to this broad-spectrum activity, amidochelocardin might eventually be a promising candidate for broad-spectrum antimicrobial therapy, which is still inevitable in severe cases, such as the treatment of septic shock patients (Strich *et al.*, 2020; L. Evans *et al.*, 2021; Rhee *et al.*, 2021). Since *C. difficile* infections rank among the most prevalent forms of adverse events following broad-spectrum antibiotic therapy, broad-spectrum antibiotics with limited or no bioavailability and/or activity in the intestinal tract would be desirable (Gerding, 2004). In this light, it was unfavorable that all members of the small panel of anaerobic bacteria tested for their susceptibility towards amidochelocardin were found to be susceptible and showed similar minimal inhibitory concentrations as aerobic species tested previously (Hennesen *et al.*, 2020). However, the risk for *C. difficile* infections is especially high after therapy with antibiotics that spare *C. difficile*, such as carbapenems and cephalosporins (Gerding, 2004; Sholeh *et al.*, 2020). The substantial susceptibility of *C. difficile* to chelocardins might give reason to hope that the risk for *C. difficile* is not as high as for other broad-spectrum antibiotics. *C. difficile* was previously shown to be substantially sensitive to membrane-directed antibiotics (Wu *et al.*, 2013).

Analysis of the systemic effects of amidochelocardin stress in *C. difficile* 630 suggests that the compound dissipates the membrane potential as observed previously for chelocardin/amidochelocardin stress in *B. subtilis* (Stepanek *et al.*, 2016; Senges *et al.*, 2020). In concert, the observed effects in *C. difficile* 630 in response to the dissipation of the membrane potential, such as the increased synthesis of proteins of the chorismate biosynthesis operon and of two putative phenazine biosynthesis proteins, suggests the increased synthesis and accumulation of aromatic metabolites, including chorismate, a common precursor for most aromatic metabolites, such as aromatic amino acids, quinones, and phenazines (Hubrich *et al.*, 2021). Since the intracellular concentrations of phenylalanine and tyrosine, the two aromatic amino acids synthesized by *C. difficile* 630 *de novo*, remained constant, it was speculated that the chorismate biosynthesis pathway potentially provided chorismate as a precursor for reactions catalyzed by the two identified putative phenazine biosynthesis proteins. However, despite the similarity of the two putative phenazine biosynthesis enzymes with phenazine biosynthesis proteins of other bacterial species, no other proteins from the respective pathways of other phenazine producers, such as *P. aeruginosa*, could be identified in the genome of *C. difficile* 630 (Blankenfeldt and Parsons, 2014). Likewise, a detailed analysis of the respective operons in *C. difficile* 630 did not provide additional hints and no unknown aromatic metabolites could be identified eventually produced by the enzymes.

Discussion

In contrast, the increase of the relative intracellular tryptophan levels, an amino acid not produced *de novo* by *C. difficile* 630 due to the absence of the respective enzymes (Karasawa *et al.*, 1995; Sebahia *et al.*, 2006), supports the idea that aromatic metabolites are required by *C. difficile* to overcome amidochelecardin stress. Although it can only be speculated why it is beneficial for the pathogen to accumulate aromatic metabolites, aromatic compounds are, due to their aromatic nature, able to transport electrons, for instance as part of respiratory chains and other electron shuttling systems (Simon *et al.*, 2008; Shipps *et al.*, 2021). Likewise, phenazine production has been observed in *P. aeruginosa* biofilms under nutrient limitations, where phenazines were proposed to assist in rescuing the membrane potential (Schiessl *et al.*, 2019). Alternatively, tryptophan is also well known for its important role in anchoring of transmembrane proteins and stabilization of membranes. The amino acid is incorporated in many membrane proteins and is involved in dipolar or hydrophobic interactions (Jesus and Allen, 2013; Khemaissa *et al.*, 2021). Accumulation of tryptophan might consequently be advantageous in membrane stress to provide tryptophan to stabilize the membrane. Of note, accumulation of tryptophan has similarly been observed in *Saccharomyces cerevisiae* upon SDS exposure which likewise disturbs membrane barrier function (Schroeder and Ikui, 2019).

Although longtime neglected due to their assumed cytotoxic potential, membrane-active antibiotics are now considered highly promising due to the pleiotropic function of the membrane, such as its central role in energy metabolism (Uppu *et al.*, 2017; Belete, 2019; Dias and Rauter, 2019). In particular, the proton motive force that is established across the membrane via a selective influx and efflux of ions is of great importance as antibiotic target (Lopez and Koch, 2017; Benarroch and Asally, 2020). Moreover, antibiotics affecting the membrane potential have great potential in combination with other drugs as shown for the combinations of, e.g., doxycycline and carprofen or doxycycline and metformin (Brochmann *et al.*, 2016; Liu *et al.*, 2020). Furthermore, the membrane is not only the target of some antibiotics but is also the target of many antimicrobial peptides produced by the immune system as a first line of defense against all invading pathogens at the host-pathogen interface (Mookherjee *et al.*, 2020). Interestingly, the proteome signature of amidochelecardin stress in *C. difficile* 630 revealed elevated levels of ClnA and ClnR from the ClnRAB operon, which is supposed to specifically respond to CAMPs, such as LL-37 (Woods *et al.*, 2018). Although LL-37 and similar CAMPs kill bacteria via pore formation, which has been excluded for amidochelecardin, there is obviously some kind of similarity between CAMP and amidochelecardin stress in *C. difficile* 630. In this light, the presented data might also contribute to an increased understanding of CAMP stress in *C. difficile*.

5. Conclusion and outlook

In summary, the data discussed in the previous sections provided not only valuable insights into *C. difficile*'s stress response architecture, but also evidence that the compound classes of chlorotonils and myxopyronins are interesting lead structures for the design of new antibiotics against *C. difficile*. Both compound classes are at least in part able to address the demands for an antibiotic directed against *C. difficile* by being relatively selective for *C. difficile* while severely affecting *C. difficile*'s central metabolism. In addition, both compound classes are able to reduce toxin levels *in vitro* in case of myxopyronin B (section 3.2.3) or *in vivo* in case of chlorotonils (Bublitz *et al.*, in revision). Moreover, the presented data indicate that *C. difficile* is essentially sensitive to antibiotics that either disturb metal homeostasis or dissipate the membrane potential. Especially, disturbance of metal homeostasis is a promising feature for an antibiotic directed against *C. difficile* due to the high sensitivity of strict anaerobes to transient metal toxicity, including vulnerability of *C. difficile*'s various [4Fe4S]-dependent enzymes like the TCA cycle enzyme fumarate hydratase as already outlined in the introduction (section 1.3.2). Future experiments addressing the efficiency and safety as well as the mode-of-action of chlorotonils are required to promote the compound class as new promising therapeutic against *C. difficile*.

Despite low resistance rates of *C. difficile* against fidaxomicin and vancomycin, new antibiotics are urgently required. The reduction of antibiotic prescription and more sophisticated treatment guidelines successfully stopped the rise in *C. difficile* infections per year (Dingle *et al.*, 2017; Guh *et al.*, 2020). Also a decline of healthcare-associated *C. difficile* infections in the US becomes visible when data are curated for improved testing strategies. However, the same study reported increasing numbers in community-acquired infections resulting in an overall constant level of infections (Guh *et al.*, 2020). Since the recent decline in healthcare-associated infections is drawn back to the reduced prescription of fluoroquinolone antibiotics (Dingle *et al.*, 2017; Guh *et al.*, 2020), reduction of carbapenem and third- and fourth-generation cephalosporin therapy is expected to further reduce the numbers of *C. difficile* infections (Slimings and Riley, 2021). Nevertheless, the therapy of the infection remains challenging. By the introduction of fidaxomicin in 2011, a selective RNA polymerase inhibitor with the ability to reduce toxin synthesis and sporulation rates, recurrence events were only slightly reduced (Louie *et al.*, 2012; Aldape *et al.*, 2017). In addition, emerging fidaxomicin-resistant strains give further cause for concerns (Leeds *et al.*, 2014; Schwanbeck *et al.*, 2019).

At this point, alternative strategies, such as pre- and probiotic and FMT therapies, have been discussed and are further developed in order to directly address the restoration of colonization resistance provided by the complex intestinal community (Laffin *et al.*, 2017;

Conclusion and outlook

Shen *et al.*, 2017; Hui *et al.*, 2019). Indeed, clinical trials successfully proved the suitability of FMT and probiotics and have likewise been shown to valuably contribute to infection management in *C. difficile* patients (Quraishi *et al.*, 2017; Shen *et al.*, 2017; Hui *et al.*, 2019). Moreover, monoclonal antibodies inhibiting toxin-mediated cell damage or stimulating the immune system have recently gained attention as modulators of disease severity (Wilcox *et al.*, 2017; Monaghan *et al.*, 2021). Nevertheless, neither monoclonal antibodies nor pre- and probiotic therapy are suited as stand-alone therapy. Furthermore, FMT is still critically discussed due to the risk of transplanting pathogenic species and the still scarce knowledge on the critical factors underlying successful FMT therapy (Moss *et al.*, 2017; Yadav and Khanna, 2021).

Therefore, antibiotics are still inevitable for the therapy of *C. difficile* infections. However, only a few candidate antibiotics have made it into clinical testing until now, of which none has reached non-inferiority compared to fidaxomicin by now (Boix *et al.*, 2017; Petrosillo *et al.*, 2018; Gerding *et al.*, 2019; Monaghan *et al.*, 2021). In this light, chlorotolils and myxopyronins can eventually promote the therapy of *C. difficile* infections in the future.

6. Materials and methods

6.1 Antibiotics

6.1.1 Natural products

Natural products were provided as lyophilized powder by the department of Microbial Natural Products at the Helmholtz Institute for Pharmaceutical Research in Saarbrücken, Germany.

Chlorotonil A

Chlorotonils were first dissolved at a concentration of 1 mg/ml (w/v) in DMSO (Sigma Aldrich, St. Louis, MO, USA) in an ultrasonic bath. Subsequently, the compounds were serially diluted in DMSO to obtain working stocks with 0.1 or 0.01 mg/ml, which were kept in aliquots at -20 °C until use. Aliquots were preferentially used as single-use stocks or were not defrosted more than three times to avoid degradation of the compound. Additional information on the purification and synthesis of chlorotonils can be obtained from (Hofer *et al.*, 2022).

Myxopyronin B

Myxopyronin A and B were first dissolved at a concentration of 10 mg/ml (w/v) in DMSO (Sigma Aldrich, St. Louis, MO, USA). Subsequently, the compounds were serially diluted in DMSO to obtain working stocks with 0.1 mg/ml, which were kept in aliquots at -20 °C until use. Aliquots were only used once and were discarded after use. Additional information on the purification and synthesis of chlorotonils can be obtained from Brauer *et al.* (2022).

Amidochelocardin

Chelocardin (CHD) and amidochelocardin (CDCHD) were provided in complex with citrate in a ratio of 2:1. CHD/citrate and CDCHD/citrate were dissolved in MS-pure water at a concentration of 1.5 mg/ml to obtain stock solutions containing 1 mg/ml chelocardin/amidochelocardin. Aliquots of the solved compounds were kept in aliquots at -20 °C until use. Aliquots were only used once and were discarded after use. Additional information on the purification and synthesis of chelocardin and amidochelocardin can be obtained from Lesnik *et al.* (2015) and Brauer *et al.* (in preparation for re-submission).

6.1.2 Commercial antibiotics

Rifaximin and fidaxomicin were obtained from Sigma Aldrich (St. Louis, MO, USA) and Selleck Chemicals (Houston, Texas, TX, USA) and were dissolved in DMSO (Sigma Aldrich, St. Louis, MO, USA). Stock solutions of 1 mg/ml were serially diluted to appropriate working stocks and aliquots were kept at -20 °C until use. Aliquots were not used more than three times.

Materials and methods

6.2 *In vitro* experiments

The following section provides information about the experimental procedures of all *in vitro* experiments done with *C. difficile* and commensal bacteria, comprising cultivation experiments and downstream omics analyses.

6.2.1 Bacterial strains and handling

6.2.1.1 Routine growth conditions

For all *in vitro* experiments, bacteria were routinely grown in an anaerobic workstation (Whitley DG250 anaerobic work station; 98% N₂, 2% H₂) at 37 °C with the exception of *E. faecalis* and *L. casei*. *E. faecalis* was cultivated at 37 °C and 180 rpm under aerobic condition. *L. casei* was cultivated at 37 °C under micro-aerophilic conditions without shaking. All bacteria were routinely grown in Brain Heart Infusion (BHI) broth (Oxoid, Wesel, Germany), which was prepared according to the manufacturer's recommendations. After autoclaving, medium flasks were closed with rubber plugs and oxygen was removed from the medium by gasing with pure nitrogen for at least 15 minutes. In addition, remaining oxygen was allowed to diffuse from the medium when medium flasks were left loosely closed in the anaerobic chamber overnight.

Bacterial strains used in this thesis are listed in **Table 6.1**.

6.2.1.2 Maintenance of strains

For long term conservation, all strains were maintained as glycerol stocks at -70 °C in 30% glycerol.

For preparation of spore suspensions, *C. difficile* was allowed to grow for 24 h at 37 °C and for additional 48 h at room temperature (RT) in BHI medium to allow sporulation. Subsequently, spores, vegetative cells and cell debris were collected by centrifugation for 10 min at 10,000 g. Supernatants were discarded and pellets were suspended in half of the initial volume aerobic BHI to concentrate spore suspensions. Suspensions were kept in 200 µl aliquots at 4 °C for a couple of months.

6.2.1.3 Preparation of overnight cultures

Prior to all experiments performed with *C. difficile*, spores of the respective strains were allowed to germinate in BHI supplemented with 5% yeast extract and 0.1% taurocholic acid at 37 °C for 24 h and vegetative cells were subsequently used to inoculate overnight cultures. Overnight cultures for all other species were inoculated directly from glycerol stocks. Overnight cultures were grown for 12 h and used to inoculate main cultures.

Table 6.1: Bacterial strains

Species	Strain designation	# DSMZ	Date & place of isolation	Reference
<i>Clostridioides difficile</i> (012)	630	27543	Zurich, Switzerland, 1982	(Wüst et al., 1982)
<i>Clostridioides difficile</i> (012)	630Δerm	28645	Derivative of 630	(Hussain et al., 2005)
<i>Clostridioides difficile</i> (027)	R20291	27147	Aylesbury, UK, 2006	(Stabler et al., 2009)
<i>Clostridioides difficile</i> (001)	1780	1296	Unknown	-
<i>Clostridioides difficile</i> (007/014/025)	Goe-91	105001	Goettingen, Germany	(Schwanbeck et al., 2019)
<i>Clostridioides difficile</i> (087)	VPI10463	-	Unknown	(Lyery et al., 1983; 1986)
<i>Clostridioides difficile</i> (126)	11S0047 (rt126)	-	Jena, Germany	(Schneeberg et al., 2013)
<i>Clostridioides difficile</i> (078)	12S0133 (rt78)	-	Jena, Germany	(Schneeberg et al., 2013)
<i>Terrisporobacter glycolicus</i>	JCM 1401	1288	Maryland, USA, before 1978	(Gerritsen et al., 2014)
<i>Terrisporobacter</i> sp.	CCK3R4-PYG-107	29186	Munich, Germany, 2012	(Lagkouvardos et al., 2016)
<i>Paeniclostridium sordellii</i>	211	2141	Unknown, before 1981	(Sasi Jyothsna et al., 2016)
<i>Intestinibacter bartlettii</i>	WAL 16138	16795	Chicago, USA, before 2005	(Gerritsen et al., 2014)
<i>Peptostreptococcus anaerobius</i>	VPI 4330	2949	Unknown	(Murdoch et al., 2000)
<i>Paraclostridium bifermentans</i>	701	631	Unknown, before 1975	(Sasi Jyothsna et al., 2016)
<i>Clostridium scindens</i>	VPI 13733	5676	USA, before 1984	(Morris et al., 1985)
<i>Bifidobacterium longum</i> subsp. <i>Infantis</i>	S12	20088	Unknown, before 1990	(Mattarelli et al., 2008)
<i>Lactobacillus casei</i>	3	20011	Unknown, before 1972	(Zhang et al., 2010)
<i>Enterococcus faecalis</i>	H1	-	Italy, 2008	(Pessione et al., 2012)
<i>Bacteroides fragilis</i>	VPI 2553	2151	UK	(Castellani A, 1919)
<i>Bacteroides thetaiotaomicron</i>	WAL 2926	2255	Unknown	(Castellani A, 1919)

Materials and methods

6.2.1.4 Chemical defined medium for routine growth of *C. difficile*

If indicated, *C. difficile* was grown in a chemical defined medium composed of an amino acid mix, glucose, vitamins, trace elements and a phosphate buffer, described by Cartman and Minton *et al.* (2010) and modified by Neumann-Schaal *et al.* (2015) (Cartman and Minton, 2010; Neumann-Schaal *et al.*, 2015) (Table 6.2).

Table 6.2: Chemical defined medium (CDMM). All components were obtained from Carl Roth (Karlsruhe, Germany) with the exception of cobalt dichloride hexahydrate and sodium selenite pentahydrate, which was obtained from Sigma Aldrich (St. Louis, MO, USA). ¹ Concentrations of stock solutions.

Component	Concentration ¹	Sterilization
10 x CDMM buffer		Autoclaved
di-Sodium hydrogen phosphate	50 g/l	
Sodium dihydrogen phosphate dihydrate	20 g/l	
Potassium dihydrogen phosphate	9 g/l	
Sodium chloride	9 g/l	
5 x Casamino acid mix		Sterilized by filtration
Casamino acids	50 g/l	
L-Cysteine	2.5 g/l	
L-Tryptophan	0.5 g/l	
100 x Trace salt mix		Sterilized by filtration
di-Ammonium sulfate	4 g/l	
Calcium dichloride dihydrate	2.6 g/l	
Magnesium dichloride hexahydrate	2 g/l	
Mangan dichloride tetrahydrate	1 g/l	
Cobalt dichloride hexahydrate	0.1 g/l	
Sodium selenite pentahydrate	0.015 g/l	
500 x Iron solution		Sterilized by filtration
Iron(II)sulfate heptahydrate	2 g/l	
200 x Vitamin solution		Sterilized by filtration
D-Biotin	0.06 g/l	
Calcium-D-panthotenate	0.2 g/l	
Pyridoxine hydrochloride	0.2 g/l	
100 x Glucose solution		Sterilized by filtration
D-Glucose monohydrate	200 g/l	
A. dest	Ad 1000 ml	Autoclaved

6.2.1.5 Cell disruption

If required, cells were disrupted in screw cap tubes with 1 ml of Tris-EDTA, pH 7.5 buffer (Table 6.3) and 500 μ l of glass beads (0.1 to 0.11 mm, Satorius Stedim Biotech, Göttingen, Germany) by three cycles of bead beating at 6.5 m/s for 30 s in FastPrep-24™5G homogenizer (M.P. Biomedicals, Santa Ana, CA, USA). Subsequently, glass beads and cell debris were removed by three centrifugation steps at 20,000 x *g* at 4 °C.

Optionally, the volume of Tris-EDTA buffer and glass beads was adjusted depending on the cell pellet size.

Table 6.3: Tris-EDTA buffer, pH 7.5

Component	Concentration
Tris, pH 7.5	10 mM
EDTA, pH 8.0	1 mM

Materials and methods

6.2.2 Physiological assays

6.2.2.1 Growth experiments

For analysis of growth rates, a respective volume of either BHI or CDMM was inoculated from an overnight culture to an OD_{600nm} of 0.05. In the following, growth was monitored in adequate intervals by optical density measurements at OD_{600nm} .

6.2.2.2 Antibiotic susceptibility assays

Serial broth dilution assays

Minimal inhibitory concentrations were determined in serial broth dilution assays. Briefly, antibiotics were diluted in two-fold serial dilutions in adequate concentration ranges in supplemented BHI (BHIS) medium (Table 6.4) and 100 μ l of the respective dilutions were transferred to 96-well plates (Brand™, cellGrade, F-bottom; Thermo Scientific, Rockford, IL, USA). Each well was subsequently inoculated with 100 μ l of a bacterial suspension prepared by diluting overnight cultures of each individual strain 1:100 in BHIS medium. Plates were incubated at 37 °C and minimal inhibitory concentrations, the lowest concentrations where no growth could be observed, were determined after 24 h. All experiments were conducted in technical duplicates and biological triplicates at least.

Table 6.4: Supplemented Brain infusion broth for minimal inhibitory concentration assays.

Component	Final concentration
Brain Heart Infusion Broth®	37 g/l
Yeast extract	5 g/l
L-Cysteine	1 g/l
Vitamin K1	0.1%
Hemin(chloride)	0.5%
A. dest	Ad 1 l

Stress experiments

For antibiotic stress experiments a batch culture of each bacterial strain was inoculated to an OD_{600nm} of 0.05 and was grown to mid-exponential phase in BHI medium. At an OD_{600nm} of approximately 0.5, the batch cultures were split to subcultures of 30 ml and treated with serial dilutions of the antibiotics of interests. Subsequently, the optical densities of all subcultures were monitored for several hours. If required, colony forming units were determined at selected timepoints by plating serial dilutions onto BHIS agar plates, which were incubated for 24 h until colony forming units could be counted. Experiments were conducted in at least three biological replicates.

6.2.2.3 Toxin western blots

Toxins of *C. difficile* were detected and quantified either within cytosolic or extracellular protein extracts of *C. difficile*. Cytosolic proteins were extracted as described in section **6.2.1.5**. For precipitation of extracellular proteins, 10 ml culture supernatants were separated from bacterial cells by filtering through a 0.2 µm filter followed by precipitation of proteins with 10% trichloroacetic acid (Carl Roth, Karlsruhe, Germany) overnight at 4 °C. Precipitated proteins were collected by centrifugation for 1 h at 10,000 x g at 4 °C. Subsequently, protein pellets were washed twice with 70% ethanol and once with 100% ethanol. Protein pellets were dried and dissolved in 500 µl 3x SDS sample buffer (**Tab. 6.5**). Either 50 µg of cytosolic protein samples mixed with an appropriate volume of 3x SDS sample buffer or 30 µl of precipitated extracellular protein extracts were separated by SDS PAGE on 8% SDS gels (**Table 6.6, Table 6.7**) for 3 h at 80 V in running buffer (**Table 6.8**). Separated proteins were either stained with colloidal Coomassie (**Table 6.9**) or blotted on PVDF membranes (Merck Millipore, Burlington, VT, USA) for 1.5 h at 100 V (**Table 6.10**). Blotted membranes were blocked in 5% skim milk in 1x TBS (**Table 6.11**) prior to incubation with primary antibodies against toxin A (tgcBiomics, Bingen, Germany) or toxin B (provided by Ralf Gerhardt, Hannover Medical School, Hannover, Germany) in volume-to-volume ratio of 1:5000 in 5% skim milk at 4 °C overnight. Unbound antibodies were washed off by three washing steps in TBST for 5 min (TBS, 0.1% Tween 20). Depending on the primary antibody used, membranes were incubated with an alkaline phosphatase-coupled anti-mouse (toxin A) or anti-rabbit (toxin B) secondary antibody (both Sigma Aldrich, St. Louis, MO, USA) in volume-to-volume ratio of 1:30,000 for 1 h at RT. Unbound secondary antibodies were washed off by three wash steps with dH₂O. Prior to detection, membranes were incubated for 30 min in AP buffer (**Table 6.12**). Finally, toxin signals were detected with a NBT/BCIP reaction solution (Carl Roth, Karlsruhe, Germany) in AP buffer (**Table 6.13**). For quantification of toxin signals, blots were scanned and signals were quantified using ImageJ (Schneider et al., 2012). Statistical testing was performed with the R package “ggpubr” using multiple pairwise comparisons (t-test) (version: 0.4.0) (Kassambara, 2020).

Materials and methods

Table 6.5: 3x SDS sample buffer for SDS PAGE

Component	Final concentration
Tris, pH 6.8	300 mM
EDTA	6 mM
SDS	3%
β -mercaptoethanol	3%
Glycerol	30%
Bromphenol blue	

Table 6.6: Stacking gel for SDS PAGE

Component	Final concentration
Tris, pH 6.8	250 mM
Bis-acrylamide	4%
SDS	0.1%
Ammoniumpersulfat	0.1%
TEMED	0.1%

Table 6.7: Separation gel for SDS PAGE

Component	Final concentration
Tris, pH 7.5	250 mM
Bis-acrylamide	8%
SDS	0.1%
Ammoniumpersulfat	0.1%
TEMED	0.1%

Table 6.8: Running buffer for SDS PAGE

Component	Final concentration
Tris	250 mM
Glycine	2 M
SDS	35 mM

Table 6.9: Colloidal Coomassie blue silver staining buffer (Candiano *et al.*, 2004)

Component	Final concentration
Ammonium sulfate	600 mM
Methanol	20%
Phosphoric acid	8%
Coomassie G250 C47	1 mM

Table 6.10: Transfer buffer for western blot analysis

Component	Final concentration
Tris	25 mM
Glycine	100 mM
Methanol	15%

Table 6.11: 10x TBS (Tris-buffered saline)

Component	Final concentration
Tris, pH 7.6	500 mM
Sodium chloride	1.5 M

Table 6.12: Alkaline phosphatase (AP) buffer

Component	Final concentration
Tris	100 mM
Sodium chloride	100 mM
Magnesium chloride	10 mM

Table 6.13: NBT/BCIP solution for detection of alkaline phosphatase signals

Component	Final concentration
NBT (5% w/v in 70% dimethylformamide)	3%
BCIP (5% w/v in 100% dimethylformamide)	1.5%
AP buffer	99.5%

Materials and methods

6.2.2.4 Fluorescence-based determination of the membrane potential

To analyze changes in the proton motive force across *C. difficile*'s membrane, a CDMM *C. difficile* culture was grown to mid-exponential phase. Subsequently, cells were treated with 0.5 μM of the fluorescent dye DISC₃(5) solved in DMSO (Sigma Aldrich, St. Louis, MO, USA). The dye was allowed to accumulate within the cell membrane for several minutes until the total quenching of the fluorescent signal. Subsequently, cells were treated with the antibiotic of interest and immediately transferred to black 96-well plates. Fluorescence signals were recorded at an excitation of 500 nm and an emission at 675 nm in a SynergyMx Microplate reader (BioTek Instruments, Winooski, VT, USA) for 30 min with measurements taken every minute. Experiments were conducted in at least three biological replicates. Statistical testing was performed with the R package "rstatix" using multiple pairwise comparisons (t-test) against the controls as reference group (version: 0.7.0) (Kassambara, 2021).

6.2.2.5 Luminescence-based quantification of intra- and extracellular ATP levels

Intracellular and extracellular ATP levels of *C. difficile* were determined using the CellTiter-Glo® 2.0 Assay according to the manufacturer's recommendations (Promega, Madison, WI, USA). As before, a *C. difficile* culture in CDMM was grown to mid-exponential phase and split to subcultures of 30 ml that were immediately treated with respective antibiotics. Prior and 30, 60 and 90 minutes after stress, 1 ml samples of each culture were collected by centrifugation. Subsequently, 100 μl of supernatants or 100 μl of cell suspension obtained by re-suspending cell pellets in 1 ml CDMM were mixed with 100 μl of the CellTiter-Glo® 2.0 Assay reagent in opaque 96-well plates. After luminescence signals were stable, the luminescence signals were recorded in a SynergyMx Microplate reader (BioTek Instruments, Winooski, VT, USA). Experiments were conducted in at least three biological replicates. Statistical testing was performed with the R package "rstatix" using multiple pairwise comparisons (t-test) against the controls as reference group (version: 0.7.0) (Kassambara, 2021).

6.2.3 Proteomics experiments

6.2.3.1 Cultivation and cell harvest

For proteomics experiments, *C. difficile* 630 was grown in CDMM to mid-exponential phase and stressed with a sublethal concentration of the respective antibiotics of interest or an equal volume of DMSO (Sigma Aldrich, St. Louis, MO, USA) (Suppl. figure S3). After 90 min of growth in the presence of the antibiotics, treated and untreated cells were collected by centrifugation for 5 min at 10,000 x *g* at 4 °C and cell pellets were washed once with Tris-EDTA buffer (Table 6.3). Cell pellets were lysed as described in section 6.2.1.5 and protein concentrations were determined with Roti® NanoQuant (Carl Roth, Karlsruhe, Germany) according to manufacturer's instructions. Protein extracts were stored at -70 °C until further analysis.

6.2.3.2 S-trap digestion

Protein samples were prepared for LC-MS/MS measurements by S-traps® digestion according to the manufacturer's recommendations (ProtiFi, Huntington, NY, USA). Briefly, 50 µg of each extract were filled up to 25 µl with 100 mM tetraethylammonium bicarbonate (TEAB, Sigma Aldrich, St. Louis, MO, USA) and mixed with 25 µl of 10% SDS, 100 mM TEAB. Proteins were first reduced with 10 mM dithiothreitol (Sigma Aldrich, St. Louis, MO, USA) for 10 min at 95 °C followed by alkylation with 20 mM iodoacetamide (Sigma Aldrich, St. Louis, MO, USA) for 20 min at RT in the dark. Alkylated samples were acidified with 12% phosphoric acid (Carl Roth, Karlsruhe, Germany) in a relation of 1:6 and mixed with seven volumes of S-trap buffer composed of 90% methanol, 100 mM TEAB. Diluted samples were applied onto S-trap columns in several centrifugation steps at 4,000 x *g*. Subsequently, columns were washed four times with S-trap buffer. Sequencing grade trypsin (Promega, Madison, WI, USA) was activated in 100 µl of the provided activation buffer for 15 min at 37 °C and diluted 1:5 in 100 mM TEAB. 25 µl of diluted trypsin was applied to each column and columns were incubated for 3 h at 47 °C. Tryptic peptides were eluted from the columns in three steps by centrifugation for 1 min at 4,000 *g* starting with 40 µl of 100 mM TEAB for elution of hydrophilic peptides, followed by 40 µl of 0.1% acetic acid for elution of median hydrophilic peptides and 35 µl of 60% acetonitrile, 0.1% acetic acid to allow elution of hydrophobic peptides. All elution fractions were pooled and dried by vacuum centrifugation. Dried peptides were stored at -20 °C.

Materials and methods

6.2.3.3 High pH reversed-phase fractionation

Trypsinized peptides were desalted and fractionated by high pH reversed-phase fractionation according to (Mücke *et al.*, 2020). Briefly, Pierce™ micro-spin columns (Thermo Scientific, Rockford, IL, USA) were packed with 18 mg of Reprosil Gold C₁₈ material (Dr. Maisch GmbH, Ammerbuch-Entringen, Germany) followed by activation and washing of C₁₈ with 300 µl acetonitrile for four times for 2 min at 3,000 x *g*. Subsequently, columns were equilibrated with 300 µl of 0.1% trifluoroacetic acid (Sigma Aldrich, St. Louis, MO, USA) for 2 min at 3,000 x *g*. Peptides from S-trap digestion were suspended in 300 µl of 0.1% trifluoroacetic acid and applied to the columns by centrifugation for 4 min at 3,000 *g*. Columns were then washed once with MS-pure H₂O for 4 min at 3,000 *g*. Afterwards peptides were eluted from the columns in eight centrifugation steps with increasing concentrations of acetonitrile in 0.1% triethylamine (Carl Roth, Karlsruhe, Germany) starting with 5% acetonitrile and step-wise increase to 20% acetonitrile followed by a last elution step with 50% acetonitrile. To reduce sample numbers, fractions 1 and 5, 2 and 6, 3 and 7, and 4 and 8 were pooled and all samples were dried in MS vials by vacuum centrifugation. Prior to LC-MS/MS analysis samples were suspended in 20 µl of 0.1 acetic acid (Carl Roth, Karlsruhe, Germany).

6.2.3.4 LC-MS/MS measurements

Mass spectrometry samples were analyzed on a Q Exactive™ HF Hybrid Quadrupole-Orbitrap™ Mass Spectrometer coupled to an EASY nLC 1200 HPLC (Thermo Fisher Scientific, Waltham, MA, USA). Prior to LC-MS/MS analysis, peptides were loaded onto self-packed C₁₈ reverse phase analytical columns (3 µm, Dr. Maisch GmbH, Ammerbuch-Entringen, Germany) with an integrated emitter (100 µm x 20 cm). For injection into the mass spectrometer, peptides were eluted from the HPLC column using a 85 min gradient from 5 to 50% of acetonitrile, 0.1% acetic acid with a constant flow rate set to 300 nl/min. First, full survey scans were performed with a resolution of 60,000 in the range of 333 – 1650 *m/z* followed by MS/MS scans for the fifteen most abundant precursor ions per scan cycle. Unassigned charge states and singly charged ions were excluded. In addition, repeated measures of the same peptide were permitted by enabling dynamic exclusion for 30 s. The internal lock mass calibration was set to a lock mass of 445.12003.

6.2.3.5 Data base search and data preparation

MS raw files were searched against strain specific databases obtained from NCBI or Uniprot (Table 6.14) with the Andromeda-based search engine MaxQuant (Tyanova *et al.*, 2016) applying the search parameters listed in Table 6.15. To increase protein identification, “match-between-runs” was enabled between biological replicates of each specific stress

conditions. Obtained search results were filtered for proteins identified with at least 2 unique peptides. Proteins were considered as identified if iBAQ values are provided for at least two out of three (ChB1-Epo2, MyxB dataset) or three out of four (ChA, CDCHD dataset) biological replicates. Finally, fold changes between treated and untreated sample sets were calculated using the LFQ intensities if LFQ intensities were provided for at least two out of three (ChB1-Epo2, MyxB dataset) or three out of four (ChA, CDCHD dataset) biological replicates. Fold changes were further subjected to log2 transformation. Furthermore, proteins were considered as exclusively present in stress samples (“ON”), if proteins were identified in at least three vs. zero biological replicates, or absent (“OFF”) if proteins were identified in zero vs. at least three biological replicates.

Table 6.14: Databases used for MaxQuant dataset searches.

Database	Source/date	# entries
20210803_Cdiff_NC_009089	NCBI, 03.08.2021	3560
20210315_Cdiff_630_uniprot_RefProteome_UP000001978	UniProt, 15.03.2021	3762
20210604_Tglycolicus_uniprot_proteome_UP000183495	UniProt, 04.06.2021	3774

Table 6.15: Parameter sets used for MaxQuant dataset searches.

* Parameter used for ChA/ChtB1-Epo₂ stress and adaptation experiments; ** Parameters used for amidochelocardin and rifaximin/fidaxomicin/myxopyronin B experiments.

Parameter	Value
Version	2.0.1.0 * / 1.6.17.0 **
PSM FDR	0.01
Minimal peptide Length	7
Minimal peptide length for unspecific search	8
Maxima peptide length for unspecific search	25
Minimal unique peptides	0
Minimal peptides	1
Maximum missed cleavages	2
Fixed modifications	Carbamidomethylation of cysteine
Variable modifications	Oxidation of methionine
Peptides used for protein quantification	Razor
Decoy mode	Revert
Include contaminants	True

6.2.3.6 Statistical analysis

Statistical analysis of MaxQuant derived MS data was done with the R package “DEqMS” (version: 1.8.0) (Zhu *et al.*, 2020). Analyses were done pairwise based on MaxQuant derived LFQ intensities and respective peptide counts. Changes in protein intensities were considered to be significant if the DEqMS derived adjusted p values were below the threshold of 0.05.

Materials and methods

6.2.3.7 Bioinformatic analyses

For further data analysis, additional information on the function and subcellular localization of a respective protein as well as information on functional domains, required cofactors or operon associations were obtained from various open-source platforms listed in **Table 6.16**.

Table 6.16: Databases, online repositories and tools used for annotations.

Source	Annotation type	Reference	Link
UniProt	Gene name Protein name Locus tag PATRIC ID STRING ID Gene ontology Required cofactors Domains	(UniProt Consortium, 2021)	www.uniprot.org
PSORTb	Subcellular localization	(Yu <i>et al.</i> , 2010)	www.psortb.org
PATRIC DB	Role ID Role name Superclass Class Subclass Subsystem name	(Davis <i>et al.</i> , 2020)	www.patricbrc.org
MicrobesOnline	Operon predictions Strand information Start and stop sites	(Dehal <i>et al.</i> , 2010)	www.microbesonline.org
ProOpDB	Operon predictions	(Taboada <i>et al.</i> , 2012)	www.operons.ibt.unam.mx
DOOR2	Operon predictions	(Mao <i>et al.</i> , 2014)	www.csbl.bmb.uga.edu/DOOR
RegPrecise	Regulon predictions	(Novichkov <i>et al.</i> , 2013)	www.regprecise.lbl.gov
TransportDB 2.0	Membrane transport substrates	(Elbourne <i>et al.</i> , 2017)	www.membranetransport.org
InterPro	Domains	(Jones <i>et al.</i> , 2014)	https://www.ebi.ac.uk/interpro/

6.2.3.8 Gene set enrichment analysis

Predicted metabolic pathways, operons and enzyme functions were used to define gene sets of at least four proteins. For the gene set enrichment analysis, all identified proteins were ranked according to their \log_2 fold changes and mean rank sums for every gene set were calculated. Gene sets can be found in the supplementary material (**Suppl. table S13**).

6.2.4 qPCR analysis

6.2.4.1 Cell harvest and RNA extraction

C. difficile 630 was cultivated as done for the proteomics experiment described in section 6.2.3.1. When reaching an $OD_{600\text{ nm}}$ of 0.5 cells were treated with 1.5 $\mu\text{g/ml}$ amidochelocardin and were allowed to grow in the presence of the antibiotic for additional 10 minutes. Subsequently, cells were cooled down in liquid nitrogen and collected by centrifugation for 3 min at 10,000 $\times g$ and 4 °C. RNA was extracted using TRIzol reagent (Invitrogen, Waltham, MA, USA) according to the manufacturer's recommendations. Purified RNA was solubilized in diethyl pyrocarbonate (DEPC)-treated water followed by treatment with DNase I (Roche, Basel, Switzerland).

6.2.4.2 cDNA synthesis and qPCR analysis

500 ng of the RNA samples were used for cDNA synthesis using the RevertAid RT kit (Thermo Fisher Scientific Baltics, Vilnius, Lithuania). The mRNA expression of five genes from each of the five predicted/putative operons of interest were analyzed by quantitative PCR using the Luna Universal qPCR Master Mix (New England Biolabs, Ipswich, MA, USA) and a qTOWER 3 quantitative PCR thermocycler (Analytik Jena, Jena, Germany) according to the manufacturer's recommendations. Primers were designed for an annealing temperature of 60 °C and are listed in Table 6.17. Expression of *codY* was used as internal reference and relative expression was calculated according to the Pfaffl method. Finally, statistical testing was performed using the R package "rstatix" using t-testing (version: 0.7.0) (Kassambara, 2021).

Table 6.17: Primers for qPCR analysis.

Gene	Orientation	Primer
<i>aroF1</i>	forward	TGGCTGGAGGAAATGAAAATG
	reverse	AGTCAACCATCCATGATTTACC
<i>clnR</i>	forward	GAAACAGTGAGAGCACTAGC
	reverse	TCTCCACATTAGCTATTTCC
<i>CD630_0310</i>	forward	AGCCTTACACCAGAAAAACAG
	reverse	CCAGGTTTCCAATGCTTGTG
<i>CD630_17590</i>	forward	GCAAACCTTTGTAATAACCG
	reverse	CCCATAGTCATACTATCGTC
<i>CD630_30350</i>	forward	ATACCTTTTGGTGAAATCCTG
	reverse	ATCAACTTCTAAACCTGGTGTG
<i>codY</i>	forward	TCAAATTCATTCAATGATGATGATTTAG
	reverse	TCTTCTAATTCTTCACCTATTGCTC

Materials and methods

6.2.5 Inductively-coupled plasma-mass spectrometry analysis (ICP-MS)

6.2.5.1 Cultivation and cell harvest

C. difficile was cultivated and treated with 4.69 ng/ml ChB1-Epo2 as done for the proteomics experiment described in section 6.2.3.1. Subsequently, cells were collected by centrifugation for 5 min at 10,000 x *g* at 4 °C. Cells were washed once in 10 mM Tris-HCl, pH 7.4 and after an additional centrifugation step, cells were suspended in 1 ml 10 mM Tris-HCl, pH 7.4 and lysed as described in section 6.2.1.5. Finally, the cytoplasmic fractions of cell lysates were transferred to low-binding tubes (Sorenson™ BioScience, Murray, UT, USA).

6.2.5.2 ICP-MS analysis

20 µl cellular extract or 9.37 µl dissolved compound were used to determine intracellular levels of elements. First, the extract was separated on a Superose 6 Increase 3.2x300 gel-filtration column (Cytiva Lifescience, Freiburg, Germany) by isocratic elution with 10 mM Tris-HCl, pH 7.4 at a flow rate of 100 µl min⁻¹ coupled to an Agilent 7500c ICP-MS instrument (Agilent, Waldbrunn, Germany), equipped with a Scott type spray chamber and a perfluoroalkoxy µ-flow nebulizer, to monitor the intensity for several elemental isotopes over a period of 100 min. The plasma was operated at 1600 W and all other parameters were daily optimized in order to obtain stable signals for the elements of a tuning solution (10 ppb of: 6Li – ~8.0e4 cps, 89Y - ~1.3e5 cps, 140Ce - ~1.3e5 cps, 205Tl - ~ 9.6e4 cps), and stable background signals for 13C, 23Na, 39K when infusing the eluent from the gel-filtration column.

Finally, the obtained chromatograms for each isotope were corrected for the natural isotope abundance as provided by the instrument manufacturer and for sensitivity drifts by a smoothed 13C baseline using R scripts. To enable comparison between the ChB1-Epo2-treated and DMSO-control samples, protein concentrations were determined by Bradford assay with bovine serum albumin as external calibrant for each sample. The chromatograms were rescaled according to the injected protein amount. The peak fitting program Fityk 1.3.1 was finally used to integrate peak areas above the baseline for each isotope (Wojdyr, 2010). Total elemental content was calculated as the summary of peak areas. Statistical testing was performed with the R package “rstatix” using paired t-testing (version: 0.7.0) (Kassambara, 2021).

6.2.6 Metabolomics analysis

Metabolomics experiments were performed as described by Dörries *et al.* (2014) and Liebeke *et al.* (2008).

6.2.6.1 Cultivation of cells

C. difficile cultures were cultivated and stressed as done for the proteomics experiment described in section **6.2.3.1**. After 90 minutes of growth in the presence of the antibiotics, treated and untreated cells were immediately cooled down in liquid nitrogen and collected by centrifugation for 3 min at 10,000 x *g* at 4 °C. Supernatants were collected in separate 50 ml tubes and supernatant-free pellets were frozen in liquid nitrogen. 1.2 ml of each supernatant were filtered through a 0.2 µm cutoff filter and were likewise frozen in liquid nitrogen. 1 ml aliquots of the pure medium were co-frozen as blank.

6.2.6.2 Extraction of cytosolic metabolites

For extraction of the intracellular metabolites, cell pellets were suspended in 800 µl of 60% ice-cold ethanol and transferred to screw cap tubes. Two additional screw cap tubes were filled with either 500 µl of CDMM or 500 µl of MS-pure water and 800 µl of 60% ethanol as medium or empty control. 200 µl of an internal GC-MS standard (GC4; 20 nM each of *N,N*-dimethyl-phenylalanine, *p*-chloro-phenylalanine hydroxide, norvaline, ribitol; Sigma Aldrich, St. Louis, MO, USA) were added to every tube. Cells were disrupted by three rounds of bead beating as described in section **6.2.1.5** with the exception that 60% ethanol were used instead of TE buffer. The cytosolic fraction was separated from the cell debris by centrifugation for 5 min at 20,000 x *g* at 4 °C. Supernatants were transferred to 50 ml tubes and stored on ice. Glass beads and cell debris were washed with 800 µl of MS-pure water by an additional round of bead beating followed by centrifugation for 5 min at 20,000 x *g* at 4 °C. Supernatants of both centrifugation steps were pooled and 5 ml of MS-pure water were added to every sample to lower the percentage of ethanol within the samples. Samples were transferred to -80 °C and were allowed to completely freeze for several hours. Frozen samples were lyophilized in a freeze dryer (Alpha 1-2 LDplus, Christ, Osterode am Harz, Germany) overnight. Lyophilized cytosolic extracts were suspended in 500 µl of MS-pure water and transferred to 1.7 ml low binding tubes. Samples were allowed to freeze again at -80 °C before and subjected to an additional lyophilization step.

Materials and methods

6.2.6.3 GC-MS/MS analysis

Subsequently, lyophilized samples were derivatized with 40 μ l methoxyamine hydrochloride for 90 min at 37 °C. Next, 80 μ l of N-methyl-N-trimethylsilyltrifluoroacetamide were added and samples were incubated for 30 min at 37 °C. 2 μ l of the derivatized samples were analyzed on an Agilent@5973 Network MSD mass selective detector (Agilent Technologies, Santa Clara, Ca, USA) coupled to an Agilent 6890N GC system with SSI-injector [Split 1:25 at 250 °C; inlet split flow: 20 ml/min; carrier gas: helium 1 ml/min (60 kPa) at 110 °C; pressure rise: 6 kPa/min]. First, samples were separated on a 30-m DB-5MS column (30 m x 0,25 mm x 0,25 μ m; Agilent Technologies, Santa Clara, Ca, USA) using an four-step oven program ((1) initial temperature hold at 70 °C for 1 min, (2) stepwise heating with 1.5 °C/min up to 76 °C (3) stepwise heating with 5 °C/min up to 220 °C, (3) stepwise heating with 20 °C/min up to 320 °C, (4) hold at 320 °C for 5 min). Subsequently, analytes were transferred to the mass selective detector via the transfer line at 280 °C. Operating in electron ionization mode with an ionization energy of 70 eV, full scans were performed from 50 to 550 m/z at a scan rate of 2.74 scans per second with a 6 min solvent delay. Statistical testing was performed with the R package “rstatix” using multiple pairwise comparisons (t-test) against the controls as reference group (version: 0.7.0) (Kassambara, 2021).

6.2.7 Subcellular localization analysis

Subcellular fractionation and localization experiments were performed by modifying a previously established protocol (Prochnow *et al.*, 2019).

6.2.7.1 Cultivation and harvest

C. difficile were grown in CDMM to an OD_{600nm} of 0.8 and were exposed to 10 µg/ml amidochelocardin for 10 min. Treated cells and untreated controls were harvested by centrifugation for 5 min at 10,000 x *g* at 4 °C. Cell pellets were suspended in 2 ml 50 mM Tris, pH 7.6, 150 mM NaCl and were split to two equal subsamples. Cells were collected by centrifugation for 5 min at 4,500 x *g* at 4 °C and were washed once with 1 ml of 25 mM Tris, pH 7.4. After an additional centrifugation step, supernatants were discarded.

6.2.7.2 Subcellular fractionation

Cells were suspended in 190 µl 10 mM Tris, pH 7.4 and were subjected to five cycles of ultrasonication of 30 s at an amplitude of 60% with pulse ratio 0.1/0.5 s (Sonopuls Ultrasonic Homogenizer, Bandelin electronic GmbH & Co. KG, Berlin, Germany). To remove DNA from the samples, each sample was treated with 2.8 ng/ml DNase I (Roche, Basel, Switzerland) for 15 min at 37 °C and 1,000 rpm. One subsample of both conditions was transferred to ultracentrifuge tubes (Thermo Scientific, Rockford, IL, USA) and the cytosol fraction was separated from the envelope fraction by ultracentrifugation for 1 h at 100,000 x *g* at 4 °C (Sorvall Discovery M150 SE, Thermo Fisher Scientific, Waltham, MA, USA). The supernatants were collected as cytoplasmic fraction. Cell envelope pellets were carefully washed with 200 µl 10 mM Tris, pH 7.4 without disrupting the pellet followed by an additional centrifugation step for 1 min at 16,000 x *g* at 4 °C. Supernatants were discarded and the envelope pellets were suspended in 200 µl 0.5 M MgSO₄ in an ultrasonic bath.

Materials and methods

6.2.7.3 LC-MS analysis

The amount of amidochelocardin taken up by *C. difficile* was quantified on an AbSciex QTrap6500 Linear Ion Trap Quadrupole LC-MS/MS Mass Spectrometer (AB Sciex Germany GmbH, Darmstadt, Germany) coupled to an Agilent 1290 Infinity II (Agilent Technologies, Santa Clara, CA, USA) in negative ion mode. Briefly, proteins were precipitated using 80 μ l of sample mixed with 80 μ l H₂O, 120 μ l of acetonitrile and 120 μ l of methanol followed by centrifugation at 2250 x *g* for 60 min at 4 °C. Subsequently, 320 μ l of supernatant were dried overnight in a CentriVap equipped with a -50 °C cold trap (Labconco, Kansas, MO, USA). Prior to injection into the LC, dried samples were reconstituted in 40 μ l MS-Buffer (40% H₂O, 30% acetonitrile and 30% methanol), containing 100 ng/ml Glipizide as internal standard. Liquid chromatography separation was done using a reversed-phase column (Phenomenex Gemini® 3 μ m NX-C18 110A; 50 x 2 mm) equipped with respective guard column (5 x 2 mm) (Phenomenex, Torrance, CA, USA) at a flow rate of 700 μ l/min applying a linear gradient starting at 1 min 5% B, which steadily increased up to 95% B in 5 min plus an additional 1 min 95% B (A: 0.1% formic acid; B: acetonitrile, 0.1% formic acid). Targeted analyses in negative mode were done using multiple reaction monitoring with the following MRM settings for detection: the internal standard was measured as m/z: 443.9, with fragments: m/z: 319.1 (Declustering Potential -66; Collision Energy: -26; Cell Exit Potential: -21) and m/z: 170.1 (Declustering Potential -66; Collision Energy: -40; Cell Exit Potential: -7). For detection of amidochelocardin (m/z: 411.1), its fragments m/z: 269.1 (Declustering Potential -5.0; Collision Energy: -20; Cell Exit Potential: -13) and m/z: 141.0 (Declustering Potential -5.0; Collision Energy: -20; Cell Exit Potential: -9) were quantified using the software Analyst 1.6.3 and MultiQuant 3.0 (AB Sciex Germany GmbH, Darmstadt, Germany).

6.2.8 Transmission electron microscopy

Sample preparation for transmission electron microscopy was done as described previously in Metzendorf *et al.* (2022).

6.2.8.1 Cultivation of cells and cell harvest

Cells were grown in CDMM to mid-exponential phase and were stressed with a sublethal concentration as done for the proteomics experiments described in section **6.2.3.1**. Subsequently, 15 ml of stressed and unstressed cells were harvested by centrifugation for 10 min at 2,250 x *g* at 4 °C for 10 min. Cells were washed once in 1 ml 1x PBS (Table 6.18), transferred to low-binding tubes (Sorenson™ BioScience, Murray, UT, USA) and collected again by centrifugation 3,500 x *g* at 4 °C for 10 min. Supernatants were discarded and cells were suspended in 200 µl 1x PBS (Table 6.18).

Table 6.18: Phosphate-buffered saline (PBS)

Component	Final concentration
Sodium chloride	137 mM
Di-sodium hydrogen phosphate	10 mM
Potassium chloride	2.7 mM
Potassium dihydrogen phosphate	1.8 mM

6.2.8.2 Fixation of cells

For fixation, 1 ml of fixation buffer (Table 6.19) was added to the cells and samples were first incubated with slow agitation at RT for 10 min and subsequently at 4 °C overnight. Fixed cells were washed three times in 100 mM cacodylate, pH 7.4 and were pelleted after each wash step at 6,000 x *g* at 4 °C for 3 min. Finally, fixed cells were suspended in 200 µl 100 mM cacodylate, pH 7.4 followed by a final centrifugation step at 6,000 x *g* at 4 °C for 3 min.

Table 6.19: Fixation buffer, pH 7.4

Component	Final concentration
Cacodylate	100 mM
Sodium azide	50 mM
Magnesium chloride	10 mM
Calcium chloride	5 mM
Glutaraldehyde	2%
Paraformaldehyde	2%

Materials and methods

6.2.8.3 Preparation for transmission electron microscopy and image acquisition

Fixed cells were embedded in low gelling agarose and were prepared for transmission electron microscopy as described in Metzendorf *et al.* (2022). The morphology of cells was then analyzed with a transmission electron microscope LEO 906 (Carl Zeiss Microscopy GmbH, Oberkochen, Germany) and images were acquired with a wide-angle dual speed CCD camera Sharpeye (Tröndle, Moorenweis, Germany), which was operated by the ImageSP software. Finally, all micrographs were edited by using Adobe Photoshop CS6.

6.3 *In vivo* experiments: Metaproteomics analyses

The following section provides information about the experimental procedures applied for the analyses of piglet fecal samples obtained during a piglet feeding trial conducted at the Friedrich-Loeffler-Institute (FLI, Jena, Germany).

6.3.1 Extraction of proteins

6.3.1.1 Differential centrifugation and filtration of samples

Approximately 400 mg of each fecal sample, which had been homogenized directly after sampling prior freezing, were suspended in 5 ml ice-cold 1x PBS (Table 6.18), 0.03% sodium deoxycholate (Sigma Aldrich, St. Louis, MO, USA) with brief vortexing. Samples were incubated on a tube rotator for 10 min at full speed at 4 °C followed by vigorous vortexing. Fiber material was separated from the supernatant by low-speed centrifugation for 5 min at 200 x *g* at 4 °C. Supernatants were collected in a new tube and the fiber pellets were washed again in 5 ml 1x PBS (Table 6.18), 0.03% sodium deoxycholate by vortexing two times for 30 s. Fiber material was pelleted once again for 5 min at 200 x *g* at 4 °C. The wash step was repeated two times and the supernatants were pooled. Subsequently, supernatants were filtered through stomacher strainer bags (stomacher® 400 Circulating strainer bags, Seward Ltd., Worthing, UK) and bacterial cells were pelleted for 20 min at 10,000 x *g* at 4 °C. Obtained cell pellets were stored at -70 °C.

6.3.1.2 Phenol-based extraction of proteins

Proteins were extracted from fecal material according to the protocol of Heyer *et al.* (2019) with minor modifications. Frozen cell pellets were suspended in 800 µl Tris-HCl, pH 7.5, 1% SDS and transferred to 2 ml screw cap tubes containing 500 µl glass beads (0.1 to 0.11 mm, Satorius Stedim Biotech, Göttingen, Germany). Subsequently, cells were lysed by mechanical disruption in a FastPrep homogenizer at 6.5 m/s in three cycles à 30 s (FastPrep-24™5G homogenizer; M.P. Biomedicals, Santa Ana, CA, USA). In between runs, samples were cooled down on ice for 1 min. To remove glass beads, cell debris and aggregates samples were centrifuged for 5 min at 15,000 x *g* at 4 °C. The supernatants were transferred to a 15 ml falcon tube and the glass beads/debris pellets were washed once with 400 µl of Tris-HCl, pH 7.5, 1% SDS. Samples were centrifuged again for 5 min at 15,000 x *g* at 4 °C and supernatants of both cycles were pooled. 2 ml phenol solution equilibrated with 10 mM Tris-HCl, pH 8.0, 1 mM EDTA and 1 ml dH₂O were added to each sample and samples were incubated on a tube rotator for 1 h at highest speed at 4 °C. Phase separation was achieved by centrifugation for 30 min at 10,000 x *g* and RT. The lower phenol phase was transferred to a new 15 ml falcon tube and mixed with an equal volume of dH₂O. Samples were again incubated on a tube rotator for 30 min at highest

Materials and methods

speed at 4 °C followed by centrifugation for 30 min at 10,000 x *g* and RT. The lower phenol phase was transferred to a new 50 ml falcon tube and proteins were precipitated with five volumes of 0.1 M ammonium acetate in methanol overnight at -20 °C. Precipitated proteins were collected for 30 min at 10,000 x *g* at 4 °C and washed twice with 1 ml of 0.1 M ammonium acetate in methanol for 15 min at -20 °C in 1.5 ml microcentrifuge tubes followed by centrifugation for 10 min at 15,000 x *g* at 4 °C. Obtained protein pellets were dried and suspended in an appropriate volume of 1% SDS at 50 °C and 900 rpm until pellets were fully dissolved. Protein extracts were stored at -20 °C.

6.3.2 LC-MS/MS sample preparation and analysis

6.3.2.1 Determination of protein concentrations

Protein contents of extracts were determined using Pierce™ BCA Protein Assay Kit (Thermo Scientific, Rockford, IL, USA) according to the manufacturer's recommendations. Briefly, 100 µl of a 1:10 dilution of each protein extract was mixed with 2 ml working reagent prepared from 50 parts of reagent A and 1 part of reagent B. Samples were incubated for 30 min at 37 °C and the optical density was read at 562 nm blanked against dH₂O. Protein contents of samples were calculated based on a respective standard curve.

6.3.2.2 S-trap digestion of fecal proteins and high pH reversed phase purification and fractionation

Fecal protein samples were prepared for LC-MS/MS measurements as described in sections **6.2.3.2** and **6.2.3.3** with the exception that final peptide fractions were not pooled and each fraction was suspended in 40 µl of 0.1 acetic acid prior to the LC-MS/MS measurements.

6.3.2.3 LC-MS/MS measurements

For separation of peptide mixtures, peptides were loaded onto self-packed analytical columns with integrated emitter (100 µm x 20 cm) containing C₁₈ reverse phase material (3 µm, Dr. Maisch GmbH, Ammerbuch-Entringen, Germany) of an EASY nLC 1000 coupled to an Orbitrap-Velos Pro™ mass spectrometer (Thermo Fisher Scientific, Waltham, MA, USA). Peptides were eluted using a 85 min gradient from 5 to 50% of acetonitrile, 0.1% acetic acid at a constant flow rate of 300 nl/min. First, full survey scans were performed with a resolution of 30,000 in the range of 300 – 2000 *m/z*. Subsequently, the twenty most abundant precursor ions per scan cycle were subjected to collision-induced dissociation (CID) with a normalized collision energy of 35 and MS/MS scans were performed in the LTQ-part of the instrument. Unassigned charge states and singly charged ions were excluded from the analysis with a dynamic exclusion enabled for 20 s. Internal lock mass calibration was applied (lock mass 445.120025).

6.3.3 Database search and analysis

6.3.3.1 Database search and post-processing

Raw files were converted to mgf format using the ProteoWizard tool MSConvert and a threshold peak filter for the 500 most intense peaks (Chambers *et al.*, 2012). The commercial search engine Mascot (Matrix Science Inc., Boston, MA, USA; version 2.6.2) was used to search raw files against a sample specific database created on the basis of 16S rRNA (5,425,260 entries) processed and clustered with the FASTA TOOLKIT and cd-hit (Fuchs; Li and Godzik, 2006; Fu *et al.*, 2012). For the search, carbamidomethylation of cysteine was set as fixed modification and oxidation of methionine was set as variable modification. In addition, fragment tolerance was set to 0.5 Da and parent tolerance was set to 10 ppm and up to two missed cleavages were allowed. Mascot generic files were subjected to a second round of database search using the search algorithm X! Tandem Alanine (version 2017.2.1.4) implemented in Scaffold (Proteome Software, Inc., Portland, OR, USA; version 4.11.1). Subsequently, Scaffold was used for post-processing and validation selecting the experiment-wide grouping algorithm. Finally, the dataset was filtered for protein groups identified by at least two peptides and a peptide threshold of 95% and a protein threshold of 99% were applied.

6.3.3.2 Metaproteomics data analysis

Taxonomic and functional annotations for the identified protein groups were obtained from NCBI (taxonomy) and eggNOG (function) by subjecting the Scaffold protein report to ProPhane analysis (version 4.2.2) (Schiebenhoefer *et al.*, 2020). Data were further analyzed using RStudio Desktop (version: 1.4.1103; RStudio, Boston, MS, USA) and the R packages listed in Table 6.20.

Table 6.20: R packages used for metaproteomics data analysis.

R Package	Version	Type of analysis	Reference
Indicspecies	1.7.9	Indicator species analysis	(Cáceres and Legendre, 2009)
Limma	3.46.0	Differential expression analysis	(Ritchie <i>et al.</i> , 2015)
Vegan	2.5-7	Diversity analysis	(Oksanen <i>et al.</i> , 2020)
zCompositions	1.4.0	multivariate imputation of left-censored data under a compositional approach	(Palarea-Albaladejo and Martín-Fernández, 2015)

6.3 Comparative BLASTp analysis

To comparatively analyze the theoretical protein repertoire of species with higher or lower susceptibility to chlorotoniols, the theoretical proteome of 17 strains selected bacterial species was downloaded from Uniprot (Table 6.21). Strains were selected based on susceptibility screening dataset provided by Arne Bublitz (Helmholtz Centre for Infection Research, Braunschweig, see Suppl. figure S2).

Table 6.21: Reference proteomes for comparative BLASTp analysis.

Species	Proteome	Download date
<i>Akkermansia muciniphila</i>	UP000001031	23.11.2021
<i>Bacteroides caecimuris</i>	UP000092631	25.10.2021
<i>Bacteroides fragilis</i>	UP000006731	18.03.2021
<i>Bacteroides thetaiotaomicron</i>	UP000001414	18.03.2021
<i>Bifidobacterium longum subsp. infantis</i>	UP000001360	07.12.2020
<i>Clostridioides difficile</i>	UP000001978	23.11.2020
<i>Clostridium clostridioforme</i>	UP000013180	25.10.2021
<i>Clostridium scindens</i>	UP000003459	25.01.2021
<i>Enterococcus faecalis</i>	UP000001415	25.01.2021
<i>Extibactermuris muris</i>	UP000295710	24.11.2021
<i>Flavonifractor plautii</i>	UP000004459	25.10.2021
<i>Limosilactobacillus reuteri</i>	UP000001991	23.11.2021
<i>Muribaculum intestinale</i>	UP000186351	25.10.2021
<i>Paeniclostridium sordellii</i>	UP000036161	26.01.2021
<i>Paraclostridium bifermentans</i>	UP000015688	25.02.2021
<i>Peptostreptococcus anaerobius</i>	UP000004206	25.02.2021
<i>Terrisporobacter glycolicus</i>	UP000183495	07.12.2020

All theoretical proteomes were searched against the proteome of *C. difficile* 630, which was used as reference dataset, using BLASTp (version: 2.11.0, downloaded Oct. 6, 2020) applying an e value threshold of 1×10^{-5} (Camacho *et al.*, 2009).

6.4 Data visualization

Data were visualized using RStudio Desktop (version: 1.4.1103; RStudio, Boston, MS, USA) and the various R packages (Table 6.22). Voronoi treemaps were further created using the treemap builder “Paver” (Decodon GmbH, Greifswald, Germany). Figures and images were created and/or adjusted using Microsoft PowerPoint 2019 (Microsoft, Albuquerque, NM, USA).

Table 6.22: R packages used to analyze and visualize metaproteomics data.

R Package	Version	Type of analysis	Reference
Broom	0.7.12	Data organization	(Wickham, 2022)
ComplexHeatmap	2.6.2	Creation of heatmaps	(Gu <i>et al.</i> , 2016)
dplyr	1.0.8	Data organization	(Wickham <i>et al.</i> , 2021)
ggplot2	3.3.5	Visualization	(Wickham, 2016)
ggpubr	0.4.0	Data organization	(Kassambra, 2020)
ggvenn	0.1.9	Venn diagrams	(Yan, 2021)
Pheatmap	1.0.12	Heatmaps	(Kolde, 2019)
RColorBrewer	1.1-2	Colors	(Neuwirth, 2014)
Stringr	1.4.0	Data organization	(Wickham, 2019)
Tidyr	1.2.0	Data organization	(Wickham, 2021)

6.5 Data availability

Proteomics data sets are available at the ProteomeXchange Consortium via the PRIDE partner repository (<http://proteomecentral.proteomexchange.org>). Individual data sets were deposited separately and were assigned individual identifiers (Table 6.23).

Table 6.23: Proteomics data depository.

Data set	Identifier	Username	Password
ChA stress experiment	PXD033805	reviewer_pxd033805@ebi.ac.uk	h0mX74ST
ChB1-Epo2 stress experiment	PXD029243	reviewer_pxd029243@ebi.ac.uk	7s5wLD0u
ChB1-Epo2 long-term stress experiment	PXD029251	reviewer_pxd029251@ebi.ac.uk	NVTpzqdf
<i>T. glycolicus</i> stress experiment	PXD033806	reviewer_pxd033806@ebi.ac.uk	h4GyAZ7e
MyxB stress experiment	PXD027366	publicly available	
CDCHD stress experiment	PXD029250	reviewer_pxd029250@ebi.ac.uk	aTWIUiMM
Metaproteomics experiment	PXD033822	reviewer_pxd033822@ebi.ac.uk	UVyPm0Jj

7 References

- AbdelKhalek, A., Mohammad, H., Mayhoub, A. S., and Seleem, M. N. (2020). Screening for potent and selective anticlostridial leads among FDA-approved drugs. *J Antibiot (Tokyo)* 73, 392–409. doi: 10.1038/s41429-020-0288-3
- Abraham, E. P., and Chain, E. (1988). An enzyme from bacteria able to destroy penicillin. 1940. *Rev Infect Dis* 10, 677–678.
- Aldape, M. J., Packham, A. E., Heeney, D. D., Rice, S. N., Bryant, A. E., and Stevens, D. L. (2017). Fidaxomicin reduces early toxin A and B production and sporulation in *Clostridium difficile* *in vitro*. *J Med Microbiol* 66, 1393–1399. doi: 10.1099/jmm.0.000580
- Aldape, M. J., Packham, A. E., Nute, D. W., Bryant, A. E., and Stevens, D. L. (2013). Effects of ciprofloxacin on the expression and production of exotoxins by *Clostridium difficile*. *J Med Microbiol* 62, 741–747. doi: 10.1099/jmm.0.056218-0
- Aldape, M. J., Rice, S. N., Field, K. P., Bryant, A. E., and Stevens, D. L. (2018). Sub-lethal doses of surotomycin and vancomycin have similar effects on *Clostridium difficile* virulence factor production *in vitro*. *J Med Microbiol* 67, 1689–1697. doi: 10.1099/jmm.0.000852
- Almutairi, M. S., Gonzales-Luna, A. J., Anezary, F. S., Fallatah, S. B., Alam, M. J., Begum, K., et al. (2021). Comparative clinical outcomes evaluation of hospitalized patients infected with *Clostridioides difficile* ribotype 106 vs. other toxigenic strains. *Anaerobe* 72, 102440. doi: 10.1016/j.anaerobe.2021.102440
- Alquethamy, S. F., Adams, F. G., Maharjan, R., Delgado, N. N., Zang, M., Ganio, K., et al. (2021). The Molecular Basis of *Acinetobacter baumannii* Cadmium Toxicity and Resistance. *Appl Environ Microbiol* 87, e0171821. doi: 10.1128/AEM.01718-21
- Aminov, R. I. (2010). A brief history of the antibiotic era: lessons learned and challenges for the future. *Front. Microbiol.* 1, 134. doi: 10.3389/fmicb.2010.00134
- Anahar, M. N., Gootenberg, D. B., Mitchell, C. M., and Kwon, D. S. (2018). Cervicovaginal Microbiota and Reproductive Health: The Virtue of Simplicity. *Cell Host Microbe* 23, 159–168. doi: 10.1016/j.chom.2018.01.013
- D. I. Andersson, N. Q. Balaban, F. Baquero, P. Courvalin, P. Glaser, U. Gophna, et al. (2020). Antibiotic resistance: turning evolutionary principles into clinical reality. *FEMS Microbiol Rev* 44, 171–188. doi: 10.1093/femsre/fuaa001
- J. A. Andersson, A. G. Peniche, C. L. Galindo, P. Boonma, J. Sha, R. A. Luna, et al. (2020). New Host-Directed Therapeutics for the Treatment of *Clostridioides difficile* Infection. *mBio* 11. doi: 10.1128/mBio.00053-20
- Antunes, A., Camiade, E., Monot, M., Courtois, E., Barbut, F., Sernova, N. V., et al. (2012). Global transcriptional control by glucose and carbon regulator CcpA in *Clostridium difficile*. *Nucleic acids research* 40, 10701–10718. doi: 10.1093/nar/gks864
- Argüello, J. M., Raimunda, D., and Padilla-Benavides, T. (2013). Mechanisms of copper homeostasis in bacteria. *Front. Cell. Infect. Microbiol.* 3, 73. doi: 10.3389/fcimb.2013.00073
- Artsimovitch, I., Seddon, J., and Sears, P. (2012). Fidaxomicin is an inhibitor of the initiation of bacterial RNA synthesis. *Clin Infect Dis* 55 Suppl 2, S127-31. doi: 10.1093/cid/cis358
- Aslam, B., Wang, W., Arshad, M. I., Khurshid, M., Muzammil, S., Rasool, M. H., et al. (2018). Antibiotic resistance: a rundown of a global crisis. *Infect Drug Resist* 11, 1645–1658. doi: 10.2147/IDR.S173867
- Azzouzi, A., Steunou, A.-S., Durand, A., Khalfaoui-Hassani, B., Bourbon, M.-L., Astier, C., et al. (2013). Coproporphyrin III excretion identifies the anaerobic coproporphyrinogen III oxidase HemN as a copper target in the Cu⁺-ATPase mutant *copA*⁻ of *Rubrivivax gelatinosus*. *Mol Microbiol* 88, 339–351. doi: 10.1111/mmi.12188
- Babakhani, F., Seddon, J., and Sears, P. (2014). Comparative microbiological studies of transcription inhibitors fidaxomicin and the rifamycins in *Clostridium difficile*. *Antimicrob Agents Chemother* 58, 2934–2937. doi: 10.1128/AAC.02572-13

- Balabanova, L., Averianova, L., Marchenok, M., Son, O., and Tekutyeva, L. (2021). Microbial and Genetic Resources for Cobalamin (Vitamin B12) Biosynthesis: From Ecosystems to Industrial Biotechnology. *Int J Mol Sci* 22. doi: 10.3390/ijms22094522
- Baldoni, D., Gutierrez, M., Timmer, W., and Dingemans, J. (2014). Cadazolid, a novel antibiotic with potent activity against *Clostridium difficile*: safety, tolerability and pharmacokinetics in healthy subjects following single and multiple oral doses. *J Antimicrob Chemother* 69, 706–714. doi: 10.1093/jac/dkt401
- Barka, E. A., Vatsa, P., Sanchez, L., Gaveau-Vaillant, N., Jacquard, C., Meier-Kolthoff, J. P., et al. (2016). Taxonomy, Physiology, and Natural Products of Actinobacteria. *Microbiol Mol Biol Rev* 80, 1–43. doi: 10.1128/MMBR.00019-15
- Barwinska-Sendra, A., and Waldron, K. J. (2017). The Role of Intermetal Competition and Mis-Metalation in Metal Toxicity. *Adv Microb Physiol* 70, 315–379. doi: 10.1016/bs.ampbs.2017.01.003
- Bassères, E., Endres, B. T., Khaleduzzaman, M., Miraftehi, F., Alam, M. J., Vickers, R. J., et al. (2016). Impact on toxin production and cell morphology in *Clostridium difficile* by ridinilazole (SMT19969), a novel treatment for *C. difficile* infection. *J Antimicrob Chemother* 71, 1245–1251. doi: 10.1093/jac/dkv498
- Basu, P., Dinani, A., Rayapudi, K., Pacana, T., Shah, N. J., Hampole, H., et al. (2010). Rifaximin therapy for metronidazole-unresponsive *Clostridium difficile* infection: a prospective pilot trial. *Therap Adv Gastroenterol* 3, 221–225. doi: 10.1177/1756283X10372985
- Battaglioli, E. J., Hale, V. L., Chen, J., Jeraldo, P., Ruiz-Mojica, C., Schmidt, B. A., et al. (2018). *Clostridioides difficile* uses amino acids associated with gut microbial dysbiosis in a subset of patients with diarrhea. *Sci. Transl. Med.* 10. doi: 10.1126/scitranslmed.aam7019
- Bauer, M. A., Kainz, K., Carmona-Gutierrez, D., and Madeo, F. (2018). Microbial wars: Competition in ecological niches and within the microbiome. *Microb Cell* 5, 215–219. doi: 10.15698/mic2018.05.628
- Begg, S. L., Eijkelkamp, B. A., Luo, Z., Couñago, R. M., Morey, J. R., Maher, M. J., et al. (2015). Dysregulation of transition metal ion homeostasis is the molecular basis for cadmium toxicity in *Streptococcus pneumoniae*. *Nat Commun* 6, 6418. doi: 10.1038/ncomms7418
- Belenky, P., Ye, J. D., Porter, C. B. M., Cohen, N. R., Lobritz, M. A., Ferrante, T., et al. (2015). Bactericidal Antibiotics Induce Toxic Metabolic Perturbations that Lead to Cellular Damage. *Cell Rep* 13, 968–980. doi: 10.1016/j.celrep.2015.09.059
- Belete, T. M. (2019). Novel targets to develop new antibacterial agents and novel alternatives to antibacterial agents. *Human Microbiome Journal* 11, 100052. doi: 10.1016/j.humic.2019.01.001
- Benarroch, J. M., and Asally, M. (2020). The Microbiologist's Guide to Membrane Potential Dynamics. *Trends Microbiol* 28, 304–314. doi: 10.1016/j.tim.2019.12.008
- Berkell, M., Mysara, M., Xavier, B. B., van Werkhoven, C. H., Monsieurs, P., Lammens, C., et al. (2021). Microbiota-based markers predictive of development of *Clostridioides difficile* infection. *Nat Commun* 12, 2241. doi: 10.1038/s41467-021-22302-0
- Binyamin, D., Nitzan, O., Azrad, M., Hamo, Z., Koren, O., and Peretz, A. (2021). The microbial diversity following antibiotic treatment of *Clostridioides difficile* infection. *BMC Gastroenterol* 21, 166. doi: 10.1186/s12876-021-01754-0
- Bird, L. J., Coleman, M. L., and Newman, D. K. (2013). Iron and copper act synergistically to delay anaerobic growth of bacteria. *Appl Environ Microbiol* 79, 3619–3627. doi: 10.1128/AEM.03944-12
- Blanco, P., Hernando-Amado, S., Reales-Calderon, J. A., Corona, F., Lira, F., Alcalde-Rico, M., et al. (2016). Bacterial Multidrug Efflux Pumps: Much More Than Antibiotic Resistance Determinants. *Microorganisms* 4. doi: 10.3390/microorganisms4010014
- Blankenfeldt, W., and Parsons, J. F. (2014). The structural biology of phenazine biosynthesis. *Curr Opin Struct Biol* 29, 26–33. doi: 10.1016/j.sbi.2014.08.013
- Bloom, D. E., and Cadarette, D. (2019). Infectious Disease Threats in the Twenty-First Century: Strengthening the Global Response. *Front. Immunol.* 10, 549. doi: 10.3389/fimmu.2019.00549

References

- Blum, M., Chang, H.-Y., Chuguransky, S., Grego, T., Kandasaamy, S., Mitchell, A., et al. (2021). The InterPro protein families and domains database: 20 years on. *Nucleic acids research* 49, D344–D354. doi: 10.1093/nar/gkaa977
- Boersch, M., Rudrawar, S., Grant, G., and Zunk, M. (2018). Menaquinone biosynthesis inhibition: a review of advancements toward a new antibiotic mechanism. *RSC Adv.* 8, 5099–5105. doi: 10.1039/C7RA12950E
- Boix, V., Fedorak, R. N., Mullane, K. M., Pesant, Y., Stoutenburgh, U., Jin, M., et al. (2017). Primary Outcomes From a Phase 3, Randomized, Double-Blind, Active-Controlled Trial of Surotomyacin in Subjects With *Clostridium difficile* Infection. *Open Forum Infect Dis* 4, ofw275. doi: 10.1093/ofid/ofw275
- Bouillaut, L., Dubois, T., Francis, M. B., Daou, N., Monot, M., Sorg, J. A., et al. (2019). Role of the global regulator Rex in control of NAD⁺ -regeneration in *Clostridioides (Clostridium) difficile*. *Mol Microbiol* 111, 1671–1688. doi: 10.1111/mmi.14245
- Bousis, S., Setyawati, I., Diamanti, E., Slotboom, D. J., and Hirsch, A. K. H. (2019). Energy-Coupling Factor Transporters as Novel Antimicrobial Targets. *Adv. Therap.* 2, 1800066. doi: 10.1002/adtp.201800066
- Brauer M, Lassek C, Hinze C, Hoyer J, Becher D, Jahn D, Sievers S and Riedel K (2021). What's a Biofilm?—How the Choice of the Biofilm Model Impacts the Protein Inventory of *Clostridioides difficile*. *Front. Microbiol.* 12:682111. doi: 10.3389/fmicb.2021.682111
- Brauer, M., Herrmann, J., Zühlke, D., Müller, R., Riedel, K., and Sievers, S. (2022). Myxopyronin B inhibits growth of a Fidaxomicin-resistant *Clostridioides difficile* isolate and interferes with toxin synthesis. *Gut Pathog* 14, 4. doi: 10.1186/s13099-021-00475-9
- Brochmann, R. P., Helmfrid, A., Jana, B., Magnowska, Z., and Guardabassi, L. (2016). Antimicrobial synergy between carprofen and doxycycline against methicillin-resistant *Staphylococcus pseudintermedius* ST71. *BMC Vet Res* 12, 126. doi: 10.1186/s12917-016-0751-3
- Bruxelle, J. F., Tsapis, N., Hoys, S., Collignon, A., Janoir, C., Fattal, E., et al. (2018). Protection against *Clostridium difficile* infection in a hamster model by oral vaccination using flagellin FliC-loaded pectin beads. *Vaccine* 36, 6017–6021. doi: 10.1016/j.vaccine.2018.08.013
- Bruxelle, J.-F., Mizrahi, A., Hoys, S., Collignon, A., Janoir, C., and Péchiné, S. (2016). Immunogenic properties of the surface layer precursor of *Clostridium difficile* and vaccination assays in animal models. *Anaerobe* 37, 78–84. doi: 10.1016/j.anaerobe.2015.10.010
- Buffie, C. G., Bucci, V., Stein, R. R., McKenney, P. T., Ling, L., Gouberne, A., et al. (2015). Precision microbiome reconstitution restores bile acid mediated resistance to *Clostridium difficile*. *Nature* 517, 205–208. doi: 10.1038/nature13828
- Buffie, C. G., and Pamer, E. G. (2013). Microbiota-mediated colonization resistance against intestinal pathogens. *Nat Rev Immunol* 13, 790–801. doi: 10.1038/nri3535
- Butler, M. S., Gigante, V., Sati, H., Paulin, S., Al-Sulaiman, L., Rex, J. H., et al. (2022). Analysis of the Clinical Pipeline of Treatments for Drug-Resistant Bacterial Infections: Despite Progress, More Action Is Needed. *Antimicrob Agents Chemother* 66, e0199121. doi: 10.1128/AAC.01991-21
- Cáceres, M. de, and Legendre, P. (2009). Associations between species and groups of sites: indices and statistical inference. *Ecology* 90, 3566–3574. doi: 10.1890/08-1823.1
- Cai, L., Friedman, N., and Xie, X. S. (2006). Stochastic protein expression in individual cells at the single molecule level. *Nature* 440, 358–362. doi: 10.1038/nature04599
- Camacho, C., Coulouris, G., Avagyan, V., Ma, N., Papadopoulos, J., Bealer, K., et al. (2009). BLAST+: architecture and applications. *BMC Bioinformatics* 10, 421. doi: 10.1186/1471-2105-10-421
- Candiano, G., Bruschi, M., Musante, L., Santucci, L., Ghiggeri, G. M., Carnemolla, B., et al. (2004). Blue silver: a very sensitive colloidal Coomassie G-250 staining for proteome analysis. *Electrophoresis* 25, 1327–1333. doi: 10.1002/elps.200305844
- Cartman, S. T., and Minton, N. P. (2010). A mariner-based transposon system for *in vivo* random mutagenesis of *Clostridium difficile*. *Appl Environ Microbiol* 76, 1103–1109. doi: 10.1128/AEM.02525-09

- Cassini, A., Högberg, L. D., Plachouras, D., Quattrocchi, A., Hoxha, A., Simonsen, G. S., et al. (2019). Attributable deaths and disability-adjusted life-years caused by infections with antibiotic-resistant bacteria in the EU and the European Economic Area in 2015: a population-level modelling analysis. *Lancet Infect Dis* 19, 56–66. doi: 10.1016/S1473-3099(18)30605-4
- Cassini, A., Plachouras, D., Eckmanns, T., Abu Sin, M., Blank, H.-P., Ducomble, T., et al. (2016). Burden of Six Healthcare-Associated Infections on European Population Health: Estimating Incidence-Based Disability-Adjusted Life Years through a Population Prevalence-Based Modelling Study. *PLoS Med* 13, e1002150. doi: 10.1371/journal.pmed.1002150
- Castellani A, C. A. J. (1919). Manual of tropical medicine, 3rd ed. *William Wood and Co., NY* 1919, 959–960.
- Castro-Córdova, P., Mora-Uribe, P., Reyes-Ramírez, R., Cofré-Araneda, G., Orozco-Aguilar, J., Brito-Silva, C., et al. (2021). Entry of spores into intestinal epithelial cells contributes to recurrence of *Clostridioides difficile* infection. *Nat Commun* 12, 1140. doi: 10.1038/s41467-021-21355-5
- Chaar, A., and Feuerstadt, P. (2021). Evolution of clinical guidelines for antimicrobial management of *Clostridioides difficile* infection. *Therap Adv Gastroenterol* 14, 17562848211011953. doi: 10.1177/17562848211011953
- Chambers, M. C., Maclean, B., Burke, R., Amodei, D., Ruderman, D. L., Neumann, S., et al. (2012). A cross-platform toolkit for mass spectrometry and proteomics. *Nat Biotechnol* 30, 918–920. doi: 10.1038/nbt.2377
- Chan, A. N., Shiver, A. L., Wever, W. J., Razvi, S. Z. A., Traxler, M. F., and Li, B. (2017). Role for dithiolopyrrolones in disrupting bacterial metal homeostasis. *PNAS* 114, 2717–2722. doi: 10.1073/pnas.1612810114
- Chandrangsu, P., Dusi, R., Hamilton, C. J., and Helmann, J. D. (2014). Methylglyoxal resistance in *Bacillus subtilis*: contributions of bacillithiol-dependent and independent pathways. *Mol Microbiol* 91, 706–715. doi: 10.1111/mmi.12489
- Chandrangsu, P., Rensing, C., and Helmann, J. D. (2017). Metal homeostasis and resistance in bacteria. *Nat Rev Microbiol* 15, 338–350. doi: 10.1038/nrmicro.2017.15
- Chen, W., Liu, F., Ling, Z., Tong, X., and Xiang, C. (2012). Human intestinal lumen and mucosa-associated microbiota in patients with colorectal cancer. *PLOS ONE* 7, e39743. doi: 10.1371/journal.pone.0039743
- Chey, W. D., Shah, E. D., and DuPont, H. L. (2020). Mechanism of action and therapeutic benefit of rifaximin in patients with irritable bowel syndrome: a narrative review. *Therap Adv Gastroenterol* 13, 1756284819897531. doi: 10.1177/1756284819897531
- Chilton, C. H., Crowther, G. S., Baines, S. D., Todhunter, S. L., Freeman, J., Locher, H. H., et al. (2014). *In vitro* activity of cadazolid against clinically relevant *Clostridium difficile* isolates and in an *in vitro* gut model of *C. difficile* infection. *J Antimicrob Chemother* 69, 697–705. doi: 10.1093/jac/dkt411
- Cho, I., and Blaser, M. J. (2012). The human microbiome: at the interface of health and disease. *Nat Rev Genet* 13, 260–270. doi: 10.1038/nrg3182
- Cho, J. C., Crotty, M. P., and Pardo, J. (2019). Ridinilazole: a novel antimicrobial for *Clostridium difficile* infection. *Ann Gastroenterol* 32, 134–140. doi: 10.20524/aog.2018.0336
- Choi, Y. H., and Verpoorte, R. (2014). Metabolomics: what you see is what you extract. *Phytochem Anal* 25, 289–290. doi: 10.1002/pca.2513
- Chopra, I. (1994). Tetracycline analogs whose primary target is not the bacterial ribosome. *Antimicrob Agents Chemother* 38, 637–640. doi: 10.1128/AAC.38.4.637
- Christensen, S. B. (2021). Drugs That Changed Society: History and Current Status of the Early Antibiotics: Salvarsan, Sulfonamides, and β -Lactams. *Molecules* 26. doi: 10.3390/molecules26196057
- Christgen, S. L., and Becker, D. F. (2019). Role of Proline in Pathogen and Host Interactions. *Antioxid Redox Signal* 30, 683–709. doi: 10.1089/ars.2017.7335

References

- Chu, M., Mallozzi, M. J. G., Roxas, B. P., Bertolo, L., Monteiro, M. A., Agellon, A., et al. (2016). A *Clostridium difficile* Cell Wall Glycopolymer Locus Influences Bacterial Shape, Polysaccharide Production and Virulence. *PLoS Pathog* 12, e1005946. doi: 10.1371/journal.ppat.1005946
- Colebrook, L. (1936). The Mode of Action of *p*-aminobenzenesulphonamide and Prontosil in Hemolytic Streptococcal Infections. *The Lancet* 228, 1323–1326. doi: 10.1016/S0140-6736(00)48181-X
- Cornely, O. A., Crook, D. W., Esposito, R., Poirier, A., Somero, M. S., Weiss, K., et al. (2012). Fidaxomicin versus vancomycin for infection with *Clostridium difficile* in Europe, Canada, and the USA: a double-blind, non-inferiority, randomised controlled trial. *The Lancet Infectious Diseases* 12, 281–289. doi: 10.1016/S1473-3099(11)70374-7
- Crobach, M. J. T., Ducarmon, Q. R., Terveer, E. M., Harmanus, C., Sanders, I. M. J. G., Verduin, K. M., et al. (2020). The Bacterial Gut Microbiota of Adult Patients Infected, Colonized or Noncolonized by *Clostridioides difficile*. *Microorganisms* 8. doi: 10.3390/microorganisms8050677
- Ctortekca, C., and Mechtler, K. (2021). The rise of single-cell proteomics. *Analytical Science Advances* 2, 84–94. doi: 10.1002/ansa.202000152
- Cupp-Sutton, K. A., and Wu, S. (2020). High-throughput quantitative top-down proteomics. *Mol Omics* 16, 91–99. doi: 10.1039/c9mo00154a
- Cyphert, E. L., Wallat, J. D., Pokorski, J. K., and Recum, H. A. von (2017). Erythromycin Modification That Improves Its Acidic Stability while Optimizing It for Local Drug Delivery. *Antibiotics (Basel)* 6. doi: 10.3390/antibiotics6020011
- Czepiel, J., Krutova, M., Mizrahi, A., Khanafer, N., Enoch, D. A., Patyi, M., et al. (2021). Mortality Following *Clostridioides difficile* Infection in Europe: A Retrospective Multicenter Case-Control Study. *Antibiotics (Basel)* 10. doi: 10.3390/antibiotics10030299
- Da Farrell, L. J., Lo, R., Wanford, J. J., Jenkins, A., Maxwell, A., and Piddock, L. J. V. (2018). Revitalizing the drug pipeline: AntibioticDB, an open access database to aid antibacterial research and development. *J Antimicrob Chemother* 73, 2284–2297. doi: 10.1093/jac/dky208
- Daley, P., Louie, T., Lutz, J. E., Khanna, S., Stoutenburgh, U., Jin, M., et al. (2017). Surotomycin versus vancomycin in adults with *Clostridium difficile* infection: primary clinical outcomes from the second pivotal, randomized, double-blind, Phase 3 trial. *J Antimicrob Chemother* 72, 3462–3470. doi: 10.1093/jac/dkx299
- Dang, U. T., Zamora, I., Hevener, K. E., Adhikari, S., Wu, X., and Hurdle, J. G. (2016). Rifamycin Resistance in *Clostridium difficile* Is Generally Associated with a Low Fitness Burden. *Antimicrob Agents Chemother* 60, 5604–5607. doi: 10.1128/AAC.01137-16
- Davis, J. J., Wattam, A. R., Aziz, R. K., Brettin, T., Butler, R., Butler, R. M., et al. (2020). The PATRIC Bioinformatics Resource Center: expanding data and analysis capabilities. *Nucleic acids research* 48, D606–D612. doi: 10.1093/nar/gkz943
- Debast, S. B., van Leengoed, L. A. M. G., Goorhuis, A., Harmanus, C., Kuijper, E. J., and Bergwerff, A. A. (2009). *Clostridium difficile* PCR ribotype 078 toxinotype V found in diarrhoeal pigs identical to isolates from affected humans. *Environ Microbiol* 11, 505–511. doi: 10.1111/j.1462-2920.2008.01790.x
- Dehal, P. S., Joachimiak, M. P., Price, M. N., Bates, J. T., Baumohl, J. K., Chivian, D., et al. (2010). MicrobesOnline: an integrated portal for comparative and functional genomics. *Nucleic acids research* 38, D396–400. doi: 10.1093/nar/gkp919
- Dembek, M., Barquist, L., Boinett, C. J., Cain, A. K., Mayho, M., Lawley, T. D., et al. (2015). High-throughput analysis of gene essentiality and sporulation in *Clostridium difficile*. *mBio* 6, e02383. doi: 10.1128/mBio.02383-14
- Dethlefsen, L., and Relman, D. A. (2011). Incomplete recovery and individualized responses of the human distal gut microbiota to repeated antibiotic perturbation. *PNAS* 108 Suppl 1, 4554–4561. doi: 10.1073/pnas.1000087107
- Dias, C., and Rauter, A. P. (2019). Membrane-targeting antibiotics: recent developments outside the peptide space. *Future Med Chem*. doi: 10.4155/fmc-2018-0254

- Dingle, K. E., Didelot, X., Quan, T. P., Eyre, D. W., Stoesser, N., Golubchik, T., et al. (2017). Effects of control interventions on *Clostridium difficile* infection in England: an observational study. *The Lancet Infectious Diseases* 17, 411–421. doi: 10.1016/S1473-3099(16)30514-X
- Division, A. R. (2019). No time to Wait: Securing the future from drug-resistant infections. *World Health Organization*.
- Donnelly, D. P., Rawlins, C. M., DeHart, C. J., Fornelli, L., Schachner, L. F., Lin, Z., et al. (2019). Best practices and benchmarks for intact protein analysis for top-down mass spectrometry. *Nat Methods* 16, 587–594. doi: 10.1038/s41592-019-0457-0
- Dörries, K., Schlueter, R., and Lalk, M. (2014). Impact of antibiotics with various target sites on the metabolome of *Staphylococcus aureus*. *Antimicrob Agents Chemother* 58, 7151–7163. doi: 10.1128/AAC.03104-14
- Dubois, T., Tremblay, Y. D. N., Hamiot, A., Martin-Verstraete, I., Deschamps, J., Monot, M., et al. (2019). A microbiota-generated bile salt induces biofilm formation in *Clostridium difficile*. *NPJ Biofilms Microbiomes* 5, 14. doi: 10.1038/s41522-019-0087-4
- Dupree, E. J., Jayathirtha, M., Yorkey, H., Mihasan, M., Petre, B. A., and Darie, C. C. (2020). A Critical Review of Bottom-Up Proteomics: The Good, the Bad, and the Future of this Field. *Proteomes* 8. doi: 10.3390/proteomes8030014
- Dwyer, D. J., Belenky, P. A., Yang, J. H., MacDonald, I. C., Martell, J. D., Takahashi, N., et al. (2014). Antibiotics induce redox-related physiological alterations as part of their lethality. *PNAS* 111, E2100-9. doi: 10.1073/pnas.1401876111
- Eckburg, P. B., Bik, E. M., Bernstein, C. N., Purdom, E., Dethlefsen, L., Sargent, M., et al. (2005). Diversity of the human intestinal microbial flora. *Science* 308, 1635–1638. doi: 10.1126/science.1110591
- Ehrlich, P. (1910). Die experimentelle Chemotherapie der Spirillosen.
- Eichel-Streiber, C. von, Laufenberg-Feldmann, R., Sartingen, S., Schulze, J., and Sauerborn, M. (1992). Comparative sequence analysis of the *Clostridium difficile* toxins A and B. *Mol Gen Genet* 233, 260–268. doi: 10.1007/BF00587587
- Elbourne, L. D. H., Tetu, S. G., Hassan, K. A., and Paulsen, I. T. (2017). TransportDB 2.0: a database for exploring membrane transporters in sequenced genomes from all domains of life. *Nucleic acids research* 45, D320-D324. doi: 10.1093/nar/gkw1068
- Emmerich, R., and Löw, O. (1899). Bakteriolytische Enzyme als Ursache der erworbenen Immunität und die Heilung von Infektionskrankheiten durch dieselben. *Zeitschr. f. Hygiene*. 31, 1–65. doi: 10.1007/BF02206499
- Ernst, K., Landenberger, M., Nieland, J., Nørgaard, K., Frick, M., Fois, G., et al. (2021). Characterization and Pharmacological Inhibition of the Pore-Forming *Clostridioides difficile* CDTb Toxin. *Toxins (Basel)* 13. doi: 10.3390/toxins13060390
- L. Evans, A. Rhodes, W. Alhazzani, M. Antonelli, C. M. Coopersmith, C. French, et al. (2021). Surviving sepsis campaign: international guidelines for management of sepsis and septic shock 2021. *Intensive Care Med* 47, 1181–1247. doi: 10.1007/s00134-021-06506-y
- R. M. Evans, N. Krahn, B. J. Murphy, H. Lee, F. A. Armstrong, and D. Söll (2021). Selective cysteine-to-selenocysteine changes in a NiFe-hydrogenase confirm a special position for catalysis and oxygen tolerance. *PNAS* 118. doi: 10.1073/pnas.2100921118
- Ezhilarasan, V., Sharma, O. P., and Pan, A. (2013). *In silico* identification of potential drug targets in *Clostridium difficile* R20291: modeling and virtual screening analysis of a candidate enzyme MurG. *Med Chem Res* 22, 2692–2705. doi: 10.1007/s00044-012-0262-0
- Faber, F., Tran, L., Byndloss, M. X., Lopez, C. A., Velazquez, E. M., Kerrinnes, T., et al. (2016). Host-mediated sugar oxidation promotes post-antibiotic pathogen expansion. *Nature* 534, 697–699. doi: 10.1038/nature18597
- Ferreya, J. A., Wu, K. J., Hryckowian, A. J., Bouley, D. M., Weimer, B. C., and Sonnenburg, J. L. (2014). Gut microbiota-produced succinate promotes *C. difficile* infection after antibiotic treatment or motility disturbance. *Cell Host Microbe* 16, 770–777. doi: 10.1016/j.chom.2014.11.003

References

- Finegold, S. M., Molitoris, D., and Väisänen, M.-L. (2009). Study of the *in vitro* activities of rifaximin and comparator agents against 536 anaerobic intestinal bacteria from the perspective of potential utility in pathology involving bowel flora. *Antimicrob Agents Chemother* 53, 281–286. doi: 10.1128/AAC.00441-08
- Finn, E., Andersson, F. L., and Madin-Warburton, M. (2021). Burden of *Clostridioides difficile* infection (CDI) - a systematic review of the epidemiology of primary and recurrent CDI. *BMC Infect Dis* 21, 456. doi: 10.1186/s12879-021-06147-y
- Fleming, A. (1929). On the Antibacterial Action of Cultures of a Penicillium, with Special Reference to their Use in the Isolation of B. influenzae. *Br J Exp Pathol* 10, 226–236.
- Fletcher, J. R., Erwin, S., Lanzas, C., and Theriot, C. M. (2018). Shifts in the Gut Metabolome and *Clostridium difficile* Transcriptome throughout Colonization and Infection in a Mouse Model. *mSphere* 3. doi: 10.1128/mSphere.00089-18
- Fletcher, J. R., Pike, C. M., Parsons, R. J., Rivera, A. J., Foley, M. H., McLaren, M. R., et al. (2021). *Clostridioides difficile* exploits toxin-mediated inflammation to alter the host nutritional landscape and exclude competitors from the gut microbiota. *Nat Commun* 12, 462. doi: 10.1038/s41467-020-20746-4
- Flint, H. J., Scott, K. P., Duncan, S. H., Louis, P., and Forano, E. (2012). Microbial degradation of complex carbohydrates in the gut. *Gut Microbes* 3, 289–306. doi: 10.4161/gmic.19897
- Foster, A. W., Osman, D., and Robinson, N. J. (2014). Metal preferences and metallation. *J Biol Chem* 289, 28095–28103. doi: 10.1074/jbc.R114.588145
- Freeman, J., Baines, S. D., Jabes, D., and Wilcox, M. H. (2005). Comparison of the efficacy of ramoplanin and vancomycin in both *in vitro* and *in vivo* models of clindamycin-induced *Clostridium difficile* infection. *J Antimicrob Chemother* 56, 717–725. doi: 10.1093/jac/dki321
- Fu, L., Niu, B., Zhu, Z., Wu, S., and Li, W. (2012). CD-HIT: accelerated for clustering the next-generation sequencing data. *Bioinformatics (Oxford, England)* 28, 3150–3152. doi: 10.1093/bioinformatics/bts565
- Fu, Y., Luo, Y., and Grinspan, A. M. (2021). Epidemiology of community-acquired and recurrent *Clostridioides difficile* infection. *Therap Adv Gastroenterol* 14, 17562848211016248. doi: 10.1177/17562848211016248
- Fuchs, S. FASTA TOOLKIT.
- Garey, K. W., Ghantouji, S. S., Shah, D. N., Habib, M., Arora, V., Jiang, Z.-D., et al. (2011). A randomized, double-blind, placebo-controlled pilot study to assess the ability of rifaximin to prevent recurrent diarrhoea in patients with *Clostridium difficile* infection. *J Antimicrob Chemother* 66, 2850–2855. doi: 10.1093/jac/dkr377
- Geers, A. U., Buijs, Y., Strube, M. L., Gram, L., and Bentzon-Tilia, M. (2022). The natural product biosynthesis potential of the microbiomes of Earth - Bioprospecting for novel anti-microbial agents in the meta-omics era. *Comput Struct Biotechnol J* 20, 343–352. doi: 10.1016/j.csbj.2021.12.024
- Gehin, M., Desnica, B., and Dingemans, J. (2015). Minimal systemic and high faecal exposure to cadazolid in patients with severe *Clostridium difficile* infection. *International journal of antimicrobial agents* 46, 576–581. doi: 10.1016/j.ijantimicag.2015.07.015
- Gencic, S., and Grahame, D. A. (2020). Diverse Energy-Conserving Pathways in *Clostridium difficile*: Growth in the Absence of Amino Acid Stickland Acceptors and the Role of the Wood-Ljungdahl Pathway. *J Bacteriol* 202. doi: 10.1128/JB.00233-20
- Gerber, J. S., Ross, R. K., Bryan, M., Localio, A. R., Szymczak, J. E., Wasserman, R., et al. (2017). Association of Broad- vs Narrow-Spectrum Antibiotics With Treatment Failure, Adverse Events, and Quality of Life in Children With Acute Respiratory Tract Infections. *JAMA* 318, 2325–2336. doi: 10.1001/jama.2017.18715
- Gerding, D. N. (2004). Clindamycin, cephalosporins, fluoroquinolones, and *Clostridium difficile*-associated diarrhea: this is an antimicrobial resistance problem. *Clin Infect Dis* 38, 646–648. doi: 10.1086/382084
- Gerding, D. N., Cornely, O. A., Grill, S., Kracker, H., Marrast, A. C., Nord, C. E., et al. (2019). Cadazolid for the treatment of *Clostridium difficile* infection: results of two double-blind, placebo-

- controlled, non-inferiority, randomised phase 3 trials. *The Lancet Infectious Diseases* 19, 265–274. doi: 10.1016/S1473-3099(18)30614-5
- Gerritsen, J., Fuentes, S., Grievink, W., van Niftrik, L., Tindall, B. J., Timmerman, H. M., et al. (2014). Characterization of *Romboutsia ilealis* gen. nov., sp. nov., isolated from the gastrointestinal tract of a rat, and proposal for the reclassification of five closely related members of the genus *Clostridium* into the genera *Romboutsia* gen. nov., *Intestinibacter* gen. nov., *Terrisporobacter* gen. nov. and *Asaccharospora* gen. nov. *Int. J. Syst. Evol.* 64, 1600–1616. doi: 10.1099/ijs.0.059543-0
- Gerth, K., Steinmetz, H., Höfle, G., and Jansen, R. (2008). Chlorotonil A, ein Macrolid mit einzigartigem Dichlor-1,3-dionfunktion aus *Sorangium cellulosum*, So ce1525. *Angew. Chem.* 120, 610–613. doi: 10.1002/ange.200703993
- Gest, H. (2004). The discovery of microorganisms by Robert Hooke and Antoni Van Leeuwenhoek, fellows of the Royal Society. *Notes Rec R Soc Lond* 58, 187–201. doi: 10.1098/rsnr.2004.0055
- Gierse, L. C., Meene, A., Schultz, D., Schwaiger, T., Karte, C., Schröder, C., et al. (2020). A Multi-Omics Protocol for Swine Feces to Elucidate Longitudinal Dynamics in Microbiome Structure and Function. *Microorganisms* 8. doi: 10.3390/microorganisms8121887
- Girinathan, B. P., DiBenedetto, N., Worley, J. N., Peltier, J., Arrieta-Ortiz, M. L., Immanuel, S. R. C., et al. (2021). *In vivo* commensal control of *Clostridioides difficile* virulence. *Cell Host Microbe* 29, 1693-1708.e7. doi: 10.1016/j.chom.2021.09.007
- Gould, K. (2016). Antibiotics: from prehistory to the present day. *J Antimicrob Chemother* 71, 572–575. doi: 10.1093/jac/dkv484
- Granata, G., Petrosillo, N., Adamoli, L., Bartoletti, M., Bartoloni, A., Basile, G., et al. (2021). Prospective Study on Incidence, Risk Factors and Outcome of Recurrent *Clostridioides difficile* Infections. *J Clin Med* 10. doi: 10.3390/jcm10051127
- Grandclaudon, C., Birudukota, N. V. S., Elgaher, W. A. M., Jumde, R. P., Yahiaoui, S., Arisetti, N., et al. (2020). Semisynthesis and biological evaluation of amidochelocardin derivatives as broad-spectrum antibiotics. *European Journal of Medicinal Chemistry* 188, 112005. doi: 10.1016/j.ejmech.2019.112005
- Gu, Z., Eils, R., and Schlesner, M. (2016). Complex heatmaps reveal patterns and correlations in multidimensional genomic data. *Bioinformatics (Oxford, England)* 32, 2847–2849. doi: 10.1093/bioinformatics/btw313
- Guery, B., Berger, P., Gauzit, R., Gourdon, M., Barbut, F., Dafne, S. G., et al. (2021). A prospective, observational study of fidaxomicin use for *Clostridioides difficile* infection in France. *J Int Med Res* 49, 3000605211021278. doi: 10.1177/03000605211021278
- Guh, A. Y., Mu, Y., Winston, L. G., Johnston, H., Olson, D., Farley, M. M., et al. (2020). Trends in U.S. Burden of *Clostridioides difficile* Infection and Outcomes. *N Engl J Med* 382, 1320–1330. doi: 10.1056/NEJMoa1910215
- Gülke, I., Pfeifer, G., Liese, J., Fritz, M., Hofmann, F., Aktories, K., et al. (2001). Characterization of the enzymatic component of the ADP-ribosyltransferase toxin CDTa from *Clostridium difficile*. *Infect Immun* 69, 6004–6011. doi: 10.1128/IAI.69.10.6004-6011.2001
- Gupta, A., and Ananthakrishnan, A. N. (2021). Economic burden and cost-effectiveness of therapies for *Clostridioides difficile* infection: a narrative review. *Therap Adv Gastroenterol* 14, 17562848211018654. doi: 10.1177/17562848211018654
- Hadadi, N., Berweiler, V., Wang, H., and Trajkovski, M. (2021). Intestinal microbiota as a route for micronutrient bioavailability. *Curr Opin Endocr Metab Res* 20, 100285. doi: 10.1016/j.coemr.2021.100285
- Hansen, C., and Paintsil, E. (2016). Infectious Diseases of Poverty in Children: A Tale of Two Worlds. *Pediatric Clinics of North America* 63, 37–66. doi: 10.1016/j.pcl.2015.08.002
- Harbison-Price, N., Ferguson, S. A., Heikal, A., Taiaroa, G., Hards, K., Nakatani, Y., et al. (2020). Multiple Bactericidal Mechanisms of the Zinc Ionophore PBT2. *mSphere* 5. doi: 10.1128/mSphere.00157-20

References

- Hassan, K. A., Pederick, V. G., Elbourne, L. D. H., Paulsen, I. T., Paton, J. C., McDevitt, C. A., et al. (2017). Zinc stress induces copper depletion in *Acinetobacter baumannii*. *BMC Microbiol* 17, 59. doi: 10.1186/s12866-017-0965-y
- He, M., Sebahia, M., Lawley, T. D., Stabler, R. A., Dawson, L. F., Martin, M. J., et al. (2010). Evolutionary dynamics of *Clostridium difficile* over short and long time scales. *PNAS* 107, 7527–7532. doi: 10.1073/pnas.0914322107
- Healy, J., Ekkerman, S., Pliotas, C., Richard, M., Bartlett, W., Grayer, S. C., et al. (2014). Understanding the structural requirements for activators of the Kef bacterial potassium efflux system. *Biochemistry* 53, 1982–1992. doi: 10.1021/bi5001118
- Heath, R. J., and Rock, C. O. (2000). A triclosan-resistant bacterial enzyme. *Nature* 406, 145–146. doi: 10.1038/35018162
- Heidebrecht, H.-J., Lagkouvardos, I., Reitmeier, S., Hengst, C., Kulozik, U., and Pfaffl, M. W. (2021). Alteration of Intestinal Microbiome of *Clostridioides difficile*-Infected Hamsters during the Treatment with Specific Cow Antibodies. *Antibiotics (Basel)* 10. doi: 10.3390/antibiotics10060724
- Heintz-Buschart, A., and Wilmes, P. (2018). Human Gut Microbiome: Function Matters. *Trends Microbiol* 26, 563–574. doi: 10.1016/j.tim.2017.11.002
- Held, J., Gebru, T., Kalesse, M., Jansen, R., Gerth, K., Müller, R., et al. (2014). Antimalarial activity of the myxobacterial macrolide chlorotonil a. *Antimicrob Agents Chemother* 58, 6378–6384. doi: 10.1128/AAC.03326-14
- Hennessen, F., Miethke, M., Zaburanyi, N., Loose, M., Lukežič, T., Bernecker, S., et al. (2020). Amidochelocardin Overcomes Resistance Mechanisms Exerted on Tetracyclines and Natural Chelocardin. *Antibiotics (Basel)* 9, 619. doi: 10.3390/antibiotics9090619
- Hernandez, B. G., Vinithakumari, A. A., Sponseller, B., Tangudu, C., and Mooyottu, S. (2020). Prevalence, Colonization, Epidemiology, and Public Health Significance of *Clostridioides difficile* in Companion Animals. *Front Vet Sci* 7, 512551. doi: 10.3389/fvets.2020.512551
- Heyer, R., Schallert, K., Büdel, A., Zoun, R., Dorl, S., Behne, A., et al. (2019). A Robust and Universal Metaproteomics Workflow for Research Studies and Routine Diagnostics Within 24 h Using Phenol Extraction, FASP Digest, and the MetaProteomeAnalyzer. *Front. Microbiol.* 10, 1883. doi: 10.3389/fmicb.2019.01883
- Heyer, R., Schallert, K., Zoun, R., Becher, B., Saake, G., and Benndorf, D. (2017). Challenges and perspectives of metaproteomic data analysis. *J Biotechnol* 261, 24–36. doi: 10.1016/j.jbiotec.2017.06.1201
- Hinzke, T., Kouris, A., Hughes, R.-A., Strous, M., and Kleiner, M. (2019). More Is Not Always Better: Evaluation of 1D and 2D-LC-MS/MS Methods for Metaproteomics. *Front. Microbiol.* 10, 238. doi: 10.3389/fmicb.2019.00238
- Hofer, W., Müller, R., Oueis, E., Abou Fayad, A., Deschner, F., Andreas, A., et al. (2022). Regio- and Stereoselective Epoxidation and Acidic Epoxide Opening of Antibacterial and Antiplasmodial Chlorotonils Yield Highly Potent Derivatives. *Angew Chem Int Ed Engl.* doi: 10.1002/anie.202202816
- Huang, Y. Y., Martínez-Del Campo, A., and Balskus, E. P. (2018). Anaerobic 4-hydroxyproline utilization: Discovery of a new glycy radical enzyme in the human gut microbiome uncovers a widespread microbial metabolic activity. *Gut Microbes* 9, 437–451. doi: 10.1080/19490976.2018.1435244
- Hubrich, F., Müller, M., and Andexer, J. N. (2021). Chorismate- and isochorismate converting enzymes: versatile catalysts acting on an important metabolic node. *Chem Commun (Camb)* 57, 2441–2463. doi: 10.1039/d0cc08078k
- Hui, W., Li, T., Liu, W., Zhou, C., and Gao, F. (2019). Fecal microbiota transplantation for treatment of recurrent *C. difficile* infection: An updated randomized controlled trial meta-analysis. *PLoS One* 14, e0210016. doi: 10.1371/journal.pone.0210016
- Hussain, H. A., Roberts, A. P., and Mullany, P. (2005). Generation of an erythromycin-sensitive derivative of *Clostridium difficile* strain 630 (630Deltaerm) and demonstration that the

- conjugative transposon Tn916DeltaE enters the genome of this strain at multiple sites. *J Med Microbiol* 54, 137–141. doi: 10.1099/jmm.0.45790-0
- Hutchings, M. I., Truman, A. W., and Wilkinson, B. (2019). Antibiotics: past, present and future. *Curr Opin Microbiol* 51, 72–80. doi: 10.1016/j.mib.2019.10.008
- Irschik, H., Gerth, K., Höfle, G., Kohl, W., and Reichenbach, H. (1983). The myxopyronins, new inhibitors of bacterial RNA synthesis from *Myxococcus fulvus* (Myxobacterales). *J Antibiot (Tokyo)* 36, 1651–1658. doi: 10.7164/antibiotics.36.1651
- Irving, H., and Williams, R. J. P. (1948). Order of Stability of Metal Complexes. *Nature* 162, 746–747. doi: 10.1038/162746a0
- Issa Isaac, N., Philippe, D., Nicholas, A., Raoult, D., and Eric, C. (2019). Metaproteomics of the human gut microbiota: Challenges and contributions to other OMICS. *Clin Mass Spectrom* 14 Pt A, 18–30. doi: 10.1016/j.clinms.2019.06.001
- Jackson, S., Calos, M., Myers, A., and Self, W. T. (2006). Analysis of proline reduction in the nosocomial pathogen *Clostridium difficile*. *J Bacteriol* 188, 8487–8495. doi: 10.1128/JB.01370-06
- Jackson-Rosario, S., Cowart, D., Myers, A., Tarrien, R., Levine, R. L., Scott, R. A., et al. (2009). Aurano-fin disrupts selenium metabolism in *Clostridium difficile* by forming a stable Au-Se adduct. *J Biol Inorg Chem* 14, 507–519. doi: 10.1007/s00775-009-0466-z
- Janezic, S., Zidaric, V., Pardon, B., Indra, A., Kokotovic, B., Blanco, J. L., et al. (2014). International *Clostridium difficile* animal strain collection and large diversity of animal associated strains. *BMC Microbiol* 14, 173. doi: 10.1186/1471-2180-14-173
- Jarrad, A. M., Karoli, T., Blaskovich, M. A. T., Lyras, D., and Cooper, M. A. (2015). *Clostridium difficile* drug pipeline: challenges in discovery and development of new agents. *Journal of Medicinal Chemistry* 58, 5164–5185. doi: 10.1021/jm5016846
- Jenior, M. L., Leslie, J. L., Young, V. B., and Schloss, P. D. (2017). *Clostridium difficile* Colonizes Alternative Nutrient Niches during Infection across Distinct Murine Gut Microbiomes. *mSystems* 2. doi: 10.1128/mSystems.00063-17
- Jenior, M. L., Leslie, J. L., Young, V. B., and Schloss, P. D. (2018). *Clostridium difficile* Alters the Structure and Metabolism of Distinct Cecal Microbiomes during Initial Infection To Promote Sustained Colonization. *mSphere* 3. doi: 10.1128/mSphere.00261-18
- Jenjaroenpun, P., Wongsurawat, T., Pereira, R., Patumcharoenpol, P., Ussery, D. W., Nielsen, J., et al. (2018). Complete genomic and transcriptional landscape analysis using third-generation sequencing: a case study of *Saccharomyces cerevisiae* CEN.PK113-7D. *Nucleic acids research* 46, e38. doi: 10.1093/nar/gky014
- Jesus, A. J. de, and Allen, T. W. (2013). The role of tryptophan side chains in membrane protein anchoring and hydrophobic mismatch. *Biochimica et biophysica acta* 1828, 864–876. doi: 10.1016/j.bbamem.2012.09.009
- Jones, J. A., Prior, A. M., Marreddy, R. K. R., Wahrmund, R. D., Hurdle, J. G., Sun, D., et al. (2019). Small-Molecule Inhibition of the *C. difficile* FAS-II Enzyme, FabK, Results in Selective Activity. *ACS Chemical Biology* 14, 1528–1535. doi: 10.1021/acscchembio.9b00293
- Jones, P., Binns, D., Chang, H.-Y., Fraser, M., Li, W., McAnulla, C., et al. (2014). InterProScan 5: genome-scale protein function classification. *Bioinformatics (Oxford, England)* 30, 1236–1240. doi: 10.1093/bioinformatics/btu031
- Jungmann, K., Jansen, R., Gerth, K., Huch, V., Krug, D., Fenical, W., et al. (2015). Two of a Kind—The Biosynthetic Pathways of Chlorotoniol and Anthracimycin. *ACS Chemical Biology* 10, 2480–2490. doi: 10.1021/acscchembio.5b00523
- Just, I., Selzer, J., Wilm, M., Eichel-Streiber, C. von, Mann, M., and Aktories, K. (1995a). Glucosylation of Rho proteins by *Clostridium difficile* toxin B. *Nature* 375, 500–503. doi: 10.1038/375500a0
- Just, I., Wilm, M., Selzer, J., Rex, G., Eichel-Streiber, C. von, Mann, M., et al. (1995b). The enterotoxin from *Clostridium difficile* (ToxA) monoglucosylates the Rho proteins. *J Biol Chem* 270, 13932–13936. doi: 10.1074/jbc.270.23.13932

References

- Juste, C., Kreil, D. P., Beauvallet, C., Guillot, A., Vaca, S., Carapito, C., et al. (2014). Bacterial protein signals are associated with Crohn's disease. *Gut* 63, 1566–1577. doi: 10.1136/gutjnl-2012-303786
- Juttukonda, L. J., Beavers, W. N., Unsihuay, D., Kim, K., Pishchany, G., Horning, K. J., et al. (2020). A Small-Molecule Modulator of Metal Homeostasis in Gram-Positive Pathogens. *mBio* 11. doi: 10.1128/mBio.02555-20
- Kang, J. D., Myers, C. J., Harris, S. C., Kakiyama, G., Lee, I.-K., Yun, B.-S., et al. (2019). Bile Acid 7 α -Dehydroxylating Gut Bacteria Secrete Antibiotics that Inhibit *Clostridium difficile*: Role of Secondary Bile Acids. *Cell Chem Biol* 26, 27-34.e4. doi: 10.1016/j.chembiol.2018.10.003
- Kao, D., Wong, K., Franz, R., Cochrane, K., Sherriff, K., Chui, L., et al. (2021). The effect of a microbial ecosystem therapeutic (MET-2) on recurrent *Clostridioides difficile* infection: a phase 1, open-label, single-group trial. *The Lancet Gastroenterology & Hepatology* 6, 282–291. doi: 10.1016/S2468-1253(21)00007-8
- Karakonstantis, S., Kritsotakis, E. I., and Gikas, A. (2020). Pandrug-resistant Gram-negative bacteria: a systematic review of current epidemiology, prognosis and treatment options. *J Antimicrob Chemother* 75, 271–282. doi: 10.1093/jac/dkz401
- Karasawa, T., Ikoma, S., Yamakawa, K., and Nakamura, S. (1995). A defined growth medium for *Clostridium difficile*. *Microbiology* 141 (Pt 2), 371–375. doi: 10.1099/13500872-141-2-371
- Kashaf, S. S., Angione, C., and Lió, P. (2017). Making life difficult for *Clostridium difficile*: augmenting the pathogen's metabolic model with transcriptomic and codon usage data for better therapeutic target characterization. *BMC Syst Biol* 11, 25. doi: 10.1186/s12918-017-0395-3
- Kassambara, A. (2021). *rstatix: Pipe-friendly framework for basic statistical tests: R package version 0.7.0*, <https://rdr.io/github/kassambara/rstatix/>
- Kassambara, A. (2020). *ggpubr: 'ggplot2' Based Publication Ready Plots*.
- Khanna, S., Montassier, E., Schmidt, B., Patel, R., Knights, D., Pardi, D. S., et al. (2016). Gut microbiome predictors of treatment response and recurrence in primary *Clostridium difficile* infection. *Aliment Pharmacol Ther* 44, 715–727. doi: 10.1111/apt.13750
- Khanna, S., Pardi, D. S., Aronson, S. L., Kammer, P. P., Orenstein, R., St Sauver, J. L., et al. (2012). The epidemiology of community-acquired *Clostridium difficile* infection: a population-based study. *Am J Gastroenterol* 107, 89–95. doi: 10.1038/ajg.2011.398
- Khemaissa, S., Sagan, S., and Walrant, A. (2021). Tryptophan, an Amino-Acid Endowed with Unique Properties and Its Many Roles in Membrane Proteins. *Crystals* 11, 1032. doi: 10.3390/cryst11091032
- Khodadadi, E., Zeinalzadeh, E., Taghizadeh, S., Mehramouz, B., Kamounah, F. S., Khodadadi, E., et al. (2020). Proteomic Applications in Antimicrobial Resistance and Clinical Microbiology Studies. *Infect Drug Resist* 13, 1785–1806. doi: 10.2147/IDR.S238446
- Kint, N., Alves Feliciano, C., Martins, M. C., Morvan, C., Fernandes, S. F., Folgosa, F., et al. (2020). How the Anaerobic Enteropathogen *Clostridioides difficile* Tolerates Low O₂ Tensions. *mBio* 11. doi: 10.1128/mBio.01559-20
- Klein, E. Y., van Boeckel, T. P., Martinez, E. M., Pant, S., Gandra, S., Levin, S. A., et al. (2018). Global increase and geographic convergence in antibiotic consumption between 2000 and 2015. *PNAS* 115, E3463-E3470. doi: 10.1073/pnas.1717295115
- Knetsch, C. W., Connor, T. R., Mutreja, A., van Dorp, S. M., Sanders, I. M., Browne, H. P., et al. (2014). Whole genome sequencing reveals potential spread of *Clostridium difficile* between humans and farm animals in the Netherlands, 2002 to 2011. *Eurosurveillance* 19, 20954. doi: 10.2807/1560-7917.ES2014.19.45.20954
- Knight, D. R., Elliott, B., Chang, B. J., Perkins, T. T., and Riley, T. V. (2015). Diversity and Evolution in the Genome of *Clostridium difficile*. *Clin Microbiol Rev* 28, 721–741. doi: 10.1128/CMR.00127-14
- Knight, D. R., Kullin, B., Androga, G. O., Barbut, F., Eckert, C., Johnson, S., et al. (2019). Evolutionary and Genomic Insights into *Clostridioides difficile* Sequence Type 11: a Diverse Zoonotic and Antimicrobial-Resistant Lineage of Global One Health Importance. *mBio* 10. doi: 10.1128/mBio.00446-19

- Knight-Connoni, V., Mascio, C., Chesnel, L., and Silverman, J. (2016). Discovery and development of surotomycin for the treatment of *Clostridium difficile*. *J Ind Microbiol Biotechnol* 43, 195–204. doi: 10.1007/s10295-015-1714-6
- Knippel, R. J., Wexler, A. G., Miller, J. M., Beavers, W. N., Weiss, A., Crécy-Lagard, V. de, et al. (2020). *Clostridioides difficile* Senses and Hijacks Host Heme for Incorporation into an Oxidative Stress Defense System. *Cell Host Microbe* 28, 411–421.e6. doi: 10.1016/j.chom.2020.05.015
- Kochan, T. J., Somers, M. J., Kaiser, A. M., Shoshiev, M. S., Hagan, A. K., Hastie, J. L., et al. (2017). Intestinal calcium and bile salts facilitate germination of *Clostridium difficile* spores. *PLoS Pathog* 13, e1006443. doi: 10.1371/journal.ppat.1006443
- Koene, M. G. J., Mevius, D., Wagenaar, J. A., Harmanus, C., Hensgens, M. P. M., Meetsma, A. M., et al. (2012). *Clostridium difficile* in Dutch animals: their presence, characteristics and similarities with human isolates. *Clin Microbiol Infect* 18, 778–784. doi: 10.1111/j.1469-0691.2011.03651.x
- Köhler, T., Perron, G. G., Buckling, A., and van Delden, C. (2010). Quorum sensing inhibition selects for virulence and cooperation in *Pseudomonas aeruginosa*. *PLoS Pathog* 6, e1000883. doi: 10.1371/journal.ppat.1000883
- Kolde, R. (2019). pheatmap: Pretty Heatmaps: R package version 1.0.12, <https://CRAN.R-project.org/package=pheatmap>
- Kongpracha, P., Wiriyasermkul, P., Isozumi, N., Moriyama, S., Kanai, Y., and Nagamori, S. (2022). Simple but efficacious enrichment of integral membrane proteins and their interactions for in-depth membrane proteomics. *MCP*, 100206. doi: 10.1016/j.mcpro.2022.100206
- Koo, H. L., DuPont, H. L., and Huang, D. B. (2009). The role of rifaximin in the treatment and chemoprophylaxis of travelers' diarrhea. *Ther Clin Risk Manag* 5, 841–848. doi: 10.2147/tcrm.s4442
- Köpke, M., Straub, M., and Dürre, P. (2013). *Clostridium difficile* is an autotrophic bacterial pathogen. *PLoS One* 8, e62157. doi: 10.1371/journal.pone.0062157
- Kordus, S. L., Thomas, A. K., and Lacy, D. B. (2021). *Clostridioides difficile* toxins: mechanisms of action and antitoxin therapeutics. *Nat Rev Microbiol*. doi: 10.1038/s41579-021-00660-2
- Kraus, C. N., Lyerly, M. W., and Carman, R. J. (2015). Ambush of *Clostridium difficile* spores by ramoplanin: activity in an *in vitro* model. *Antimicrob Agents Chemother* 59, 2525–2530. doi: 10.1128/AAC.04853-14
- Kulecka, M., Waker, E., Ambrozkiwicz, F., Paziewska, A., Skubisz, K., Cybula, P., et al. (2021). Higher genome variability within metabolism genes associates with recurrent *Clostridium difficile* infection. *BMC Microbiol* 21, 36. doi: 10.1186/s12866-021-02090-9
- Kumar, D., Bansal, G., Narang, A., Basak, T., Abbas, T., and Dash, D. (2016). Integrating transcriptome and proteome profiling: Strategies and applications. *Proteomics* 16, 2533–2544. doi: 10.1002/pmic.201600140
- Kumar, N., Browne, H. P., Viciani, E., Forster, S. C., Clare, S., Harcourt, K., et al. (2019). Adaptation of host transmission cycle during *Clostridium difficile* speciation. *Nat Genet* 51, 1315–1320. doi: 10.1038/s41588-019-0478-8
- Laffin, M., Millan, B., and Madsen, K. L. (2017). Fecal microbial transplantation as a therapeutic option in patients colonized with antibiotic resistant organisms. *Gut Microbes* 8, 221–224. doi: 10.1080/19490976.2016.1278105
- Lagkouvardos, I., Pukall, R., Abt, B., Foessel, B. U., Meier-Kolthoff, J. P., Kumar, N., et al. (2016). The Mouse Intestinal Bacterial Collection (miBC) provides host-specific insight into cultured diversity and functional potential of the gut microbiota. *Nat Microbiol* 1, 16131. doi: 10.1038/nmicrobiol.2016.131
- Landenberger, M., Nieland, J., Roeder, M., Nørgaard, K., Papatheodorou, P., Ernst, K., et al. (2021). The cytotoxic effect of *Clostridioides difficile* pore-forming toxin CDTb. *Biochim Biophys Acta Biomembr* 1863, 183603. doi: 10.1016/j.bbmem.2021.183603
- Larocque, M., Chénard, T., and Najmanovich, R. (2014). A curated *C. difficile* strain 630 metabolic network: prediction of essential targets and inhibitors. *BMC Syst Biol* 8, 117. doi: 10.1186/s12918-014-0117-z

References

- Larsson, D. G. J., and Flach, C.-F. (2022). Antibiotic resistance in the environment. *Nat Rev Microbiol* 20, 257–269. doi: 10.1038/s41579-021-00649-x
- Lee, C. H., Patino, H., Stevens, C., Rege, S., Chesnel, L., Louie, T., et al. (2016). Surotomycin versus vancomycin for *Clostridium difficile* infection: Phase 2, randomized, controlled, double-blind, non-inferiority, multicentre trial. *J Antimicrob Chemother* 71, 2964–2971. doi: 10.1093/jac/dkw246
- Leeds, J. A., Sachdeva, M., Mullin, S., Barnes, S. W., and Ruzin, A. (2014). *In vitro* selection, via serial passage, of *Clostridium difficile* mutants with reduced susceptibility to fidaxomicin or vancomycin. *J Antimicrob Chemother* 69, 41–44. doi: 10.1093/jac/dkt302
- Leshner, G. Y., Froehlich, E. J., Gruett, M. D., Bailey, J. H., and Brundage, R. P. (1962). 1,8-Naphthyridine derivatives. A new class of chemotherapeutic agents. *J. Med. Chem.* 91, 1063–1065. doi: 10.1021/jm01240a021
- Leslie, J. L., Jenior, M. L., Vendrov, K. C., Standke, A. K., Barron, M. R., O'Brien, T. J., et al. (2021). Protection from Lethal *Clostridioides difficile* Infection via Intraspecies Competition for Cogerminant. *mBio* 12. doi: 10.1128/mBio.00522-21
- Lesniak, N. A., Schubert, A. M., Sinani, H., and Schloss, P. D. (2021). Clearance of *Clostridioides difficile* Colonization Is Associated with Antibiotic-Specific Bacterial Changes. *mSphere* 6. doi: 10.1128/mSphere.01238-20
- Lešnik, U., Lukežič, T., Podgoršek, A., Horvat, J., Polak, T., Šala, M., et al. (2015). Construction of a new class of tetracycline lead structures with potent antibacterial activity through biosynthetic engineering. *Angew Chem Int Ed Engl* 54, 3937–3940. doi: 10.1002/anie.201411028
- Li, L., and Figeys, D. (2020). Proteomics and Metaproteomics Add Functional, Taxonomic and Biomass Dimensions to Modeling the Ecosystem at the Mucosal-luminal Interface. *MCP* 19, 1409–1417. doi: 10.1074/mcp.R120.002051
- Li, W., and Godzik, A. (2006). Cd-hit: a fast program for clustering and comparing large sets of protein or nucleotide sequences. *Bioinformatics (Oxford, England)* 22, 1658–1659. doi: 10.1093/bioinformatics/btl158
- Liao, C.-H., Ko, W.-C., Lu, J.-J., and Hsueh, P.-R. (2012). Characterizations of clinical isolates of *Clostridium difficile* by toxin genotypes and by susceptibility to 12 antimicrobial agents, including fidaxomicin (OPT-80) and rifaximin: a multicenter study in Taiwan. *Antimicrob Agents Chemother* 56, 3943–3949. doi: 10.1128/AAC.00191-12
- Liebeke, M., Pöther, D.-C., van Duy, N., Albrecht, D., Becher, D., Hochgräfe, F., et al. (2008). Depletion of thiol-containing proteins in response to quinones in *Bacillus subtilis*. *Mol Microbiol* 69, 1513–1529. doi: 10.1111/j.1365-2958.2008.06382.x
- Lim, S.-C., Knight, D. R., Moono, P., Foster, N. F., and Riley, T. V. (2020). *Clostridium difficile* in soil conditioners, mulches and garden mixes with evidence of a clonal relationship with historical food and clinical isolates. *Environ Microbiol Rep* 12, 672–680. doi: 10.1111/1758-2229.12889
- Lira, R., Xiang, A. X., Doundoulakis, T., Biller, W. T., Agrios, K. A., Simonsen, K. B., Webber, S. E., Sisson, W., Aust, R. M., Shah, A. M., Showalter, R. E., Banh, V. N., Steffy, K. R., & Appleman, J. R. (2007). Syntheses of novel myxopyronin B analogs as potential inhibitors of bacterial RNA polymerase. *Bioorganic & medicinal chemistry letters*, 17(24), 6797–6800. doi: 10.1016/j.bmcl.2007.10.017
- Liu, L., Oza, S., Hogan, D., Chu, Y., Perin, J., Zhu, J., et al. (2016). Global, regional, and national causes of under-5 mortality in 2000–15: an updated systematic analysis with implications for the Sustainable Development Goals. *The Lancet* 388, 3027–3035. doi: 10.1016/S0140-6736(16)31593-8
- Liu, Y., Jia, Y., Yang, K., Li, R., Xiao, X., Zhu, K., et al. (2020). Metformin Restores Tetracyclines Susceptibility against Multidrug Resistant Bacteria. *Adv Sci (Weinh)* 7, 1902227. doi: 10.1002/advs.201902227
- Liu, Z., Dumville, J. C., Norman, G., Westby, M. J., Blazeby, J., McFarlane, E., et al. (2018). Intraoperative interventions for preventing surgical site infection: an overview of Cochrane Reviews. *Cochrane Database Syst Rev* 2, CD012653. doi: 10.1002/14651858.CD012653.pub2

- Lobritz, M. A., Belenky, P., Porter, C. B. M., Gutierrez, A., Yang, J. H., Schwarz, E. G., et al. (2015). Antibiotic efficacy is linked to bacterial cellular respiration. *PNAS* 112, 8173–8180. doi: 10.1073/pnas.1509743112
- Locher, H. H., Caspers, P., Bruyère, T., Schroeder, S., Pfaff, P., Knezevic, A., et al. (2014a). Investigations of the mode of action and resistance development of cadazolid, a new antibiotic for treatment of *Clostridium difficile* infections. *Antimicrob Agents Chemother* 58, 901–908. doi: 10.1128/AAC.01831-13
- Locher, H. H., Seiler, P., Chen, X., Schroeder, S., Pfaff, P., Enderlin, M., et al. (2014b). *In vitro* and *in vivo* antibacterial evaluation of cadazolid, a new antibiotic for treatment of *Clostridium difficile* infections. *Antimicrob Agents Chemother* 58, 892–900. doi: 10.1128/AAC.01830-13
- Locke, J. C. W., Young, J. W., Fontes, M., Hernández Jiménez, M. J., and Elowitz, M. B. (2011). Stochastic pulse regulation in bacterial stress response. *Science* 334, 366–369. doi: 10.1126/science.1208144
- Lohani, M., Dhasmana, A., Haque, S., Wahid, M., Jawed, A., Dar, S. A., et al. (2017). Proteome mining for the identification and *in-silico* characterization of putative drug targets of multi-drug resistant *Clostridium difficile* strain 630. *Journal of Microbiological Methods* 136, 6–10. doi: 10.1016/j.mimet.2017.02.008
- Looft, T., Allen, H. K., Cantarel, B. L., Levine, U. Y., Bayles, D. O., Alt, D. P., et al. (2014). Bacteria, phages and pigs: the effects of in-feed antibiotics on the microbiome at different gut locations. *ISME J* 8, 1566–1576. doi: 10.1038/ismej.2014.12
- Lopez, C. A., Beavers, W. N., Weiss, A., Knippel, R. J., Zackular, J. P., Chazin, W., et al. (2019). The Immune Protein Calprotectin Impacts *Clostridioides difficile* Metabolism through Zinc Limitation. *mBio* 10. doi: 10.1128/mBio.02289-19
- Lopez, C. A., McNeely, T. P., Nurmakova, K., Beavers, W. N., and Skaar, E. P. (2020). *Clostridioides difficile* proline fermentation in response to commensal clostridia. *Anaerobe* 63, 102210. doi: 10.1016/j.anaerobe.2020.102210
- Lopez, D., and Koch, G. (2017). Exploring functional membrane microdomains in bacteria: an overview. *Curr Opin Microbiol* 36, 76–84. doi: 10.1016/j.mib.2017.02.001
- Louie, T., Nord, C. E., Talbot, G. H., Wilcox, M., Gerding, D. N., Buitrago, M., et al. (2015). Multicenter, Double-Blind, Randomized, Phase 2 Study Evaluating the Novel Antibiotic Cadazolid in Patients with *Clostridium difficile* Infection. *Antimicrob Agents Chemother* 59, 6266–6273. doi: 10.1128/AAC.00504-15
- Louie, T. J., Cannon, K., Byrne, B., Emery, J., Ward, L., Eyben, M., et al. (2012). Fidaxomicin preserves the intestinal microbiome during and after treatment of *Clostridium difficile* infection (CDI) and reduces both toxin reexpression and recurrence of CDI. *Clin Infect Dis* 55 Suppl 2, S132-42. doi: 10.1093/cid/cis338
- Lozupone, C. A., Stombaugh, J. I., Gordon, J. I., Jansson, J. K., and Knight, R. (2012). Diversity, stability and resilience of the human gut microbiota. *Nature* 489, 220–230. doi: 10.1038/nature11550
- Lu, Z., and Imlay, J. A. (2021). When anaerobes encounter oxygen: mechanisms of oxygen toxicity, tolerance and defence. *Nat Rev Microbiol* 19, 774–785. doi: 10.1038/s41579-021-00583-y
- Lucas, J. M., Gora, E., Salzberg, A., and Kaspari, M. (2019). Antibiotics as chemical warfare across multiple taxonomic domains and trophic levels in brown food webs. *Proceedings. Biological sciences* 286, 20191536. doi: 10.1098/rspb.2019.1536
- Lukežič, T., Fayad, A. A., Bader, C., Harmrolfs, K., Bartuli, J., Groß, S., et al. (2019). Engineering Atypical Tetracycline Formation in *Amycolatopsis sulphurea* for the Production of Modified Chelocardin Antibiotics. *ACS Chemical Biology* 14, 468–477. doi: 10.1021/acscchembio.8b01125
- Lukežič, T., Lešnik, U., Podgoršek, A., Horvat, J., Polak, T., Šala, M., et al. (2013). Identification of the chelocardin biosynthetic gene cluster from *Amycolatopsis sulphurea*: a platform for producing novel tetracycline antibiotics. *Microbiology* 159, 2524–2532. doi: 10.1099/mic.0.070995-0

References

- Lukežič, T., Pikel, Š., Zaburanyi, N., Remškar, M., Petković, H., and Müller, R. (2020). Heterologous expression of the atypical tetracycline chelocardin reveals the full set of genes required for its biosynthesis. *Microb Cell Fact* 19, 230. doi: 10.1186/s12934-020-01495-x
- Luong, T., Salabarria, A.-C., and Roach, D. R. (2020). Phage Therapy in the Resistance Era: Where Do We Stand and Where Are We Going? *Clin Ther* 42, 1659–1680. doi: 10.1016/j.clinthera.2020.07.014
- Lyerly, D. M., Phelps, C. J., Toth, J., and Wilkins, T. D. (1986). Characterization of toxins A and B of *Clostridium difficile* with monoclonal antibodies. *Infect Immun* 54, 70–76. doi: 10.1128/iai.54.1.70-76.1986
- Lyerly, D. M., Sullivan, N. M., and Wilkins, T. D. (1983). Enzyme-linked immunosorbent assay for *Clostridium difficile* toxin A. *Journal of clinical microbiology* 17, 72–78. doi: 10.1128/jcm.17.1.72-78.1983
- Magill, S. S., O’Leary, E., Janelle, S. J., Thompson, D. L., Dumyati, G., Nadle, J., et al. (2018). Changes in Prevalence of Health Care-Associated Infections in U.S. Hospitals. *N Engl J Med* 379, 1732–1744. doi: 10.1056/NEJMoa1801550
- Maia, A. R., Reyes-Ramírez, R., Pizarro-Guajardo, M., Saggese, A., Ricca, E., Baccigalupi, L., et al. (2020). Nasal Immunization with the C-Terminal Domain of BclA3 Induced Specific IgG Production and Attenuated Disease Symptoms in Mice Infected with *Clostridioides difficile* Spores. *Int J Mol Sci* 21. doi: 10.3390/ijms21186696
- Major, G., Bradshaw, L., Boota, N., Sprange, K., Diggle, M., Montgomery, A., et al. (2019). Follow-on RifAximin for the Prevention of recurrence following standard treatment of Infection with *Clostridium Difficile* (RAPID): a randomised placebo controlled trial. *Gut* 68, 1224–1231. doi: 10.1136/gutjnl-2018-316794
- Mao, X., Ma, Q., Zhou, C., Chen, X., Zhang, H., Yang, J., et al. (2014). DOOR 2.0: presenting operons and their functions through dynamic and integrated views. *Nucleic acids research* 42, D654-9. doi: 10.1093/nar/gkt1048
- Marrakchi, H., Dewolf, W. E., Quinn, C., West, J., Polizzi, B. J., So, C. Y., et al. (2003). Characterization of *Streptococcus pneumoniae* enoyl-(acyl-carrier protein) reductase (FabK). *Biochem J* 370, 1055–1062. doi: 10.1042/BJ20021699
- Marreddy, R. K. R., Wu, X., Sapkota, M., Prior, A. M., Jones, J. A., Sun, D., et al. (2019). The Fatty Acid Synthesis Protein Enoyl-ACP Reductase II (FabK) is a Target for Narrow-Spectrum Antibacterials for *Clostridium difficile* Infection. *ACS Infect Dis* 5, 208–217. doi: 10.1021/acsinfecdis.8b00205
- Martin-Verstraete, I., Peltier, J., and Dupuy, B. (2016). The Regulatory Networks That Control *Clostridium difficile* Toxin Synthesis. *Toxins (Basel)* 8. doi: 10.3390/toxins8050153
- Mattarelli, P., Bonaparte, C., Pot, B., and Biavati, B. (2008). Proposal to reclassify the three biotypes of *Bifidobacterium longum* as three subspecies: *Bifidobacterium longum* subsp. longum subsp. nov., *Bifidobacterium longum* subsp. infantis comb. nov. and *Bifidobacterium longum* subsp. suis comb. nov. *Int. J. Syst. Evol.* 58, 767–772. doi: 10.1099/ijms.0.65319-0
- McAllister, K. N., Martinez Aguirre, A., and Sorg, J. A. (2021). The selenophosphate synthetase, *selD*, is important for *Clostridioides difficile* physiology. *J Bacteriol.* doi: 10.1128/JB.00008-21
- McDonald, J. A. K., Mullish, B. H., Pechlivanis, A., Liu, Z., Brignardello, J., Kao, D., et al. (2018). Inhibiting Growth of *Clostridioides difficile* by Restoring Valerate, Produced by the Intestinal Microbiota. *Gastroenterology* 155, 1495-1507.e15. doi: 10.1053/j.gastro.2018.07.014
- McEwen, S. A., and Collignon, P. J. (2018). Antimicrobial Resistance: a One Health Perspective. *Microbiol Spectr* 6. doi: 10.1128/microbiolspec.ARBA-0009-2017
- McFarland, L. V. (2015). Probiotics for the Primary and Secondary Prevention of *C. difficile* Infections: A Meta-analysis and Systematic Review. *Antibiotics (Basel)* 4, 160–178. doi: 10.3390/antibiotics4020160
- McKee, H. K., Kajiwara, C., Yamaguchi, T., Ishii, Y., Shimizu, N., Ohara, A., et al. (2021). *Clostridioides difficile* toxins enhanced the *in vitro* production of CXC chemokine ligand 2 and tumor necrosis factor- α via Toll-like receptors in macrophages. *J Med Microbiol* 70. doi: 10.1099/jmm.0.001342

- Metzendorf, N. G., Lange, L. M., Lainer, N., Schlüter, R., Dittmann, S., Paul, L.-S., et al. (2022). Destination and Specific Impact of Different Bile Acids in the Intestinal Pathogen *Clostridioides difficile*. *Front. Microbiol.* 13, 814692. doi: 10.3389/fmicb.2022.814692
- Mileto, S. J., Jardé, T., Childress, K. O., Jensen, J. L., Rogers, A. P., Kerr, G., et al. (2020). *Clostridioides difficile* infection damages colonic stem cells via TcdB, impairing epithelial repair and recovery from disease. *Proc Natl Acad Sci U S A* 117, 8064–8073. doi: 10.1073/pnas.1915255117
- Mitcheltree, M. J., Pisipati, A., Syroegin, E. A., Silvestre, K. J., Klepacki, D., Mason, J. D., et al. (2021). A synthetic antibiotic class overcoming bacterial multidrug resistance. *Nature* 599, 507–512. doi: 10.1038/s41586-021-04045-6
- Mitosch, K., Rieckh, G., and Bollenbach, T. (2017). Noisy Response to Antibiotic Stress Predicts Subsequent Single-Cell Survival in an Acidic Environment. *Cell Syst* 4, 393–403.e5. doi: 10.1016/j.cels.2017.03.001
- Mitscher, L. A., Juvarkar, J. V., Rosenbrook, W., Andres, W. W., Schenk, J., and Egan, R. S. (1970). Structure of chelocardin, a novel tetracycline antibiotic. *J. Am. Chem. Soc.* 92, 6070–6071. doi: 10.1021/ja00723a049
- Molnar, V., Matković, Z., Tambić, T., and Kozma, C. (1977). Klinicko-farmakolosko ispitivanje kelokardina u bolesnika s infekcijom mokraćnih putova. *Liječnički vjesnik* 99, 560–562.
- Monaghan, T. M., Seekatz, A. M., Mullish, B. H., Moore-Gillon, C. C. E. R., Dawson, L. F., Ahmed, A., et al. (2021). *Clostridioides difficile*: innovations in target discovery and potential for therapeutic success. *Expert Opin Ther Targets* 25, 949–963. doi: 10.1080/14728222.2021.2008907
- Mondal, S. I., Draper, L. A., Ross, R. P., and Hill, C. (2020). Bacteriophage endolysins as a potential weapon to combat *Clostridioides difficile* infection. *Gut Microbes* 12, 1813533. doi: 10.1080/19490976.2020.1813533
- Mookherjee, N., Anderson, M. A., Haagsman, H. P., and Davidson, D. J. (2020). Antimicrobial host defence peptides: functions and clinical potential. *Nat Rev Drug Discov* 19, 311–332. doi: 10.1038/s41573-019-0058-8
- Morens, D. M., Folkers, G. K., and Fauci, A. S. (2004). The challenge of emerging and re-emerging infectious diseases. *Nature* 430, 242–249. doi: 10.1038/nature02759
- Morris, G. N., Winter, J., Cato, E. P., Ritchie, A. E., and v. d. Bokkenheuser (1985). *Clostridium scindens* sp. nov., a Human Intestinal Bacterium with Desmolytic Activity on Corticoids. *International Journal of Systematic Bacteriology* 35, 478–481. doi: 10.1099/00207713-35-4-478
- Moss, E. L., Falconer, S. B., Tkachenko, E., Wang, M., Systrom, H., Mahabamunuge, J., et al. (2017). Long-term taxonomic and functional divergence from donor bacterial strains following fecal microbiota transplantation in immunocompromised patients. *PLOS ONE* 12, e0182585. doi: 10.1371/journal.pone.0182585
- Motamedi, H., Fathollahi, M., Abiri, R., Kadivar, S., Rostamian, M., and Alvandi, A. (2021). A worldwide systematic review and meta-analysis of bacteria related to antibiotic-associated diarrhea in hospitalized patients. *PLoS One* 16, e0260667. doi: 10.1371/journal.pone.0260667
- Mücke, P.-A., Maaß, S., Kohler, T. P., Hammerschmidt, S., and Becher, D. (2020). Proteomic Adaptation of *Streptococcus pneumoniae* to the Human Antimicrobial Peptide LL-37. *Microorganisms* 8, 413. doi: 10.3390/microorganisms8030413
- Muhammad, A., Madhav, D., Rawish, F., Viveksandeep, T. C., Albert, E., Mollie, J., et al. (2019). Surotomycin (A Novel Cyclic Lipopeptide) vs. Vancomycin for the Treatment of *Clostridioides difficile* Infection: A Systematic Review and Meta-analysis. *Current clinical pharmacology* 14, 166–174. doi: 10.2174/1574884714666190328162637
- Muhammad, A., Simcha, W., Rawish, F., Sabih, R., Albert, E., and Ali, N. (2020). Cadazolid vs Vancomycin for the Treatment of *Clostridioides difficile* Infection: Systematic Review with Meta-analysis. *Current clinical pharmacology* 15, 4–10. doi: 10.2174/1574884714666190802124301
- Mukhopadhyay, J., Das, K., Ismail, S., Koppstein, D., Jang, M., Hudson, B., et al. (2008). The RNA polymerase “switch region” is a target for inhibitors. *Cell* 135, 295–307. doi: 10.1016/j.cell.2008.09.033

References

- Mulani, M. S., Kamble, E. E., Kumkar, S. N., Tawre, M. S., and Pardesi, K. R. (2019). Emerging Strategies to Combat ESKAPE Pathogens in the Era of Antimicrobial Resistance: A Review. *Front. Microbiol.* 10, 539. doi: 10.3389/fmicb.2019.00539
- Murdoch, D., Shah, H., Gharbia, S., and Rajendram, D. (2000). Proposal to Restrict the Genus *Peptostreptococcus* (Kluyver & van Niel 1936) to *Peptostreptococcus anaerobius*. *Anaerobe* 6, 257–260. doi: 10.1006/anae.2000.0344
- Murdoch, C. C., and Skaar, E. P. (2022). Nutritional immunity: the battle for nutrient metals at the host-pathogen interface. *Nat Rev Microbiol.* doi: 10.1038/s41579-022-00745-6
- Myles, I. A. (2014). Fast food fever: reviewing the impacts of the Western diet on immunity. *Nutr J* 13, 61. doi: 10.1186/1475-2891-13-61
- Nang, S. C., Azad, M. A. K., Velkov, T., Zhou, Q. T., and Li, J. (2021). Rescuing the Last-Line Polymyxins: Achievements and Challenges. *Pharmacol Rev* 73, 679–728. doi: 10.1124/pharmrev.120.000020
- Nawrocki, K. L., Wetzell, D., Jones, J. B., Woods, E. C., and McBride, S. M. (2018). Ethanolamine is a valuable nutrient source that impacts *Clostridium difficile* pathogenesis. *Environ Microbiol* 20, 1419–1435. doi: 10.1111/1462-2920.14048
- Nayfach, S., Roux, S., Seshadri, R., Udvariy, D., Varghese, N., Schulz, F., et al. (2021). A genomic catalog of Earth's microbiomes. *Nat Biotechnol* 39, 499–509. doi: 10.1038/s41587-020-0718-6
- Neumann-Schaal, M., Hofmann, J. D., Will, S. E., and Schomburg, D. (2015). Time-resolved amino acid uptake of *Clostridium difficile* 630 Δ erm and concomitant fermentation product and toxin formation. *BMC Microbiol* 15, 281. doi: 10.1186/s12866-015-0614-2
- Neumann-Schaal, M., Jahn, D., and Schmidt-Hohagen, K. (2019). Metabolism the Difficile Way: The Key to the Success of the Pathogen *Clostridioides difficile*. *Front. Microbiol.* 10, 219. doi: 10.3389/fmicb.2019.00219
- Neumann-Schaal, M., Metzendorf, N. G., Troitzsch, D., Nuss, A. M., Hofmann, J. D., Beckstette, M., et al. (2018). Tracking gene expression and oxidative damage of O₂-stressed *Clostridioides difficile* by a multi-omics approach. *Anaerobe* 53, 94–107. doi: 10.1016/j.anaerobe.2018.05.018
- Neuwirth, E. (2014). RColorBrewer: ColorBrewer Palettes: R package version 1.1-2., <https://CRAN.R-project.org/package=RColorBrewer>
- Neville, S. L., Eijkelkamp, B. A., Lothian, A., Paton, J. C., Roberts, B. R., Rosch, J. W., et al. (2020). Cadmium stress dictates central carbon flux and alters membrane composition in *Streptococcus pneumoniae*. *Commun Biol* 3, 694. doi: 10.1038/s42003-020-01417-y
- Newman, J. R. S., Ghaemmaghami, S., Ihmels, J., Breslow, D. K., Noble, M., DeRisi, J. L., et al. (2006). Single-cell proteomic analysis of *S. cerevisiae* reveals the architecture of biological noise. *Nature* 441, 840–846. doi: 10.1038/nature04785
- Ng, K. M., Ferreyra, J. A., Higginbottom, S. K., Lynch, J. B., Kashyap, P. C., Gopinath, S., et al. (2013). Microbiota-liberated host sugars facilitate post-antibiotic expansion of enteric pathogens. *Nature* 502, 96–99. doi: 10.1038/nature12503
- Ng, Q. X., Loke, W., Foo, N. X., Mo, Y., Yeo, W.-S., and Soh, A. Y. S. (2019). A systematic review of the use of rifaximin for *Clostridium difficile* infections. *Anaerobe* 55, 35–39. doi: 10.1016/j.anaerobe.2018.10.011
- Normington, C., Moura, I. B., Bryant, J. A., Ewin, D. J., Clark, E. V., Kettle, M. J., et al. (2021). Biofilms harbour *Clostridioides difficile*, serving as a reservoir for recurrent infection. *NPJ Biofilms Microbiomes* 7, 16. doi: 10.1038/s41522-021-00184-w
- Novichkov, P. S., Kazakov, A. E., Ravcheev, D. A., Leyn, S. A., Kovaleva, G. Y., Sutormin, R. A., et al. (2013). RegPrecise 3.0--a resource for genome-scale exploration of transcriptional regulation in bacteria. *BMC genomics* 14, 745. doi: 10.1186/1471-2164-14-745
- Ofori, E., Ramai, D., Dhawan, M., Mustafa, F., Gasperino, J., and Reddy, M. (2018). Community-acquired *Clostridium difficile*: epidemiology, ribotype, risk factors, hospital and intensive care unit outcomes, and current and emerging therapies. *Journal of Hospital Infection* 99, 436–442. doi: 10.1016/j.jhin.2018.01.015

- Oksanen, J., Blanchet, F. G., Friendly, M., Kindt, R., Legendre, P., McGlinn, D., et al. (2020). vegan: Community Ecology Package: R package version 2.5-7, <https://CRAN.R-project.org/package=vegan>
- Oliva, B., and Chopra, I. (1992). Tet determinants provide poor protection against some tetracyclines: further evidence for division of tetracyclines into two classes. *Antimicrob Agents Chemother* 36, 876–878. doi: 10.1128/AAC.36.4.876
- Oliva, B., Gordon, G., McNicholas, P., Ellestad, G., and Chopra, I. (1992). Evidence that tetracycline analogs whose primary target is not the bacterial ribosome cause lysis of *Escherichia coli*. *Antimicrob Agents Chemother* 36, 913–919. doi: 10.1128/AAC.36.5.913
- Oliveira, D. M. P. de, Forde, B. M., Kidd, T. J., Harris, P. N. A., Schembri, M. A., Beatson, S. A., et al. (2020). Antimicrobial Resistance in ESKAPE Pathogens. *Clin Microbiol Rev* 33. doi: 10.1128/CMR.00181-19
- Oliver, T. J., and Sinclair, A. (2021). US3155582A - Antibiotic m-319 - Google Patents. Accessed October 08, 2021, <https://patents.google.com/patent/US3155582A/en>
- Ong, C. Y., Walker, M. J., and McEwan, A. G. (2015). Zinc disrupts central carbon metabolism and capsule biosynthesis in *Streptococcus pyogenes*. *Sci Rep* 5, 10799. doi: 10.1038/srep10799
- O'Rourke, A., Beyhan, S., Choi, Y., Morales, P., Chan, A. P., Espinoza, J. L., et al. (2020). Mechanism-of-Action Classification of Antibiotics by Global Transcriptome Profiling. *Antimicrob Agents Chemother* 64. doi: 10.1128/AAC.01207-19
- Osman, D., Cooke, A., Young, T. R., Deery, E., Robinson, N. J., and Warren, M. J. (2021). The requirement for cobalt in vitamin B12: A paradigm for protein metalation. *Biochim Biophys Acta Mol Cell Res* 1868, 118896. doi: 10.1016/j.bbamcr.2020.118896
- Pal, C., Bengtsson-Palme, J., Kristiansson, E., and Larsson, D. G. J. (2015). Co-occurrence of resistance genes to antibiotics, biocides and metals reveals novel insights into their co-selection potential. *BMC genomics* 16, 964. doi: 10.1186/s12864-015-2153-5
- Pal, R., Dai, M., and Seleem, M. N. (2021). High-throughput screening identifies a novel natural product-inspired scaffold capable of inhibiting *Clostridioides difficile* *in vitro*. *Sci Rep* 11, 10913. doi: 10.1038/s41598-021-90314-3
- Palarea-Albaladejo, J., and Martín-Fernández, J. A. (2015). zCompositions — R package for multivariate imputation of left-censored data under a compositional approach. *Chemometrics and Intelligent Laboratory Systems* 143, 85–96. doi: 10.1016/j.chemolab.2015.02.019
- Panina, E. M., Mironov, A. A., and Gelfand, M. S. (2003). Comparative genomics of bacterial zinc regulons: enhanced ion transport, pathogenesis, and rearrangement of ribosomal proteins. *Proceedings of the National Academy of Sciences* 100, 9912–9917. doi: 10.1073/pnas.1733691100
- Park, Y. J., and Lee, H. K. (2017). The Role of Skin and Orogenital Microbiota in Protective Immunity and Chronic Immune-Mediated Inflammatory Disease. *Front. Immunol.* 8, 1955. doi: 10.3389/fimmu.2017.01955
- Passmore, I. J., Letertre, M. P. M., Preston, M. D., Bianconi, I., Harrison, M. A., Nasher, F., et al. (2018). Para-cresol production by *Clostridium difficile* affects microbial diversity and membrane integrity of Gram-negative bacteria. *PLoS Pathog* 14, e1007191. doi: 10.1371/journal.ppat.1007191
- Peláez, T., Alcalá, L., Alonso, R., Martín-López, A., García-Arias, V., Marín, M., et al. (2005). *In vitro* activity of ramoplanin against *Clostridium difficile*, including strains with reduced susceptibility to vancomycin or with resistance to metronidazole. *Antimicrob Agents Chemother* 49, 1157–1159. doi: 10.1128/AAC.49.3.1157-1159.2005
- Peng, T., Lin, J., Xu, Y.-Z., and Zhang, Y. (2016). Comparative genomics reveals new evolutionary and ecological patterns of selenium utilization in bacteria. *ISME J* 10, 2048–2059. doi: 10.1038/ismej.2015.246
- Peniche, A. G., Spinler, J. K., Boonma, P., Savidge, T. C., and Dann, S. M. (2018). Aging impairs protective host defenses against *Clostridioides (Clostridium) difficile* infection in mice by suppressing neutrophil and IL-22 mediated immunity. *Anaerobe* 54, 83–91. doi: 10.1016/j.anaerobe.2018.07.011

References

- Pereira, F. C., and Berry, D. (2017). Microbial nutrient niches in the gut. *Environ Microbiol* 19, 1366–1378. doi: 10.1111/1462-2920.13659
- Perelle, S., Gibert, M., Bourlioux, P., Corthier, G., and Popoff, M. R. (1997). Production of a complete binary toxin (actin-specific ADP-ribosyltransferase) by *Clostridium difficile* CD196. *Infect Immun* 65, 1402–1407. doi: 10.1128/iai.65.4.1402-1407.1997
- Pérez, J., Contreras-Moreno, F. J., Marcos-Torres, F. J., Moraleda-Muñoz, A., and Muñoz-Dorado, J. (2020). The antibiotic crisis: How bacterial predators can help. *Comput Struct Biotechnol J* 18, 2547–2555. doi: 10.1016/j.csbj.2020.09.010
- Perkel, J. M. (2021). Single-cell proteomics takes centre stage. *Nature* 597, 580–582. doi: 10.1038/d41586-021-02530-6
- Pessione, A., Lamberti, C., Cocolin, L., Campolongo, S., Grunau, A., Giubergia, S., et al. (2012). Different protein expression profiles in cheese and clinical isolates of *Enterococcus faecalis* revealed by proteomic analysis. *Proteomics* 12, 431–447. doi: 10.1002/pmic.201100468
- Petrosillo, N., Granata, G., and Cataldo, M. A. (2018). Novel Antimicrobials for the Treatment of *Clostridium difficile* Infection. *Front Med (Lausanne)* 5, 96. doi: 10.3389/fmed.2018.00096
- Pinu, F. R., Goldansaz, S. A., and Jaine, J. (2019). Translational Metabolomics: Current Challenges and Future Opportunities. *Metabolites* 9. doi: 10.3390/metabo9060108
- Plackett, B. (2020). Why big pharma has abandoned antibiotics. *Nature* 586, S50–S52. doi: 10.1038/d41586-020-02884-3
- Ponziani, F. R., Zocco, M. A., D'Aversa, F., Pompili, M., and Gasbarrini, A. (2017). Eubiotic properties of rifaximin: Disruption of the traditional concepts in gut microbiota modulation. *World J Gastroenterol* 23, 4491–4499. doi: 10.3748/wjg.v23.i25.4491
- Poquet, I., Saujet, L., Canette, A., Monot, M., Mihajlovic, J., Ghigo, J.-M., et al. (2018). *Clostridium difficile* biofilm: Remodeling metabolism and cell surface to build a sparse and heterogeneously aggregated architecture. *Front. Microbiol.* 9:2084. doi: 10.3389/fmicb.2018.02084
- Prochnow, H., Fetz, V., Hotop, S.-K., García-Rivera, M. A., Heumann, A., and Brønstrup, M. (2019). Subcellular Quantification of Uptake in Gram-Negative Bacteria. *Anal Chem* 91, 1863–1872. doi: 10.1021/acs.analchem.8b03586
- Proctor, R., Craig, W., and Kunin, C. (1978). Cetocycline, tetracycline analog: *in vitro* studies of antimicrobial activity, serum binding, lipid solubility, and uptake by bacteria. *Antimicrob Agents Chemother* 13, 598–604. doi: 10.1128/AAC.13.4.598
- Qian, C., and Hettich, R. L. (2017). Optimized Extraction Method To Remove Humic Acid Interferences from Soil Samples Prior to Microbial Proteome Measurements. *J Proteome Res* 16, 2537–2546. doi: 10.1021/acs.jproteome.7b00103
- Quraishi, M. N., Widlak, M., Bhala, N., Moore, D., Price, M., Sharma, N., et al. (2017). Systematic review with meta-analysis: the efficacy of faecal microbiota transplantation for the treatment of recurrent and refractory *Clostridium difficile* infection. *Aliment Pharmacol Ther* 46, 479–493. doi: 10.1111/apt.14201
- Raj, A., and van Oudenaarden, A. (2008). Nature, nurture, or chance: stochastic gene expression and its consequences. *Cell* 135, 216–226. doi: 10.1016/j.cell.2008.09.050
- Rajasingham, R., Enns, E. A., Khoruts, A., and Vaughn, B. P. (2020). Cost-effectiveness of Treatment Regimens for *Clostridioides difficile* Infection: An Evaluation of the 2018 Infectious Diseases Society of America Guidelines. *Clin Infect Dis* 70, 754–762. doi: 10.1093/cid/ciz318
- Rana, P., Ghouse, S. M., Akunuri, R., Madhavi, Y. V., Chopra, S., and Nanduri, S. (2020). FabI (enoyl acyl carrier protein reductase) - A potential broad spectrum therapeutic target and its inhibitors. *European Journal of Medicinal Chemistry* 208, 112757. doi: 10.1016/j.ejmech.2020.112757
- Randall, C. P., Oyama, L. B., Bostock, J. M., Chopra, I., and O'Neill, A. J. (2013). The silver cation (Ag⁺): antistaphylococcal activity, mode of action and resistance studies. *J Antimicrob Chemother* 68, 131–138. doi: 10.1093/jac/dks372
- Reed, A. D., Fletcher, J. R., Huang, Y. Y., Thanissery, R., Rivera, A. J., Parsons, R. J., et al. (2022). The Stickland Reaction Precursor trans-4-Hydroxy-L-Proline Differentially Impacts the

- Metabolism of *Clostridioides difficile* and Commensal Clostridia. *mSphere* 7, e0092621. doi: 10.1128/msphere.00926-21
- Reed, A. D., Nethery, M. A., Stewart, A., Barrangou, R., and Theriot, C. M. (2020). Strain-Dependent Inhibition of *Clostridioides difficile* by Commensal Clostridia Carrying the Bile Acid-Inducible (*bai*) Operon. *J Bacteriol* 202. doi: 10.1128/JB.00039-20
- Reed, A. D., and Theriot, C. M. (2021). Contribution of Inhibitory Metabolites and Competition for Nutrients to Colonization Resistance against *Clostridioides difficile* by Commensal *Clostridium*. *Microorganisms* 9. doi: 10.3390/microorganisms9020371
- Reyman, M., van Houten, M. A., Watson, R. L., Chu, M. L. J. N., Arp, K., Waal, W. J. de, et al. (2022). Effects of early-life antibiotics on the developing infant gut microbiome and resistome: a randomized trial. *Nat Commun* 13, 893. doi: 10.1038/s41467-022-28525-z
- Rhee, C., Chiotos, K., Cosgrove, S. E., Heil, E. L., Kadri, S. S., Kalil, A. C., et al. (2021). Infectious Diseases Society of America Position Paper: Recommended Revisions to the National Severe Sepsis and Septic Shock Early Management Bundle (SEP-1) Sepsis Quality Measure. *Clin Infect Dis* 72, 541–552. doi: 10.1093/cid/ciaa059
- Ritchie, M. E., Phipson, B., Di Wu, Hu, Y., Law, C. W., Shi, W., et al. (2015). limma powers differential expression analyses for RNA-sequencing and microarray studies. *Nucleic acids research* 43, e47. doi: 10.1093/nar/gkv007
- Rodionov, D. A., Arzamasov, A. A., Khoroshkin, M. S., Iablokov, S. N., Leyn, S. A., Peterson, S. N., et al. (2019). Micronutrient Requirements and Sharing Capabilities of the Human Gut Microbiome. *Front. Microbiol.* 10, 1316. doi: 10.3389/fmicb.2019.01316
- Rodionov, D. A., Vitreschak, A. G., Mironov, A. A., and Gelfand, M. S. (2003). Comparative genomics of the vitamin B12 metabolism and regulation in prokaryotes. *J Biol Chem* 278, 41148–41159. doi: 10.1074/jbc.M305837200
- Rose, E. C., Blikslager, A. T., and Ziegler, A. L. (2022). Porcine Models of the Intestinal Microbiota: The Translational Key to Understanding How Gut Commensals Contribute to Gastrointestinal Disease. *Front Vet Sci* 9, 834598. doi: 10.3389/fvets.2022.834598
- Roshan, N., Hammer, K. A., and Riley, T. V. (2018). Non-conventional antimicrobial and alternative therapies for the treatment of *Clostridium difficile* infection. *Anaerobe* 49, 103–111. doi: 10.1016/j.anaerobe.2018.01.003
- Roshan, N., Riley, T. V., and Hammer, K. A. (2017). Antimicrobial activity of natural products against *Clostridium difficile* *in vitro*. *J Appl Microbiol* 123, 92–103. doi: 10.1111/jam.13486
- Rupnik, M., and Janezic, S. (2016). An Update on *Clostridium difficile* Toxinotyping. *J Clin Microbiol* 54, 13–18. doi: 10.1128/JCM.02083-15
- Saffarian, A., Mulet, C., Regnault, B., Amiot, A., Tran-Van-Nhieu, J., Ravel, J., et al. (2019). Crypt- and Mucosa-Associated Core Microbiotas in Humans and Their Alteration in Colon Cancer Patients. *mBio* 10. doi: 10.1128/mBio.01315-19
- Sasi Jyothsna, T. S., Tushar, L., Sasikala, C., and Ramana, C. V. (2016). *Paraclostridium benzoelyticum* gen. nov., sp. nov., isolated from marine sediment and reclassification of *Clostridium bifermentans* as *Paraclostridium bifermentans* comb. nov. Proposal of a new genus *Paeniclostridium* gen. nov. to accommodate *Clostridium sordellii* and *Clostridium ghonii*. *Int. J. Syst. Evol.* 66, 1268–1274. doi: 10.1099/ijsem.0.000874
- Sattar, A., Thommes, P., Payne, L., Warn, P., and Vickers, R. J. (2015). SMT19969 for *Clostridium difficile* infection (CDI): *in vivo* efficacy compared with fidaxomicin and vancomycin in the hamster model of CDI. *J Antimicrob Chemother* 70, 1757–1762. doi: 10.1093/jac/dkv005
- Schiebenhoefer, H., Schallert, K., Renard, B. Y., Trappe, K., Schmid, E., Benndorf, D., et al. (2020). A complete and flexible workflow for metaproteomics data analysis based on MetaProteomeAnalyzer and Prophan. *Nat Protoc* 15, 3212–3239. doi: 10.1038/s41596-020-0368-7
- Schieferdecker, S., Exner, T. E., Gross, H., Roth, M., and Nett, M. (2014). New myxothiazols from the predatory bacterium *Myxococcus fulvus*. *J Antibiot (Tokyo)* 67, 519–525. doi: 10.1038/ja.2014.31

References

- Schiessl, K. T., Hu, F., Jo, J., Nazia, S. Z., Wang, B., Price-Whelan, A., et al. (2019). Phenazine production promotes antibiotic tolerance and metabolic heterogeneity in *Pseudomonas aeruginosa* biofilms. *Nat Commun* 10, 762. doi: 10.1038/s41467-019-08733-w
- Schneeberg, A., Neubauer, H., Schmooch, G., Baier, S., Harlizius, J., Nienhoff, H., et al. (2013). *Clostridium difficile* genotypes in piglet populations in Germany. *Journal of clinical microbiology* 51, 3796–3803. doi: 10.1128/JCM.01440-13
- Schneider, C. A., Rasband, W. S., and Eliceiri, K. W. (2012). NIH Image to ImageJ: 25 years of image analysis. *Nat Methods* 9, 671–675. doi: 10.1038/nmeth.2089
- Schnizlein, M. K., Vendrov, K. C., Edwards, S. J., Martens, E. C., and Young, V. B. (2020). Dietary Xanthan Gum Alters Antibiotic Efficacy against the Murine Gut Microbiota and Attenuates *Clostridioides difficile* Colonization. *mSphere* 5. doi: 10.1128/mSphere.00708-19
- Schroeder, L., and Ikui, A. E. (2019). Tryptophan confers resistance to SDS-associated cell membrane stress in *Saccharomyces cerevisiae*. *PLOS ONE* 14, e0199484. doi: 10.1371/journal.pone.0199484
- Schwanbeck, J., Riedel, T., Laukien, F., Schober, I., Oehmig, I., Zimmermann, O., et al. (2019). Characterization of a clinical *Clostridioides difficile* isolate with markedly reduced fidaxomicin susceptibility and a V1143D mutation in *rpoB*. *J Antimicrob Chemother* 74, 6–10. doi: 10.1093/jac/dky375
- Scudeller, L., Righi, E., Chiamenti, M., Bragantini, D., Menchinelli, G., Cattaneo, P., et al. (2021). Systematic review and meta-analysis of *in vitro* efficacy of antibiotic combination therapy against carbapenem-resistant Gram-negative bacilli. *International journal of antimicrobial agents* 57, 106344. doi: 10.1016/j.ijantimicag.2021.106344
- Sebaihia, M., Wren, B. W., Mullany, P., Fairweather, N. F., Minton, N., Stabler, R., et al. (2006). The multidrug-resistant human pathogen *Clostridium difficile* has a highly mobile, mosaic genome. *Nat Genet* 38, 779–786. doi: 10.1038/ng1830
- Seekatz, A. M., Rao, K., Santhosh, K., and Young, V. B. (2016). Dynamics of the fecal microbiome in patients with recurrent and nonrecurrent *Clostridium difficile* infection. *Genome Med* 8, 47. doi: 10.1186/s13073-016-0298-8
- Selle, K., Fletcher, J. R., Tuson, H., Schmitt, D. S., McMillan, L., Vridhambal, G. S., et al. (2020). *In Vivo* Targeting of *Clostridioides difficile* Using Phage-Delivered CRISPR-Cas3 Antimicrobials. *mBio* 11. doi: 10.1128/mBio.00019-20
- Senges, C. H. R., Stepanek, J. J., Wenzel, M., Raatschen, N., Ay, Ü., Märtens, Y., et al. (2020). Comparison of Proteomic Responses as Global Approach to Antibiotic Mechanism of Action Elucidation. *Antimicrob Agents Chemother* 65. doi: 10.1128/AAC.01373-20
- Shelton, A. N., Seth, E. C., Mok, K. C., Han, A. W., Jackson, S. N., Haft, D. R., et al. (2019). Uneven distribution of cobamide biosynthesis and dependence in bacteria predicted by comparative genomics. *ISME J* 13, 789–804. doi: 10.1038/s41396-018-0304-9
- Shen, A. (2020). *Clostridioides difficile* Spore Formation and Germination: New Insights and Opportunities for Intervention. *Annu Rev Microbiol* 74, 545–566. doi: 10.1146/annurev-micro-011320-011321
- Shen, N. T., Maw, A., Tmanova, L. L., Pino, A., Ancy, K., Crawford, C. V., et al. (2017). Timely Use of Probiotics in Hospitalized Adults Prevents *Clostridium difficile* Infection: A Systematic Review With Meta-Regression Analysis. *Gastroenterology* 152, 1889-1900.e9. doi: 10.1053/j.gastro.2017.02.003
- Shippo, C., Kelly, H. R., Dahl, P. J., Yi, S. M., Vu, D., Boyer, D., et al. (2021). Intrinsic electronic conductivity of individual atomically resolved amyloid crystals reveals micrometer-long hole hopping via tyrosines. *PNAS* 118. doi: 10.1073/pnas.2014139118
- Sholeh, M., Krutova, M., Forouzesh, M., Mironov, S., Sadeghifard, N., Molaeipour, L., et al. (2020). Antimicrobial resistance in *Clostridioides (Clostridium) difficile* derived from humans: a systematic review and meta-analysis. *Antimicrob Resist Infect Control* 9, 158. doi: 10.1186/s13756-020-00815-5
- Sierant, M., Leszczynska, G., Sadowska, K., Komar, P., Radzikowska-Cieciura, E., Sochacka, E., et al. (2018). *Escherichia coli* tRNA 2-selenouridine synthase (SelU) converts S2U-RNA to

- Se2U-RNA via S-geranylated-intermediate. *FEBS Lett* 592, 2248–2258. doi: 10.1002/1873-3468.13124
- Sievers, S., Metzendorf, N. G., Dittmann, S., Troitzsch, D., Gast, V., Tröger, S. M., et al. (2019). Differential View on the Bile Acid Stress Response of *Clostridioides difficile*. *Front. Microbiol.* 10, 258. doi: 10.3389/fmicb.2019.00258
- Silver, L. L. (2011). Challenges of antibacterial discovery. *Clin Microbiol Rev* 24, 71–109. doi: 10.1128/CMR.00030-10
- Simon, J., van Spanning, R. J. M., and Richardson, D. J. (2008). The organisation of proton motive and non-proton motive redox loops in prokaryotic respiratory systems. *Biochimica et biophysica acta* 1777, 1480–1490. doi: 10.1016/j.bbabi.2008.09.008
- Slimings, C., and Riley, T. V. (2021). Antibiotics and healthcare facility-associated *Clostridioides difficile* infection: systematic review and meta-analysis 2020 update. *J Antimicrob Chemother* 76, 1676–1688. doi: 10.1093/jac/dkab091
- Soavelomandroso, A. P., Gaudin, F., Hoys, S., Nicolas, V., Vedantam, G., Janoir, C., et al. (2017). Biofilm structures in a mono-associated mouse model of *Clostridium difficile* infection. *Front. Microbiol.* 8:2086. doi: 10.3389/fmicb.2017.02086
- Spencer, J. L., Abate, D., Abate, K. H., Abay, S. M., Abbafati, C., Abbasi, N., et al. (2018). Global, regional, and national incidence, prevalence, and years lived with disability for 354 diseases and injuries for 195 countries and territories, 1990–2017: a systematic analysis for the Global Burden of Disease Study 2017. *Lancet* 392, 1789–1858. doi: 10.1016/S0140-6736(18)32279-7
- Srivastava, A., Degen, D., Ebright, Y. W., and Ebright, R. H. (2012). Frequency, spectrum, and nonzero fitness costs of resistance to myxopyronin in *Staphylococcus aureus*. *Antimicrob Agents Chemother* 56, 6250–6255. doi: 10.1128/AAC.01060-12
- Srivastava, A., Talaue, M., Liu, S., Degen, D., Ebright, R. Y., Sineva, E., et al. (2011). New target for inhibition of bacterial RNA polymerase: ‘switch region’. *Curr Opin Microbiol* 14, 532–543. doi: 10.1016/j.mib.2011.07.030
- Stabler, R. A., He, M., Dawson, L., Martin, M., Valiente, E., Corton, C., et al. (2009). Comparative genome and phenotypic analysis of *Clostridium difficile* 027 strains provides insight into the evolution of a hypervirulent bacterium. *Genome Biol* 10, R102. doi: 10.1186/gb-2009-10-9-r102
- Stepanek, J. J., Lukežič, T., Teichert, I., Petković, H., and Bandow, J. E. (2016). Dual mechanism of action of the atypical tetracycline chelocardin. *Biochimica et biophysica acta* 1864, 645–654. doi: 10.1016/j.bbapap.2016.03.004
- Steunou, A. S., Durand, A., Bourbon, M.-L., Babot, M., Tambosi, R., Liotenberg, S., et al. (2020). Cadmium and Copper Cross-Tolerance. Cu⁺ Alleviates Cd²⁺ Toxicity, and Both Cations Target Heme and Chlorophyll Biosynthesis Pathway in *Rubrivivax gelatinosus*. *Front. Microbiol.* 11, 893. doi: 10.3389/fmicb.2020.00893
- Stewart, D., Anwar, F., and Vedantam, G. (2020). Anti-virulence strategies for *Clostridioides difficile* infection: advances and roadblocks. *Gut Microbes* 12, 1802865. doi: 10.1080/19490976.2020.1802865
- Stokes, J. M., Lopatkin, A. J., Lobritz, M. A., and Collins, J. J. (2019). Bacterial Metabolism and Antibiotic Efficacy. *Cell Metab* 30, 251–259. doi: 10.1016/j.cmet.2019.06.009
- Strich, J. R., Heil, E. L., and Masur, H. (2020). Considerations for Empiric Antimicrobial Therapy in Sepsis and Septic Shock in an Era of Antimicrobial Resistance. *J Infect Dis* 222, S119-S131. doi: 10.1093/infdis/jiaa221
- Sucipto, H., Pogorevc, D., Luxenburger, E., Wenzel, S. C., and Müller, R. (2017). Heterologous production of myxobacterial α -pyrone antibiotics in *Myxococcus xanthus*. *Metab Eng* 44, 160–170. doi: 10.1016/j.ymben.2017.10.004
- Suetens, C., Latour, K., Kärki, T., Ricchizzi, E., Kinross, P., Moro, M. L., et al. (2018). Prevalence of healthcare-associated infections, estimated incidence and composite antimicrobial resistance index in acute care hospitals and long-term care facilities: results from two European point prevalence surveys, 2016 to 2017. *Eurosurveillance* 23, 1800516. doi: 10.2807/1560-7917.ES.2018.23.46.1800516

References

- Sun, X., Savidge, T., and Feng, H. (2010). The enterotoxicity of *Clostridium difficile* toxins. *Toxins (Basel)* 2, 1848–1880. doi: 10.3390/toxins2071848
- Taboada, B., Ciria, R., Martinez-Guerrero, C. E., and Merino, E. (2012). ProOpDB: Prokaryotic Operon DataBase. *Nucleic acids research* 40, D627-31. doi: 10.1093/nar/gkr1020
- Tachedjian, G., Aldunate, M., Bradshaw, C. S., and Cone, R. A. (2017). The role of lactic acid production by probiotic *Lactobacillus* species in vaginal health. *Res Microbiol* 168, 782–792. doi: 10.1016/j.resmic.2017.04.001
- Tam, J., Icho, S., Utama, E., Orrell, K. E., Gómez-Biagi, R. F., Theriot, C. M., et al. (2020). Intestinal bile acids directly modulate the structure and function of *C. difficile* TcdB toxin. *PNAS* 117, 6792–6800. doi: 10.1073/pnas.1916965117
- Tan, G., Yang, J., Li, T., Zhao, J., Sun, S., Li, X., et al. (2017). Anaerobic Copper Toxicity and Iron-Sulfur Cluster Biogenesis in *Escherichia coli*. *Appl Environ Microbiol* 83. doi: 10.1128/AEM.00867-17
- Tanca, A., Palomba, A., Pisanu, S., Addis, M. F., and Uzzau, S. (2015). Enrichment or depletion? The impact of stool pretreatment on metaproteomic characterization of the human gut microbiota. *Proteomics* 15, 3474–3485. doi: 10.1002/pmic.201400573
- Tandan, M., Cormican, M., and Vellinga, A. (2018). Adverse events of fluoroquinolones vs. other antimicrobials prescribed in primary care: A systematic review and meta-analysis of randomized controlled trials. *International journal of antimicrobial agents* 52, 529–540. doi: 10.1016/j.ijantimicag.2018.04.014
- Tarrant, E., P Riboldi, G., McIlvin, M. R., Stevenson, J., Barwinska-Sendra, A., Stewart, L. J., et al. (2019). Copper stress in *Staphylococcus aureus* leads to adaptive changes in central carbon metabolism. *Metallomics* 11, 183–200. doi: 10.1039/c8mt00239h
- Thanissery, R., Winston, J. A., and Theriot, C. M. (2017). Inhibition of spore germination, growth, and toxin activity of clinically relevant *C. difficile* strains by gut microbiota derived secondary bile acids. *Anaerobe* 45, 86–100. doi: 10.1016/j.anaerobe.2017.03.004
- Thanissery, R., Zeng, D., Doyle, R. G., and Theriot, C. M. (2018). A Small Molecule-Screening Pipeline to Evaluate the Therapeutic Potential of 2-Aminoimidazole Molecules Against *Clostridium difficile*. *Front. Microbiol.* 9, 1206. doi: 10.3389/fmicb.2018.01206
- Theriot, C. M., Koenigskecht, M. J., Carlson, P. E., Hatton, G. E., Nelson, A. M., Li, B., et al. (2014). Antibiotic-induced shifts in the mouse gut microbiome and metabolome increase susceptibility to *Clostridium difficile* infection. *Nat Commun* 5, 3114. doi: 10.1038/ncomms4114
- Theriot, C. M., and Young, V. B. (2015). Interactions Between the Gastrointestinal Microbiome and *Clostridium difficile*. *Annu Rev Microbiol* 69, 445–461. doi: 10.1146/annurev-micro-091014-104115
- Thompson, L. R., Sanders, J. G., McDonald, D., Amir, A., Ladau, J., Locey, K. J., et al. (2017). A communal catalogue reveals Earth's multiscale microbial diversity. *Nature* 551, 457–463. doi: 10.1038/nature24621
- Tian, L., Wang, X.-W., Wu, A.-K., Fan, Y., Friedman, J., Dahlin, A., et al. (2020). Deciphering functional redundancy in the human microbiome. *Nat Commun* 11, 6217. doi: 10.1038/s41467-020-19940-1
- Tortajada-Girbés, M., Rivas, A., Hernández, M., González, A., Ferrús, M. A., and Pina-Pérez, M. C. (2021). Alimentary and Pharmaceutical Approach to Natural Antimicrobials against *Clostridioides difficile* Gastrointestinal Infection. *Foods* 10. doi: 10.3390/foods10051124
- Tramuta, C., Spigaglia, P., Barbanti, F., Bianchi, D. M., Boteva, C., Di Blasio, A., et al. (2021). Comparison of *Clostridioides difficile* strains from animals and humans: First results after introduction of *C. difficile* molecular typing and characterization at the Istituto Zooprofilattico Sperimentale of Piemonte, Liguria e Valle d'Aosta, Italy. *Comp Immunol Microbiol Infect Dis* 75, 101623. doi: 10.1016/j.cimid.2021.101623
- Tremblay, Y.D.N., Durand, B.A.R., Hamiot, A. et al. (2021). Metabolic adaption to extracellular pyruvate triggers biofilm formation in *Clostridioides difficile*. *ISME J* 15, 3623–3635. doi.org/10.1038/s41396-021-01042-5

- Tsakou, F., Jersie-Christensen, R., Jenssen, H., and Mojsoska, B. (2020). The Role of Proteomics in Bacterial Response to Antibiotics. *Pharmaceuticals (Basel)* 13. doi: 10.3390/ph13090214
- Turanov, A. A., Xu, X.-M., Carlson, B. A., Yoo, M.-H., Gladyshev, V. N., and Hatfield, D. L. (2011). Biosynthesis of selenocysteine, the 21st amino acid in the genetic code, and a novel pathway for cysteine biosynthesis. *Adv Nutr* 2, 122–128. doi: 10.3945/an.110.000265
- Turnbaugh, P. J., Hamady, M., Yatsunencko, T., Cantarel, B. L., Duncan, A., Ley, R. E., et al. (2009). A core gut microbiome in obese and lean twins. *Nature* 457, 480–484. doi: 10.1038/nature07540
- Tyanova, S., Temu, T., and Cox, J. (2016). The MaxQuant computational platform for mass spectrometry-based shotgun proteomics. *Nat Protoc* 11, 2301–2319. doi: 10.1038/nprot.2016.136
- Ullah, I., Ali, E., and Fakhar-ud-Din (2020). “Bioavailability of Antibiotics and Their Toxicity,” in *Antibiotics and Antimicrobial Resistance Genes: Environmental Occurrence and Treatment Technologies*, ed. M. Z. Hashmi (Cham: Springer International Publishing; Imprint Springer), 211–238.
- UniProt Consortium (2021). UniProt: the universal protein knowledgebase in 2021. *Nucleic acids research* 49, D480–D489. doi: 10.1093/nar/gkaa1100
- Uppu, D. S. S. M., Konai, M. M., Sarkar, P., Samaddar, S., Fensterseifer, I. C. M., Farias-Junior, C., et al. (2017). Membrane-active macromolecules kill antibiotic-tolerant bacteria and potentiate antibiotics towards Gram-negative bacteria. *PLOS ONE* 12, e0183263. doi: 10.1371/journal.pone.0183263
- van Goethem, M. W., Pierneef, R., Bezuidt, O. K. I., van de Peer, Y., Cowan, D. A., and Makhalanyaane, T. P. (2018). A reservoir of ‘historical’ antibiotic resistance genes in remote pristine Antarctic soils. *Microbiome* 6, 40. doi: 10.1186/s40168-018-0424-5
- van Werkhoven, C. H., Ducher, A., Berkell, M., Mysara, M., Lammens, C., Torre-Cisneros, J., et al. (2021). Incidence and predictive biomarkers of *Clostridioides difficile* infection in hospitalized patients receiving broad-spectrum antibiotics. *Nat Commun* 12, 2240. doi: 10.1038/s41467-021-22269-y
- van Zuylen, E. M., Ferguson, S. A., Hughes, A., Rennison, D., Brimble, M. A., and Cook, G. M. (2021). Disruption of Metallostasis in the Anaerobic Human Pathogen *Fusobacterium nucleatum* by the Zinc Ionophore PBT2. *ACS Infect Dis* 7, 2285–2298. doi: 10.1021/acsinfecdis.0c00887
- Verberkmoes, N. C., Russell, A. L., Shah, M., Godzik, A., Rosenquist, M., Halfvarson, J., et al. (2009). Shotgun metaproteomics of the human distal gut microbiota. *ISME J* 3, 179–189. doi: 10.1038/ismej.2008.108
- Vickers, R., Robinson, N., Best, E., Echols, R., Tillotson, G., and Wilcox, M. (2015). A randomised phase 1 study to investigate safety, pharmacokinetics and impact on gut microbiota following single and multiple oral doses in healthy male subjects of SMT19969, a novel agent for *Clostridium difficile* infections. *BMC Infect Dis* 15, 91. doi: 10.1186/s12879-015-0759-5
- Vickers, R. J., Tillotson, G. S., Nathan, R., Hazan, S., Pullman, J., Lucasti, C., et al. (2017). Efficacy and safety of ridinilazole compared with vancomycin for the treatment of *Clostridium difficile* infection: a phase 2, randomised, double-blind, active-controlled, non-inferiority study. *The Lancet Infectious Diseases* 17, 735–744. doi: 10.1016/S1473-3099(17)30235-9
- Waksman, S. A. (1941). Antagonistic relations of microorganisms. *Bacteriol Rev* 5, 231–291. doi: 10.1128/br.5.3.231-291.1941
- Waksman, S. A. (1947). What Is an Antibiotic or an Antibiotic Substance? *Mycologia* 39, 565. doi: 10.2307/3755196
- Waldron, K. J., and Robinson, N. J. (2009). How do bacterial cells ensure that metalloproteins get the correct metal? *Nat Rev Microbiol* 7, 25–35. doi: 10.1038/nrmicro2057
- Walter, B. M., Rupnik, M., Hodnik, V., Anderluh, G., Dupuy, B., Paulič, N., et al. (2014). The LexA regulated genes of the *Clostridium difficile*. *BMC Microbiol* 14, 88. doi: 10.1186/1471-2180-14-88
- Wang, H., Wang, M., Xu, X., Gao, P., Xu, Z., Zhang, Q., et al. (2021). Multi-target mode of action of silver against *Staphylococcus aureus* endows it with capability to combat antibiotic resistance. *Nat Commun* 12, 3331. doi: 10.1038/s41467-021-23659-y

References

- Wang, H., Yan, A., Liu, Z., Yang, X., Xu, Z., Wang, Y., et al. (2019). Deciphering molecular mechanism of silver by integrated omic approaches enables enhancing its antimicrobial efficacy in *E. coli*. *PLoS Biol* 17, e3000292. doi: 10.1371/journal.pbio.3000292
- Washburn, M. P., Wolters, D., and Yates, J. R. (2001). Large-scale analysis of the yeast proteome by multidimensional protein identification technology. *Nat Biotechnol* 19, 242–247. doi: 10.1038/85686
- Webb, B. J., Subramanian, A., Lopansri, B., Goodman, B., Jones, P. B., Ferraro, J., et al. (2020). Antibiotic Exposure and Risk for Hospital-Associated *Clostridioides difficile* Infection. *Antimicrob Agents Chemother* 64. doi: 10.1128/AAC.02169-19
- Weekley, C. M., and He, C. (2017). Developing drugs targeting transition metal homeostasis. *Curr Opin Chem Biol* 37, 26–32. doi: 10.1016/j.cbpa.2016.12.011
- Wenzel, M., Dekker, M. P., Wang, B., Burggraaf, M. J., Bitter, W., van Weering, J. R. T., et al. (2021). A flat embedding method for transmission electron microscopy reveals an unknown mechanism of tetracycline. *Commun Biol* 4, 306. doi: 10.1038/s42003-021-01809-8
- Wickham, H. (2016). *ggplot2: Elegant graphics for data analysis*. New York: Springer International Publishing.
- Wickham, H. (2019). *stringr: Simple, Consistent Wrappers for Common String Operations: R package version 1.4.0.*, <https://CRAN.R-project.org/package=stringr>
- Wickham, H. (2021). *tidyr: Tidy Messy Data: R package version 1.1.4.*, <https://CRAN.R-project.org/package=tidyr>
- Wickham, H. (2022). *broom: Convert Statistical Objects into Tidy Tibbles*.
- Wickham, H., François, R., Henry, L., and Müller, K. (2021). *dplyr: A Grammar of Data Manipulation: R package version 1.0.7.*, <https://CRAN.R-project.org/package=dplyr>
- Wiegand, P. N., Nathwani, D., Wilcox, M. H., Stephens, J., Shelbaya, A., and Haider, S. (2012). Clinical and economic burden of *Clostridium difficile* infection in Europe: a systematic review of healthcare-facility-acquired infection. *The Journal of hospital infection* 81, 1–14. doi: 10.1016/j.jhin.2012.02.004
- Wilcox, M. H., Gerding, D. N., Poxton, I. R., Kelly, C., Nathan, R., Birch, T., et al. (2017). Bezlotoxumab for Prevention of Recurrent *Clostridium difficile* Infection. *N Engl J Med* 376, 305–317. doi: 10.1056/NEJMoa1602615
- Willing, S. E., Richards, E. J., Sempere, L., Dale, A. G., Cutting, S. M., and Fairweather, N. F. (2015). Increased toxin expression in a *Clostridium difficile* *mfd* mutant. *BMC Microbiol* 15, 280. doi: 10.1186/s12866-015-0611-5
- Wintersdorff, C. J. H. von, Penders, J., van Niekerk, J. M., Mills, N. D., Majumder, S., van Alphen, L. B., et al. (2016). Dissemination of Antimicrobial Resistance in Microbial Ecosystems through Horizontal Gene Transfer. *Front. Microbiol.* 7, 173. doi: 10.3389/fmicb.2016.00173
- Wojdyr, M. (2010). Fityk: a general-purpose peak fitting program. *J Appl Crystallogr* 43, 1126–1128. doi: 10.1107/S0021889810030499
- Wolmeringer, A. (2017). Wirkung verschiedener Naturstoffe auf das Wachstum von *Clostridium difficile* 630 Δ erm. Bachelor's Thesis (Institute of Microbiology, University of Greifswald, Germany)
- Wood, C. L., McInturff, A., Young, H. S., Kim, D., and Lafferty, K. D. (2017). Human infectious disease burdens decrease with urbanization but not with biodiversity. *Phil. Trans. R. Soc. B* 372, 20160122. doi: 10.1098/rstb.2016.0122
- Woods, E. C., Edwards, A. N., Childress, K. O., Jones, J. B., and McBride, S. M. (2018). The *C. difficile* *clnRAB* operon initiates adaptations to the host environment in response to LL-37. *PLoS Pathog* 14, e1007153. doi: 10.1371/journal.ppat.1007153
- Woods, S. A., Schwartzbach, S. D., and Guest, J. R. (1988). Two biochemically distinct classes of fumarase in *Escherichia coli*. *Biochimica et Biophysica Acta (BBA) - Protein Structure and Molecular Enzymology* 954, 14–26. doi: 10.1016/0167-4838(88)90050-7
- Wu, X., Cherian, P. T., Lee, R. E., and Hurdle, J. G. (2013). The membrane as a target for controlling hypervirulent *Clostridium difficile* infections. *J Antimicrob Chemother* 68, 806–815. doi: 10.1093/jac/dks493

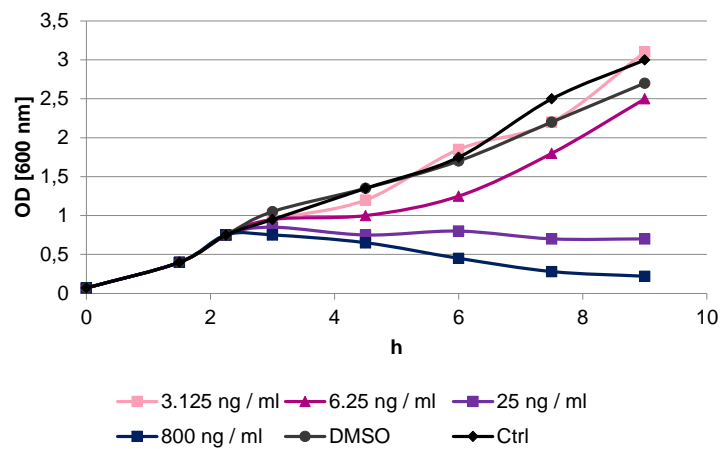
- Wüllner, D., Gesper, M., Haupt, A., Liang, X., Zhou, P., Dietze, P., et al. (2022). Adaptive Responses of *Pseudomonas aeruginosa* to Treatment with Antibiotics. *Antimicrob Agents Chemother* 66, e0087821. doi: 10.1128/AAC.00878-21
- Wüst, J., Sullivan, N. M., Hardegger, U., and Wilkins, T. D. (1982). Investigation of an outbreak of antibiotic-associated colitis by various typing methods. *J Clin Microbiol* 16, 1096–1101. doi: 10.1128/jcm.16.6.1096-1101.1982
- Xu, F. F., and Imlay, J. A. (2012). Silver(I), mercury(II), cadmium(II), and zinc(II) target exposed enzymic iron-sulfur clusters when they toxify *Escherichia coli*. *Appl Environ Microbiol* 78, 3614–3621. doi: 10.1128/AEM.07368-11
- Yadav, D., and Khanna, S. (2021). Safety of fecal microbiota transplantation for *Clostridioides difficile* infection focusing on pathobionts and SARS-CoV-2. *Therap Adv Gastroenterol* 14, 17562848211009694. doi: 10.1177/17562848211009694
- Yan, L. (2021). ggvenn: Draw Venn Diagram by “ggplot2”: R package version: 0.1.9, <https://CRAN.R-project.org/package=ggvenn>
- Yang, B., Fang, D., Lv, Q., Wang, Z., and Liu, Y. (2021). Targeted Therapeutic Strategies in the Battle Against Pathogenic Bacteria. *Front Pharmacol* 12, 673239. doi: 10.3389/fphar.2021.673239
- Yu, N. Y., Wagner, J. R., Laird, M. R., Melli, G., Rey, S., Lo, R., et al. (2010). PSORTb 3.0: improved protein subcellular localization prediction with refined localization subcategories and predictive capabilities for all prokaryotes. *Bioinformatics (Oxford, England)* 26, 1608–1615. doi: 10.1093/bioinformatics/btq249
- Yu, P., Petzoldt, S., Wilhelm, M., Zolg, D. P., Zheng, R., Sun, X., et al. (2017). Trimodal Mixed Mode Chromatography That Enables Efficient Offline Two-Dimensional Peptide Fractionation for Proteome Analysis. *Anal Chem* 89, 8884–8891. doi: 10.1021/acs.analchem.7b01356
- Yuan, C., Graham, M., Staley, C., and Subramanian, S. (2020). Mucosal Microbiota and Metabolome along the Intestinal Tract Reveal a Location-Specific Relationship. *mSystems* 5. doi: 10.1128/mSystems.00055-20
- Yuan, Y., Zallot, R., Grove, T. L., Payan, D. J., Martin-Verstraete, I., Šepić, S., et al. (2019). Discovery of novel bacterial queuine salvage enzymes and pathways in human pathogens. *PNAS* 116, 19126–19135. doi: 10.1073/pnas.1909604116
- Zhang, S.-J., Yang, Q., Xu, L., Chang, J., and Sun, X. (2012). Synthesis and antibacterial activity against *Clostridium difficile* of novel demethylvancomycin derivatives. *Bioorg Med Chem Lett* 22, 4942–4945. doi: 10.1016/j.bmcl.2012.06.039
- Zhang, W., Yu, D., Sun, Z., Wu, R., Chen, X., Chen, W., et al. (2010). Complete genome sequence of *Lactobacillus casei* Zhang, a new probiotic strain isolated from traditional homemade koumiss in Inner Mongolia, China. *J Bacteriol* 192, 5268–5269. doi: 10.1128/JB.00802-10
- Zhang, X., Ning, Z., Mayne, J., Moore, J. I., Li, J., Butcher, J., et al. (2016). MetaPro-IQ: a universal metaproteomic approach to studying human and mouse gut microbiota. *Microbiome* 4, 31. doi: 10.1186/s40168-016-0176-z
- Zhang, Y., Chowdhury, S., Rodrigues, J. V., and Shakhnovich, E. (2021). Development of antibacterial compounds that constrain evolutionary pathways to resistance. *Elife* 10. doi: 10.7554/eLife.64518
- Zhang, Y., Romero, H., Salinas, G., and Gladyshev, V. N. (2006). Dynamic evolution of selenocysteine utilization in bacteria: a balance between selenoprotein loss and evolution of selenocysteine from redox active cysteine residues. *Genome Biol* 7, R94. doi: 10.1186/gb-2006-7-10-r94
- Zhang, Y., Turanov, A. A., Hatfield, D. L., and Gladyshev, V. N. (2008). *In silico* identification of genes involved in selenium metabolism: evidence for a third selenium utilization trait. *BMC genomics* 9, 251. doi: 10.1186/1471-2164-9-251
- Zhao, Q., and Maynard, C. L. (2022). Mucus, commensals, and the immune system. *Gut Microbes* 14, 2041342. doi: 10.1080/19490976.2022.2041342
- Zheng, D., Liwinski, T., and Elinav, E. (2020). Interaction between microbiota and immunity in health and disease. *Cell Res* 30, 492–506. doi: 10.1038/s41422-020-0332-7

References

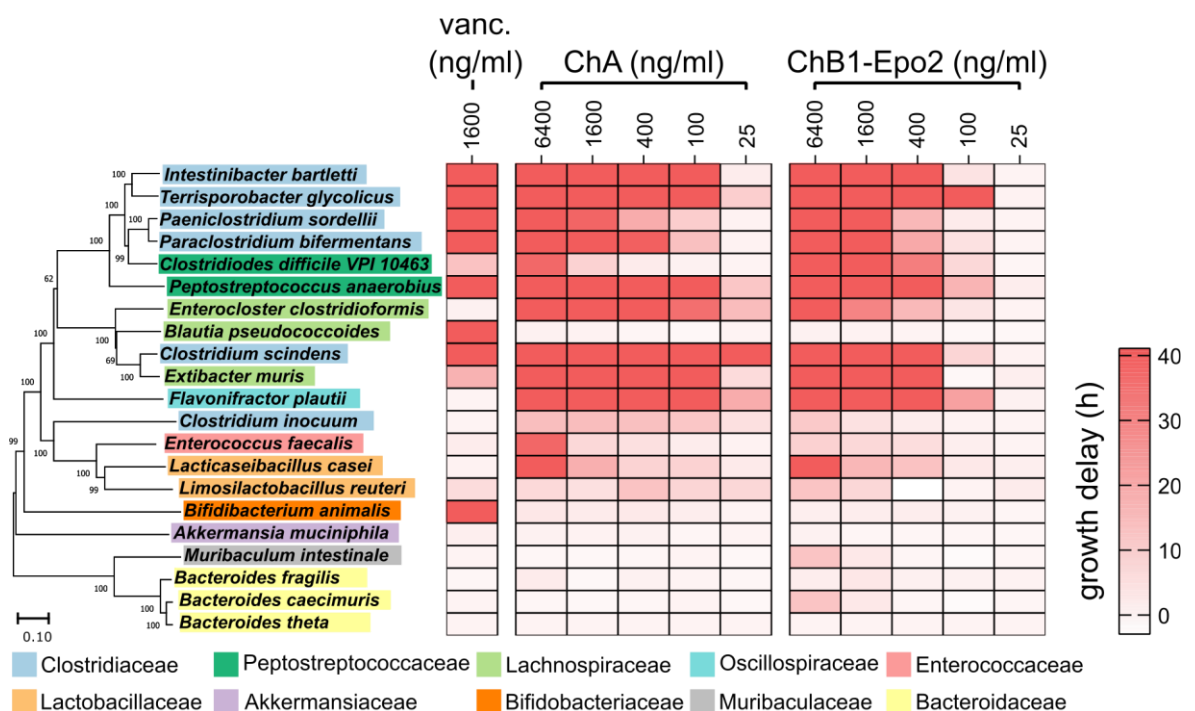
- Zhu, Y., Orre, L. M., Zhou Tran, Y., Mermelekas, G., Johansson, H. J., Malyutina, A., et al. (2020). DEqMS: A Method for Accurate Variance Estimation in Differential Protein Expression Analysis. *MCP* 19, 1047–1057. doi: 10.1074/mcp.TIR119.001646
- Zimmermann, P., Ziesenitz, V. C., Curtis, N., and Ritz, N. (2018). The Immunomodulatory Effects of Macrolides-A Systematic Review of the Underlying Mechanisms. *Front. Immunol.* 9, 302. doi: 10.3389/fimmu.2018.00302
- zur Abel Wiesch, P., Abel, S., Gkotzis, S., Ocampo, P., Engelstädter, J., Hinkley, T., et al. (2015). Classic reaction kinetics can explain complex patterns of antibiotic action. *Sci. Transl. Med.* 7, 287ra73. doi: 10.1126/scitranslmed.aaa8760

8. Appendix

8.1 Supplementary figures

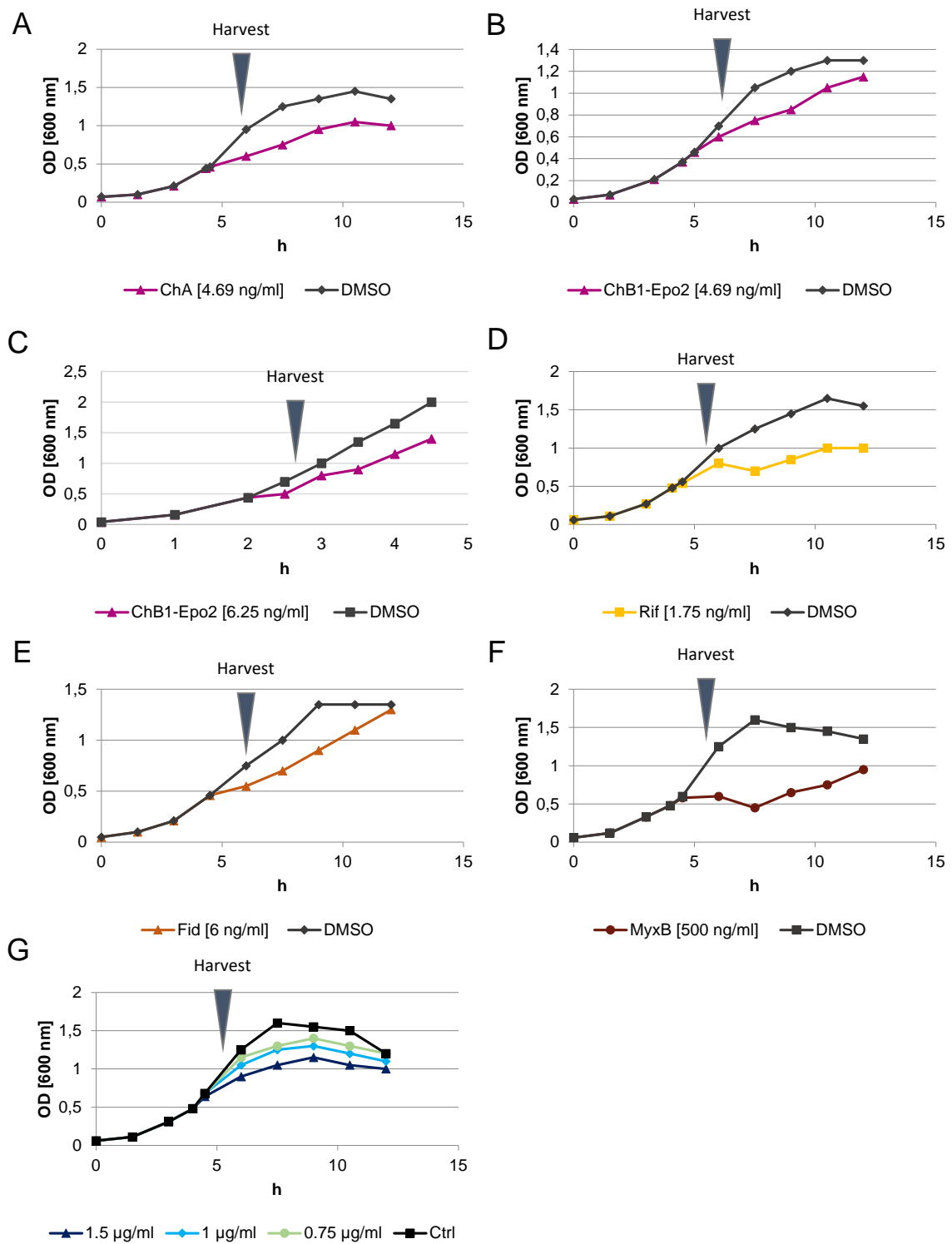


Supplementary figure S1: Growth of *C. difficile* in BHI broth is inhibited by low concentrations of chlorotonils to similar extent as in CDMM medium. Exemplarily, a selected growth curve representing $n \geq 3$ biological replicates is shown.

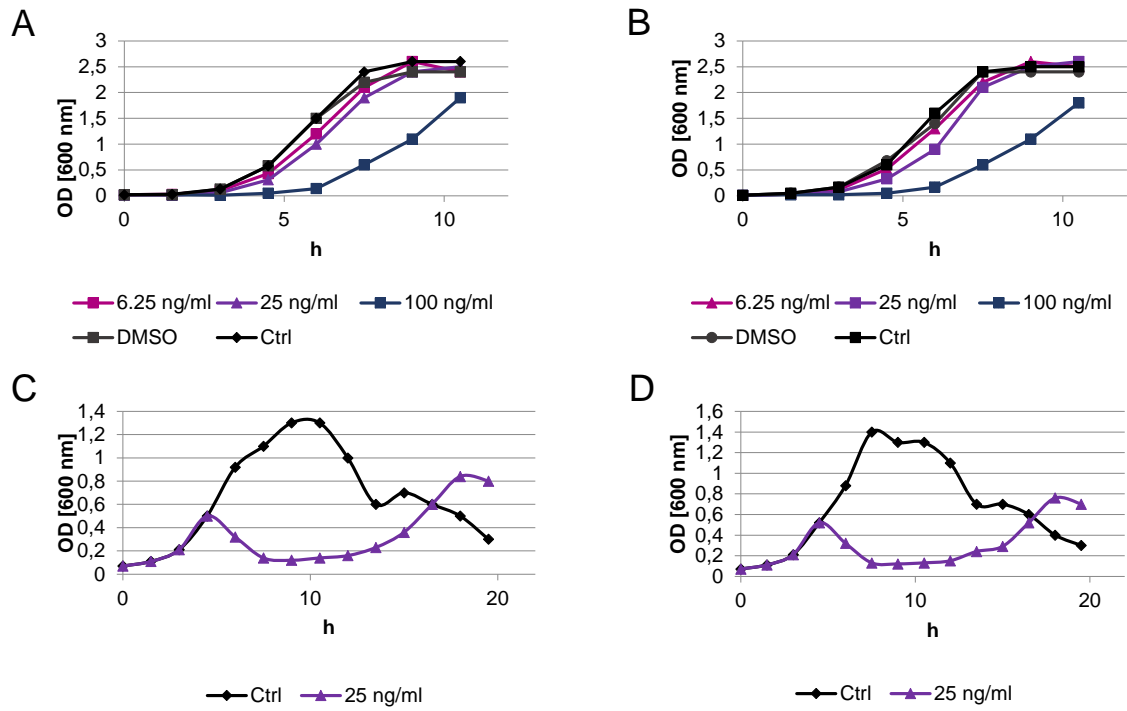


© Arne Bublitz, Helmholtz Centre for Infection Research, Braunschweig, Germany

Supplementary figure S2: Differential susceptibility of members from the intestinal community to ChA and ChB1-Epo2. Strains from ten different bacterial families were grown in BHIS in the presence of different concentrations of ChA or ChB1-Epo2. The time until cells reached an OD_{600nm} of 0.2 was measured and the growth delay is displayed in hours using a color gradient from white (no growth delay) to red (highest delay). Data and figure provided by Arne Bublitz, Helmholtz Institute for Infection Research, Braunschweig, Germany.



Supplementary figure S3: Exemplarily growth curves for the omics stress experiment. (A, B, D-G) *C. difficile* 630 was grown in CDMM to mid-exponential phase and was treated with (A) 4.69 ng/ml ChA, (B) 4.69 ng/ml ChB1-Epo2, (D) 1.75 ng/ml rifaximin (Rif), (E) 6 ng/ml fidaxomicin, (F) 500 ng/ml myxopyronin B or (G) three different concentrations of amidochelocardin (0.75 μ g/ml; 1.0 μ g/ml; 1.5 μ g/ml). (C) *T. glycolicus* DSM 1288 was grown in BHI to mid-exponential phase and was treated with 6.25 ng/ml ChB1-Epo2. Harvest points 90 minutes following stress are indicated by a triangle.



Supplementary figure S4: Adaptation of *C. difficile* to ChA. (A + B) *C. difficile* 630 was cultivated in the presence of serial dilutions of ChA in BHI broth. **(C + D)** *C. difficile* 630 is able to recover following ChA stress in CDMM medium.

8.2CD Rom content

The supplementary material included on the attached CD-ROM comprises:

Supplementray_tables.xlsx

- Tab. S1: Minimal inhibitory concentrations of ChA in different media in µg/ml.
- Tab. S2: Overview table of comparative BLASTp analysis.
- Tab. S3: Overview table of PrdB and GrdB homologous proteins submitted to the InterPro/Uniprot database. Downloaded May 9, 2022.
- Tab. S4: Table of all proteins identified in the ChA stress proteomics experiment with *C. difficile*.
- Tab. S5: Table of all proteins identified in the ChB1-Epo2 stress proteomics experiment with *C. difficile*.
- Tab. S6: Table of all proteins identified in the ChB1-Epo2 long-term stress proteomics experiment with *C. difficile*.
- Tab. S7: Table of all proteins identified in the chlorotoni proteomics experiment with *T. glycolicus*.
- Tab. S8: Table of quantitative ICP-MS data determined in the ChB1-Epo2 stress experiment with *C. difficile*.
- Tab. S9: Table of isotopes identified in complex with ChA and ChB1-Epo2.
- Tab. S10: Table of protein groups identified in the metaproteomics analysis.
- Tab. S11: Table of all proteins identified in the myxopyronin B proteomics experiment.
- Tab. S12: Table of all proteins identified in the amidochelocardin proteomics experiment.
- Tab. S13: Table of gene sets used for the gene set enrichment analysis.
- Tab. S14: Table of consumables and devices with specifications and manufacturers.

8.3 Eigenständigkeitserklärung

Hiermit erkläre ich, dass diese Arbeit bisher von mir weder an der Mathematisch-Naturwissenschaftlichen Fakultät der Universität Greifswald noch einer anderen wissenschaftlichen Einrichtung zum Zwecke der Promotion eingereicht wurde.

Ferner erkläre ich, dass ich diese Arbeit selbstständig verfasst und keine anderen als die darin angegebenen Hilfsmittel und Hilfen benutzt und keine Textabschnitte eines Dritten ohne Kennzeichnung übernommen habe.

Greifswald, 19.10.2022



Ort, Datum

Unterschrift des Promovenden

8.4 Conference contribution

- 04.2018 **Conference of the VAAM** (Leipzig, Germany)
Poster: Chelocardin and Chlorotonil A/B as novel therapeutics for the treatment of *Clostridioides difficile* infections
- 08.2018 **ISME** (Leipzig, Germany)
Poster: A multi-omics approach to characterize the new antibiotic Chlorotonil B
- 12.2018 **International Metaproteomics Symposium** (Leipzig, Germany)
Poster: A multi-omics approach to characterize the new antibiotic Chlorotonil B
- 03.2019 **Conference of the VAAM** (Mainz, Germany)
Poster: A multi-omics approach to evaluate natural products for *Clostridioides difficile* therapy
- 08.2019 **ClostPath 2019** (Leiden, Netherlands)
Poster: Chlorotonil A & B as new therapeutic options for *Clostridioides difficile* therapy
- 09.2019 **Joint meeting** of the **VAAM** special group “Qualitätssicherung und Diagnostik” and the **DGHM** special group “Diagnostische and Klinische Mikrobiologie” (Erlangen, Germany)

Talk: *Clostridioides difficile* Therapie mit Naturstoffen
- 03.2020 **Conference of the VAAM** (Leipzig, Germany)
Talk: New sustainable therapeutic options for *Clostridioides difficile* therapy (cancelled due to the Corona pandemic)
- 09.2020 **International *Clostridioides difficile* Symposium (ICDS)** (online conference)
- 09.2021 **ClostPath 2021** (online conference)

Poster: *Clostridioides difficile*'s response to dissipation of its proton motive force
- 09.2021 **International Metaproteomics Symposium** (Luxembourg, Luxembourg)

Poster: A metaproteomics approach to prove functional stability within the intestinal microbiome of piglets after challenge with Chlorotonil A

8.5 Acknowledgments

Finally, I would like to express my sincerest gratitude to those who have participated or indirectly contributed to this thesis.

First, I would like to express my special gratitude to my supervisor Prof. Kathrin Riedel for the opportunity to join her lab and conduct the work for my PhD under her supervision. I appreciated her helpful advices and guidance during my PhD and I am particularly grateful for her encouragement and support in career planning and the various opportunities to visit and to take part in conferences, symposia and workshops in Germany and abroad.

I am further very grateful to Dr. Susanne Sievers for her very helpful suggestions, her contributions to the different projects, her support during manuscript submission and revision processes, her encouragement and hours of proof-reading of manuscripts and abstracts.

I would further like to thank my collaborators from the MOASES project, including Prof. Thilo Fuchs and Stefanie Wagner from the Friedrich-Loeffler-Institute in Jena, Prof. Rolf Müller and Dr. Jennifer Herrmann from the Helmholtz Institute for Pharmaceutical Research in Saarbücken and Prof. Till Strowig and Arne Bublitz from the Helmholtz Institute for Infection Research in Braunschweig. I appreciated the constructive and successful collaboration. I would like to express my special thanks to Jenni, Stefanie and Arne for the lively exchange and scientific discussions and, in particular, for chats and laughter on the sidelines of scientific discussion. Thanks to all others who were involved in any of the projects.

I wish to extend my special thanks to all those colleagues and collaborators, namely Dr. Daniela Zühlke, Jürgen Bartel, Christian Wolff, Dr. Claudia Hirschfeld, Prof. Michael Lalk, Dr. Martina Wurster, Dr. Sven-Kevin Hotop, Prof. Mark Brönstrup, Christine Wünsche, Pierre Mücke, and Dr. Viktoria Pauker, who were involved in mass spectrometry measurements. In this respect, I would further like to thank Dr. Rabea Schlüter and Annette Meuche from the Imaging Center of the Department of Biology of University of Greifswald for performing the electron microscopy.

I further need to thank Prof. Ralf Gerhard and Daniel Henkel from the Hannover Medical School for providing antibodies directed against *C. difficile*'s toxins and Dr. Christian Seyboldt from the Friedrich-Loeffler-Institute for providing porcine *C. difficile* isolates.

Appendix

In addition, I would like to express sincere gratitude to Dr. Jörg Bernhardt, Jürgen Bartel, Siliva Dittmann, Prof. Dr. Robert Heyer, Dr. Tjorven Hinzke and Dirk Lewerentz for support during data analysis and the lab work. In this context, I further like to thank to all members from the Riedel/Sievers lab and the Institute of Microbiology for support and infrastructure, and my Bachelor and Master students for their great help.

Last but not least, it is very important for me to thank all who have supported me personally, especially the cake and coffee crew, who luckily provided a lot of cake, but also Luca Zaeck, Lars Lilge and Alexander and Anica Graf, my peers from the KarriereWegeMentoring program as well as my family and friends.

Finally, the work for this thesis was carried out at the University of Greifswald at the Institute of Microbiology and received funding from the InfectionControl 2020 research program of the Federal Ministry of Education and Research.